Investigations of Sterically Demanding Ligands in Molybdenum and Tungsten Monopyrrolide Monoalkoxide Catalysts for Olefin Metathesis

by

Laura Claire Heidkamp Gerber

B.A./M.S. in Chemistry (2007)
Brandeis University, Waltham, MA

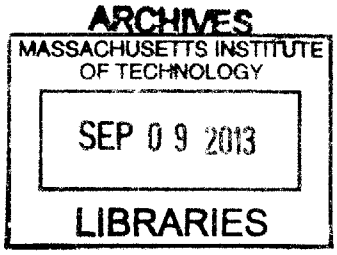

Submitted to the Department of Chemistry
in Partial Fulfillment of the Requirements for the Degree of

Doctor of Philosophy

at the
Massachusetts Institute of Technology
September 2013

Signature of Author _____
Department of Chemistry
August 12, 2013

Certified by _____
Richard R. Schrock
Frederick G. Keyes Professor of Chemistry
Thesis Supervisor

Accepted by _____
Robert W. Field
Haslam and Dewey Professor of Chemistry
Chairman, Departmental Committee on Graduate Students

This doctoral thesis has been examined by a Committee of the Department of Chemistry as follows

Professor Christopher C. Cummins
Chairman

Professor Richard R. Schrock
Thesis Supervisor

Professor Yogesh Surendranath

Investigations of Sterically Demanding Ligands in Molybdenum and Tungsten Monopyrrolide Monoalkoxide Catalysts for Olefin Metathesis

by

Laura Claire Heidkamp Gerber

Submitted to the Department of Chemistry on August 12, 2013
in Partial Fulfillment of the Requirements for the
Degree of Doctor of Philosophy in Chemistry

ABSTRACT

Chapter 2 investigates the mechanism of the temperature-controlled polymerization of 3-methyl-3-phenylcyclopropene (MPCP) by Mo(NAr)(CHCMe$_2$Ph)(Pyr)(OTPP) (Ar = 2,6-diisopropylphenyl, Pyr = pyrrolide, OTPP = 2,3,5,6-tetraphenylphenoxide). *Cis,syndiotactic* poly(MPCP) is obtained at −78 °C, while atactic poly(MPCP) is obtained at ambient temperature. The *syn* initiator (*syn* refers to the isomer in which the substituent on the alkylidene points towards the imido ligand and *anti* where the substituent points away) reacts with MPCP to form an *anti* first-insertion product at low temperatures, which continues to propagate to give *cis,syndiotactic* polymer. At higher temperatures, the *anti* alkylidenes that form initially upon reaction with MPCP rotate thermally to *syn* alkylidenes on a similar timescale as polymer propagation, giving rise to an irregular polymer structure. In this system *cis,syndiotactic* polymer is obtained through propagation of *anti* alkylidene species.

Chapters 3 – 5 detail the synthesis and reactivity of compounds containing a 2,6-dimesitylphenylimido (NAr*) ligand in order to provide a better understanding of the role of steric hindrance in olefin metathesis catalysts. A new synthetic route to imido alkylidene complexes of Mo and W, which proceeds through mixed-imido compounds containing both NAr* and N^{t}Bu ligands, was developed to incorporate the NAr* ligand. Alkylidene formation is accomplished by the addition of 3 equivalents of pyridine•HCl to Mo(NAr*)(N^{t}Bu)(CH$_2$CMe$_2$Ph)$_2$ or the addition of 1 equivalent of pyridine followed by 3 equivalents of HCl solution to W(NAr*)(N^{t}Bu)(CH$_2$CMe$_2$Ph)$_2$ to provide M(NAr*)(CHCMe$_2$Ph)Cl$_2$(py) (py = pyridine). Monoalkoxide monochloride, bispyrrolide, and monoalkoxide monopyrrolide (MAP) compounds are isolated upon substitution of the chloride ligands. Reaction of W MAP complexes (W(NAr*)(CHCMe$_2$Ph)(Me$_2$Pyr)(OR)) with ethylene allows for the isolation of unsubstituted metallacycle complexes W(N Ar*)(C$_3$H$_6$)(Me$_2$Pyr)(OR) (R = CMe(CF$_3$)$_2$, 2,6-Me$_2$C$_6$H$_3$, and SiPh$_3$). By application of vacuum to solutions of unsubstituted metallacyclebutane species, methylidene complexes W(NAr*)(CH$_2$)(Me$_2$Pyr)(OR) (R = ^{t}Bu, 2,6-Me$_2$C$_6$H$_3$, and SiPh$_3$) are isolated. Addition of one equivalent of 2,3-dicarbomethoxynorbornadiene to methylidene species allows for the observation of first-insertion products by NMR spectroscopy. Investigations of NAr* MAP compounds as catalysts for olefin metathesis reactions show that they are active catalysts, but not *E* or *Z* selective for

ring-opening metathesis polymerization the homocoupling of 1-octene or 1,3-dienes. Methylidene species W(NAr*)(CH_2)(Me_2Pyr)(OR) (R = 2,6-$Me_2C_6H_3$ or $SiPh_3$) catalyze the ring-opening metathesis or substituted norbornenes and norbornadienes with ethylene.

Thesis Supervisor: Richard R. Schrock
Title: Frederick G. Keyes Professor of Chemistry

Table of Contents

List of Figures

List of Schemes

List of Tables

List of Abbreviations

° C	degrees Celsius
Ad	1-adamantyl
anti	the alkylidene isomer in which the substituent points away from the imido ligand
Ar	2,6-diisopropylphenyl
Ar'	2,6-dimethylphenyl
Ar*	2,6-(2,4,6-trimethylphenyl)C_6H_3
atm	atmospheres
COSY	Correlation SpectroscopY
d	days or doublet
DCMNBD	2,3-dicarbomethoxynorbornadiene
DCMNBE	*rac*-2,3-dicarbomethoxynorbornene
DFT	Density Functional Theory
DME	dimethoxyethane
e	electron
Et	ethyl
EXSY	EXchange SpectroscopY
GC-MS	gas chromatography – mass spectrometry
h	hours
HIPT	2,6-(2,4,6-triisopropylphenyl)C_6H_3
HMT	2,6-(2,4,6-trimethylphenyl)C_6H_3
HRMS	high-resolution mass spectrometry
Hz	hertz, s^{-1}
^{i}Pr	isopropyl
k	rate constant
K	Kelvin
kcal	kilocalories
m	minutes or multiplet
M	molar

MAP	MonoAlkoxide Pyrrolide or MonoAryloxide Pyrrolide
Me	methyl
Me_2Pyr	2,5-dimethylpyrrolide
mesityl	2,4,6-trimethylphenyl
mL	milliliter
mmol	millimolar
MPCP	3-methyl-3-phenylcyclopropene
neophyl	2-methyl-2-phenylpropyl
$^{n}J_{AB}$	the coupling constant between atoms A and B through n bonds
NMR	nuclear magnetic resonance
OTf	triflate, trifluoromethanesulfonate
py	pyridine
Pyr	pyrrolide
rac	racemic
RCM	ring-closing metathesis
ROCM	ring-opening cross metathesis
ROMP	ring-opening metathesis polymerization
s	seconds or singlet
syn	the alkylidene isomer in which the substituent points towards the imido ligand
t	triplet
TBS	dimethyl-*tert*-butylsilyl
^{t}Bu	tertiarybutyl, 2,2-dimethylethyl
THF	tetrahydrofuran
TMS	trimethylsilyl
TPP	2,3,5,6-tetrapheylphenyl
TRIP	2,4,6-triisopropylphenyl
VT	variable temperature
δ	chemical shift
μL	microliter
μmol	micromolar

Chapter 1

General Introduction

Formation of carbon-carbon bonds is one of the most synthetically useful processes in chemistry. Olefin metathesis has emerged over the last 50 years as a practical and versatile method for the formation of carbon-carbon double bonds. It is used for polymerization as well as synthetic organic chemistry, giving rise to applications in fields such as material science, pharmaceuticals, and medicinal chemistry. Due to the utility of olefin metathesis, the 2005 Nobel Prize in Chemistry was awarded to Yves Chauvin, Robert H. Grubbs and Richard R. Schrock *"for the development of the metathesis method in organic synthesis"*.[1]

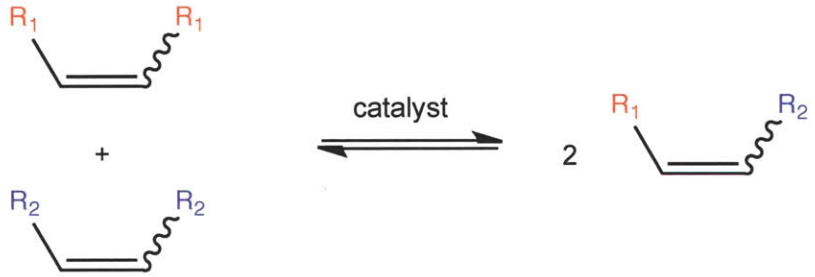

Scheme 1.1. Olefin metathesis is a process that rearranges the substituents on carbon-carbon double bonds in the presence of a catalyst.

Olefin metathesis is the process by which the substituents on carbon-carbon double bonds are rearranged (Scheme 1.1). Olefin metathesis activity was first reported in a German patent in 1960 by Dupont chemist H. S. Eleuterio.[2] Later accounts indicate that the research group of Prof. Karl Zeigler and chemists at Dupont were aware of olefin metathesis reactivity as early as 1956.[2] "Olefin disproportionation" was first reported in the chemical literature by Banks and Bailey in 1964, where the rearrangement of propylene to ethylene and butene was observed in the presence of heterogeneous molybdenum or tungsten catalysts.[3] The mechanism by which olefin metathesis proceeds was first proposed by Hérrison and Chauvin (Scheme 1.2).[4] A catalyst containing a metal-carbon double bond reacts with an alkene through a [2+2] cycloaddition to form a metallacyclobutane as an intermediate. When the metallacycle ring undergoes cycloreversion in the opposite way than it formed, a new olefin product forms, as well as a new metal-carbon double bond that can continue in the catalytic cycle.

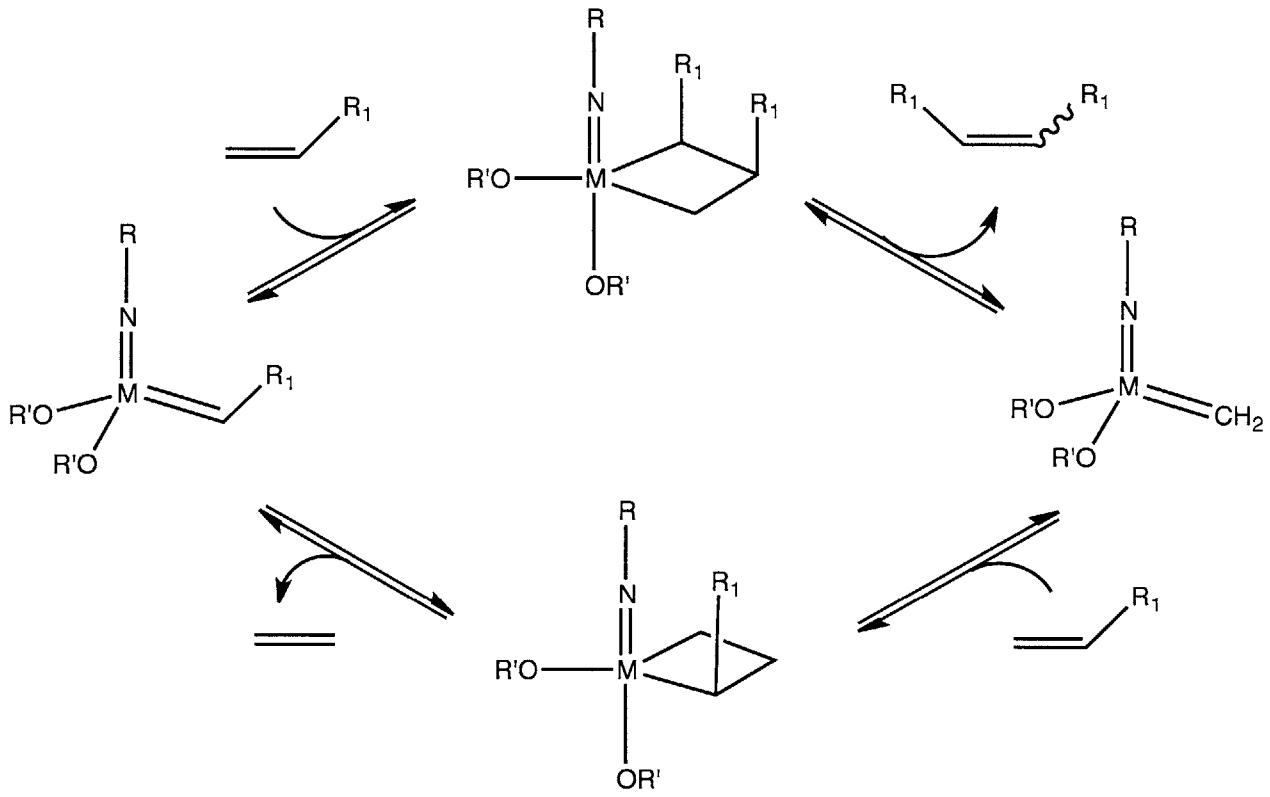

Scheme 1.2. Mechanism for olefin metathesis

Olefin metathesis has been developed into a versatile reaction that can be used for many different purposes.[5] Some examples are shown in Scheme 1.3. Cross metathesis refers to the intermolecular exchange of substituents to form a new olefin product. Ethenolysis is a reaction where ethylene is used to cleave an internal olefin to form two terminal olefins. Ethenolysis can be viewed as a subset of cross metathesis where an internal olefin is crossed with ethylene. Ring-closing metathesis is an intramolecular process where two terminal olefin moieties form a ring with ethylene as a byproduct. Ring-opening cross metathesis is where one of the partners of a cross metathesis reaction is contained in a ring, incorporating all parts of the substrates into one product. Ring-opening metathesis polymerization (ROMP) is a process by which a cyclic olefin is polymerized.

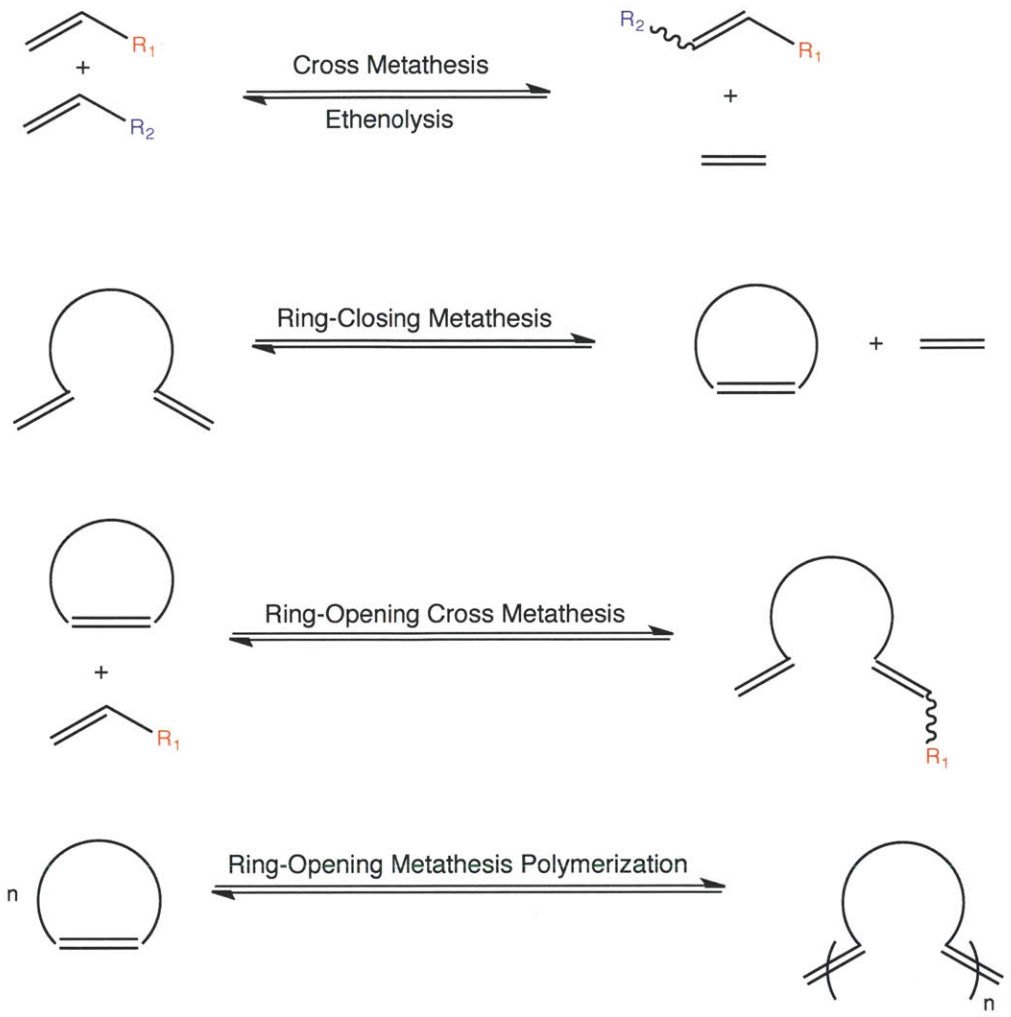

Scheme 1.3. Examples of olefin metathesis reactions.

A metal alkylidene complex, $Ta(CHCMe_3)(CH_2CMe_3)_3$ was isolated by Schrock in 1975.[6] This was the first example of a triplet carbene that is electrophilic at the metal and nucleophilic at the α-carbon, a distinct class of compounds from Fischer carbenes that are singlet carbenes, nucleophilic at the metal, and electrophilic at the α-carbon (Figure 1.1). The first examples of metal alkylidenes were not active as catalysts for olefin metathesis, but an alkylidene compound active for olefin metathesis was discovered with the synthesis of $W(O)(CHCMe_3)Cl_2(PEt_3)_2$.[7] Since that point, many catalysts have been developed for olefin metathesis, most of which are based on Mo, W, Re, and Ru.

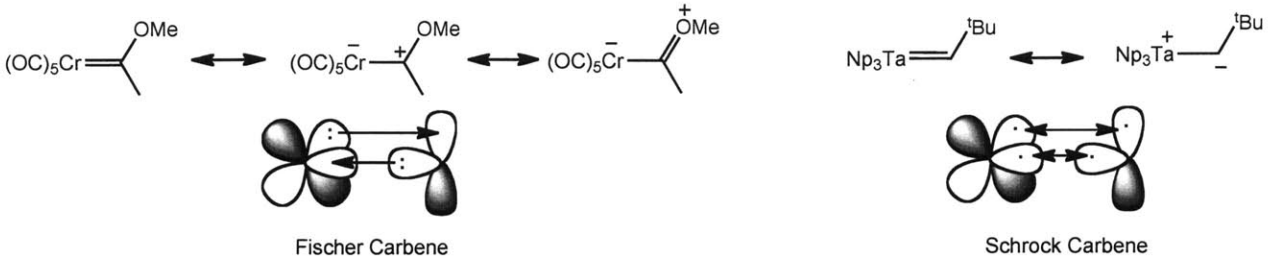

Figure 1.1. Types of metal-carbon double bonds; Fischer and Schrock carbenes.

The olefin metathesis catalysts based on Mo, W, and Ru that have proven to be most successful are of the general format shown in Figure 1.2. Ru catalysts tend to be stable to water and acidic functionalities such as carboxylates and amides, while Group 6 catalysts are stable to basic functionalities such as phosphines and amines, which provides for complimentary reactivity. For Group 6 catalysts, the initial alkylidene ligand is generally a neophylidene or a neopentylidene. The imido ligand is typically a substituted phenyl imido ligand or tertiary alkyl imido ligands. The two X-type ligands were traditionally two alkoxide ligands (Figure 1.2, **B**), with fluorinated alkoxide ligands providing for the highest activity. A second generation of catalysts was developed that contain axially chiral chelating diolate ligands for the performance of enantioselective reactions (Figure 1.2, **C**). Over the past 5 years, emphasis has been towards the development of catalysts that contain two different X-type ligands, especially catalysts that contain one pyrrolide or one alkoxide ligand (Figure 1.2, **D**).

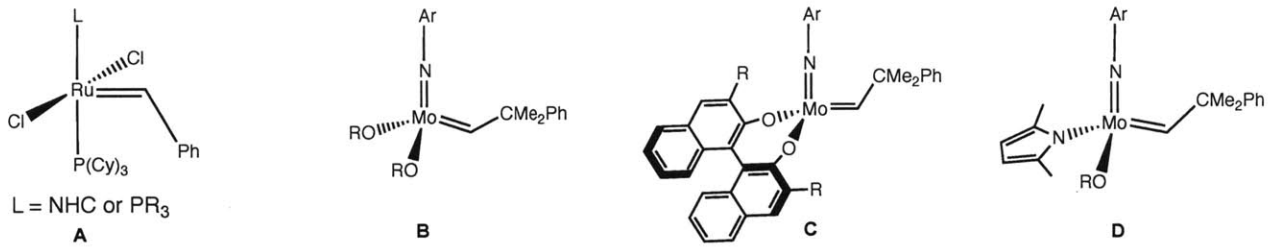

Figure 1.2. Examples of metathesis catalysts. A: Ruthenium catalysts, NHC = N-heterocyclic carbene. B: Bisalkoxide catalysts, R is typically a fluorinated alkyl group. C: Enantioselective catalysts that contain chiral, chelating diolate ligands. D: MonoAlkoxide Pyrrolide (MAP) catalysts.

A third generation of group 6 olefin metathesis catalysts, MonoAlkoxide Pyrrolide or MonoAryloxide Pyrrolide (MAP) catalysts (Figure 1.2, **D**), have been studied extensively over the past five years. MAP catalysts are typically synthesized from bispyrrolide complexes, which

were developed as precursors for the *in situ* generation of catalysts.[8] By the addition of one equivalent of an alcohol to bispyrrolide complexes, MAP catalysts are isolated.[9] Rather than showing intermediate reactivity between the inactive bispyrrolide complexes and the active bisalkoxide catalysts, the MAP catalysts showed greater catalyst efficiency in some cases as well as new types of reactivity for olefin metathesis catalysts. Group 6 olefin metathesis catalysts with two different X-type ligands have been studied computationally as well, and results indicate that two different X-type ligands provide for higher activity compared with catalysts containing two of the same X-type ligands.[10] According to these computational studies, the unsymmetrical catalysts have lower energy barriers for coordination of an olefin when compared to symmetrical catalysts, and the lower energy transition state shows olefin binding *trans* to the less electron-withdrawing ligand.

Due to the metal binding to four different ligands, MAP catalysts are chiral at the metal center. The properties of the two enantiomers have been studied by using a chiral alkoxide ligand to form diastereomers. Mo(NAr)(CHCMe$_2$Ph)(Me$_2$Pyr)(OBr$_2$Bitet) (**1**, Figure 1.3) forms as a 7:1 mixture of *S*:*R* diastereomers, each of which have been isolated and structurally characterized.[11] Solutions of pure (*S*)-**1** or (*R*)-**1** both remain unchanged over a week in C_6D_6 or THF-d_8, indicating that the two diastereomers do not interconvert under these conditions. Addition of PMe_3, $PPhMe_2$, pyridine-d_5, and acetonitrile-d_3 to (*R*)-**1** show conversion to an equilibrium mixture of (*S*)-**1** and (*R*)-**1**, which is first order in base (measured for PMe_3).[12] Structural characterization of a PMe_3 adduct of **1** shows that PMe_3 binds *trans* to the pyrrolide ligand.[12] Rearrangement of the five-coordinate species through Barry *pseudo*-rotations or turnstile rearrangements was proposed since the lack of a solvent effect argues against ionization and the variety of bases that promote the rearrangement suggests that formation of an intermediate ylide is unlikely. Addition of ethylene to (*S*)-**1** or (*R*)-**1** provides a mixture of metallacyclobutane and (*R*)- and (*S*)- methylidene species.[12] In this case, the authors propose interconversion of the diastereomers through ethylene metathesis since formation of the metallacycle is fast and an intermediate alkylidene olefin-complex is unlikely. If ethylene both approaches and leaves *trans* to the pyrrolide (consistent with both computational studies[10] and the X-ray structure of **1**(PMe_3)), then the metal inverts its configuration, as shown in Scheme 1.4.

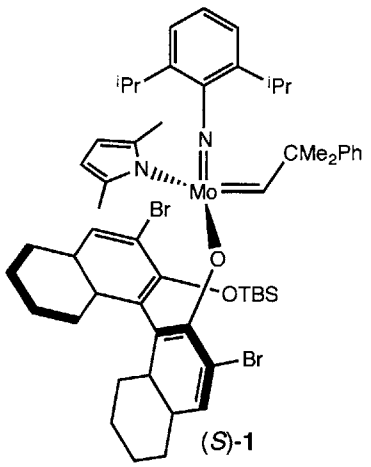

Figure 1.3. Structure of (*S*)-1. OTBS = OSi(^{t}Bu)Me$_2$.

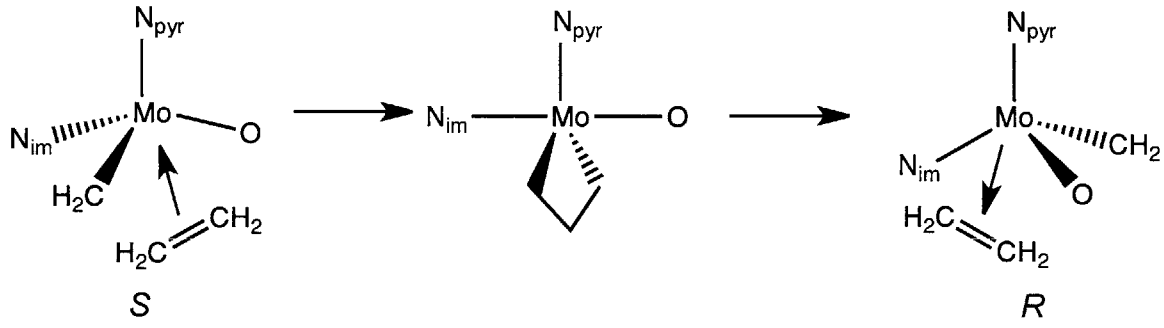

Scheme 1.4. Inversion of configuration at the metal of a MAP catalyst by ethylene metathesis. The first coordination sphere of the metal is shown.

The discovery of MAP catalysts has given rise to a great deal of new olefin metathesis activity. MAP catalysts provide new regioselectivity for intramolecular enyne metathesis reactions, forming the β isomer in several cases (Scheme 1.5).[9] Additionally, MAP catalysts containing a chiral aryloxide were used for enantioselective ring-closing metathesis reactions and applied to the synthesis of quebrachamine (Scheme 1.6), a compound that possesses adrenergic blocking activity.[11a, 13, 14] Previous enantioselective metathesis catalysts were not able to perform this reaction well.

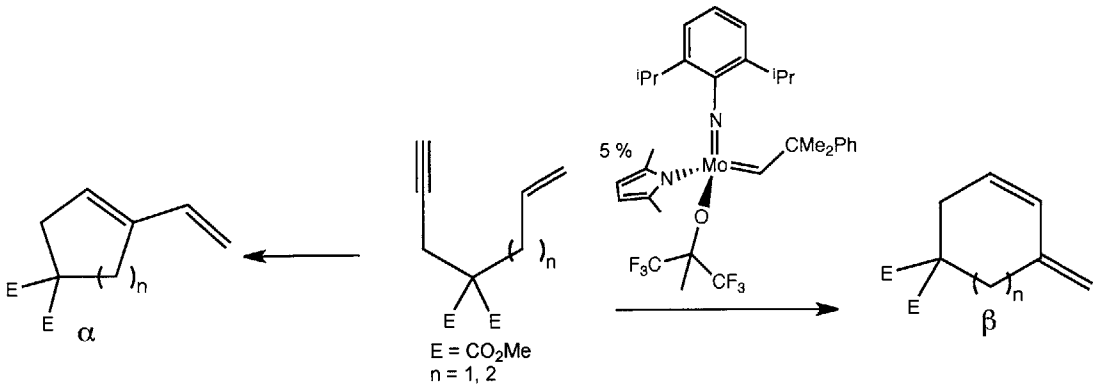

Scheme 1.5. Enyne metathesis with MAP catalysts form the β regioisomer.

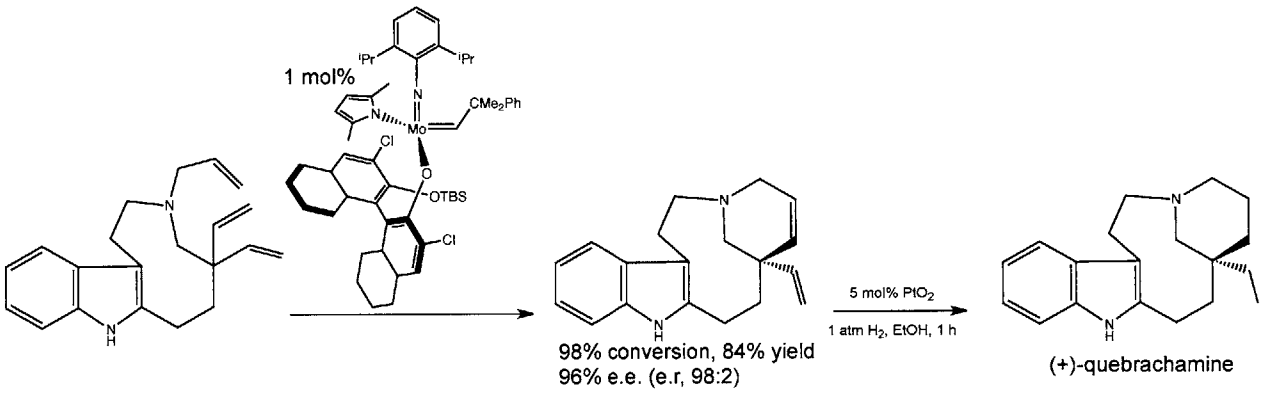

Scheme 1.6. Enantioselective synthesis of (+)-quebrachamine using a MAP catalyst.

Especially important has been the development of *Z*-selective MAP catalysts by incorporation of a sterically demanding aryloxide ligand. Typically, olefin metathesis catalysts give a thermodynamic ratio of *E* and *Z* products, which are difficult to separate. Ways to form the *E* or *Z* isomer exclusively as a kinetic product have been long sought in order to obtain higher yields of desired products and avoid difficult purification procedures. The proposed mechanism by which *Z* olefins form using MAP catalysts is shown in Scheme 1.7. The steric hindrance of the aryloxide ligand promotes the formation of an intermediate metallacyclebutane in which all substituents point away from the aryloxide. When this metallacycle opens, a *cis* olefin is formed.

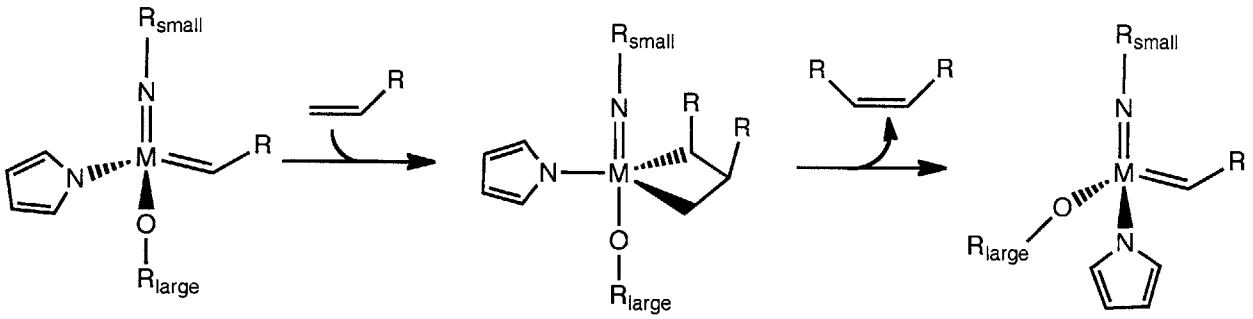

Scheme 1.7. Mechanism by which MAP catalysts form *Z* olefins

Z-selectivity was first demonstrated for ring-opening cross metathesis (ROCM). As shown in Scheme 1.8, an oxabicycle is crossed with styrene using a MAP catalyst containing an axially chiral aryloxide ligand to provide both enantio- and *Z*-selectivity.[15a] *Z*- and enantioselective ROCM has been expanded to a variety of cyclic olefins and the scope of cross partners has been expanded to include enol ethers as well as substituted styrenes.[15b] *Z*-selectivity has been achieved for the homocoupling of terminal olefins using W-based MAP catalysts with substituted terphenoxide ligands (Scheme 1.9).[16] Ethenolysis of a mixture of *E* and *Z* olefins with *Z* selective catalyst **1**, provides the unreacted *E* olefin along with terminal olefins formed from the *Z* olefin and ethylene, which can be easily separated (Scheme 1.10).[17] This process provides a convenient way to obtain pure *E* olefin. MAP catalysts have also been used for *Z*-selective ring-closing metathesis (RCM) forming important *Z* macrocyclic intermediates in natural product synthesis.[18]

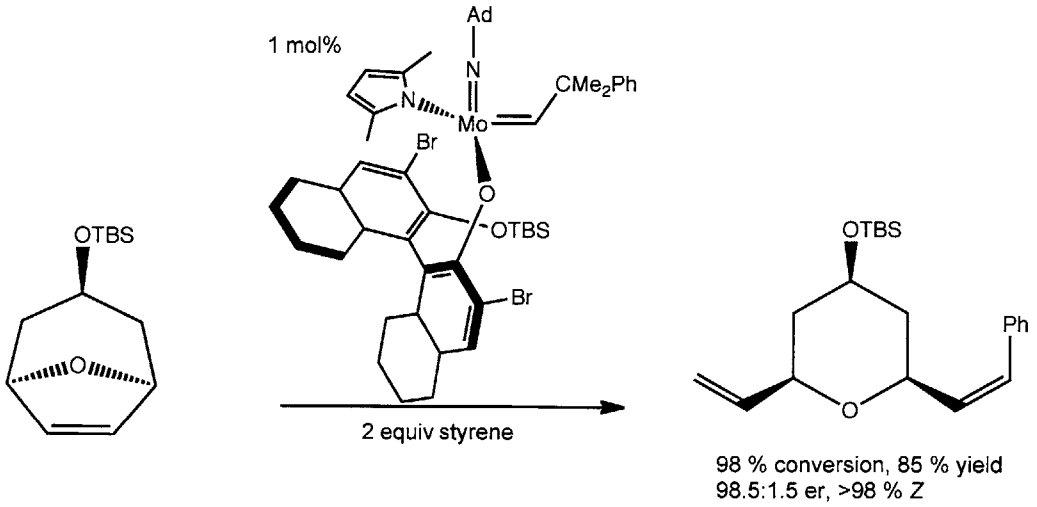

Scheme 1.8. *Z*- and enantioselective ring-opening cross metathesis using a MAP catalyst.

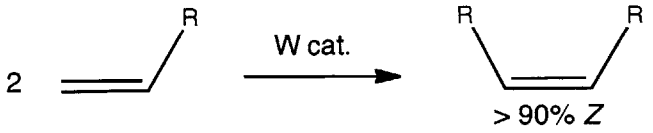

R = n-butyl, n-hexyl, CH_2Ph, CH_2SiMe_3, $(CH_2)_8CO_2Me$, $(CH_2)_7CO_2Me$, CH_2Bpin, CH_2OBn, CH_2NHTos, CH_2NhPh, CHCHMe, $CHCHMe_2$, CHCHPh, CHCH-hexyl

Scheme 1.9. *Cis* selective homocoupling of terminal olefins using MAP catalysts.

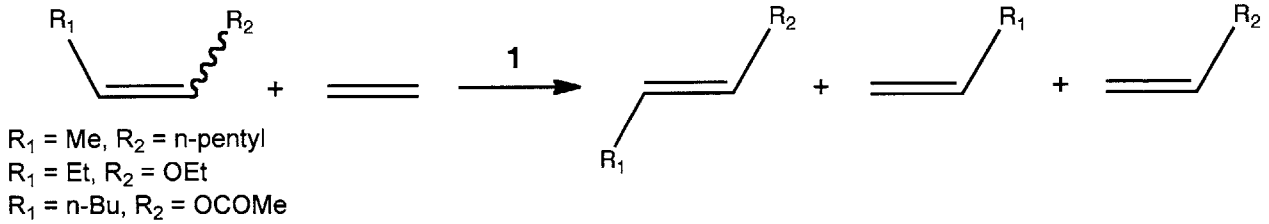

R_1 = Me, R_2 = n-pentyl
R_1 = Et, R_2 = OEt
R_1 = n-Bu, R_2 = OCOMe

E:Z mixture

Scheme 1.10. Purification of a mixture of *cis* and *trans* olefins by selective ethenolysis of the *cis* olefin.

Ring-opening metathesis polymerization (ROMP) is another area to which *Z*-selective MAP catalysts have been applied successfully. For substituted cyclic olefins, there are four possible regular structures of their polymers, illustrated in Figure 1.4 for substituted poly(norbornadienes). Bisalkoxide catalyst Mo(NAr)($CHCMe_2Ph$)(O^tBu)$_2$ (Ar = 2,6-diisopropylphenyl) gives *trans,syndiotactic* substituted poly(norbornadienes).[19] Chelating diolate catalyst, Mo(NAr')($CHCMe_2Ph$)[(±)-BINO($SiMe_2Ph$)] (Ar' = 2,6-dimethylphenyl, (±)-BINO($SiMe_2Ph$) = 3,3'-bis(dimethyl(phenyl)silyl)-[1,1'-binaphthalene]-2,2'-diolate), gives *cis,isotactic* poly(norbornadiene)s, with the tacticity controlled by the chiral ligand.[20] A new polymer structure, *cis,syndiotactic*, is observed with MAP catalyst Mo(NAd)($CHCMe_2Ph$)(pyr)(OHIPT) (Ad = 1-adamantyl, OHIPT = 2,6-bis(2,4,6-triisopropylphenyl)phenoxide) for the polymerization of substituted norbornadienes or 3-methyl-3-phenylcyclopropene.[21] Polymerization of a racemic mixture of substituted norbornenes provides a regular *cis,syndiotactic* polymer structure of alternating enantiomers.[22] The proposed mechanism by which *cis,syndiotactic* polymer forms is shown in Scheme 1.11. The large aryloxide ligand forces all substituents to be on one side of the intermediate metallacyclebutane

providing *cis* linkages, while the inversion of chirality at the metal with each forward metathesis step provides *syndiotacticity.*

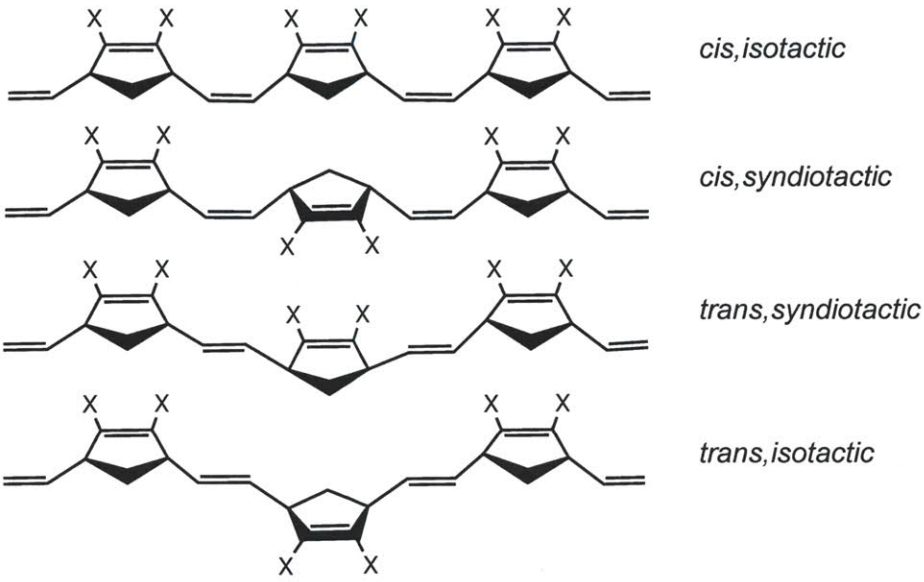

Figure 1.4. The four regular structures for poly(norbornadienes).

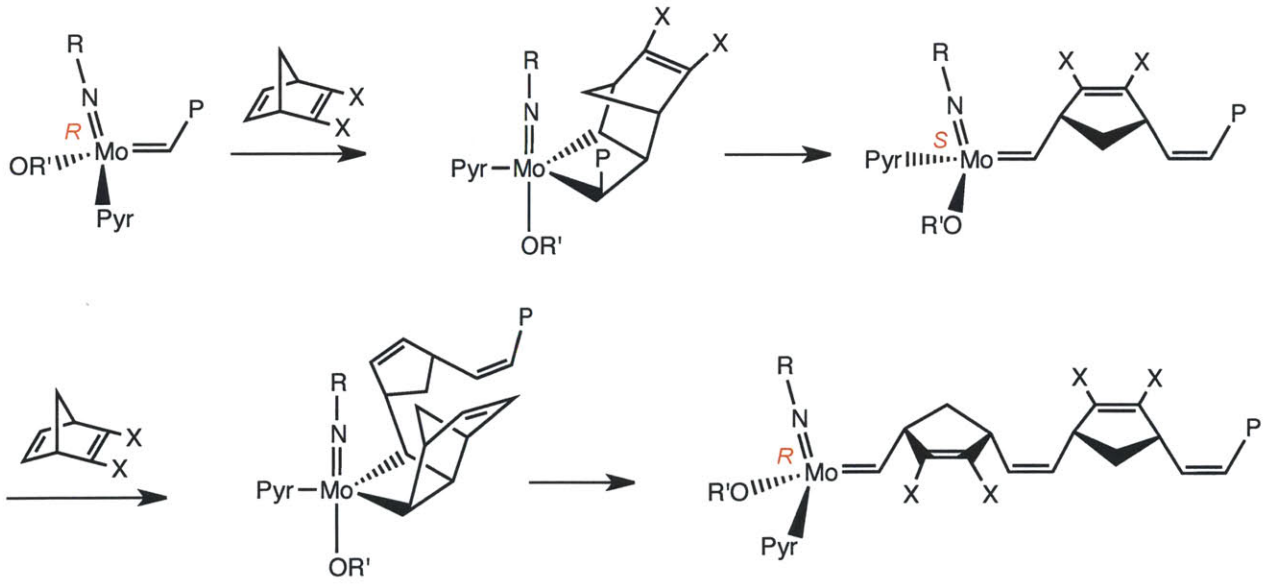

Scheme 1.11. The proposed mechanism by which *cis,syndiotactic* polymer forms using a MAP catalyst

Another important factor in olefin metathesis catalysts is created by the position of the alkylidene ligand. For Group 6 imido alkylidene metathesis catalysts, the *d*-orbital forming the

M-C π-bond is perpendicular to the imido ligand, which means the substituent on the alkylidene can point towards the imido group (*syn* alkylidene) or away from the imido group (*anti* alkylidene), as shown in Scheme 1.12. The *syn* alkylidene has an α-agostic interaction, while the *anti* alkylidene does not. Therefore, the two isomers can be distinguished by NMR spectroscopy by measurement of the αC-H coupling constants. Due to stabilization by the agostic interaction for the *syn* isomer, the equilibrium between *syn* and *anti* alkylidenes typically lies towards the *syn*, with K_{eq} values typically $>10^2$.[23] The *anti* alkylidene isomer can be generated by photolysis at low temperatures. Subsequently raising the temperature to a range where bond rotation can be observed allows rates of conversion of the *anti* alkylidene to the *syn* to be obtained.

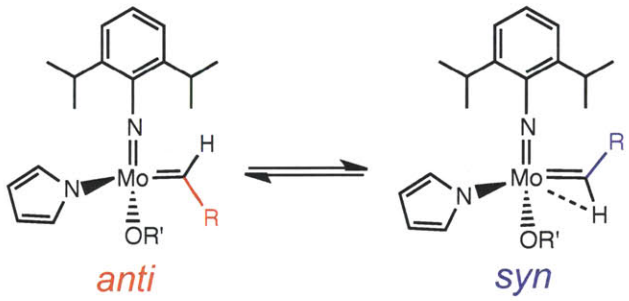

Scheme 1.12. *Anti* and *syn* isomers of metathesis catalysts.

Rotation of the alkylidene ligands in Group 6 imido alkylidene complexes has been studied computationally.[24] The alkylidene ligand is rotated by 90° in the transition state. At that point, a *p*-orbital of the αC and a *p*-orbital of N compete for the same metal d-orbital. Carbon being less electronegative than nitrogen, the metal preferentially forms a π-bond with the carbon. The loss of the triple bond character causes bending of the imido ligand at nitrogen, with bond angles calculated to be 140 – 150°, as opposed to 165 – 175° in the ground state. The ability of the metal to form a π bond with the 90° rotated alkylidene ligand causes relatively low barriers to alkylidene rotation: $\Delta G^{\ddagger}$ is measured experimentally to be 16 – 21 kcal/mol for compounds with two fluorinated alkoxide ligands,[23] and calculated to be 11 – 14 kcal/mol for dimethoxide or diethyl compounds[24]. Consistent with this theory, isolobal Re alkylidyne alkylidene complexes with a less polarizable M-C triple bond compared to the imido ligand in Mo and W imido alkylidene complexes show higher barriers to alkylidene rotation compared with analogous

Group 6 compounds (22 – 25 kcal/mol for dimethoxide or diethyl compounds calculated computationally).[24]

The recent development of *Z*-selective MAP catalysts prompted an interest in a more detailed mechanistic understanding of how MAP catalysts provide selectivity, as well as an interest in expanding the types of selective catalysts available.

Towards gaining a mechanistic understanding of *cis* selective polymerization, Chapter 2 details a mechanistic investigation into a temperature-controlled polymerization reaction. *Cis,syndiotactic* poly(3-methyl-3-phenylcyclopropene) (poly(MPCP)) is obtained at −78 °C, while atactic poly(MPCP) is obtained at ambient temperature with a Mo MAP catalyst. The *syn* initiator reacts with MPCP to form an *anti* first-insertion product at low temperatures, which continues to propagate to give *cis,syndiotactic* polymer. At higher temperatures, the *anti* alkylidenes that form initially upon reaction with MPCP rotate thermally to *syn* alkylidenes on a similar timescale as polymer propagation, giving rise to an irregular polymer structure. In this system *cis,syndiotactic* polymer is obtained through propagation of *anti* alkylidene species.

Towards the goal of developing a greater variety of selective catalysts, and gaining a better understanding of the role of steric hindrance in olefin metathesis catalysts, compounds containing a 2,6-dimesitylphenylimido (NAr*) ligand are synthesized. Chapter 3 explains the synthesis of MAP compounds containing the NAr* ligand, for which a new synthetic route was developed. Chapter 4 delves into the study of the alkylidene isomers of the NAr* MAP compounds, as well as their basic reactivity towards simple olefins, especially ethylene. Chapter 5 explores the ability of NAr* MAP compounds as catalysts for olefin metathesis.

REFERENCES

[1] Nobelprize.org. The Nobel Prize in Chemistry 2005. http://www.nobelprize.org/nobel_prizes/chemistry/laureates/2005/ (accessed May 17, 2013).

[2] Eleuterio, H. S. *J. Molec. Catal.* **1991**, *65*, 55.

[3] Banks, R. L; Bailey, G. C. *I & EC Product Research and Development* **1964**, *3* (3), 170.

[4] Hérrison, J. L.; Chauvin, Y. *Makromol. Chem.* **1971**, *141*, 161.

[5] Grubbs, R. H. *Handbook of Metathesis, Volumes 2 and 3*; Wiley-VCH, Weinheim, 2003.

[6] Schrock, R. R. *J. Am. Chem. Soc.*, 1974, 96 (21), 6796.

[7] Wengrovius, J. H.; Schrock, R. R.; Churchill, M. R.; Missert, J. R.; Youngs, W. J. *J. Am. Chem. Soc.* **1980**, *102 (13),* 4515.

[8] Hock, A. S.; Schrock, R. R.; Hoveyda, A. H. *J. Am. Chem. Soc.* **2006**, *128*, 16373.

[9] Singh, R.; Schrock, R. R.; Müller, P; Hoveyda, A. H. *J. Am. Chem. Soc.* **2007**, *129*, 12654.

[10] Poater, A.; Monfort-Solans, X.; Clot, E.; Copéret, C.; Eisenstein, O. *J. Am. Chem. Soc.* **2007**, 8207.

[11] (a) Malcolmson, S. J.; Meek, S. J.; Sattely, E. S.; Schrock, R. R.; Hoveyda, A. H. *Nature* **2008**, 933. (b) Meek, S. J.; Malcolmson, S. J.; Li, B.; Schrock, R. R.; Hoveyda, A. H. *J. Am. Chem. Soc.* **2009**, *131*, 16407.

[12] Marinescu, S. C.; Schrock, R. R.; Li, B.; Hoveyda, A. H. *J. Am. Chem. Soc.* **2009**, *131*, 58.

[13] Sattely, E. S.; Meek, S. J.; Malcolmson, S. J.; Schrock, R. R.; Hoveyda, A. H. *J. Am. Chem. Soc.* **2009**, *131*, 943.

[14] Deutsch, H. F.; Evenson, M. A.; Drescher, P.; Sparwasser, C.; Madsen, P. O. *J. Pharm. Biomed. Anal.* **1994**, *12*, 1283.

[15] (a) Ibrahem, I; Yu, M.; Schrock, R. R.; Hoveyda, A. H. *J. Am. Chem. Soc.* **2009**, *131*, 3844. (b) Yu, M.; Ibrahem, I.; Hasegawa, M.; Schrock, R. R.; Hoveyda, A. H. *J. Am. Chem. Soc.* **2012**, *134*, 2788.

[16] (a) Jiang, A. J.; Zhao, Y.; Schrock, R. R.; Hoveyda, A. H. *J. Am. Chem. Soc.* **2009**, *131*, 16630. (b) Marinescu, S. C.; Schrock, R. R.; Müller, P.; Takase, M. K.; Hoveyda, A. H. *Organometallics* **2011**, *30*, 1780. (c) Townsend, E. M.; Schrock, R. R.; Hoveyda, A. H. *J. Am. Chem. Soc.* **2012**, *134*, 11334. (d) Peryshkov, D. V.; Schrock, R. R.; Takase, M. K.; Müller, P.; Hoveyda, A. H. *J. Am. Chem. Soc.* **2011**, *133*, 20754.

[17] Marinescu, S. C.; Levine, D.; Zhao, Y.; Schrock, R. R.; Hoveyda, A. H. *J. Am. Chem. Soc.* **2011**, *133*, 11512.

[18] (a) Wang, C.; Haeffner, F.; Schrock, R. R.; Hoveyda, A. H. *Angew. Chem., Int. Ed.* **2013**, *52*, 1939. (b) Wang, C.; Yu, M.; Kyle, A. F.; Jacubec, P.; Dixon, D. J.; Schrock, R. R.; Hoveyda, A. H. *Chem. Eur. J.* **2013**, *19*, 2726.

[19] Bazan, G. C.; Khosravi, E.; Schrock, R. R.; Feast, W. J.; Gibson, V. C.; O'Regan, M. B.; Thomas, J. K.; Davis, W. M. *J. Am. Chem. Soc.* **1990**, *112*, 8378.

[20] McConville, D. H.; Wolf, J. R.; Schrock, R. R. *J. Am. Chem. Soc.* **1993**, *115*, 4413.

[21] (a) Flook, M. M.; Jiang, A. J.; Schrock, R. R.; Müller, P.; Hoveyda, A. H. *J. Am. Chem. Soc.* **2009**, *131*, 7962. (b) Flook, M. M.; Gerber, L. C. H.; Debelouchina, G. T.; Schrock, R. R. *Macromolecules* **2010**, *43*, 7515.

[22] (a) Flook, M. M.; Ng, V. W. L.; Schrock, R. R. *J. Am. Chem. Soc.* **2011**, *133*, 1784. (b) Flook, M. M.; Börner, J.; Kilyanek, S.; Gerber, L. C. H.; Schrock, R. R. *Organometallics* **2012**, *31*, 6231.

[23] (a) Oskam, J. H.; Schrock, R. R. *J. Am. Chem. Soc.* **1992**, *114*, 7588. (b) Oskam, J. H.; Schrock, R. R. *J. Am. Chem. Soc.* **1993**, *115*, 11831.

[24] Poater, A.; Monfort-Solans, X.; Clot, E.; Copéret, C.; Eisenstein, O. *Dalton Trans.* **2006**, 3077.

Chapter 2

Mechanistic Studies of a Temperature-Controlled Polymerization Reaction

Portions of this chapter have appeared in print:

Flook, M. M.; Gerber, L. C. H.; Debelouchina, G. T.; Schrock, R. R. *Z*-Selective and Syndioselective Ring-Opening Metathesis Polymerization (ROMP) Initiated by Monoaryloxidepyrrolide (MAP) Catalysts. *Macromolecules* **2010**, *43* (18), 7515 – 7522.

INTRODUCTION

Ring-opening metathesis polymerization (ROMP) is an important application of olefin metathesis. ROMP can useful for controlling polymer structures and providing narrow molecular weight distributions.[1,2,3] In order to provide the greatest utility to material scientists, controlling polymer structure is a goal in the development of new olefin metathesis catalysts for ROMP since polymer structure can have a large effect on polymer properties.[1,2] When substituted cyclic olefins are used as monomers for ROMP, four regular polymer structures are possible. The four regular structures are due to the configuration of the C=C double bonds, which can be *cis* or *trans*, and the relationship of the monomer units to one another, which can either all have the same stereochemistry (*isotactic*) or alternating stereochemistry (*syndiotactic*), as illustrated in Figure 2.1 for substituted norbornenes. *Trans,syndiotactic* poly(norbornadienes) are obtained by using $Mo(NAr)(CHCMe_2Ph)(O^tBu)_2$ (Ar = 2,6-diisopropylphenyl) as a catalyst.[4] *Cis,isotactic* poly(norbornadienes) are obtained with a chiral diolate-based catalyst, $Mo(NAr')(CHCMe_2Ph)[(\pm)\text{-}BINO(SiMe_2Ph)]_2$ (Ar' = 2,6-dimethylphenyl, (±)-BINO($SiMe_2Ph$) = 3,3'-bis(dimethyl(phenyl)silyl)-[1,1'-binaphthalene]-2,2'-diolate).[5]

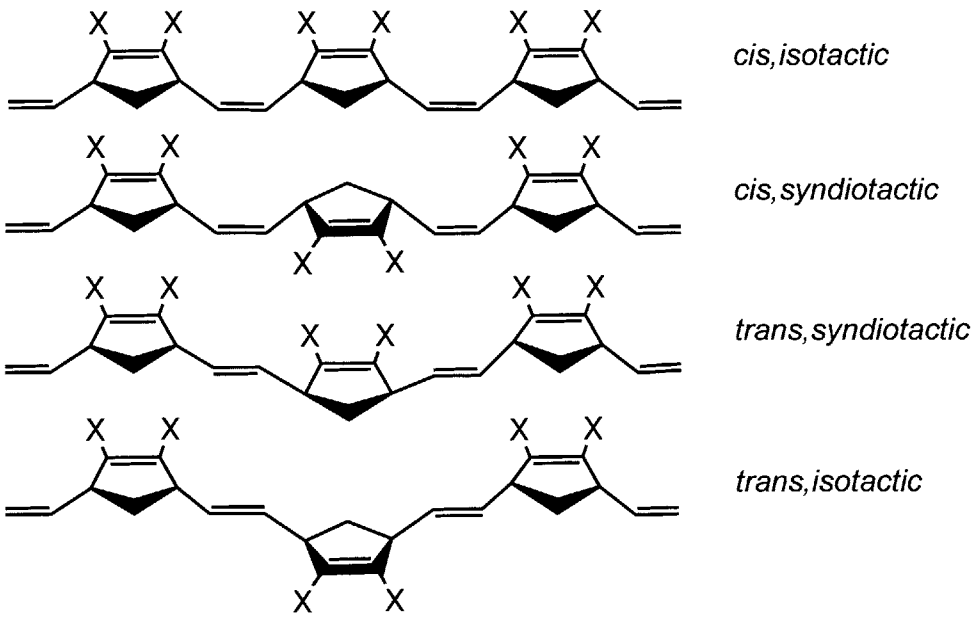

Figure 2.1. The four possible regular polymer structures for substituted poly(norbornenes).

The development of MAP catalysts led to the discovery that a new polymer structure, *cis,syndiotactic*, can be obtained in several cases. When polymerization is performed with Mo(NAd)(CHCMe$_2$Ph)(Pyr)(OHIPT) (**1**, Figure 2.2) as the catalyst, *cis,syndiotactic* polymers of 3-methyl-3-phenylcyclopropene (**MPCP**), 2,3-dicarbomethoxynorbornadiene (**DCMNBD**), 2,3-dicarbomenthoxynorbornadiene (**DCMenthNBD**), 2,3-bis(trifluoromethyl)norbornadiene (**NBDF6**) are obtained (Figure 2.3).[6, 7] Tacticity can be determined directly by NMR spectroscopy for poly(**DCMenthNBD**) that contains chiral substituents,[8] and the other polymers by analogy to poly(**DCMenthNBD**). Additionally, *cis,syndiotactic* polymers of alternating enantiomers are obtained from a racemic mixture of substituted norbornenes, using a similar catalyst to **1**: Mo(NAd)(CHCMe$_2$Ph)(pyr)(OHMT) (HMT = 2,6-dimesitylphenyl).[9]

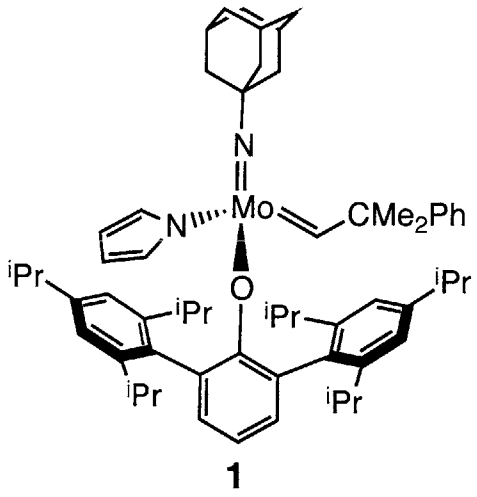

1

Figure 2.2. ***Cis,syndio*** **selective catalyst, Mo(NAd)(CHCMe$_2$Ph)(pyr)(OHIPT) (1).**

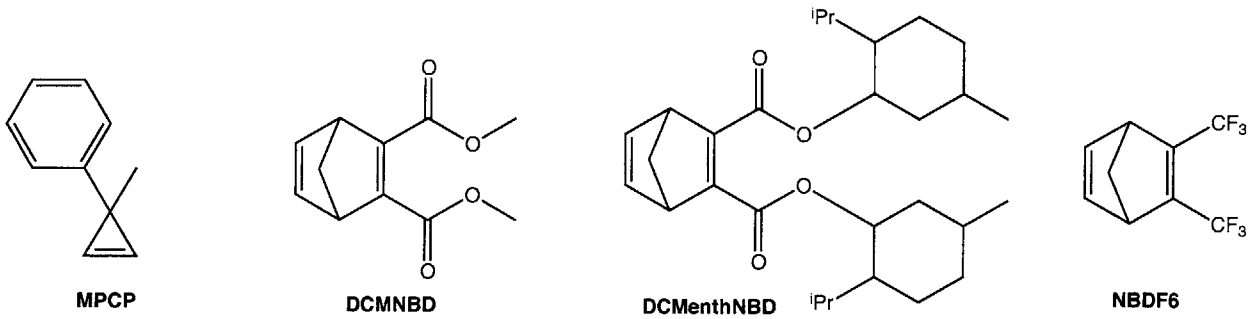

Figure 2.3. Monomers for which 1 gives *cis,syndiotactic* polymer.

The proposed mechanism by which **1** controls the formation of *cis,syndiotactic* polymer is shown in Scheme 2.1.[6] The sterically demanding aryloxide, OHIPT, forces all substituents on the metallacycle intermediates to point towards the imido ligand, which causes a *cis* double bond to be formed when the metallacycle opens. Syndiotacticity arises because of the inversion of configuration at the metal center with each metathesis step.[10]

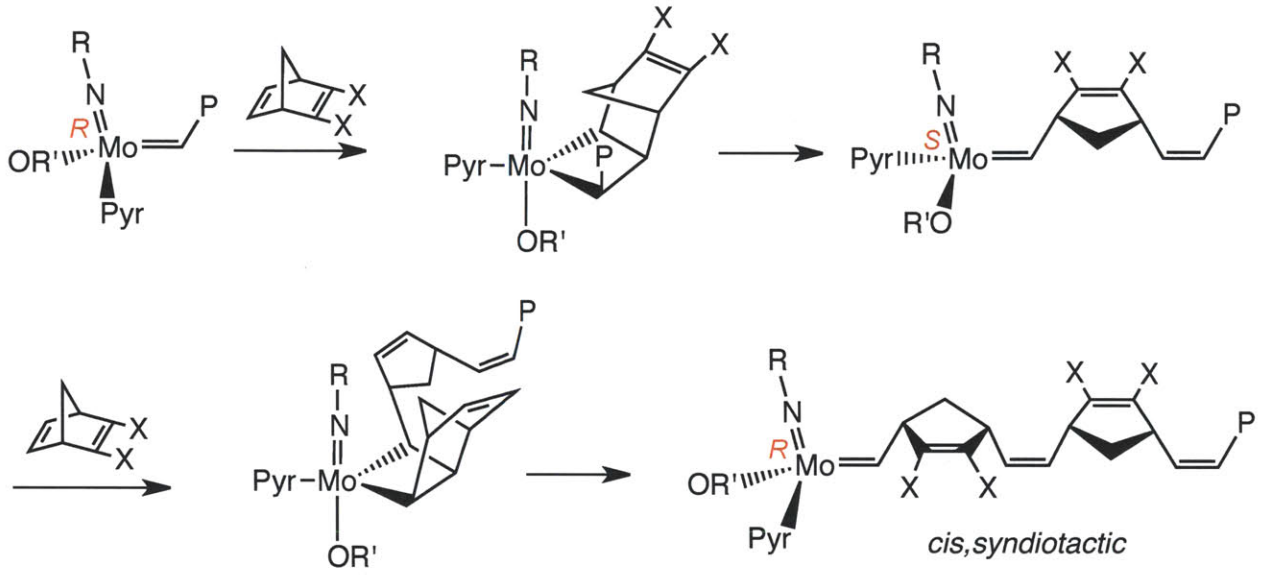

Scheme 2.1. Proposed mechanism by which 1 gives *cis,syndiotactic* polymers. R = 1-adamantyl, Pyr = pyrrolide, OR' = HIPTO, P = propagating polymer chain, X = CO_2Me, CO_2Menthyl, or CF_3

In order to better understand the formation of *cis,syndiotactic* polymer by MAP catalysts, we were interested in exploring which MAP catalysts give *cis,syndiotactic* polymer. Additionally, we wanted to perform mechanistic studies to assess the validity of the proposed mechanism shown in Scheme 2.1.

RESULTS AND DISCUSSION

I. Mechanism of ROMP of MPCP initiated by Mo(NAr)(CHCMe$_2$Ph)(Pyr)(OTPP)

A. Polymerization of MPCP by Mo(NAr)(CHCMe$_2$Ph)(Pyr)(OTPP)

When Mo(NAr)(CHCMe$_2$Ph)(Pyr)(OTPP) (**2**, Ar = 2,6-diisopropylphenyl, Pyr = pyrrolide, OTPP = 2,3,5,6-tetraphenylphenoxide, Figure 2.4) is used as a ROMP initiator for

MPCP the *cis/trans* content of the polymer depends on the reaction temperature (Figure 2.5). Regular *cis,syndiotactic* polymer is obtained when the polymerization reaction is conducted at −78 °C. As the reaction temperature is increased, in separate experiments, the regularity of the polymer structure decreases, with increasing *trans* content at higher temperatures. By 20 °C, no regular structure is observed.

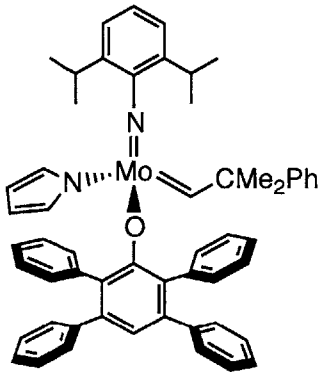

2

Figure 2.4. Structure of compound 2.

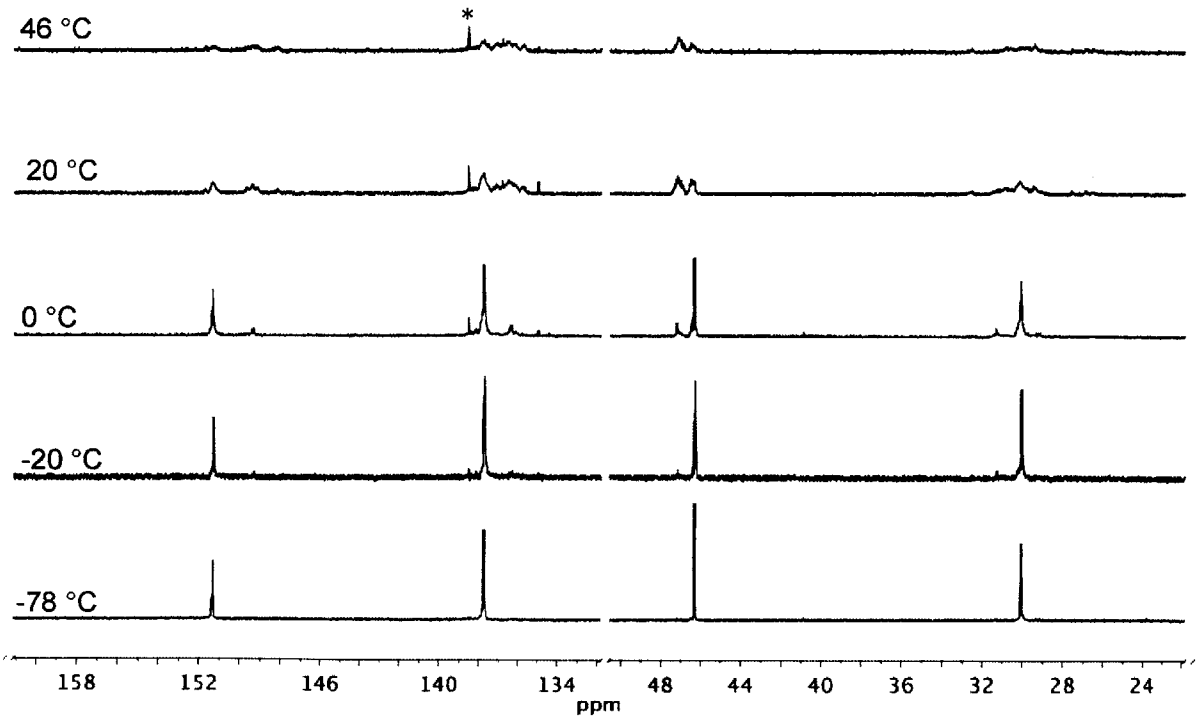

Figure 2.5. Selected regions of the $^{13}C\{^1H\}$ NMR spectra of poly(MPCP) (CD_2Cl_2, 125 MHz) synthesized at various temperatures with 2 as initiator. * = residual toluene.

A similar temperature dependence of the *cis/trans* ratio was observed for the ROMP of **DCMNBD** and **NBDF6** with various bisalkoxide initiators, with higher *trans* content at higher reaction temperatures.[11] Schrock *et al.* proposed that higher *trans* content is observed at higher temperatures due to faster interconversion of *anti* and *syn* alkylidene isomers at higher temperatures. Specifically, it was proposed that the monomer approaches consistently with its substituents pointing towards the imido ligand (ene_{syn}). Thus, if the monomer reacts with a *syn* alkylidene a *cis* double bond results, and if the monomer reacts with an *anti* alkylidene a *trans* double bond results. The higher the reaction temperature, the faster the *syn* to *anti* alkylidene rotation, which gives rise to more propagating *anti* species, and thus more *trans* linkages.

Since the factors controlling the formation of *cis,syndiotactic* poly(**MPCP**) become active during a temperature range that can be studied easily, this system seemed ideal for mechanistic studies directed towards understanding how MAP catalysts provide *cis,syndiotactic* polymer.

B. Kinetic Studies of Alkylidene Rotation for Mo(NAr)(CHCMe$_2$Ph)(Pyr)(OTPP)

It has been proposed that the rate of alkylidene rotation can affect polymer structure,[11] and it has been shown that the different alkylidene isomers can have different reactivity towards monomer.[12, 13] Therefore, study of the kinetics of alkylidene rotation is important to understanding this system.

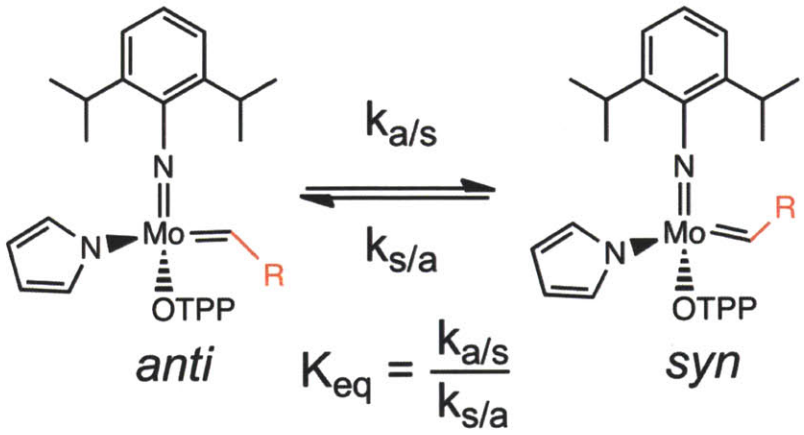

Figure 2.6. ***Anti*** **and** ***syn*** **alkylidene isomers.**

Syn and *anti* alkylidene isomers are usually characterized by the $^1J_{CH}$ for the alkylidene resonance, where 115 – 125 Hz is characteristic of *syn* alkylidenes and 145 – 155 Hz is typical for *anti* alkylidenes.[12] The lower coupling constant for the *syn* alkylidenes is due to an α-agostic interaction that is present in the *syn* alkylidene and not the *anti*. The equilibrium constant for **2** is 400 at 298 K. By exposing **2** to 366 or 350 nm light at −78 °C for 3 h, up to 23 % *anti* alkylidene is generated. The NMR spectrum observed at −70 °C in toluene-d_8 after photolysis at −78 °C shows a new resonance at 13.6 ppm with a $^1J_{CH}$ value of 143 Hz, which is downfield of *syn*-**2** (*syn*-**2**: 12.1 ppm, $^1J_{CH}$ = 122 Hz). This resonance is assigned as *anti*-**2**, which decays to *syn*-**2** upon warming. The decay back to equilibrium was followed at several temperatures over a 20 °C range. The decay fits a first-order plot, consistent with an intramolecular process. Rate constants ($k_{a/s}$ as defined in Figure 2.6) are obtained from the slope of the linear regression in accordance with $\ln(c_o/c) = kt$ (where c_o = initial concentration, c = concentration, t = time in seconds), Table 2.1.[14]

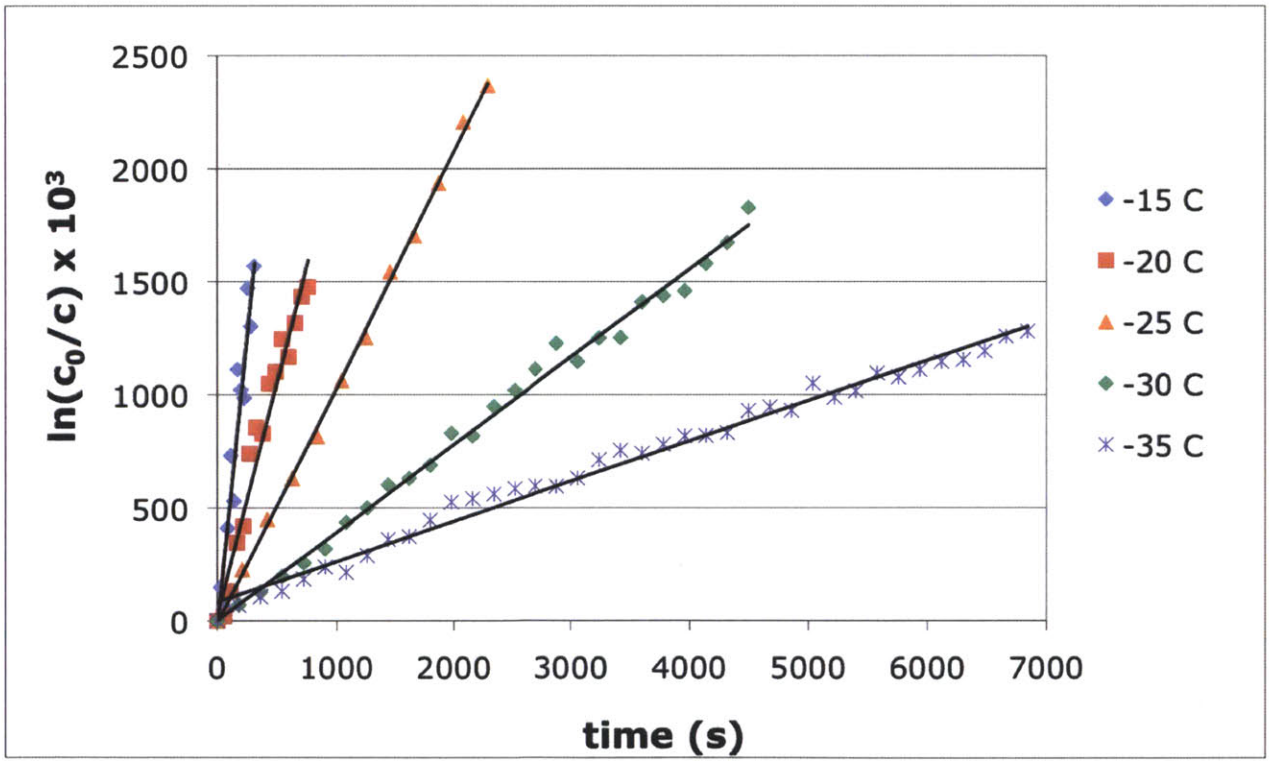

Figure 2.7. Decay of *anti*-2 to *syn*-2 at various temperatures.

Table 2.1. Rate constants ($k_{a/s}$) for 2.

T (°C)	$k_{a/s}$ (s^{-1})
−15	$(5.2 \pm 0.5) \times 10^{-3}$
−20	$(2.1 \pm 0.1) \times 10^{-3}$
−25	$(5.6 \pm 0.2) \times 10^{-4}$
−30	$(4.1 \pm 0.1) \times 10^{-4}$
−35	$(1.9 \pm 0.1) \times 10^{-4}$

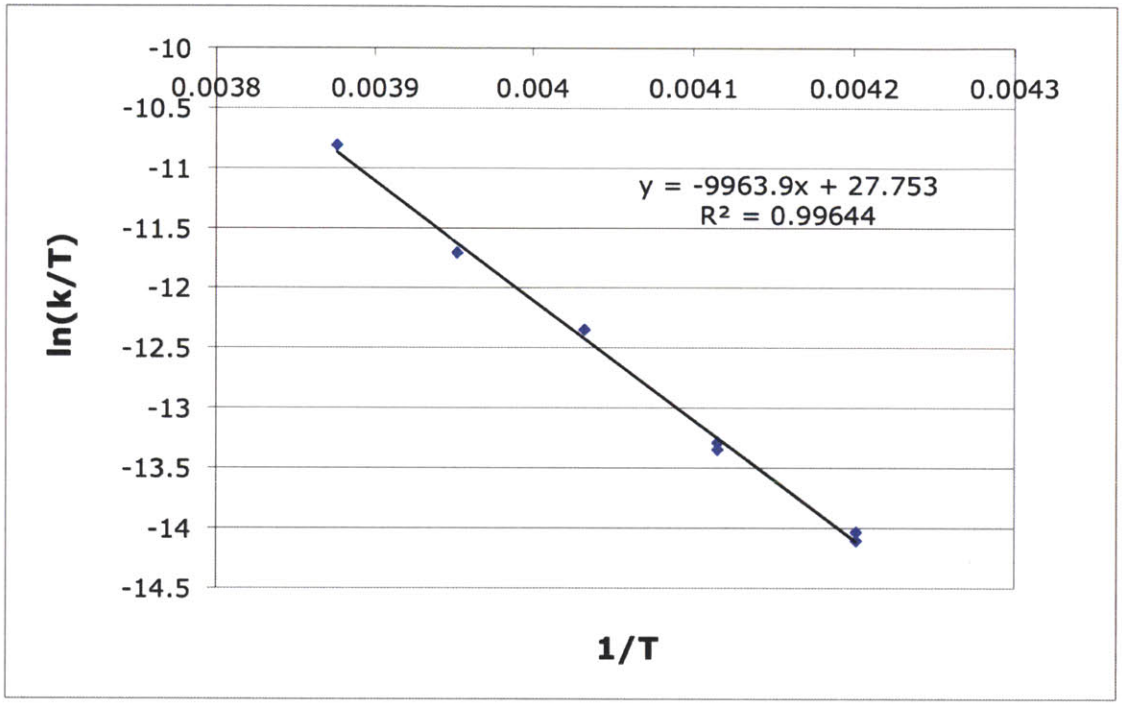

Figure 2.8. Eyring plot for 2. $\Delta H^{\ddagger} = 20 \pm 2$ kcal/mol and $\Delta S^{\ddagger} = 7 \pm 1$ eu.

Values for $\Delta H^{\ddagger}$ and $\Delta S^{\ddagger}$ were determined by constructing an Eyring plot (Figure 2.8). $\Delta H^{\ddagger} = 20 \pm 2$ kcal/mol and $\Delta S^{\ddagger} = 7 \pm 1$ eu. At 298 K, $\Delta G^{\ddagger}$ is calculated to be 2 ± 2 kcal/mol, which is consistent with the observed fast decay of *anti*-**2** to *syn*-**2** at room temperature. Extrapolation of the rate constant data to room temperature gives $k_{a/s}$ as 3 s^{-1} at 298 K. With $k_{a/s}$ in hand, $k_{s/a}$ is calculated to be 8×10^{-3} s^{-1} at 298 K.

Table 2.2. Rate and equilibrium constant data for 2 and other catalysts. R_{F3} = $CMe_2(CF_3)$, R_{F6} = $CMe(CF_3)_2$, R_{F9} = $C(CF_3)_3$, and R_{F13} = $C(CF_3)_2(CF_2CF_2CF_3)$, Ar = 2,6-diisopropylphenyl

Catalyst	$k_{a/s}$ (s^{-1}, 298 K)	K_{eq} (298 K)	$k_{s/a}$ (s^{-1}, 298 K)	Reference
Mo(NAr)($CHCMe_2Ph$)(Pyr)(OTPP) (**2**)	3	400	8×10^{-3}	This work
Mo(NAd)($CHCMe_2Ph$)(Pyr)(OHIPT) (**1**)	0.96	> 4000	$< 2.5 \times 10^{-4}$	15
Mo(NAr)($CHCMe_2Ph$)($OCMe_3$)$_2$	~ 500	1200	~ 0.4	12
Mo(NAr)($CHCMe_2Ph$)(OR_{F3})$_2$	6.8	1800	4×10^{-3}	12
Mo(NAr)($CHCMe_2Ph$)(OR_{F6})$_2$	0.10	1400	7×10^{-5}	12
Mo(NAr)($CHCMe_2Ph$)(OR_{F9})$_2$	1.5×10^{-3}	190	8×10^{-6}	12
Mo(NAr)($CHCMe_2Ph$)(OR_{F13})$_2$	3.4×10^{-3}	600	6×10^{-6}	12

The data for **2** can be compared with data previously obtained for other Mo alkylidene complexes (Table 2.2). Although K_{eq} for **2** is similar to Mo(NAr)($CHCMe_2Ph$)(OR_{F9})$_2$ and Mo(NAr)($CHCMe_2Ph$)(OR_{F13})$_2$ (where R_{F9} = $C(CF_3)_3$ and R_{F13} = $C(CF_3)_2(CF_2CF_2CF_3)$), both $k_{a/s}$ and $k_{s/a}$ are both about 3 orders of magnitude larger for **2**, indicating much faster alkylidene rotation for **2**. The rates of alkylidene interconversion are similar for **2** and Mo(NAr)($CHCMe_2Ph$)(OR_{F3})$_2$ (where R_{F3} = $CMe_2(CF_3)$). Comparing with the other MAP complex, **1**, the rates of *anti*-to-*syn* alkylidene rotation are similar, but the K_{eq} for **1** is at least an order of magnitude larger and the *syn*-to-*anti* alkylidene rotation is at least an order of magnitude slower. This difference is likely due to the greater steric hindrance of OHIPT compared to OTPP.

C. Stoichiometric reactions of MPCP with Mo(NAr)($CHCMe_2Ph$)(Pyr)(OTPP)

Reaction of **2** with one equivalent of **MPCP** (added at −78 °C followed by warming the sample to ambient temperature) results in the formation of a first-insertion product, *syn*-**2**+1_{MPCP}, that can be observed by NMR spectroscopy (Scheme 2.2). The coupling constants of the olefinic and alkylidene resonances, $^3J_{HH}$ = 16 Hz and $^1J_{CH}$ = 124 Hz, respectively, determined with ^{1}H NMR spectroscopy, indicate that the C=C bond is *trans* and that the alkylidene is in the *syn* orientation. Unfortunately, **2**+1_{MPCP} cannot be isolated as a pure compound because k_p/k_i is large enough that a small percentage of **2** propagates beyond the first-insertion product, and starting material remains even with the addition of excess monomer. Observation of a *trans* double bond is surprising, since under the same conditions for polymerization, a *cis* polymer is obtained. This result indicates that even though *cis* polymer is obtained upon propagation, a *trans* double bond forms upon initiation.

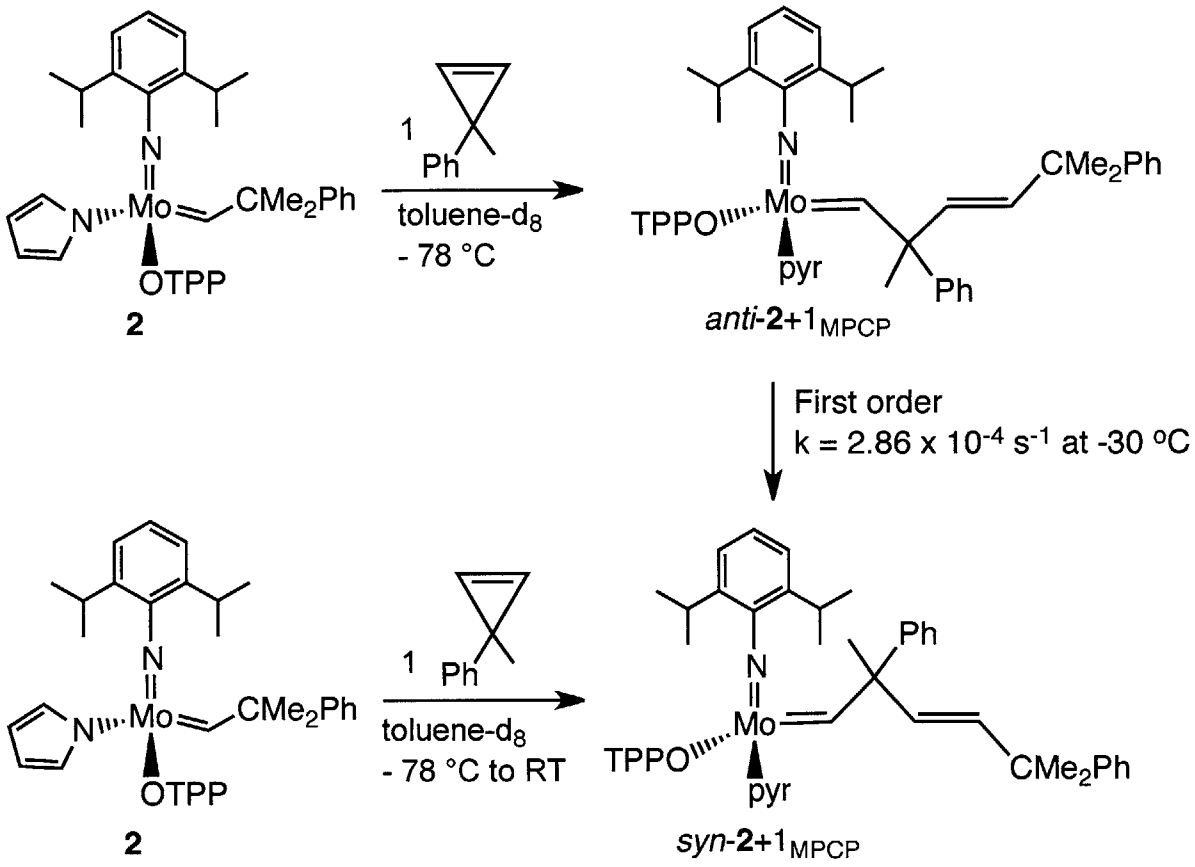

Scheme 2.2. Reaction of one molar equivalent of MPCP with 2.

When 0.8 molar equivalents of **MPCP** is added to **2** at −78 °C and the sample is not warmed, then *anti*-**2**+1_{MPCP} is observed by ^{1}H NMR spectroscopy at −70 °C. The ^{1}H NMR spectrum of *anti*-**2**+1_{MPCP} displays an alkylidene resonance at 14.1 ppm with a $^1J_{CH}$ value of 144 Hz and olefinic resonances that both have a $^3J_{HH}$ value of 16 Hz, indicating a *trans* double bond. The $^1J_{CH}$ value for the alkylidene resonance was determined by employing partially ^{13}C-labeled **MPCP**. Upon raising the temperature of the NMR spectrometer to −30 °C, *anti*-**2**+1_{MPCP} decays to *syn*-**2**+1_{MPCP} with first-order kinetics (Figure 2.9) and the rate constant was determined to be 2.9×10^{-4} s^{-1}.

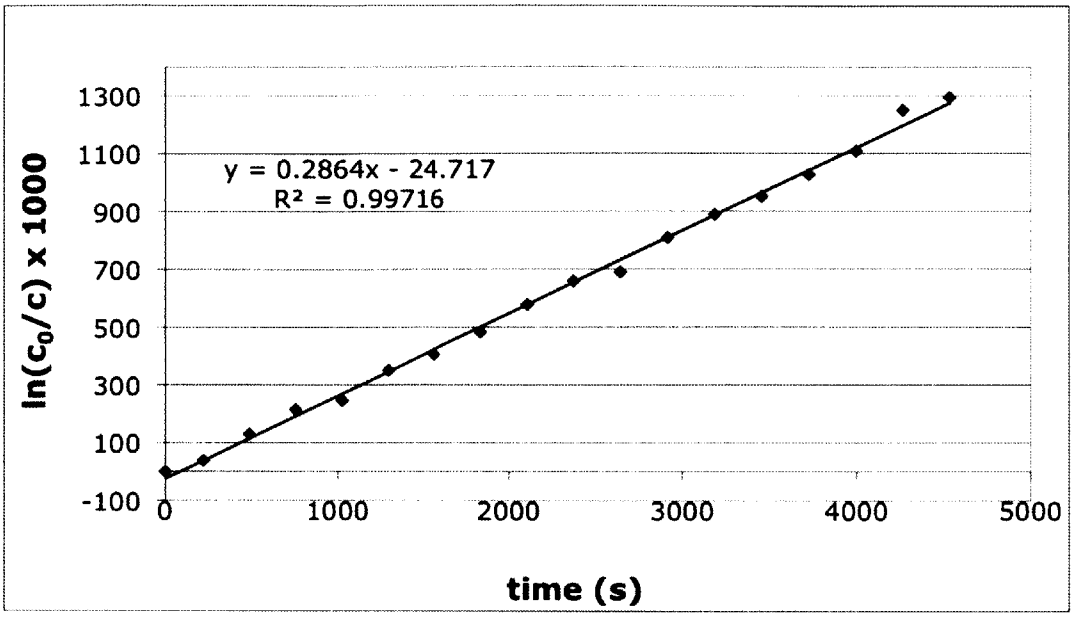

Figure 2.9. First-order plot for the conversion of *anti*-2+1$_{MPCP}$ to *syn*-2+1$_{MPCP}$ at −30 °C.

Upon addition of 3 molar equivalents of **MPCP** to **2** at −70 °C, several new resonances are observed in the *anti* region of the NMR spectrum (13.6 – 14.3 ppm), but none in the *syn* region (11.3 – 12.2 ppm). This result indicates that at −70 °C, further *anti* insertion products are formed, but *syn* species are not formed, neither directly nor through alkylidene rotation of the *anti* products. Raising the temperature of the sample to 20 °C results in disappearance of the resonances in the *anti* region and appearance of several resonances in the *syn* region. The *anti* insertion products likely decay through alkylidene rotation to the *syn* products. The olefinic region was too complicated to determine if the coupling constants indicated *cis* or *trans* double bonds in the multiple insertion products.

To determine the relative reactivity of *syn*-**2** and *anti*-**2**, a mixture of *syn*-**2** and *anti*-**2** was generated by irradiation at −78 °C. To this mixture ~0.1 equivalents of **MPCP** was added to form *anti*-**2**+1$_{MPCP}$. Figure 2.10 shows the ^{1}H NMR spectrum at −60 °C of the mixture of *syn*-**2** and *anti*-**2** generated by irradiation as well as the spectrum after the addition of ~0.1 equivalents of **MPCP**. *Anti*-**2** persists in the presence of **MPCP**, indicating that *syn*-**2** reacts with **MPCP** to form *anti*-**2**+1$_{MPCP}$. This result is contrary to previous results where 5 equivalents of **NBDF6** was added to a mixture of *syn* and *anti* Mo(NAr)(CHCMe$_2$Ph)(OR$_{F6}$); at −30 °C, only the *anti* alkylidene reacted with **NBDF6**, and not until the temperature was raised to 0 °C did the *syn* reactant or the *syn* product react with excess **NBDF6**.[12]

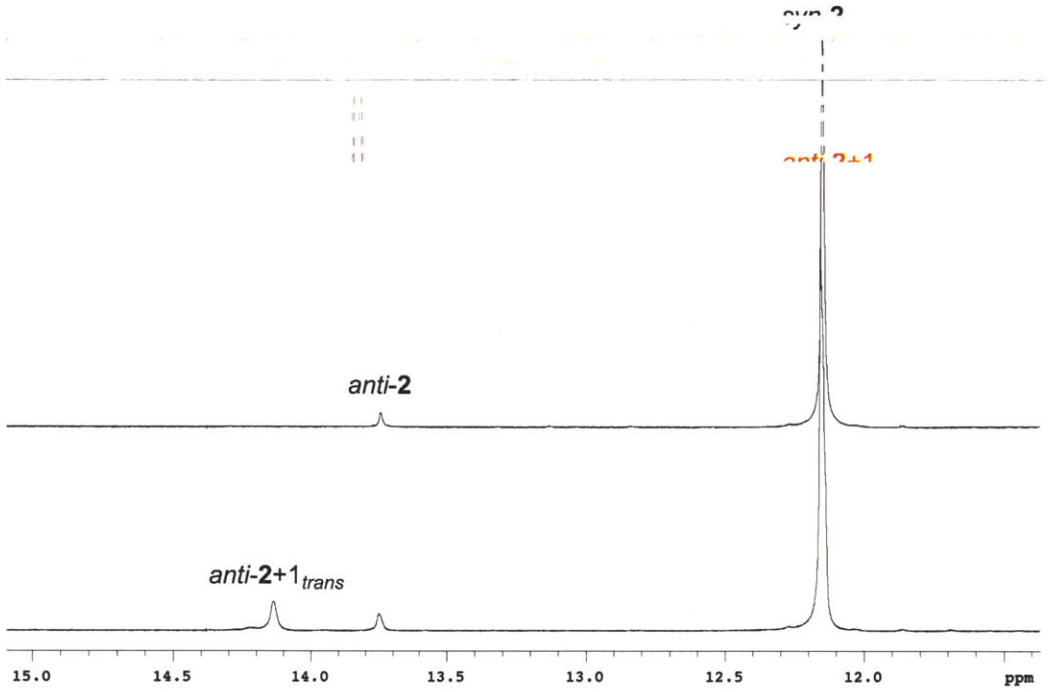

Figure 2.10. ^{1}H NMR spectra at −60 °C of (top) the mixture of *syn*-2 and *anti*-2 generated by irradiation and (bottom) after addition of ~0.1 molar equivalents of MPCP to the mixture.

D. Proposed mechanism for the formation of poly(MPCP) by Mo(NAr)(CHCMe$_2$Ph)(Pyr)(OTPP)

At low temperatures, the *anti* species are relatively stable (the calculated half-life of *anti*-**2** is 5 x 10^6 s at −78 °C). It is only upon warming the sample that their decay to *syn* species can be observed in a reasonable time frame. At −78 °C, *cis* polymer is obtained. It is proposed that polymerization initiation occurs when **MPCP** approaches *syn*-**2** in an ene$_{anti}$ fashion to form *anti*-**2**+1$_{MPCP}$. The observation of further *anti* alkylidenes and no *syn* alkylidenes indicate that propagation occurs through all *anti* alkylidenes and **MPCP** continues to approach ene$_{anti}$, as shown in Scheme 2.3.

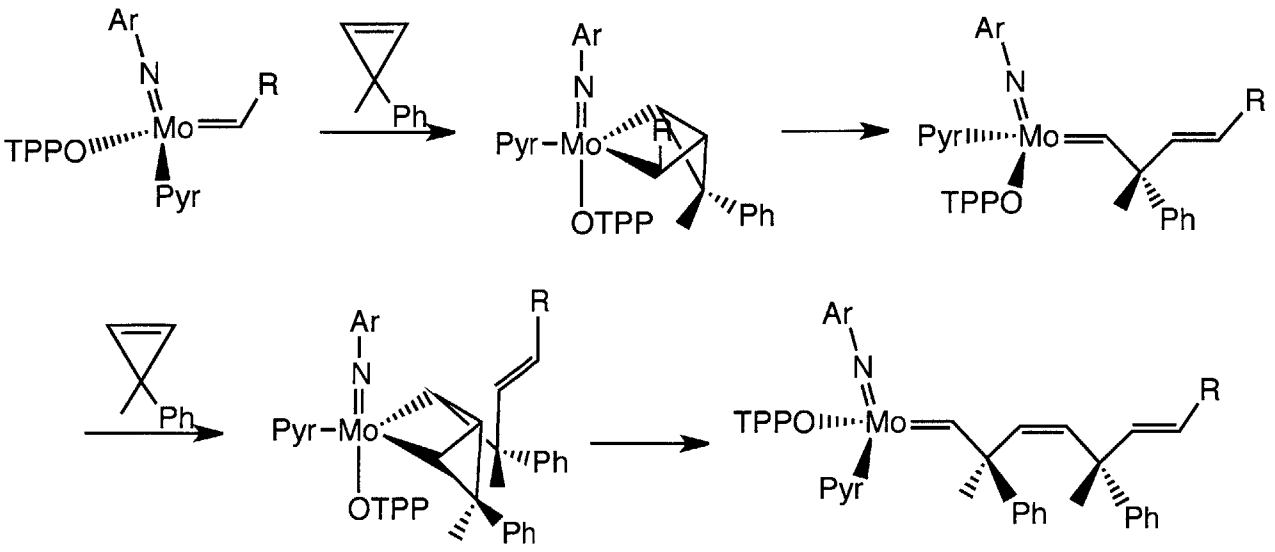

Scheme 2.3. Proposed mechanism by which Mo(NAr)(CHCMe$_2$Ph)(Pyr)(OTPP) forms *cis,syndiotactic* poly(MPCP) at −78 °C.

As the temperature is raised from −78 °C, alkylidene rotation becomes more and more facile. Once the rate of alkylidene rotation becomes competitive with the rate of polymer propagation then both *anti* and *syn* alkylidene species are available to propagate. If **MPCP** continues to approach the catalyst ene$_{anti}$, both *cis* and *trans* double bonds will be obtained depending on if a *syn* or an *anti* alkylidene reacts. The higher *trans* content in poly(**MPCP**) observed with increasing temperatures, as well as the decay of *anti* propagating species to *syn* propagating species by raising the temperature, are consistent with this proposal.

The mechanism proposed for the formation of *cis,syndiotactic* poly(**MPCP**) by **2** through all *anti* alkylidenes based on these mechanistic studies is contrary to the mechanism proposed for the formation of *cis,syndiotactic* polymers with **1** through all *syn* alkylidenes. The question arises as to whether this mechanism applies to all MAP catalysts that yield *cis,syndiotactic* polymer, or if it only applies to the system studied here. Flook *et al.*'s studies of the polymerization of **DCMNBD** with various MAP catalysts show that **1** gives >99 % *cis* content. Changing the imido substituent to 2,6-diisopropylphenyl lowers the *cis* content to 70 % and changing the aryloxide to OTPP reduces the *cis* content to 83 %.[6] This observation shows that these specific changes in the ligand set alter the system substantially.

X-ray crystal structures have previously been determined for tungsten metallacyclobutanes that contain OHIPT and OTPP ligands.[6a, 16] Space-filling diagrams of

W(NAr)(C_3H_6)(Pyr)(OHIPT) and W(NAr)(C_3H_6)(Pyr)(OTPP) are shown in Figure 2.11. Examination of these models shows the drastic difference in steric hindrance that these two terphenoxide ligands provide. HIPTO very effectively blocks the bottom side of the metallacycle; it seems unlikely that any substituent on a metallacycle would be able to point towards the OHIPT ligand. The W metallacycle containing the 2,6-diisopropylphenylimido ligand and the OTPP ligand (the ligands used in these mechanistic studies) shows a very different situation. Both sides of the metallacycle are relatively unhindered, so substitution would be possible on either side of the metallacyclebutane ring. Based on these observations, it does not seem prudent to extrapolate the mechanism observed for formation of *cis,syndiotactic* poly(**MPCP**) with **2** to other MAP catalysts.

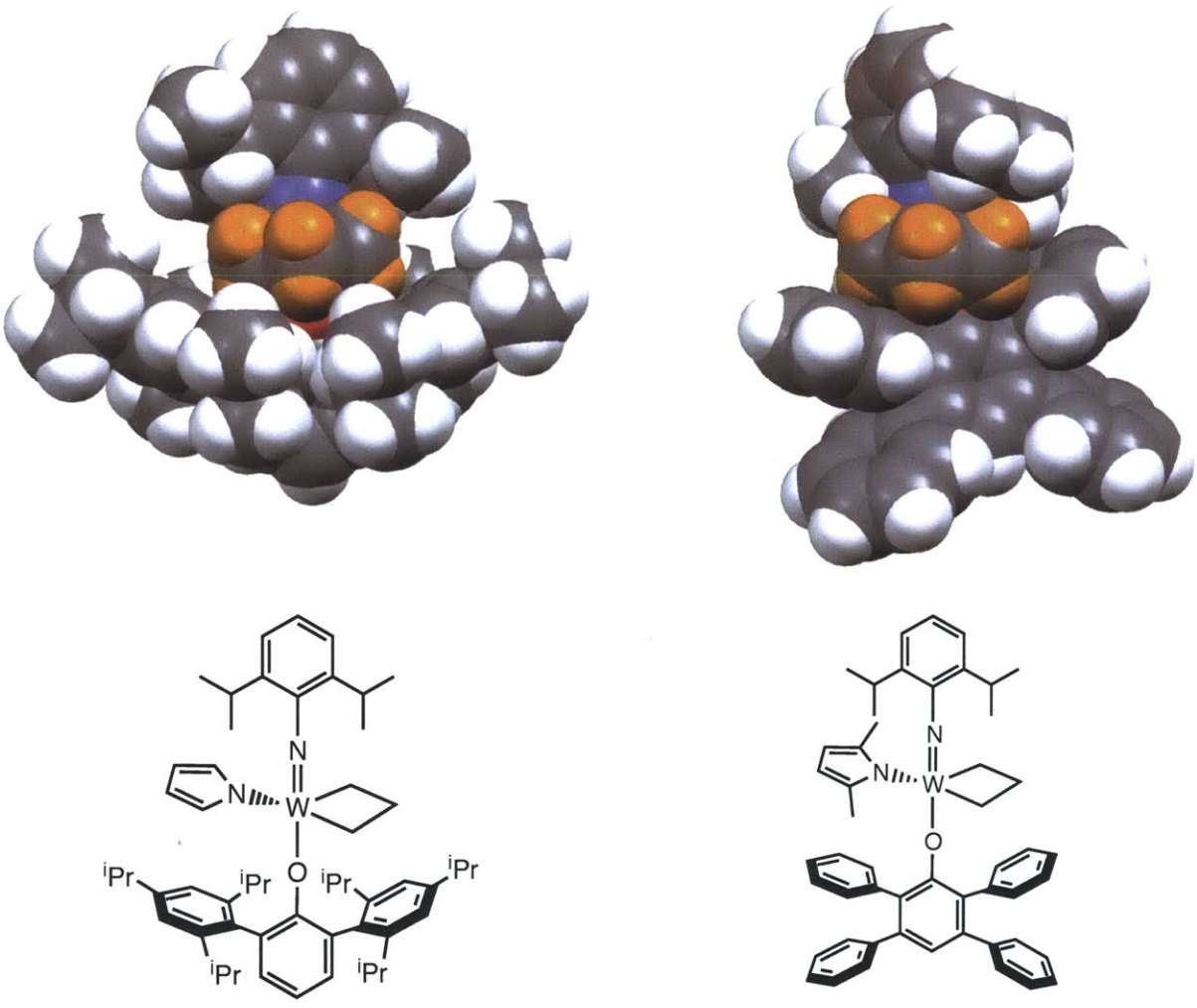

Figure 2.11. Space-filling diagrams of W(NAr)(C_3H_6)(pyr)(OHIPT) and W(NAr)(C_3H_6)(Me_2pyr)(OTPP). The hydrogen atoms in the tungstacyclobutane are orange. The imido ligands are oriented up and the aryloxide ligands are oriented down.

Additionally, when comparing **1** to **2**, the much lower K_{eq} and much faster rate of *anti*-to-*syn* alkylidene rotation indicate that the *anti* alkylidenes for **1** are much more destabilized. These factors also indicate that even though **2** polymerizes **MPCP** through all *anti* propagating species, it does not seem reasonable to extend this mechanism to polymerization initiated by **1**.

It is interesting that two MAP catalysts give *cis,syndiotactic* polymer through two different mechanisms. When catalyst **1** with the bulky ligand OHIPT is used, it is proposed that the polymer is obtained through all *syn* alkylidenes, but when catalyst **2** with the smaller OTPP ligand is used, the polymer propagates through *anti* alkylidenes after the initiation step, shown in Scheme 2.4. These studies indicate that although catalyst sterics can successfully be used to control the polymer structure, the systems are extremely sensitive to even minor changes. Although it may seem intuitive that these two similar catalysts with terphenoxide ligands would provide both *cis* polymer through a similar mechanism, the changes in stability between the alkylidene isomers has a drastic affect on how these catalysts operate. Understanding alkylidene rotation has also been key to understanding how different bisalkoxide catalysts provide different polymer structures.[11, 12]

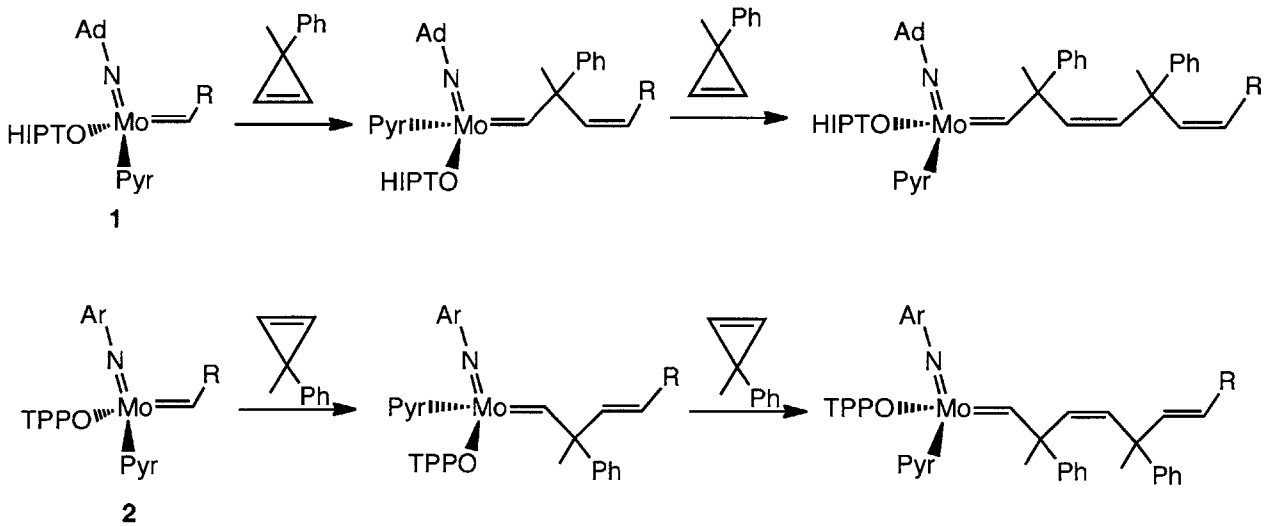

Scheme 2.4. The two distinct mechanisms by which 1 and 2 give *cis* poly(MPCP)

II. Reaction of Mo(NAr)(CHCMe$_2$Ph)(Pyr)(OTPP) with Norbornadienes

A. Polymerization of DCMNBD by Mo(NAr)(CHCMe$_2$Ph)(Pyr)(OTPP)

Reaction of **2** with 100 molar equivalents of **DCMNBD** provided no poly(**DCMNBD**) at −78 °C or −20 °C over four hours. At 0 °C the yield of polymer is low after 4 h and the polymer structure is 70 % *cis*. At room temperature and at 45 °C, polymerization is complete after 4 hours, and the polymer structure is 37 % *cis* in both cases. Ring-opening metathesis polymerization is driven by the release of ring strain. **DCMNBD** is likely to be less reactive than **MPCP** because of its lower ring strain: cyclopropene has 55 kcal/mol of ring strain while norbornadiene has 33 kcal/mol.[17] The higher *cis* content observed when polymerization is conducted at lower temperatures is consistent with **DCMNBD** reacting by a similar mechanism to **MPCP**.

Reaction of **2** with one equivalent of **DCMNBD** provided a first-insertion product (**2**+1$_{DCMNBD}$) at room temperature (Figure 2.12). All aliphatic and olefinic proton resonances in the ^{1}H NMR spectrum can be assigned by the aid of gCOSY NMR spectroscopy. The C=C bond is *trans* ($^3J_{HH}$ = 16 Hz) and the alkylidene is *anti* ($^1J_{CH}$ = 152 Hz). Monitoring **2**+1$_{DCMNBD}$ over 1 week at ambient temperature shows that **2**+1$_{DCMNBD}$ is stable as an *anti* alkylidene. After heating a sample of **2**+1$_{DCMNBD}$ overnight at 50 °C, significant decomposition to unidentifiable products is observed. Crystallization of **2**+1$_{DCMNBD}$ was unsuccessful, but it is possible that chelation of the carbonyl group stabilizes the *anti* alkylidene at room temperature. Chelation of a carbonyl group to stabilize an *anti* alkylidene has been observed for Re(C^{t}Bu)[OCMe(CF$_3$)]$_2$[CH(N(CH$_2$)$_3$)CO][18] and Mo(NAr)(Me$_2$Pyr)(OTPP)[CH(N(CH$_2$)$_3$)CO][19].

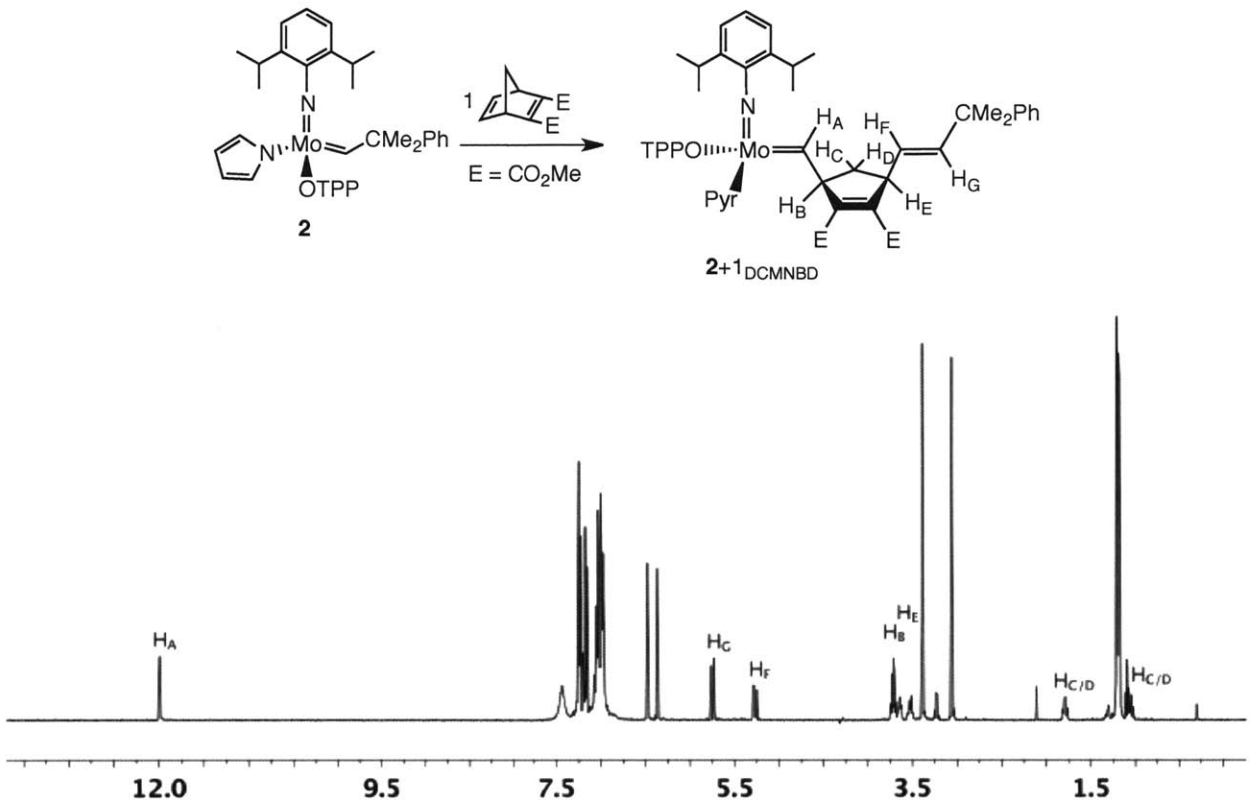

Figure 2.12. Reaction of DCMNBD with 2 and ^{1}H NMR spectrum of 2+1$_{DCMNBD}$.

When one equivalent of **DCMNBD** is added at −70 °C to a mixture of *syn*-**2** and *anti*-**2** formed by irradiation, *syn*-**2** reacts cleanly to form **2**+1$_{DCMNBD}$ while *anti*-**2** does not react with **DCMNBD**, similar to the reactivity with **MPCP**.

Reaction of **2** with two equivalents of **DCMNBD,** either sequentially (second equivalent added at ambient temperature or −78 °C) or concurrently, leads to a large mixture of products. Once the second-insertion product forms, propagation occurs rapidly, preventing the isolation or observation of a second-insertion product.

These results are consistent with the mechanism of polymerization of **DCMNBD** by **2** being similar to the polymerization of **MPCP** by **2**. The higher *trans* content in the polymer at lower temperatures and the reaction of *syn*-**2** to form *anti*-**2**+1$_{DCMNBD}$ is consistent with initiation occurring through the *syn* alkylidene to form an *anti* alkylidene, which is the species that propagates at low temperatures until bond rotation is competitive at higher temperatures.

B. Polymerization of NBDF6 by Mo(NAr)(CHCMe$_2$Ph)(Pyr)(OTPP)

Polymerizations of **NBDF6** were carried out at −78 °C, −20 °C, 0 °C, and 22 °C. Polymers synthesized at −78 °C, −20 °C and 0 °C were insoluble in dichloromethane or chloroform. The polymer synthesized at 22 °C is partially soluble in chloroform, and is 38 % *cis*.[20] Insoluble poly(**NBDF6**) is also synthesized with **1** as initiator, which gives *cis,syndiotactic* poly(**DCMenthoxyNBD**). IR, solid state NMR, and solubility studies indicate that the insoluble poly(**NBDF6**) is highly *cis,syndiotactic*.[7] Based on this theory, if the poly(**NBDF6**) synthesized with **2** at lower temperatures has more *cis,syndiotactic* linkages, as with poly(**MPCP**), then it would be expected to be insoluble in common organic solvents, as observed. IR spectra of the poly(**NBDF6**) show an absorption at 970 cm^{-1} which is stronger in the polymers synthesized at the higher temperatures than in the polymer synthesized at −78 °C. Although the *cis* or *trans* content of the polymer cannot be quantified by IR spectroscopy, the spectra are consistent with higher *trans* content at higher temperatures.

Reaction of **2** with one molar equivalent of **NBDF6** added at −78 °C produced several new alkylidene peaks. There are 2 major resonances in addition to **2**, which are assigned as the first and second-insertion products. Two resonances are observed for the olefinic protons of these species, and they are *trans* in both cases, based on the $^1J_{CH}$ values of 16 Hz. The observation of the *trans* terminal olefins in the first- and second-insertion products despite obtaining a *cis* polymer structure is consistent with the polymerization of **NBDF6** by **2** operating in a similar mechanism to polymerization of **MPCP** by **2**.

CONCLUSIONS

Mo(NAr)(CHCMe$_2$Ph)(Pyr)(OTPP) provides *cis,syndiotactic* polymer when the reaction is conducted at −78 °C, and higher *trans* content at when the reaction is conducted at higher temperatures. Mechanistic studies indicate that the *syn* initiator reacts with monomer to give an *anti* first-insertion product that then continues to propagate through *anti* alkylidenes. At higher temperatures, *anti*-to-*syn* bond rotation becomes competitive with polymerization to give more *trans* content. This mechanism of polymerization is likely distinct from the mechanism by which Mo(NAd)(CHCMe$_2$Ph)(Pyr)(OHIPT) provides *cis,syndiotactic* polymer, which is proposed to propagate through all *syn* alkylidenes.

These studies show that alkylidene bond rotation is extremely important in the determination of the structure of the product during olefin metathesis. Controlling alkylidene rotation is key to controlling selectivity in olefin metathesis. In the system studied here, which propagates through all *anti* alkylidenes, the alkylidene rotation is controlled by the reaction temperature. The low temperatures render the *anti* alkylidenes stable and allow *cis,syndiotactic* polymer to form. Control of alkylidene rotation in Mo(NAd)($CHCMe_2Ph$)(Pyr)(OHIPT) is achieved by steric control: the sterically demanding terphenoxide ligand destabilizes the *anti* alkylidene even further and allows for propagation through all *syn* alkylidenes. Interestingly, these two different mechanisms of control of the rate of alkylidene rotation can be utilized to give *cis,syndiotactic* polymer through two different mechanisms.

EXPERIMENTAL

General Considerations

All air-sensitive manipulations were performed under nitrogen atmosphere in a drybox or an air-free dual-manifold Schlenk line. All glassware was oven-dried and allowed to cool under vacuum before use. NMR spectra were obtained on Varian 500, Bruker 400 MHz, or Bruker 600 MHz spectrometers, reported in δ (parts per million) relative to tetramethylsilane, and referenced directly to a tetramethylsilane internal standard or to residual $^{1}H/^{13}C$ signals of the deuterated solvent (^{1}H (δ): benzene 7.16, chloroform 7.27, methylene chloride 5.32, toluene 2.09. ^{13}C (δ): benzene 128.39, chloroform 77.23, methylene chloride 54.00, toluene 20.40). Diethyl ether, toluene, tetrahydrofuran, pentane, and dichloromethane were sparged with nitrogen and passed through activated alumina. All solvents were stored over 4 Å molecular sieves. Benzaldehyde was distilled and stored under nitrogen. All other reagents were used as received. HOTPP,[21] 3-Methyl-3-Phenyl-cyclopropene (**MPCP**),[22] and Mo(NAr)($CHCMe_2Ph$)$(Pyr)_2$[23] were prepared according to literature procedures.

Mo(NAr)(Pyr)(OTPP)($CHCMe_2Ph$) (2). Mo(NAr)($CHCMe_2Ph$)$(Pyr)_2$ (0.489 g, 0.913 mmol) was dissolved in 8 mL of diethyl ether in a scintillation vial. TPPOH (0.364 g, 0.913 mmol) was added as a solid and a yellow precipitate formed. The mixture was stirred for 1.5 h and the yellow solid was collected on a frit and dried *in vacuo*. The filtrate was concentrated and chilled

to –25° C overnight and a second crop was collected; total yield 0.668 g (84 %). ^{1}H NMR (benzene-d_6) δ 11.96 (s, 1H, $^1J_{CH}$ = 125 Hz, MoC*H*), 7.32 – 6.89 (overlapping, Ar-*H*), 6.84 (t, J_{HH} = 7.5 Hz, 2H, Ar-H_{para}), 6.44 (d, J_{HH} = 2Hz, 2H, pyr), 6.42 (d, J_{HH} = 2Hz, 2H, pyr), 3.25 (septet, J_{HH} = 7Hz, 2H, C*H*Me$_2$), 1.48 (s, 3H, C(C*H*$_3$)$_2$(Ph)), 1.31 (s, 3H, C(C*H*$_3$)$_2$(Ph)), 1.06 (d, J_{HH} = 7Hz, 6H, CH(C*H*$_3$)$_2$), 1.02 (d, J_{HH} = 7Hz, 6H, CH(C*H*$_3$)$_2$); ^{13}C{^{1}H} NMR (benzene-d_6) δ 291.6, 159.4, 153.8, 148.5, 146.9, 142.7, 142.2, 138.3, 133.0, 131.9, 131.3, 130.4, 129.1, 128.9, 128.4, 127.5, 127.1, 126.9, 126.8, 126.6, 123.5, 110.6, 55.6, 31.8, 30.9, 29.1, 24.9, 23.7. Anal. Calcd for $C_{56}H_{54}MoN_2O$: C, 77.38; H, 6.27; N, 3.20. Found: C, 77.58; H, 6.28; N, 3.23.

Representative polymerization reaction. This procedure is representative for ROMP reactions with other monomers and other temperatures. Mo(NAr)(CHCMe$_2$Ph)(Pyr)(OTPP) (6.7 mg, 7.7 μmol) was dissolved in 2 mL toluene and cooled to 0° C. A solution of MPCP (0.1 g, 0.78 mmol) in 0.3 mL toluene was added by syringe. The reaction was stirred 2 hr at 0° C and then 0.1 mL benzaldehyde was added and stirred 1 hr. Solution was concentrated *in vacuo*. MeOH was added and a white precipitate formed immediately. The solid was collected on a frit, washed with MeOH, and dried *in vacuo*.

Kinetic Studies of Conversion of *anti*-2 to *syn*-2. Samples were irradiated at 350 nm at −78 °C for 3 h in a Rayonet RPR-200 Photoreactor in teflon-stoppered NMR tubes. The samples were kept at −78 °C until being placed in the preequilibrated 500-MHz ^{1}H NMR probe. Data were collected over at least 2 half-lives by observing the disappearance of the *anti*-**2** resonance with respect to an internal standard (anthracene, poly(dimethylsiloxane), or tetramethylsilane).

Observation of Mo(NAr)[CHC(Me)(Ph)(CH)$_2$CMe$_2$Ph](OTPP)(Pyr) (*syn*-2+1$_{MPCP}$). Mo(NAr)(CHCMe$_2$Ph)(OTPP)(pyr) (0.188 g, 0.217 mmol) was dissolved in 4 mL toluene in a 10 mL Schlenk tube and the solution was cooled to −78 °C. A solution of **MPCP** (27.7 μL, 0.217 mmol) in 0.5 mL toluene was added. The yellow solution turned dark orange. The reaction was stirred 15 min at −78 °C and 2 h at room temperature. The volatiles were removed *in vacuo*: ^{1}H NMR (benzene-d_6, 293 K) δ 12.14 (s, 1H, MoC*H*), 7.35 – 6.72 (overlapping Ar-H, pyr), 6.55 (t, J_{HH} = 2Hz, 2H, pyr), 5.65 (d, J_{HH} = 16 Hz, 1H, olefinic C*H*), 5.43 (d, J_{HH} = 16 Hz, 1H, olefinic C*H*), 3.25 (septet, J_{HH} = 6.5 Hz, C*H*Me$_2$), 1.89 (s, 3H, MoCHC(C*H*$_3$)), 1.31 (d, J_{HH} = 12 Hz, 6H,

terminal C(Ph)(CH_3)$_2$), 0.99 (d, J_{HH} = 6.5 Hz, 6H, CHC(CH_3)$_2$), 0.96 (d, J_{HH} = 6.5 Hz, 6H, CHC(CH_3)$_2$).

Observation of Mo(NAr)[^{13}CHC(Me)(Ph)^{13}CH$_2$CH$_2$CMe$_2$Ph](OTPP)(Pyr) (*syn*-2+1$_{MPCP}$). A solution of MPCP (66 % ^{13}C labeled at one olefinic position) in 0.3 mL toluene was added to a −78 °C solution of **2** in 2 mL of toluene. The mixture was stirred 1.5 h at −78 °C and then 1 h at RT. The volatiles were removed *in vacuo*. ^{1}H NMR (benzene-d_6, 293 K) δ 12.14 (1/3 d, $^1J_{CH}$ = 124 Hz, Mo=^{13}CH), 5.43 (1/3 dd, $^1J_{CH}$ = 154 Hz, $^3J_{HH}$ = 16 Hz, ^{13}CH=CH), all other resonances are the same as in the unlabeled species; ^{13}C NMR (benzene-d_6, 293 K) δ 290.4 (d, $^1J_{CH}$ = 125 Hz, Mo=^{13}CH), 133.2 (d, $^1J_{CH}$ = 154 Hz, ^{13}CH=CH).

Observation of *anti*-(Mo)(NAr)(CHC(Me)(Ph)(CH)$_2$CMe$_2$Ph)(OTPP)(Pyr) (*anti*-2+1$_{MPCP}$). An NMR sample of **2** (20.5 mg, 22.6 μmol) in toluene-d$_8$ in a screw-capped NMR tube with a septum top was cooled to −70 °C in the NMR probe. ^{13}C-labeled (33 %) MPCP (3 μL, 23 μmol) was added by syringe, the tube inverted once to mix and returned to the probe. ^{1}H NMR (toluene-d_8, characteristic resonances, 203 K) δ 14.15 ($^1J_{CH}$ = 144 Hz, Mo=CH), 6.29 (d, $^3J_{HH}$ = 16 Hz, CH=CH), 5.79 (d, $^3J_{HH}$ = 16 Hz, CH=CH).

Observation of Labeled *syn*-2+1$_{MPCP}$ at 203 K generated from *anti*-2+1$_{MPCP}$. After observation of *anti*-**2**+1$_{MPCP}$ by ^{1}H NMR spectroscopy (see above), the sample was removed from the probe and allowed to warm to room temperature before being reinserted into the cold probe: ^{1}H NMR (toluene-d_8, characteristic peaks, 203 K) δ 12.55 ($^1J_{CH}$ = 124 Hz, Mo=C*H*), 5.66 (d, $^3J_{HH}$ = 16 Hz, CH=CH), 5.38 (d, $^3J_{HH}$ = 16 Hz, CH=CH).

Observation of 2+1$_{DCMNBD}$. DCMNBD (37.3 mg, 0.179 mmol) was added as a solution in 1 mL toluene to a stirring solution of **2** (155.4 mg, 0.179 mmol) in 4 mL toluene. The solution immediately changed from yellow to wine red. The reaction was stirred for 3 h at RT and the volatiles removed *in vacuo*. The red oil was triturated with pentane to provide a red powder. ^{1}H NMR (benzene-d_6, 293 K, protons labeled in Figure 2.12) δ 11.99 (d, 3JHH = 3 Hz, $^1J_{CH}$ = 152 Hz, 1H, Mo=CH), 7.44 (br s, Ar-H), 7.26 – 6.97 (overlapping Ar-H), 6.48 (t, J_{HH} = 2Hz, 2H, pyr-H), 6.37 (t, J_{HH} = 2 Hz, 2H, pyr-H), 5.75 (d, 1H, J_{HH} = 16 Hz, H_G), 5.27 (dd, J_{HH} = 16 Hz, J_{HH} =

9 Hz, 1H, H_F), 3.70 (septet, J_{HH} = 7 Hz, 2H, C*H*Me$_2$) 3.64 (m, 1H, H_B), 3.52 (m, 1H, H_E), 3.39 (s, 3H, CO_2CH_3), 3.06 (s, 3H, CO_2CH_3), 1.79 (m, 1H, H_C), 1.21 (s, 6H, C*Me*$_2$Ph), 1.19 (dd, J_{HH} = 3Hz, J_{HH} = 7 Hz, 12H, CH(C*H*$_3$)$_2$), 1.06 (m, 1H, H_D); $^{13}C\{^1H\}$ NMR (benzene-d^6, 293 K): δ 280.2 (Mo=C), 171.1, 165.9, 161.8, 152.0, 151.4, 150.6, 150.5, 149.0, 144.5, 143.2, 142.5, 142.3, 142.1, 139.3, 136.8, 135.6, 132.9, 131.9, 130.7, 129.7, 129.3, 127.8, 127.1, 126.6, 126.0, 125.4, 125.2, 124.7, 123.5, 109.0, 55.4, 55.0, 52.0, 51.5, 40.9, 40.6, 29.1, 29.0, 28.8, 25.1, 24.8.

Observation of First- and Second-Insertion Products of NBDF6.

Mo(NAr)(CHCMe$_2$Ph)(Pyr)(OTPP) (**2**) (20 mg, 0.023 mmol) was dissolved in 2 mL of toluene and cooled to −78 °C. **NBDF6** (between 0.5 and 2 equivalents) were added as a solution in 0.3 mL of toluene. The mixtures were stirred for 30 min at −78 °C, warmed to 22 °C, and stirred for 2 h. The volatiles were removed *in vacuo* and ^{1}H NMR was used to assign the first and second-insertion products based on the relative ratios. First-insertion product, ^{1}H NMR (benzene-d_6, 294 K) δ 12.06 (d, J_{HH} = 8 Hz, 1H, Mo=CH), 5.61 (d, J_{HH} = 16 Hz, 1H, C*H*CMe$_2$Ph), 5.24 (dd, J_{HH} = 16 Hz, J_{HH} = 9 Hz, 1H, C*H*CHCMe$_2$Ph); Second-insertion product, ^{1}H NMR (benzene-d_6, 294 K) δ 11.81 (d, J_{HH} = 8 Hz, Mo=CH), 5.66 (d, J_{HH} = 16 Hz, C*H*CMe$_2$Ph), 5.31 (dd, J_{HH} = 16 Hz, J_{HH} = 9 Hz, C*H*CHCMe$_2$Ph).

REFERENCES

[1] Khosravi, E.; Szymanska-Buzar, T. *Ring Opening Metathesis Polymerisation and Related Chemistry*; Kluwer Academic Publishers: Dordrecht, 2002.

[2] Buchmeiser, M. R. *Chem. Rev.* **2000**, *100*, 1565.

[3] Schrock, R. R. *Acc. Chem. Res.* **1990**, *23*, 158.

[4] Bazan, G. C.; Khosravi, E.; Schrock, R. R.; Feast, W. J.; Gibson, V. C.; O'Regan, M. B.; Thomas, J. K.; Davis, W. M. *J. Am. Chem. Soc.* **1990**, *112*, 8378.

[5] McConville, D. H.; Wolf, J. R.; Schrock, R. R. *J. Am. Chem. Soc.* **1993**, *115*, 4413.

[6] Flook, M. M.; Jiang, A. J.; Schrock, R. R.; Müller, P.; Hoveyda, A. H. *J. Am. Chem. Soc.* **2009**, *131*, 7962.

[7] Flook, M. M.; Gerber, L. C. H.; Debelouchina, G. T.; Schrock, R. R. *Macromolecules* **2010**, *43*, 7515.

[8] O'Dell, R.; McConville, D. H.; Hofmeister, G. E.; Schrock, R. R. *J. Am. Chem. Soc.* **1994**, *116*, 3414.

[9] (a) Flook, M. M.; Ng, V. W. L.; Schrock, R. R. *J. Am. Chem. Soc.* **2011**, *133*, 1784. (b) Flook, M. M.; Börner, J.; Kilyanek, S.; Gerber, L. C. H.; Schrock, R. R. *Organometallics* **2012**, *31*, 6231.

[10] (a) Marinescu, S. C.; Schrock, R. R.; Li, B.; Hoveyda, A. H. *J. Am. Chem. Soc.* **2009**, *131*, 58. (b) Poater, A.; Monfort-Solans, X.; Clot, E.; Copéret, C.; Eisenstein, O. *J. Am. Chem. Soc.* **2007**, 8207.

[11] Schrock, R. R.; Lee, J.-K.; O'Dell, R.; Oskam, J. H. *Macromolecules* **1995**, *28*, 5933.

[12] (a) Oskam, J. H.; Schrock, R. R. *J. Am. Chem. Soc.* ***1992***, *114*, 7588. (b) Oskam, J. H.; Schrock, R. R. *J. Am. Chem. Soc.* **1993**, *115*, 11831.

[13] Feast, W. J.; Gibson, V. C.; Ivin, K. J.; Kenwright, A. M.; Khosravi, E. *J. Mol. Cat.* **1994**, *90*, 87.

[14] Moore, J. W.; Pearson, R. G. *Kinetics and Mechanism*; John Wiley & Sons: New York, 1981.

[15] Flook, M. M.; Börner, J.; Kilyanek, S. M.; Gerber, L. C. H.; Schrock, R. R. *Organometallics*, **2012**, *31*, 6231.

[16] Jiang, A. J.; Simpson, J. H.; Müller, P.; Schrock, R. R. *J. Am. Chem. Soc.* **2009**, *131*, 7770.

[17] Khoury, P. R.; Goddard, J. D.; Tam, W. *Tetrahedron* **2004**, *60*, 8103.

[18] Toreki, R.; Vaughan, G. A.; Schrock, R. R.; Davis, W. M. *J. Am. Chem. Soc.* **1993**, *115*, 127.

[19] Townsend, E. M., Kilyanek, S. M.; Schrock, R. R.; Müller, P.; Smith, S. J.; Hoveyda, A. H. *Organometallics* **2013**, ASAP August 7, 2013.

[20] ^{13}C NMR resonances assigned for *cis* and *trans* poly(**NBDF6**) in Feast, W. J.; Gibson, V. C.; Marshall, E. L. *J. Chem. Soc., Chem. Commun.* **1992**, 1157.

[21] Yates, P.; Hyre, J. E. *J. Org. Chem.* **1962**, *27*, 4101.

[22] Rubin, M.; Gevorgyan, V. *Synthesis* **2004**, 796.

[23] Hock, A. S.; Schrock, R. R. *J. Am. Chem. Soc.* **2006**, *128*, 16373.

Chapter 3

Synthesis of Molybdenum and Tungsten Alkylidene Compounds Containing a 2,6-Dimesitylphenylimido Ligand

Portions of this chapter have appeared in print:

Gerber, L. C. H.; Schrock, R. R.; Müller, P.; Takase, M. K. Synthesis of Molybdenum Alkylidene Complexes That Contain the 2,6-Dimesitylphenylimido Ligand. *J. Am. Chem. Soc.* **2011**, *133,* 18142.

Gerber, L. C. H.; Schrock, R. R.; Müller, P. Molybdenum and Tungsten Monoalkoxide Pyrrolide (MAP) Alkylidene Complexes That Contain a 2,6-Dimesitylphenylimido Ligand. *Organometallics* **2013**, *32*, 2373.

INTRODUCTION

Recently, much effort has focused on the development of olefin metathesis catalysts with bulky aryloxide ligands. Sterically demanding ligands such as mono-protected bitet ligands and substituted *ortho*-terphenols (Figure 3.1) have been particularly successful in promoting *Z*-selective olefin metathesis reactions including ring-opening metathesis polymerization (ROMP),[1] homocoupling,[2] ring-opening cross-metathesis,[3] ethenolysis,[4] and formation of natural products through ring-closing reactions.[5] The utility of bulky aryloxides led us to investigate the effect that bulky arylimido ligands would have on olefin metathesis catalysts. We were interested in exploring the effect of placing sterically demanding ligands at other positions in metathesis catalysts and studying the changes in selectivity and reactivity.

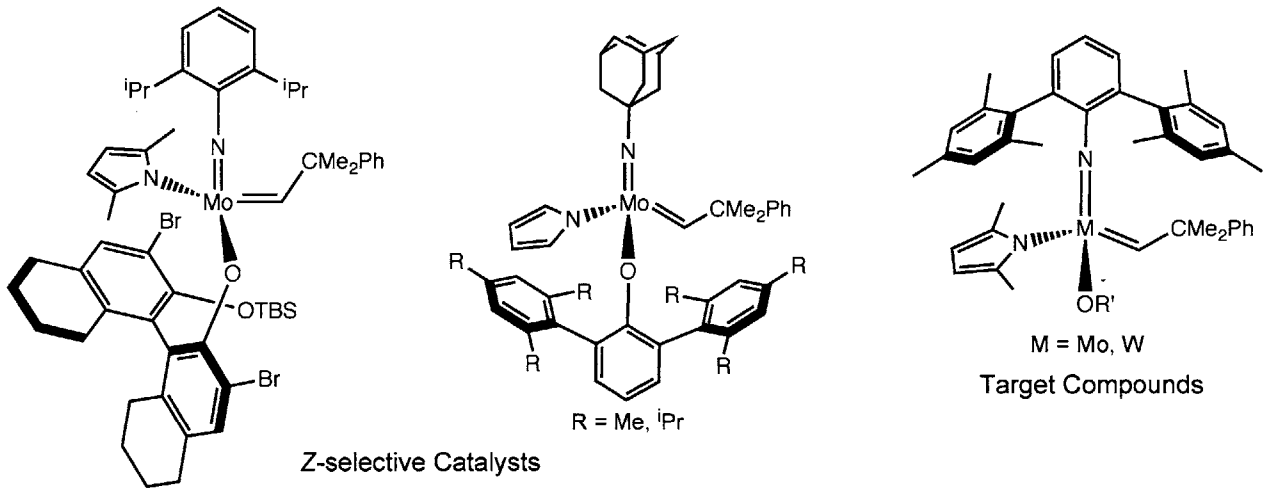

Figure 3.1. Examples of *Z*-selective olefin metathesis catalysts containing sterically demanding aryloxide ligands (left, middle) and targeted compounds (right).

Exploration of new imido ligands for group 6 metathesis catalysts is a greater undertaking than new aryloxide ligands since imido ligands are typically installed during the first step of a several step synthesis, while alcohols can easily be added to a catalyst precursor *in situ*. 2,6-Dimesitylphenyl (Ar*) was chosen as the target imido substituent because the same substituent at the aryloxide ligand is a successful *Z*-selective catalyst (Figure 3.1). Additionally, despite the steric hindrance imposed by the Ar* substituent, Ar* substituted imido moieties have been installed previously at main group metals[6] as well as Ni[7] and Ta[8]. Attempts to install an Ar*

imido group on Mo or W via synthetic routes that are typically used in the synthesis of imido alkylidene complexes had previously been unsuccessful (Scheme 3.1), and thus a new synthetic route to imido alkylidenes needed to be developed.[9] $Mo(NAr)_2Cl_2(DME)$ compounds are typically synthesized by addition of $ArNH_2$, Et_3N, and TMSCl to Na_2MoO_4. Attempts to synthesize $Mo(NAr^*)_2Cl_2(DME)$ via a similar synthetic route were not successful as a consequence of no reaction occurring. Reaction of MCl_4L_2 (M = Mo, L = THF; M = W, L_2 = DME) with Ar^*N_3, reaction of Ar*NCO with $W(O)Cl_4$, or reaction of $W(C^tBu)Cl_3(DME)$ with Ar*NH(Li) either led to decomposition or gave no reaction.

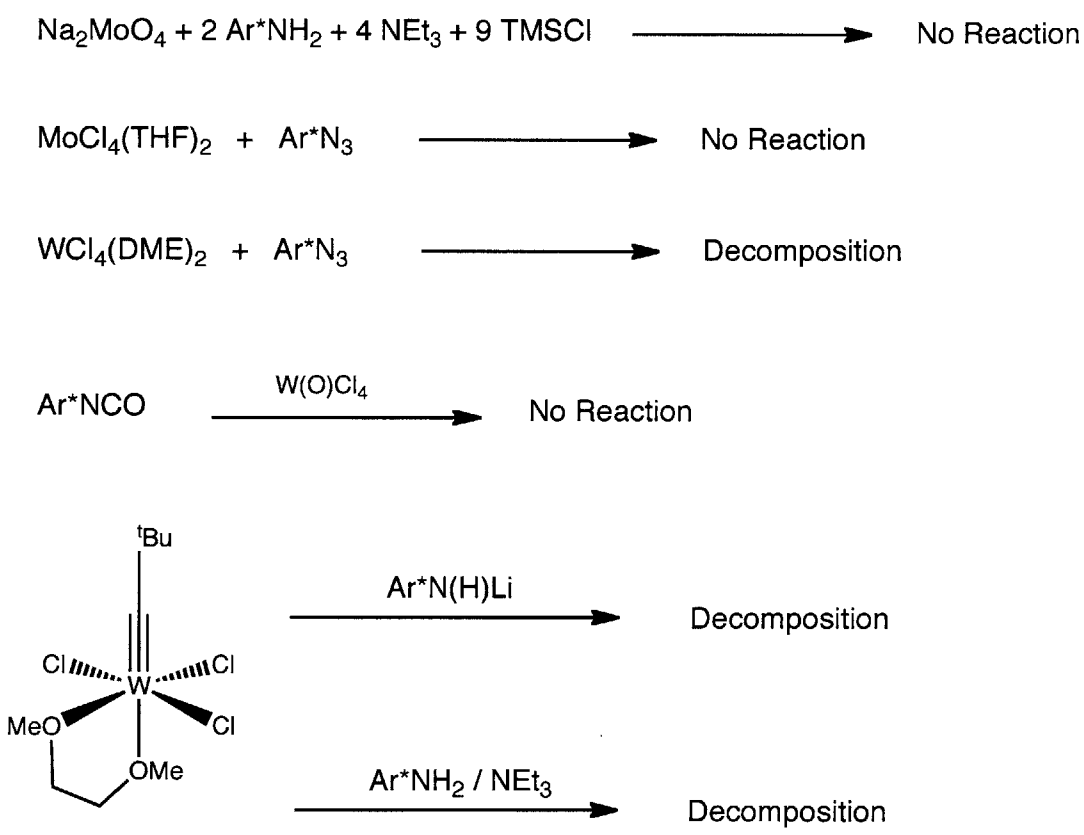

Scheme 3.1. Previous attempts towards installing the Ar* imido ligand at Mo or W.

However, Mo imido alkylidene complexes can be synthesized starting from $Mo(N^tBu)_2Cl_2(DME)$, as shown in Scheme 3.2.[10] Reaction of $Mo(N^tBu)_2Cl_2(DME)$ with H_2NAr (Ar = 2,6-diisopropylphenyl) leads to protonation of the ^{t}BuN ligand to give the mixed-imido species $Mo(NAr)(N^tBu)Cl_2(DME)$. This mixed-imido species can then be alkylated to give $Mo(NAr)(N^tBu)(CH_2CMe_2R)_2$ (R = Me or Ph). Using pentafluorophenol to protonate

$Mo(NAr)(N^tBu)(CH_2CMe_2R)_2$ gives $Mo(NAr)(CHCMe_2R)(OC_6F_5)_2$ exclusively with no evidence for protonation of the 2,6-diisopropylphenylimido ligand. Inspired by Gibson *et al.*'s work, a similar route of synthesis was targeted to install the NAr* ligand on Mo and W. This synthetic route has several advantages for the NAr* ligand over the traditional synthetic route to imido alkylidene complexes: first, one equivalent of the non-commercially available H_2NAr^* is not sacrificed during synthesis; second, sterically congested intermediates with two NAr* ligands are avoided; and third, employing a more basic t-butylimido ligand allows a weaker acid source to be used.

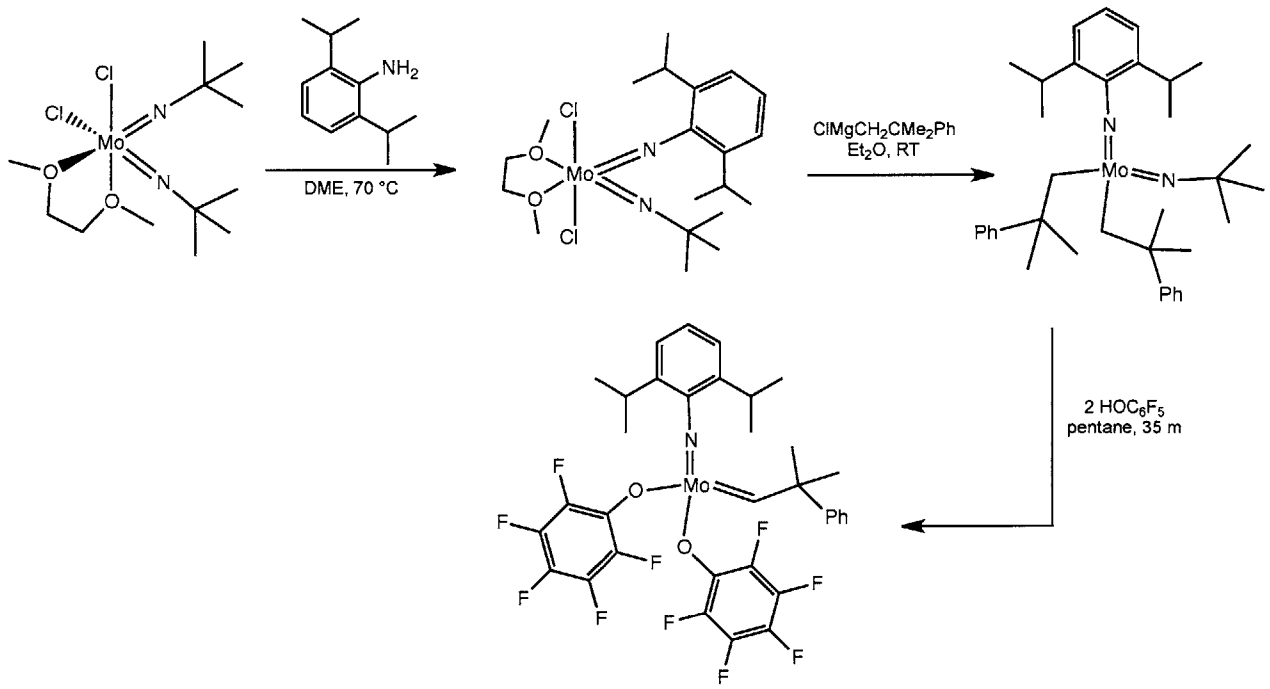

Scheme 3.2. Mixed-imido synthetic route to imido alkylidene compounds starting from $Mo(N^tBu)_2Cl_2(DME)$.

This chapter details the synthesis of Mo and W alkylidene MonoAryloxide Pyrrolide (MAP) complexes containing the 2,6-dimesitylphenylimido ligand through a mixed-imido synthetic route.

RESULTS AND DISCUSSION

I. Mixed-Imido Route for the Synthesis of 2,6-Dimesitylphenylimido Compounds

A. Synthesis of M(NAr*)(N^{t}Bu)Cl(NH^{t}Bu)

$Mo(N^tBu)_2Cl_2(DME)$ did not react with Ar^*NH_2 at ambient temperature. Upon heating solutions of $Mo(N^tBu)_2Cl_2(DME)$ and Ar^*NH_2 to 80 °C, the yellow solution became red after several hours. The solution returned to yellow when the temperature was returned to 22 °C. ^1H NMR spectra of the solution showed only starting materials. To preclude the possibility of an equilibrium that lies towards the desired product at higher temperatures, the reaction mixture was heated to 80 °C under vacuum in attempt to drive the equilibrium by removing $^tBuNH_2$ (bp 46 °C). The product remained red at room temperature. The product mixture was separated with pentane to provide an insoluble yellow powder, which was $Mo(^tBu)_2Cl_2$ (solvent free), confirmed by its conversion to $Mo(N^tBu)_2Cl_2(DME)$ upon addition of DME. A pentane soluble red oil was also isolated, which contained Ar^*NH_2 and minor highly-colored impurities.

Since a method directly analogous to the synthesis of $Mo(NAr)(N^tBu)Cl_2(DME)$ from $Mo(N^tBu)_2Cl_2(DME)$[10] was unsuccessful, an anionic route was targeted (Scheme 3.3). Addition of $Ar^*NHLi(Et_2O)$ to a solution of $Mo(N^tBu)_2Cl_2(DME)$ in Et_2O at −25 °C provided $Mo(N^tBu)_2Cl(NHAr^*)$. Addition of NEt_3 to $Mo(N^tBu)_2Cl(NHAr^*)$ gave $Mo(NAr^*)(N^tBu)Cl(NH^tBu)$ ($\mathbf{1_{Mo}}$). After optimization, $\mathbf{1_{Mo}}$ was obtained in 69 % isolated yield in one step from $Mo(N^tBu)_2Cl_2(DME)$ with Ar^*NH_2 by *in situ* preparation of Ar^*NHLi.

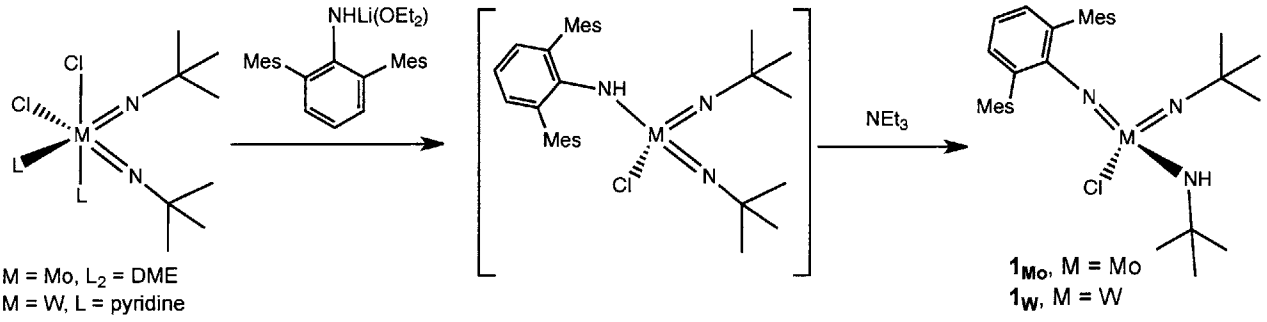

Scheme 3.3. Synthesis of M(NAr*)(N^{t}Bu)Cl(NH^{t}Bu) ($\mathbf{1_{Mo}}$ and $\mathbf{1_W}$).

$Mo(N^tBu)_2Cl(NHAr^*)$ and $\mathbf{1_{Mo}}$ can be distinguished by their ^1H NMR spectra, which are shown in Figure 3.2. The spectrum of $Mo(N^tBu)_2Cl(NHAr^*)$ displays one t-butyl resonance, while the spectrum of $\mathbf{1_{Mo}}$ displays two t-butyl resonances, indicative of the two different t-BuN moieties. Additionally, the N*H* resonance in the spectrum of $\mathbf{1_{Mo}}$ is upfield of that in the spectrum of $Mo(N^tBu)_2Cl(NHAr^*)$.

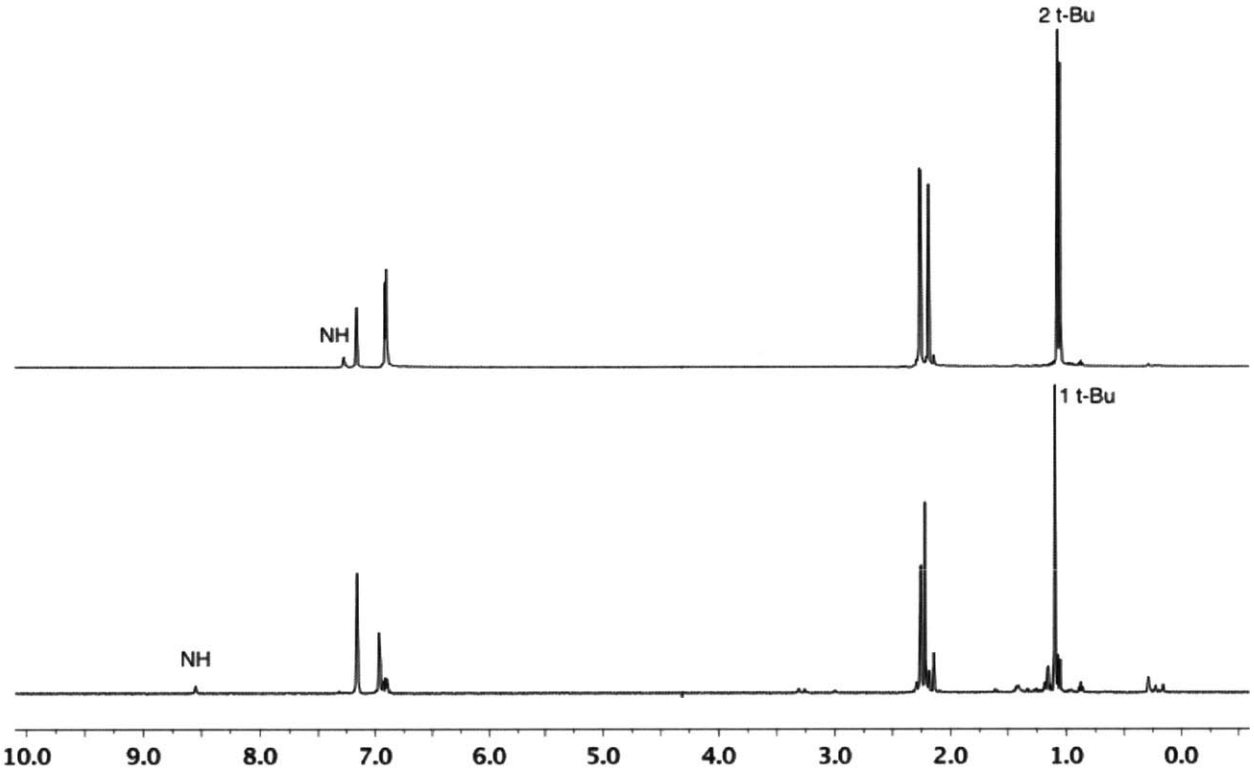

Figure 3.2. ^1H NMR spectra of $Mo(N^tBu)_2Cl(NHAr^*)$ and $Mo(NAr^*)(N^tBu)Cl(NH^tBu)$ (1_{Mo}). Bottom: ^1H NMR spectrum of $Mo(N^tBu)_2Cl(NHAr^*)$ obtained *in situ*. Top: ^1H NMR spectrum of $Mo(NAr^*)(N^tBu)Cl(NH^tBu)$ (1_{Mo}).

An X-ray diffraction study confirmed that $\mathbf{1_{Mo}}$ contains an Ar*N imido moiety and both an amide and imido t-BuN moiety (structure shown in Figure 3.3). The Mo1-N1 bond length of 1.7545(8) and the Mo1-N3 distance of 1.7425(9) are typical for a Mo=N distances in diimdo complexes. The Mo1-N1-C1 and the Mo1-N3-C29 angles of 165.16(7) and 157.39(8), respectively, are also typical for Mo diimido complexes. N2 is identified as an amide due to the longer Mo1-N2 bond length of 1.9403(9) and the smaller Mo1-N2-C25 angle of 135.53(7). Additionally, the hydrogen atom bonded to N2 was located in the difference map.

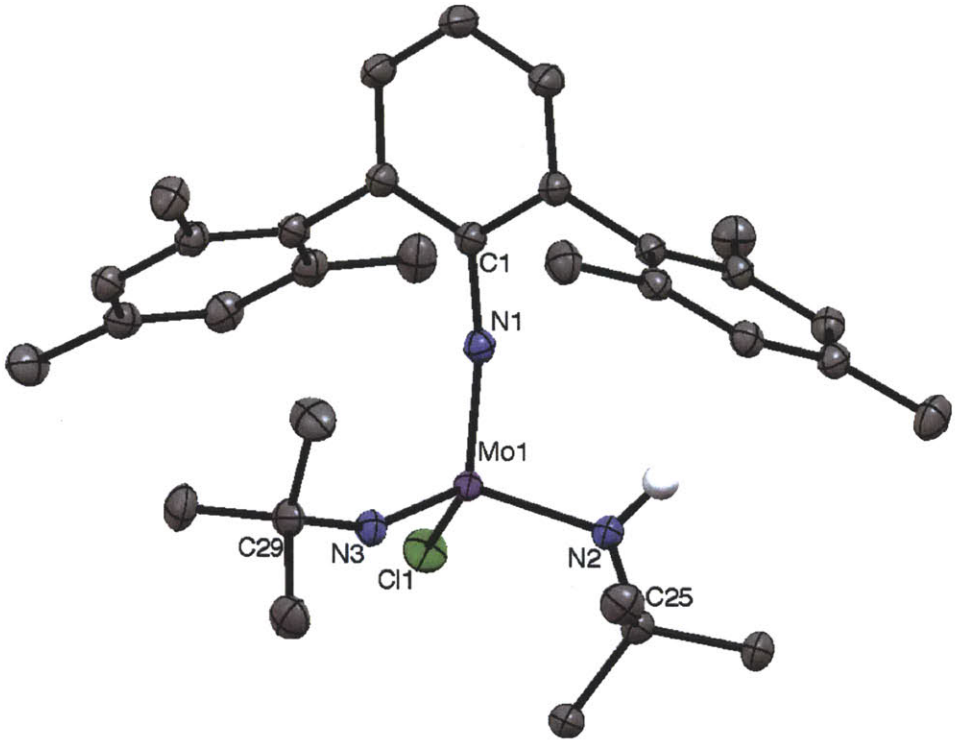

Figure 3.3. Thermal ellipsoid (50 %) drawing of Mo(NAr*)(N^{t}Bu)Cl(NH^{t}Bu), $\mathbf{1_{Mo}}$. Hydrogen atoms are omitted for clarity except for the hydrogen atom attached to N2. Selected lengths (Å) and angles (°): Mo1-N3 = 1.7425(9), Mo1-N1 = 1.7545(8), Mo1-N2 = 1.9403(9), Mo1-Cl1 = 2.3308(3), N1-C1 = 1.3874(13), N2-C25 = 1.4763(13), N3-C29 = 1.4602(13); N3-Mo1-N1 = 111.90(4), N3-Mo1-N2 = 107.89(4) N1-Mo1-N2 = 103.69(4), N3-Mo1-Cl1 = 108.87(3), N1-Mo1-Cl1 = 110.50(3), N2-Mo1-Cl1 = 113.94(3), C1-N1-Mo1 = 165.16(7), C25-N2-Mo1 = 130.53(7), C29-N3-Mo1 = 157.38(8).

W(N^{t}Bu)(NAr*)Cl(NH^{t}Bu) ($\mathbf{1_W}$) was isolated by a procedure similar to the Mo analog. The tungsten starting material W(N^{t}Bu)$_2$Cl$_2$(py)$_2$ was utilized since W(N^{t}Bu)Cl$_2$(DME) has not been previously reported. Upon addition of LiNHAr* to W(N^{t}Bu)$_2$Cl$_2$(py)$_2$, intermediate W(N^{t}Bu)$_2$Cl(NHAr*) is formed *in situ* and can be observed by ^{1}H NMR spectroscopy. After addition of NEt$_3$, W(NAr*)(N^{t}Bu)Cl(NH^{t}Bu) was isolated in 74 % yield. Attempts to use aniline Ar*NH$_2$ directly in a method analogous to Gibson *et al.*'s (as opposed to anilide LiNHAr*) were unsuccessful: W(N^{t}Bu)$_2$Cl$_2$(py)$_2$ does not react with H$_2$NAr* with after 16 h at 80 °C.

Attempts were made to use [(^{t}BuN)$_2$WCl$_2$(NH$_2$^{t}Bu)]$_2$ as a starting material since it is an intermediate in the synthesis of W(N^{t}Bu)$_2$Cl$_2$(py)$_2$, and its use would eliminate one synthetic step. Use of [(^{t}BuN)$_2$WCl$_2$(NH$_2$^{t}Bu)]$_2$ as a starting material was unsuccessful. After addition of LiNHAr* and NEt$_3$, H$_2$NAr* was the major product observed in the ^{1}H NMR spectrum.

Additionally, no reaction took place between $[(^tBuN)_2WCl_2(NH_2{}^tBu)]_2$ and H_2NAr^*, even after heating the reaction mixture to 80 °C for 5 d, likely due to the stable dimeric structure of $[(^tBuN)_2WCl_2(NH_2{}^tBu)]_2$.

B. Synthesis of $M(NAr^*)(N^tBu)(CH_2CMe_2Ph)_2$

Addition of 2,6-lutidine•HCl to $\mathbf{1_{Mo}}$ gives $Mo(NAr^*)(N^tBu)Cl_2(NH_2{}^tBu)$ ($\mathbf{2_{Mo}}$) in quantitative yield. The t-butylamino ligand remains bound, which initially caused concern about its deprotonation upon addition of a Grignard reagent to $\mathbf{2_{Mo}}$, so attempts to replace $^tBuNH_2$ with another donor ligand were undertaken. Reaction of $\mathbf{2_{Mo}}$ with one equivalent or excess pyridine or trimethylphosphine provided inseparable mixtures of $Mo(NAr^*)(N^tBu)Cl_2(L)_n$ and $Mo(N^tBu)_2Cl_2(L)_n$ (L = pyridine or trimethylphosphine, n = 1 or 2). Presence of $Mo(N^tBu)_2Cl_2(L)_n$ was confirmed by independent synthesis from $Mo(N^tBu)_2Cl_2(DME)$. Despite initial worry about the H_2N^tBu ligand, reaction of $\mathbf{2_{Mo}}$ with two equivalents of Grignard reagent $ClMgCH_2CMe_2Ph$ went smoothly to provide $Mo(NAr^*)(N^tBu)(CH_2CMe_2Ph)_2$ ($\mathbf{3_{Mo}}$).

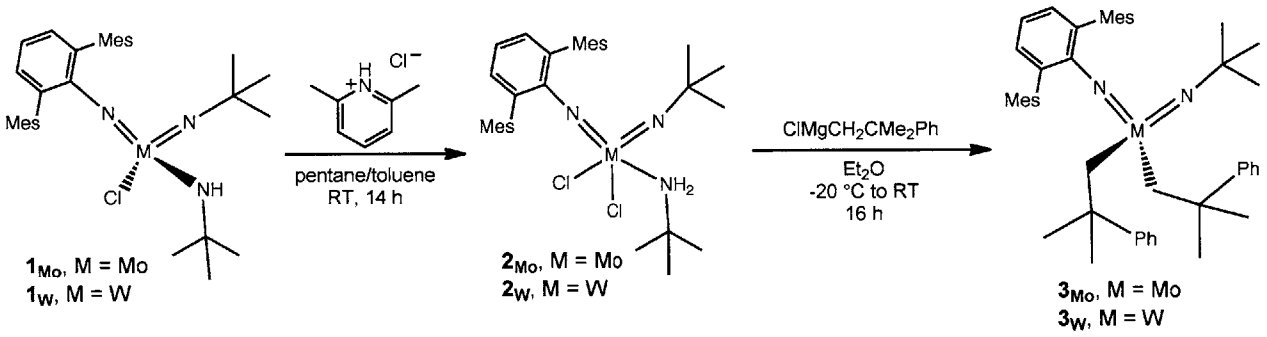

Scheme 3.4. Synthesis of $M(NAr^*)(N^tBu)(CH_2CMe_2Ph)_2$.

Compound $\mathbf{3_{Mo}}$ crystallizes in the monoclinic space group $P2_1/c$. Analysis of the crystal structure (Figure 3.4) shows the presence of the two different imido ligands. The Mo1–N1 distance of 1.7577(15) and the Mo1–N2 distance of 1.7437(15) are similar to the equivalent distances in $\mathbf{1_{Mo}}$. The C1–N1–Mo1 angle of 164.47(13) and the C25–N2–Mo1 angle of 154.65(13) are also similar to the angles in $\mathbf{1_{Mo}}$. Both $\mathbf{1_{Mo}}$ and $\mathbf{3_{Mo}}$ show slightly distorted tetrahedral geometry at Mo.

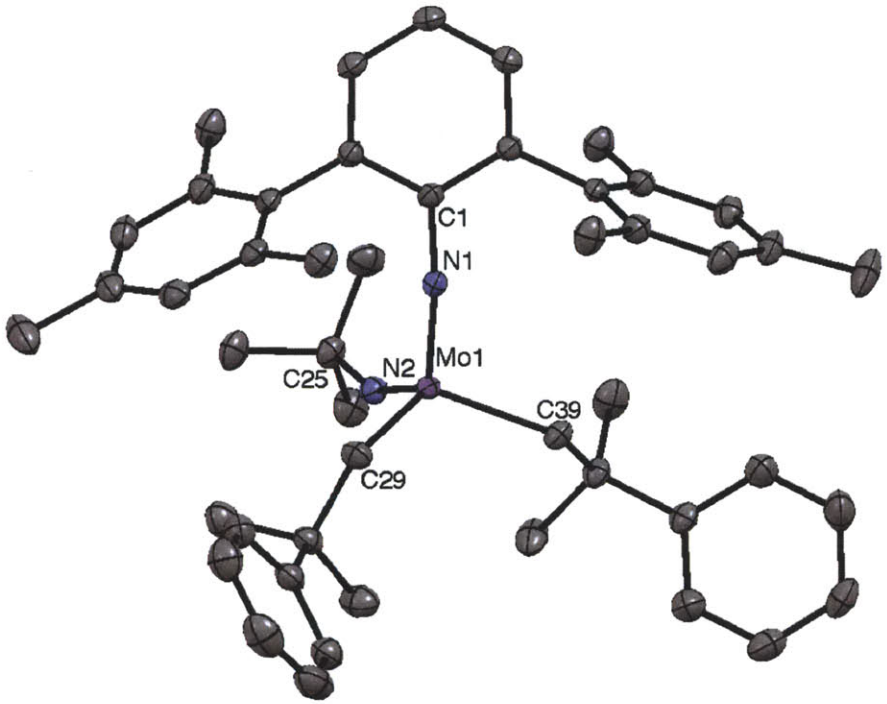

Figure 3.4. Thermal ellipsoid (50 %) drawing of Mo(NAr*)(N^{t}Bu)(CH$_2$CMe$_2$Ph)$_2$ ($\mathbf{3_{Mo}}$). Hydrogen atoms are omitted for clarity. Selected lengths (Å) and angles (°): Mo1-N2 = 1.7437(15), Mo1-N1 = 1.7577(15), Mo1-C29 = 2.1326(18), Mo1-C39 = 2.1410(17), N1-C1 = 1.389(2); N2-Mo1-N1 = 112.84(7), N2-Mo1-C29 = 111.14(7), N1-Mo1-C29 = 102.14(7), N2-Mo1-C39 = 109.20(7), N1-Mo1-C39 = 108.05(7), C29-Mo1-C39 = 113.35(7), C1-N1-Mo1 = 164.47(13), C25-N2-Mo1 = 154.65(13).

Starting from $\mathbf{1_W}$, W(NAr*)(N^{t}Bu)Cl$_2$(NH$_2$^{t}Bu) ($\mathbf{2_W}$) can be synthesized by addition of 2,6-lutidine•HCl. For the Mo analog, this reaction is quantitative, and requires no additional purification beyond filtration of the reaction mixture and removal of the volatiles *in vacuo* to obtain analytically pure product. In the case of W, this reaction is not as clean and even when excess lutidine•HCl is utilized, some $\mathbf{1_W}$ can still be observed in the ^{1}H NMR spectrum of the reaction mixture. Rather than reduce the yield of $\mathbf{2_W}$ during an extensive purification process ($\mathbf{1_W}$ and $\mathbf{2_W}$ have very similar solubilities), the reaction mixture was filtered, the volatiles removed *in vacuo*, and the crude product was used directly for the next reaction step.

W(NAr*)(N^{t}Bu)(CH$_2$CMe$_2$Ph)$_2$ ($\mathbf{3_W}$) is synthesized by the addition of two equivalents of MgClCH$_2$CMe$_2$Ph to $\mathbf{2_W}$. Despite the impurities in the starting material, W(NAr*)(N^{t}Bu)(CH$_2$CMe$_2$Ph)$_2$ was recrystallized from pentane and isolated in pure form.

II. Synthesis of Alkylidene Dichloride Compounds Containing the 2,6-Dimesitylphenylimido Ligand

A. Synthesis of Molybdenum Alkylidene Complexes

Using Mo(NAr*)(N^{t}Bu)(CH_2CMe_2Ph)$_2$ ($\mathbf{3_{Mo}}$) as a starting point, alkylidene synthesis was attempted using a variety of acids. Previously, alkylidene compounds have been synthesized from bisimido species upon treatment with triflic acid.[11] Gibson *et al.* showed that starting from a mixed-imido species they were able to use a much weaker acid, pentafluorophenol, to protonate the t-butylimido ligand and provide an alkylidene species.[10] Reaction of $\mathbf{3_{Mo}}$ with triflic acid showed the presence of five major alkylidene resonances in the ^{1}H NMR spectra, suggesting that triflic acid did not exclusively protonate the t-butylimido ligand of $\mathbf{3_{Mo}}$. A variety of HCl derived acids were then explored, including HCl, pyridine hydrochloride, 2,6-lutidine hydrochloride, 2,4-lutidine hydrochloride, and 3,5-lutidine hydrochloride. Addition of 3 equivalents of pyridine hydrochloride or 3,5-lutidine hydrochloride to $\mathbf{3_{Mo}}$ yields Mo(NAr*)($CHCMe_2Ph$)Cl_2(L) ($\mathbf{4_{Mo}}$, L = pyridine; $\mathbf{5_{Mo}}$, L = 3,5-lutidine), as shown in Scheme 3.5. No reaction was observed with the 2-substituted lutidine hydrochlorides: the steric hindrance located closer to the binding nitrogen atom in the 2-substituted lutidine hydrochlorides may prevent coordination of the lutidine and thus prevent protonation. The reaction of $\mathbf{3_{Mo}}$ with three molar equivalents of HCl solution in diethyl ether showed Ar*NH_2 as the only benzene-soluble, non-volatile product by ^{1}H NMR spectroscopy.

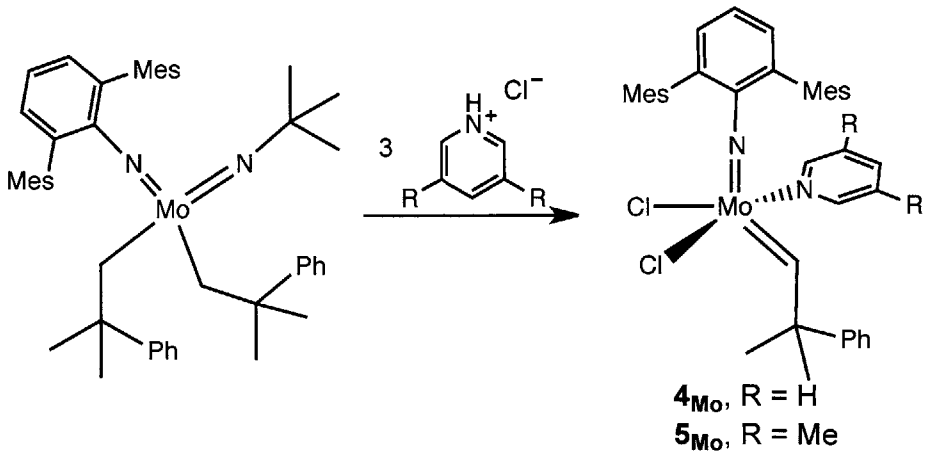

Scheme 3.5. Synthesis of Mo(NAr*)($CHCMe_2Ph$)Cl_2(py) and Mo(NAr*)($CHCMe_2Ph$)Cl_2(3,5-Lut).

The best results for the synthesis of $\mathbf{4_{Mo}}$ were obtained using a pentane/DME mixture as solvent and conducting the reaction at room temperature. Synthesis of $\mathbf{5_{Mo}}$ with a slightly larger coordinating ligand showed the best results when the reaction was conducted in benzene at 75 °C. Without heating, the reaction took several days to go to completion over which time decomposition to unidentified products was also observed.

An X-ray diffraction study of $\mathbf{4_{Mo}}$ was used to determine its crystal structure (Figure 3.5). Compound $\mathbf{4_{Mo}}$ crystallizes in the triclinic space group P$\bar{1}$. The Mo atom is five-coordinate, with the pyridine ligand coordinated opposite one of the chloride ligands. For this compound, $\tau = 0.41$ (where $\tau = 0$ for a square pyramid and $\tau = 1$ for a trigonal bipyramid),[12] indicating it is about midway between square pyramidal (SP) and trigonal bipyramidal (TBP) geometry. Bond lengths and angles are as expected for Mo imido alkylidene species, and are given in Figure 3.5. The alkylidene ligand was disordered over two positions, between an *anti* and *syn* orientation with 87 % in the *anti* orientation. Interestingly, the only atoms to be in a significantly different position between the two components of the disorder were the α-carbon, C25, and the methyl groups. The phenyl group and β-carbon, C26, are located in essentially the same place in both the *syn* and *anti* structure. The Mo=C25 bond length for the *anti* alkylidene is 1.932(2), while the Mo=C25A bond length for the *syn* alkylidene is 1.847(13). This is consistent with the *syn* alkylidene having an agostic interaction between the α-hydrogen and Mo, while *anti* alkylidene does not. Only the *anti* alkylidene is observed in the ^{1}H NMR spectrum of $\mathbf{4_{Mo}}$ in C_6D_6 or CD_2Cl_2 (12.61 ppm in CD_2Cl_2, $^1J_{CH} = 151$ Hz).

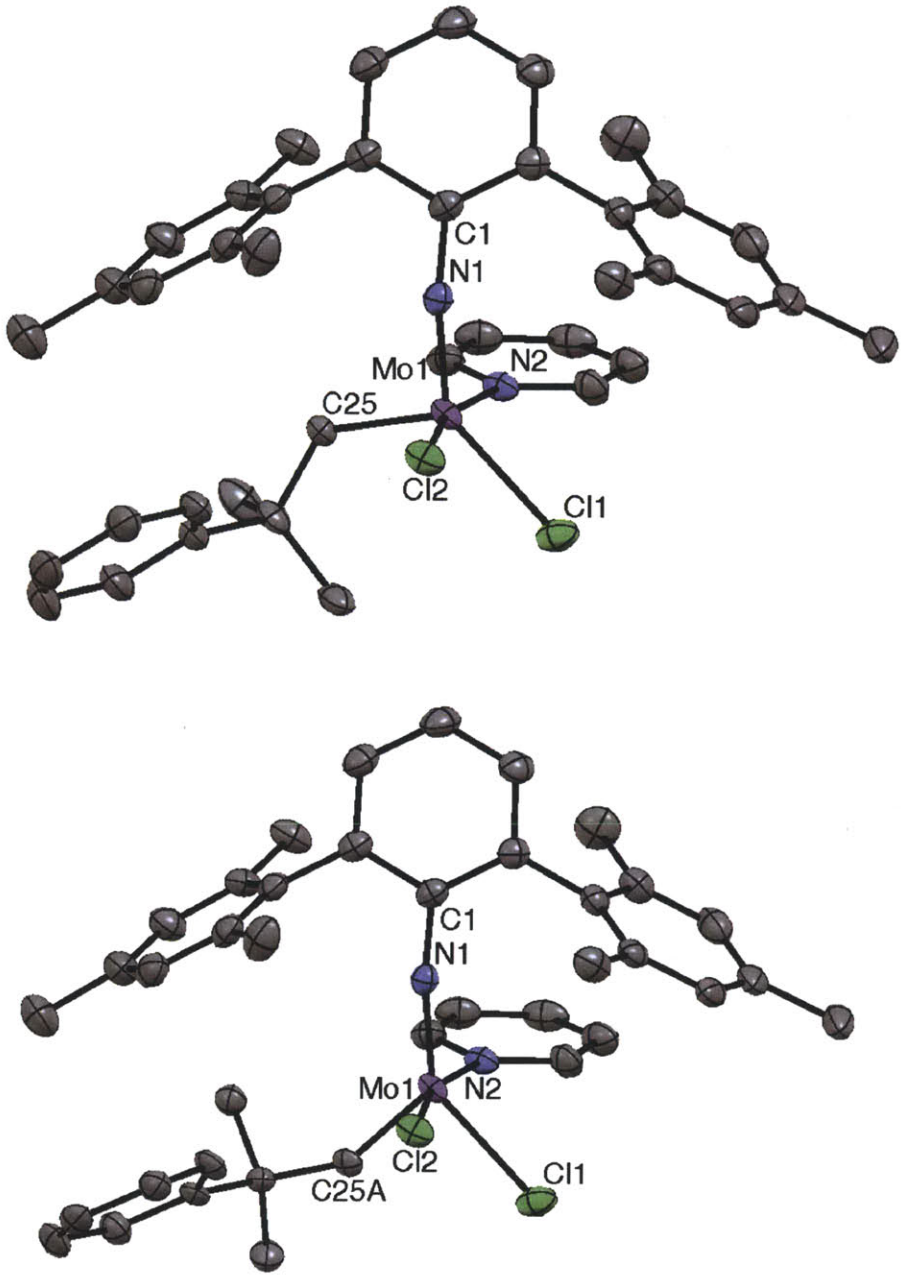

Figure 3.5. Thermal ellipsoid (50 %) drawing of the two components of disordered alkylidene ligand for Mo(NAr*)(CHCMe$_2$Ph)Cl$_2$(Py), 4$_{Mo}$. The predominant *anti* alkylidene isomer (87 %) is pictured on the top and the *syn* alkylidene isomer is pictured on the bottom. Selected bond lengths (Å) and angles (°) for both: Mo1-N1 = 1.7277(15), Mo1-N2 = 2.2280(15), Mo1-Cl1 = 2.4128(5), Mo1-Cl2 = 2.4177(5), N1-Mo1-N2 = 87.95(6), N1-Mo1-Cl1 = 141.70(5), N2-Mo1-Cl1 = 83.10(4), N1-Mo1-Cl2 = 97.42(5), N2-Mo1-Cl2 = 166.01(4), Cl1-Mo1-Cl2 = 84.731(19), C1-N1-Mo1 = 170.90(13). Selected bond lengths and angles for *anti*: Lengths (Å): Mo1-C25 = 1.932(2); Angles (°): N1-Mo1-C25 = 95.47(8), C25-Mo1-N2 = 95.16(7), C25-Mo1-Cl1 = 122.32(6), C25-Mo1-Cl2 = 97.15(6), C26-C25-Mo1 = 129.0(3). Selected bond lengths and angles for *syn*: Lengths (Å) Mo1-C25A = 1.847(13); Angles (°) N1-Mo1-C25A = 128.1(4), C25A-Mo1-N2 = 96.0(4), C25A-Mo1-Cl1 = 89.9(4), C25A-Mo1-Cl2 = 90.9(4), C26A-C25A-Mo1 = 151(2).

To the best of our knowledge, this is the first time that HCl-based acids have been employed in order to prepare Mo or W imido alkylidene complexes. Pyridine hydrochloride provides several advantages over triflic acid that has been used primarily for previous alkylidene syntheses. Pyridine hydrochloride is a solid and non-volatile, which makes it more convenient to manipulate and cause less damage in a dry box. Additionally, because triflic acid is such a strong acid, it can cause unpredictable side reactions during alkylidene synthesis, leading to failed reaction or difficult purification.

After the application of pyridine hydrochloride to alkylidene synthesis in the NAr* system, it was found that similar conditions can be employed for the synthesis of other alkylidene species that were not available using triflic acid. Specifically, other Schrock group members found that the long sought after W t-butylimido and adamantylimido alkylidene species can be synthesized by employing pyridine hydrochloride to form $W(NR)(CHCMe_3)Cl_2(py)_2$ (R = t-butyl, 1-adamantyl) from $W(NR)_2(CH_2CMe_3)_2$.[13]

B. Synthesis of Tungsten Alkylidene Complexes

With $\mathbf{3_w}$ as a starting point, a variety of acid sources were tested for the synthesis of a W NAr* alkylidene species. PyridineHCl, HCl solution in Et_2O, or triflic acid resulted in decomposition with little or no identifiable alkylidene species as determined by ^1H NMR spectroscopy. $(CF_3)_2CHOH$, pyridine•HOTf, F_5C_6OH, and $[HNEt_3][OTf]$ provided no reaction at ambient temperature in DME or at 80 °C in C_6D_6. Although use of pyridineHCl was unsuccessful, reaction of $\mathbf{3_w}$ with one molar equivalent of pyridine followed by addition of three equivalents of HCl in Et_2O gives $W(NAr^*)(CHCMe_2Ph)Cl_2(py)$ ($\mathbf{4_w}$) which was isolated in 69 % yield. Only the *anti* alkylidene isomer is visible in the ^1H NMR spectrum of $\mathbf{4_W}$ ($^1J_{CH}$ = 144 Hz).

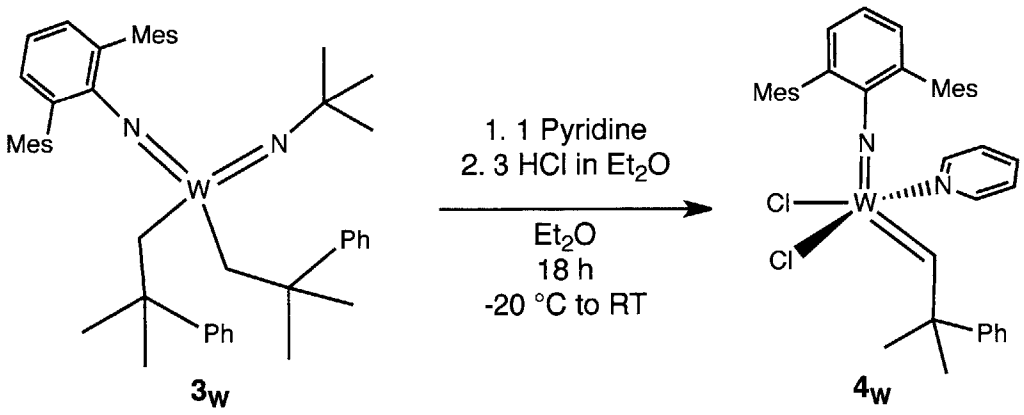

Scheme 3.6. Synthesis of W(NAr*)(CHCMe$_2$Ph)Cl$_2$(py), 4$_w$.

An alkylidene species was also synthesized by treating **3$_w$** with three equivalents of HCl in the presence of 2,2'-bipyridine (bipy) to form W(NAr*)(CHCMe$_2$Ph)Cl$_2$(bipy) (**6$_W$**, Scheme 3.7). W(NAr*)(CHCMe$_2$Ph)Cl$_2$(bipy) is insoluble in pentane, Et$_2$O, benzene, and toluene. Its low solubility in CH_2Cl_2 can be used to extract **6$_W$** from [^{t}BuNH$_3$][Cl].

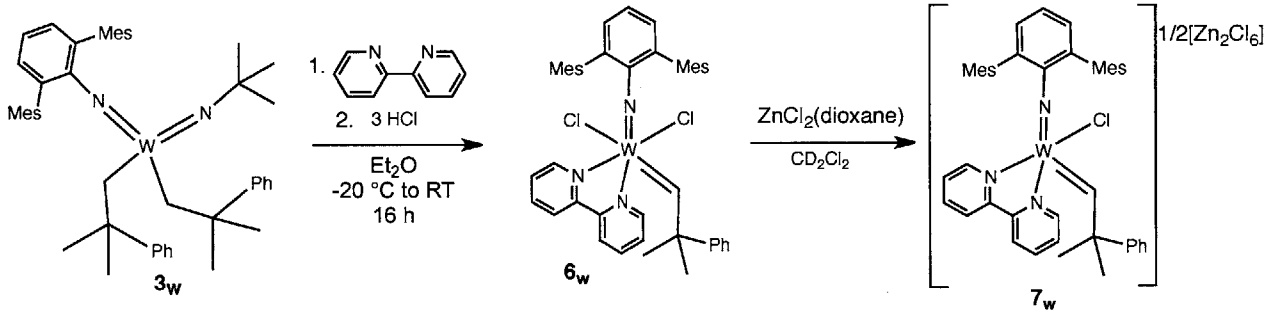

Scheme 3.7. Synthesis of W(NAr*)(CHCMe$_2$Ph)Cl$_2$(bipy), 6$_w$, and [W(NAr*)(CHCMe$_2$Ph)Cl] [Zn$_2$Cl$_6$]$_{0.5}$, 7$_w$.

$ZnCl_2$ or $ZnCl_2$(1,4-dioxane) has been used to remove 2,2'-bipyridine or 1,10-phenanthroline from Mo imido alkylidene complexes.[13, 14, 15] When $ZnCl_2$(1,4-dioxane) is added to W(NAr*)(CHCMe$_2$Ph)Cl$_2$(bipy) in CD_2Cl_2, the orange suspension becomes a clear orange solution. A new product and free 1,4-dioxane are observed by ^{1}H NMR spectroscopy, but resonances indicative of metal-bound bipyridine are visible, indicating that $ZnCl_2$(1,4-dioxane) did not remove bipyridine from the W coordination sphere. An X-ray structure of the product showed that [W(NAr*)(CHCMe$_2$Ph)Cl(bipy)][Zn$_2$Cl$_6$]$_{0.5}$ (**7$_w$**) had formed as the reaction

product: $ZnCl_2$ abstracted a chloride ligand to form a cationic W bipyridine complex (Figure 3.6).

$[W(NAr^*)(CHCMe_2Ph)Cl(bipy)][Zn_2Cl_6]_{0.5}$ crystallizes in the space group $P\bar{1}$ with one $[W(NAr^*)(CHCMe_2Ph)Cl(bipy)][Zn_2Cl_6]_{0.5}$ unit and one toluene molecule per asymmetric unit (Figure 3.6). The alkylidene ligand is in the *syn* orientation. The bipyridine ligand is disordered over two positions. The τ value is 0.34 (Where τ =1 for a perfect trigonal bipyramid and τ = 0 for a perfect square pyramid),[12] indicating that the geometry about W is best described as a distorted square pyramid with the alkylidene ligand at the apical site. The W1-N1-C11 angle of 153.52(18) is relatively small compared to many other imido alkylidene complexes, possibly due to some π interactions between the mesityl ring and one of the bipy ring system. Otherwise, the bond lengths and angles are fairly typical for W imido alkylidene complexes. The Zn atoms in the $Zn_2Cl_6^{2-}$ anion are slightly distorted tetrahedra.

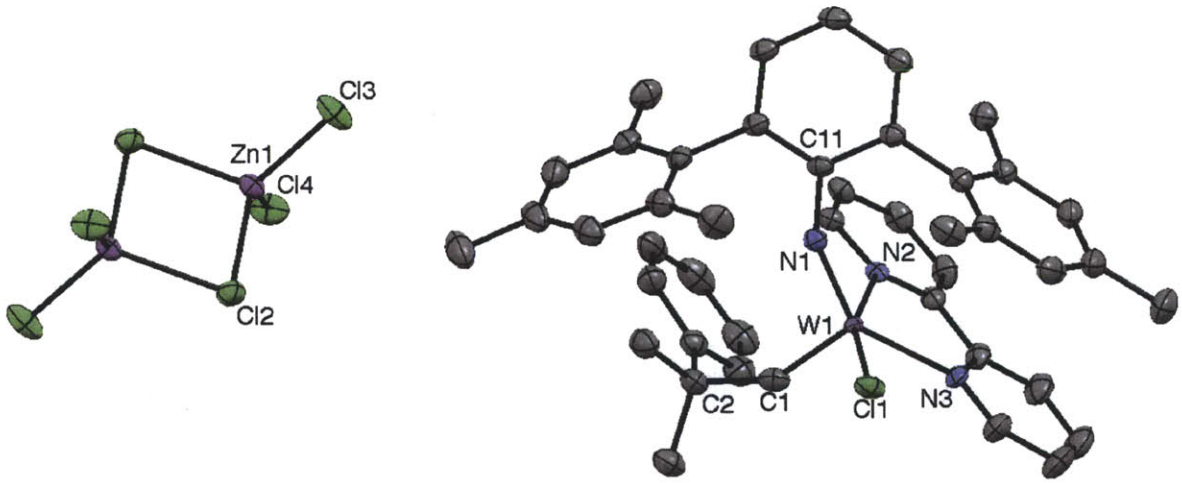

Figure 3.6. Crystal structure of $[W(NAr^*)(CHCMe_2Ph)Cl(bipy)][Zn_2Cl_6]_{0.5}$ in thermal ellipsoid representation at the 50% probability level. Only one half of the $Zn_2Cl_6^{2-}$ anion is present in the asymmetric unit, but the whole unit is pictured. Hydrogen atoms, toluene solvent molecule and minor component of disorder are omitted for clarity. Selected bond angles: C11-N1-W1 = 153.03(15), C2-C1-W1 = 148.42(17).

III. Substitution of Chloride Ligands in 2,6-Dimesitylphenylimido Alkylidene Complexes

A. Synthesis of Monochloride Monoalkoxide Complexes

In order to gauge the effects of the NAr* ligand on alkylidene complexes a small library of compounds was synthesized. The first class of complexes that was targeted were monochloride monoalkoxide complexes (Scheme 3.8), which are possible precursors to the target MAP complexes.

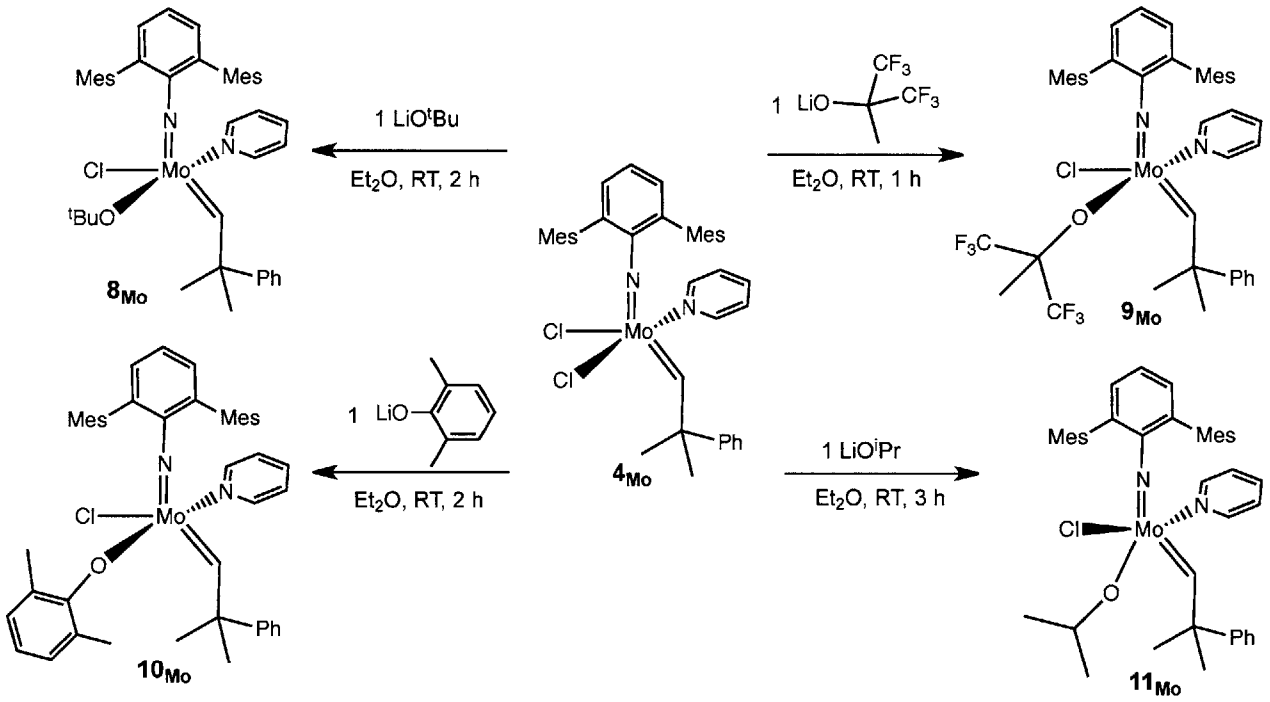

Scheme 3.8. Substitution of a chloride ligand in Mo(NAr*)(CHCMe$_2$Ph)Cl$_2$(py) to form monoalkoxide monochloride complexes.

Reaction of $\mathbf{4_{Mo}}$ with one equivalent of LiO^{t}Bu, LiOCMe(CF$_3$)$_2$, LiO(2,6-Me$_2$C$_6$H$_3$) or LiO^{i}Pr in diethyl ether at ambient temperature yields Mo(NAr*)(CHCMe$_2$Ph)Cl(O^{t}Bu)(Py) ($\mathbf{8_{Mo}}$), Mo(NAr*)(CHCMe$_2$Ph)Cl[OCMe(CF$_3$)$_2$](Py) ($\mathbf{9_{Mo}}$), Mo(NAr*)(CHCMe$_2$Ph)Cl[O(2,6-Me$_2$C$_6$H$_3$)](Py) ($\mathbf{10_{Mo}}$), and Mo(NAr*)(CHCMe$_2$Ph)Cl(O^{i}Pr)(Py) ($\mathbf{11_{Mo}}$), respectively. These reactions are more facile in diethyl ether than benzene-d$_6$ as solvent, likely because the lithium alkoxide reagents are more soluble in diethyl ether. Despite the greater steric demand of the alkoxide ligands compared with chloride, pyridine remains bound in all cases. In solution, $\mathbf{8_{Mo}}$,

$\mathbf{9_{Mo}}$, and $\mathbf{10_{Mo}}$ are observed as *anti* alkylidenes with $^1J_{CH}$ values of 148 Hz, 150 Hz, and 151 Hz, respectively, all typical $^1J_{CH}$ values for *anti* alkylidenes.

Compound $\mathbf{5_{Mo}}$ was used as a starting material with the idea that a bulkier donor ligand in the starting material may dissociate more easily upon substitution of the chloride ligands. Reaction of $\mathbf{5_{Mo}}$ with LiO^{t}Bu and LiOAr* were monitored *in situ.* In both of these reactions, no free 3,5-lutidine was observed in the ^{1}H NMR spectra; these reactions were not pursued further.

Reactions with large alkoxide ligands were explored as well. Reaction of $\mathbf{4_{Mo}}$ with one molar equivalent of LiOAr* in benzene at 80 °C for 16 h provides Mo(NAr*)(CHCMe$_2$Ph)Cl(OAr*)(Py) (Scheme 3.9). Despite the steric demands about Mo by two terphenyl-substituted ligands, pyridine remains bound to molybdenum.

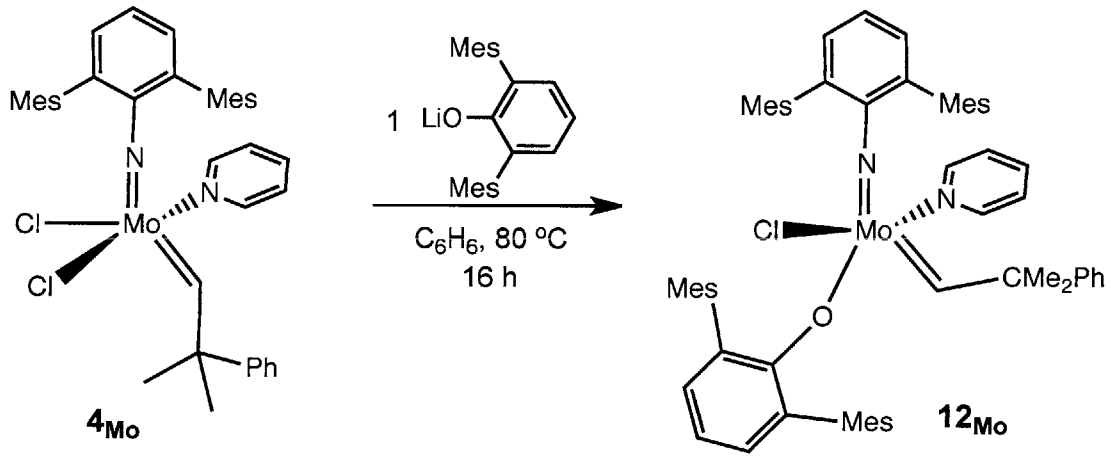

Scheme 3.9. Synthesis of Mo(NAr*)(CHCMe$_2$Ph)Cl(OAr*)(Py), $\mathbf{12_{Mo}}$.

Crystals of $\mathbf{12_{Mo}}$ were obtained by chilling a concentrated Et_2O solution. During data collection, ice accumulated on the crystal, interfering with crystal diffraction, so multiple reflections were omitted in order to find a suitable model for the data. Compound $\mathbf{12_{Mo}}$ crystallized in triclinic space group P$\bar{1}$ with two independent molecules in the asymmetric unit. There was much disorder in the structure, including in mesityl groups, the pyridine ligands, and parts of the alkylidene ligand (although neither of the α-carbon atoms was disordered).

Figure 3.7 shows one molecule of Mo(NAr*)(CHCMe$_2$Ph)Cl(OAr*)(py) ($\mathbf{12_{Mo}}$) with the disorder omitted for clarity. The geometry at Mo is a distorted square pyramid, $\tau = 0.10$ (where $\tau = 0$ for a square pyramid and $\tau = 1$ for a trigonal bipyramid), with the alkylidene ligand at the apical site. The two terphenyl-substituted ligands are located opposite one another on the base of

the square pyramid (150.95(7)°) and pyridine is opposite the chloride ligand (157.1(3) °). Mo1 sits 0.383 Å above the basal plane of the square pyramid (least squares plane of Cl11, N11, N12, and O11). Bond lengths and angles of the two independent molecules of $\mathbf{12_{Mo}}$ are similar, but the two molecules are opposite hands: the ordering of equivalent ligands about the basal plane of the square pyramid is clockwise in one and counterclockwise in the other. Although the Mo1=N11 bond is 1.7442(19) Å and the Mo1 – O11 bond length is 1.992(15) Å, the differing bond angles (C125-O11-Mo1 = 139.43(13) and C101-N11-Mo1 = 173.93(17)) mean that the NAr* and the OAr* ligand provide about similar steric protection based on the Mo – C_{ipso} distances (Mo1 – C101 and Mo1 – C125 are both 3.140 Å). The alkylidene ligands are in the *syn* orientation in both independent molecules with no disorder between *syn* and *anti*. In solution, only the *syn* isomer is observed by ^{1}H NMR spectroscopy ($^1J_{CH}$ = 127 Hz) as well.

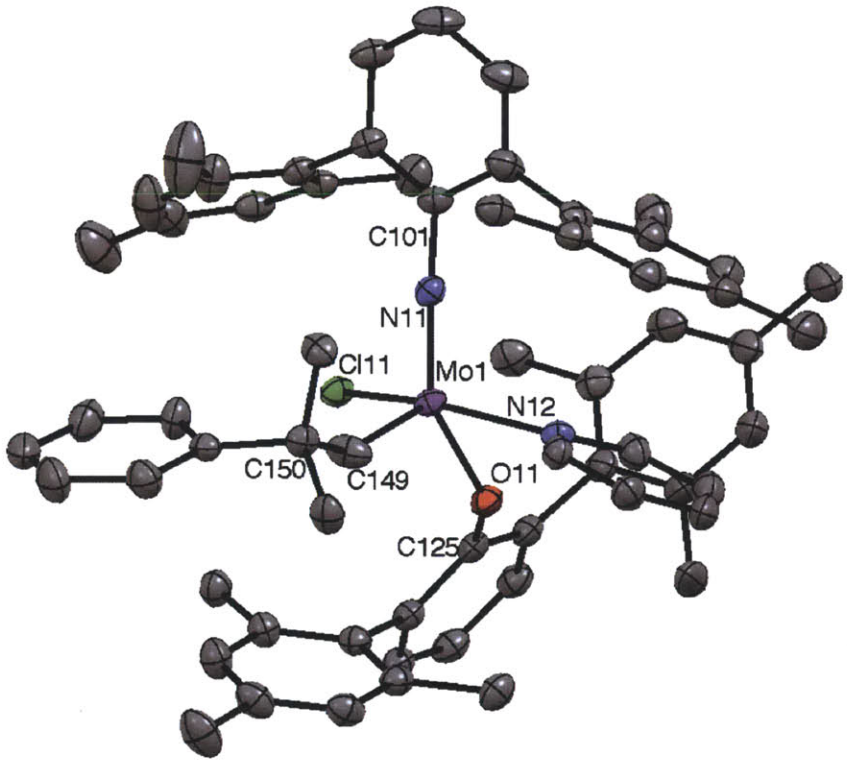

Figure 3.7.Thermal ellipsoid (50 %) drawing of 12_{Mo}. One independent molecule is shown with one component of each disorder. Hydrogen atoms were omitted for clarity. Selected bond lengths (Å) and angles (°): Mo1-N11 = 1.7442(19), Mo1-C149 = 1.874(3), Mo1-O11 = 1.992(15), Mo1-N12 = 2.267(7), Mo1-Cl11 = 2.3731(6), N11-Mo1-C149 = 102.45(10), N11-Mo1-O11 = 148.55(8), C149-Mo1-O11 = 108.32(9), N11-Mo1-N12 = 94.9(3), C149-Mo1-N12 = 98.5(2), O11-Mo1-N12 = 74.6(3), N11-Mo1-N32 = 96.6(4), N11-Mo1-Cl11 = 98.10(6), C149-Mo1-Cl11 = 99.45(8), O11-Mo1-Cl11 = 83.31(5), N12-Mo1-Cl11 = 155.0(3), C125-O11-Mo1 = 139.43(13), C150-C149-Mo1 = 146.4(3), C101-N11-Mo1 = 173.93(17).

The ^{1}H NMR spectrum of $\mathbf{12_{Mo}}$ is broad at room temperature, so a variable temperature NMR study in toluene-d_8 was conducted in order to observe coalescence and decoalescence (Figure 3.8). At −10 °C, the peaks were sharp and resonances could be observed for each methyl group. At higher temperatures, as bond rotation becomes faster, coalescence of several aromatic and methyl groups can be observed.

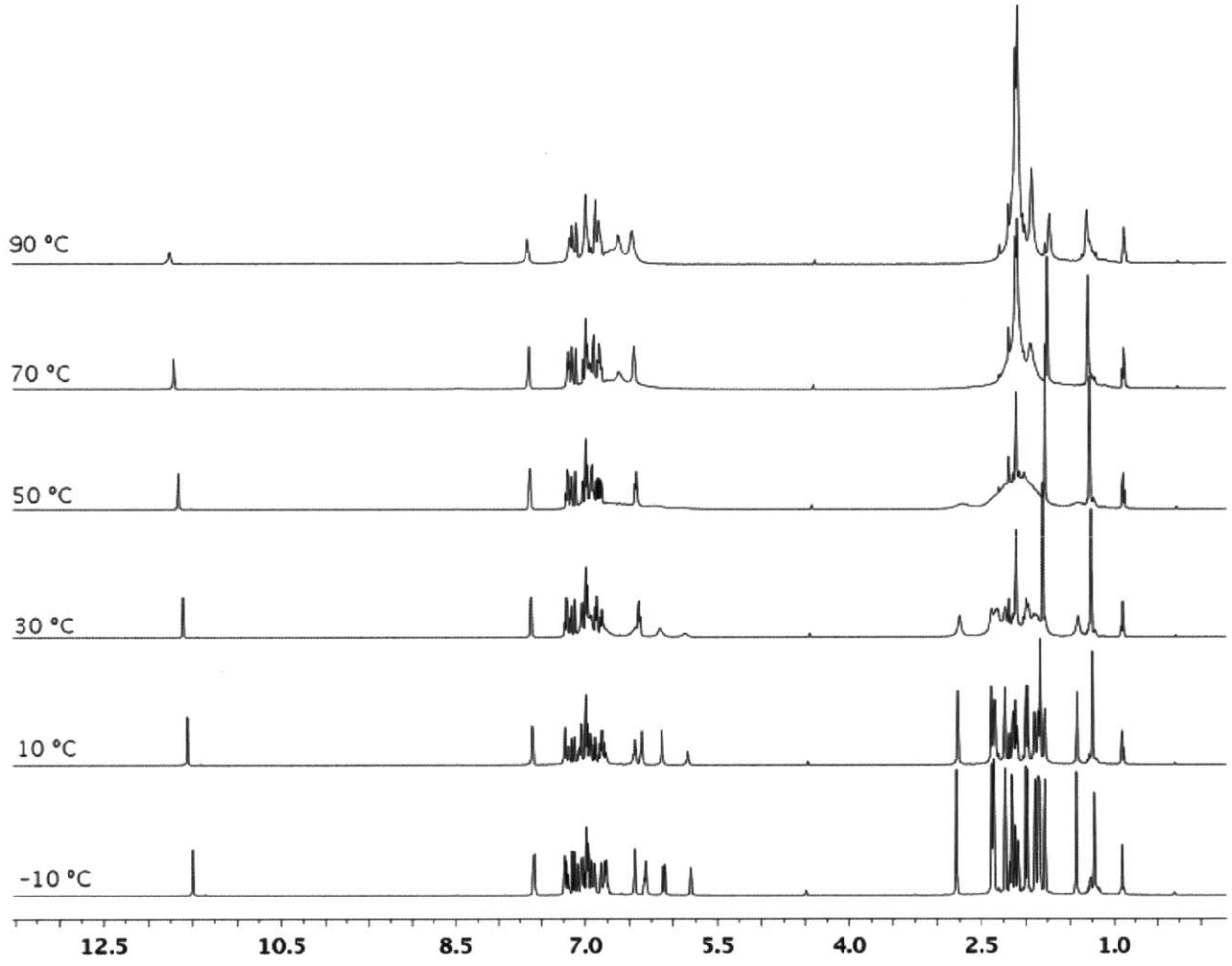

Figure 3.8. ^{1}H NMR spectra of Mo(NAr*)(CHCMe$_2$Ph)Cl(OAr*)(py) in toluene-d_8 at various temperatures.

B. Synthesis of Bispyrrolide Complexes

Bispyrrolide complexes are useful precursors for olefin metathesis catalysts. Upon addition of an alcohol, bisalkoxide or MAP complexes are synthesized. Bispyrrolide precursors are particularly useful because the byproduct of the reaction with an alcohol, pyrrole, does not interfere with olefin metathesis, thus catalysts for olefin metathesis can be synthesized *in situ*.

Another advantage is that (depending on the substituents on the pyrrolide ligand) the pyrrole byproduct can be readily removed *in vacuo*.

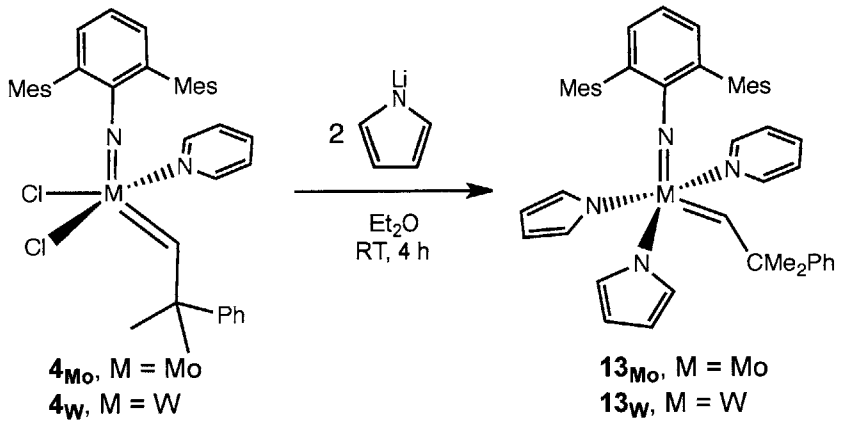

Scheme 3.10. Synthesis of M(NAr*)(CHCMe$_2$Ph)(Pyr)$_2$(Py), 13$_{Mo}$ and 13$_W$.

Upon addition of two equivalents of LiPyr (Pyr = pyrrolide = LiNC$_4$H$_4$) to **4$_{Mo}$** or **4$_W$** in Et$_2$O, M(NAr*)(CHCMe$_2$Ph)(Pyr)$_2$(Py) (M = Mo, **13$_{Mo}$**; M = W, **13$_W$**) is formed. Compounds **13$_{Mo}$** and **13$_W$** are both pyridine adducts (Scheme 3.10).

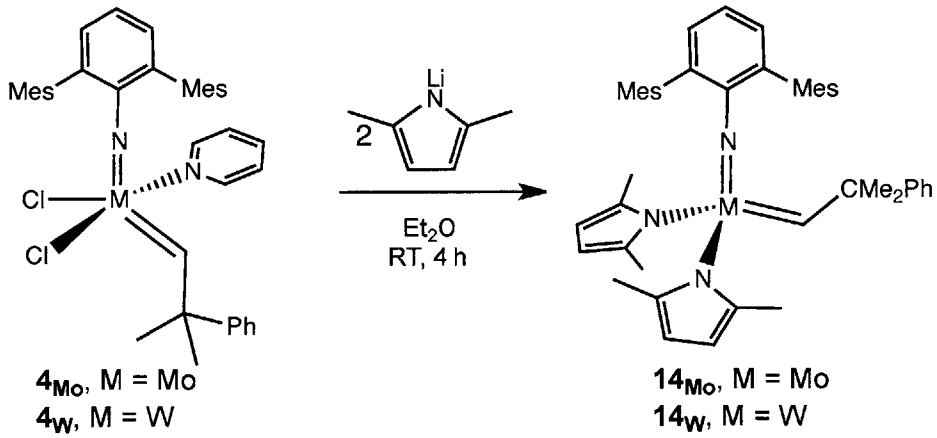

Scheme 3.11. Synthesis of M(NAr*)(CHCMe$_2$Ph)(Me$_2$Pyr), 14$_{Mo}$ and 14$_W$.

Addition of LiMe$_2$Pyr (Me$_2$Pyr = 2,5-dimethylpyrrolide = 2,5-Me$_2$NC$_4$H$_2$) to **4$_{Mo}$** or **4$_W$** in Et$_2$O gives M(NAr*)(CHCMe$_2$Ph)(Me$_2$Pyr) (M = Mo, **14$_{Mo}$**; M = W, **14$_W$**) (Scheme 3.11). Compounds **14$_{Mo}$** and **14$_W$** are not a pyridine adducts: ^{1}H NMR spectra of **14$_{Mo}$** and **14$_W$** show free pyridine unless they are thoroughly dried under vacuum. The ^{1}H NMR spectra of **14$_{Mo}$** and

$\mathbf{14_W}$ are broad at standard temperature. Variable temperature NMR studies show that at –40 °C the spectrum of $\mathbf{14_{Mo}}$ and $\mathbf{14_W}$ are sharp and all methyl and pyrrolide resonances are independent (Figure 3.9 and Figure 3.10). It is not possible to distinguish from these spectra whether the observed functionality is due to rotation about Mo-N_{pyr} bonds or the pyrrolide ligands switching between η^1 or η^5 binding modes. The $^1J_{CH}$ value for $\mathbf{14_{Mo}}$ is 130 Hz and for $\mathbf{14_W}$ is 126 Hz, which are observed at –40 °C. These values are typical for *syn* alkylidenes.

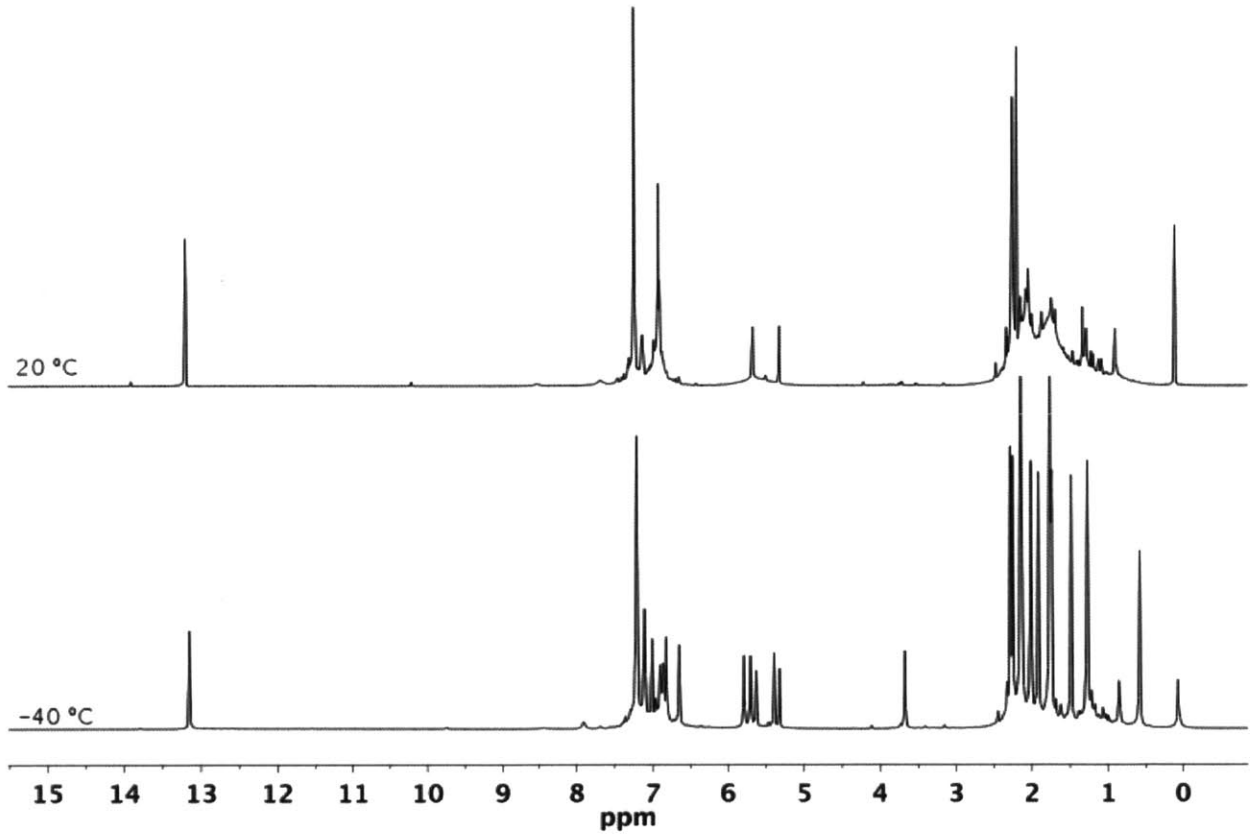

Figure 3.9. Variable temperature ^{1}H NMR spectra of Mo(NAr*)(CHCMe$_2$Ph)(Me$_2$Pyr)$_2$, $\mathbf{14_{Mo}}$.

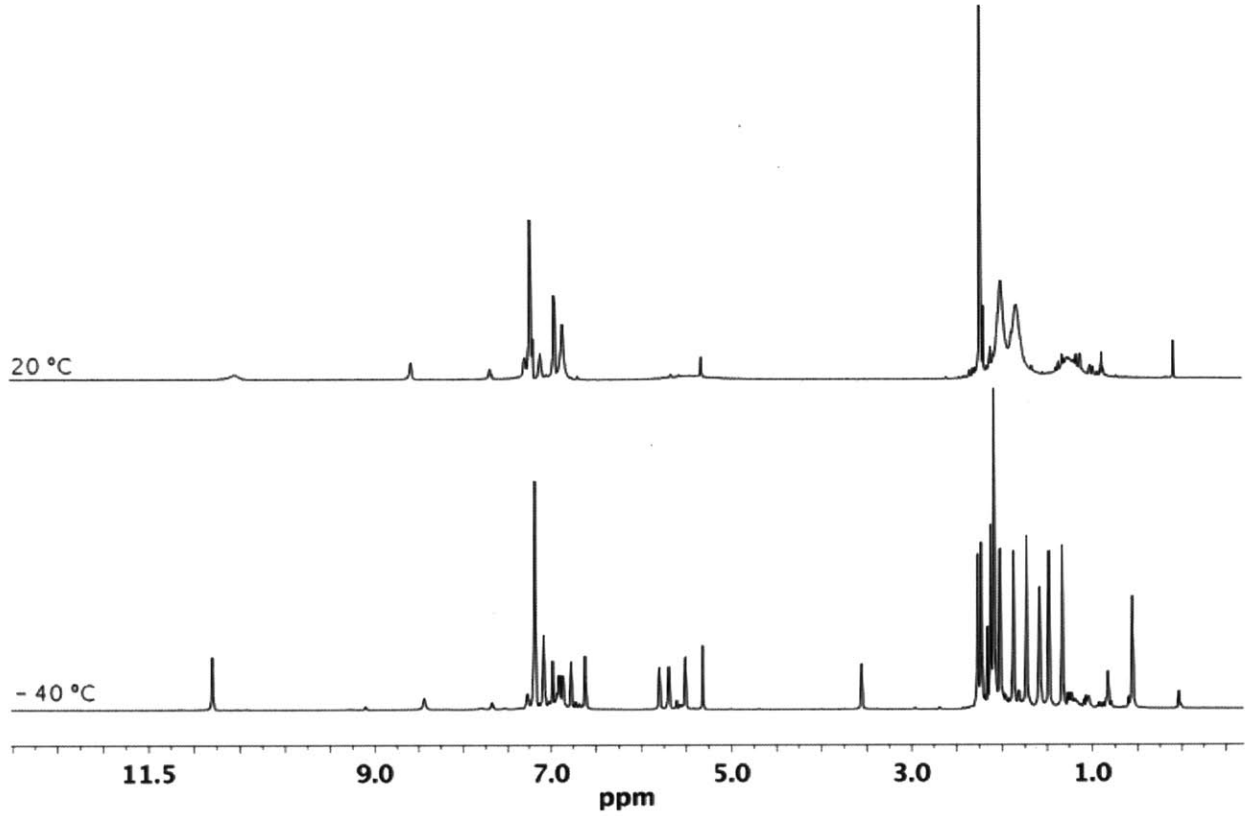

Figure 3.10. Variable temperature ^{1}H NMR spectra of W(NAr*)(CHCMe$_2$Ph)(Me$_2$Pyr)$_2$, $\mathbf{14_W}$.

C. Synthesis of Bisalkoxide Complexes

Synthesis of several types of bisalkoxide complexes was investigated. Mo(NAr*)(CHCMe$_2$Ph)(OAr′)$_2$ ($\mathbf{15_{Mo}}$, Ar′ = 2,6-Me$_2$C$_6$H$_3$) was first identified as an impurity in the reaction of one equivalent of HOAr′ with Mo(NAr*)(CHCMe$_2$Ph)(Me$_2$pyr)$_2$ ($\mathbf{14_{Mo}}$). An X-ray diffraction study was conducted on crystals obtained from the reaction mixture, and it was found that the crystal was $\mathbf{15_{Mo}}$. Compound $\mathbf{15_{Mo}}$ can be synthesized by reaction of Mo(NAr*)(CHCMe$_2$Ph)Cl$_2$(py) and two equivalents of LiOAr′. Notably, this compound is not a pyridine adduct.

The crystal structure of Mo(NAr*)(CHCMe$_2$Ph)(OAr′)$_2$ is typical for four-coordinate Mo alkylidene species (Figure 3.11). The alkylidene ligand is disordered over two positions, with 75 % in the *anti* configuration and 25 % in the *syn* configuration. The Mo=C25 bond length in the *anti* isomer is 1.950(3) while the Mo=C25a bond length of the *syn* isomer is 1.752(8). The shorter bond length of the *syn* isomer is indicative of the agostic interaction that is present in the

syn isomer, but not the *anti*. In solution, only the *anti* isomer is visible ($^1J_{CH}$ = 155 Hz). The geometry about Mo is distorted tetrahedral. Otherwise, the bond lengths and angles are typical for four-coordinate imido alkylidene complexes.

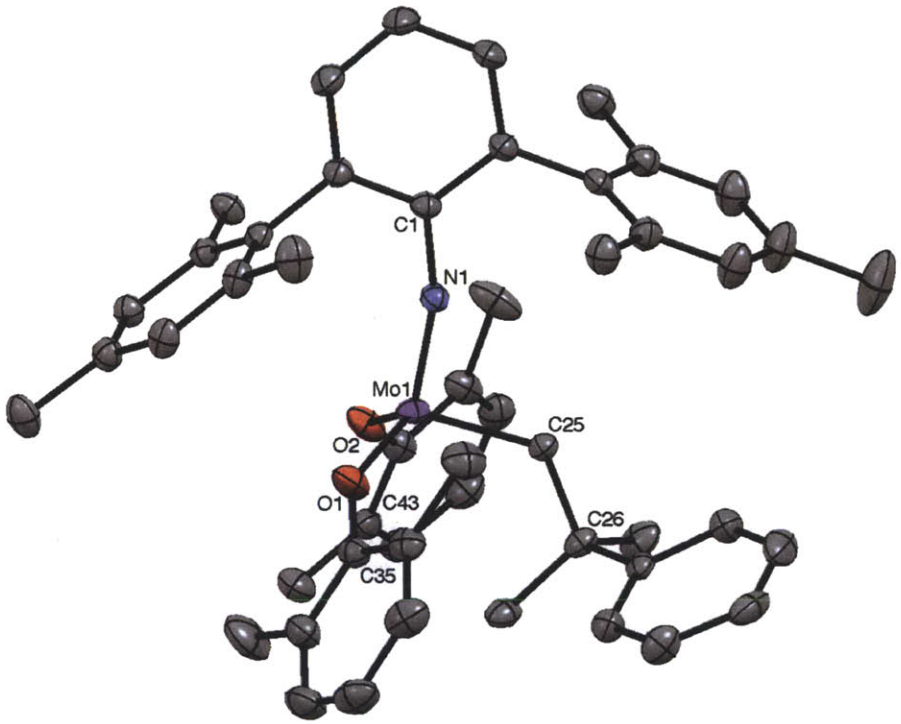

Figure 3.11. Thermal ellipsoid (50 %) representation of Mo(NAr*)(CHCMe$_2$Ph)(OAr')$_2$ (15$_{Mo}$). The alkylidene ligand is disordered with 75 % in the anti configuration (pictured), and 25 % in the syn configuration. Hydrogen atoms and minor component of the disorder are omitted for clarity. Selected bond lengths: Mo1-N1 = 1.7329(16), Mo1-O1 = 1.9118(15), Mo1-O2 = 1.9332(14), Mo1-C25 = 1.950(3) (*anti*), Mo1-C25A = 1.752(8) (*syn*). Selected bond angles (both): N1-Mo1-O1 = 116.90(7), N1-Mo1-O2 = 111.53(7), O1-Mo1-O2 = 114.60(6), C1-N1-Mo1 = 164.43(14), C43-O2-Mo1 = 137.26(14), C35-O1-Mo1 = 147.73(15). Selected bond angles (*anti*): N1-Mo1-C25 = 95.49(10), O1-Mo1-C25 = 110.13(9), O2-Mo1-C25 = 105.95(9), O2-Mo1-C25 = 105.95(9), C26-C25-Mo1 = 126.7(2), O2-Mo1-C25 = 105.95(9). Selected bond angles (*syn*): N1-Mo1-C25A = 120.5(3), C25A-Mo1-O1 = 95.8(3), C25A-Mo1-O2 = 95.0(3), C26A-C25A-Mo1 = 146.5(8), C26A-C25A-Mo1 = 146.5(8).

Attempts to isolate other bisalkoxide species have been unsuccessful. Reaction of Mo(NAr*)(CHCMe$_2$Ph)Cl$_2$(py) with excess LiO^{t}Bu showed formation a new product by ^{1}H NMR spectroscopy, but it could not be isolated. Multiple attempts have been made towards the synthesis bisalkoxide compounds containing fluorinated alkoxide ligands. Reaction of Mo(NAr*)(CHCMe$_2$Ph)Cl$_2$(py) with excess LiOCMe(CF$_3$)$_2$ or LiOCMe$_2$(CF$_3$) showed

Mo(NAr*)(CHCMe$_2$Ph)Cl(OR)(py) (R = CMe$_2$(CF$_3$) or CMe(CF$_3$)$_2$) as the major product, even with excess alkoxide or heating to 80 °C. This could be due to either steric or electronic reasons: either the crowded environment about Mo does not allow a second chloride substitution or once intermediate Mo(NAr*)(CHCMe$_2$Ph)Cl(OR)(py) (R = CMe$_2$(CF$_3$) or CMe(CF$_3$)$_2$) is formed, substitution of the alkoxide ligand is favored over the chloride ligand, making the process degenerate. Reaction of Mo(NAr*)(CHCMe$_2$Ph)(Me$_2$Pyr)$_2$ with two equivalents of HOCMe(CF$_3$)$_2$ show a mixture of 3 alkylidene products after 16 h. Reaction of Mo(NAr*)(CHCMe$_2$Ph)(Pyr)$_2$(py) with two equivalents of HOCMe(CF$_3$)$_2$ show a mixture of the MAP species and a new product (65 % new species) even after 4 d at 80 °C. The new species looks to be a pyridine adduct as well, as determined by pyridine resonances shifted from that free pyridine in the ^{1}H NMR spectrum.

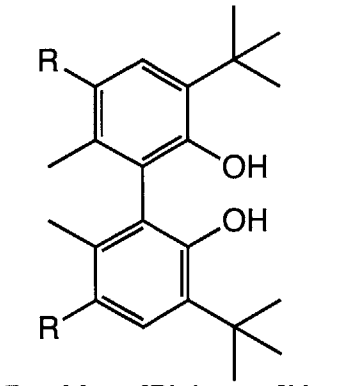

Figure 3.12. [BiphentBu]H$_2$ and [BiphenCF$_3$]H$_2$ ligands.

Isolation of compounds containing chelating diolates has been attempted. Biphen$_{CF3}$ and biphen$_{tBu}$ were chosen as diolate ligands (Figure 3.12). Reaction of [biphen$_{tBu}$]H$_2$ or [biphen$_{CF3}$]H$_2$ with excess NEt$_3$ and one equivalent of Mo(NAr*)(CHCMe$_2$Ph)Cl$_2$(py) in THF showed mostly free diol after 16 h. A stronger base was then employed to deprotonate the ligand. Reaction of [biphen$_{tBu}$]H$_2$ with two equivalents of n-butyllithium in C$_6$D$_6$ shows clean conversion to [biphen$_{tBu}$]Li$_2$. Addition of Mo(NAr*)(CHCMe$_2$Ph)Cl$_2$(py) followed by heating to 80 °C for 16 h, shows complete conversion of Mo(NAr*)(CHCMe$_2$Ph)Cl$_2$(py) and the presence of one new alkylidene. Pyridine appears to be bound in the product, as determined by resonances

shifted from that of free pyridine in the ^{1}H NMR spectrum, but attempts towards isolating the product were unsuccessful. When n-Butyllithium was added to [Biphen$_{CF3}$]H$_2$ in C_6D_6, no alcohol signal remained by ^{1}H NMR spectroscopy, upon which Mo(NAr*)(CHCMe$_2$Ph)Cl$_2$(py) was added. Only starting material was observed in the ^{1}H NMR spectrum after 16 h at 80 °C. [Biphen$_{CF3}$]H$_2$ likely decomposed before addition of Mo(NAr*)(CHCMe$_2$Ph)Cl$_2$(py) since it has been reported that [Biphen$_{CF3}$]H$_2$ is unstable in the presence of n-butyllithium.[16]

IV. Synthesis of MonoAlkoxide Pyrrolide (MAP) Complexes

A. Synthesis of MAP Complexes Containing an Unsubstituted Pyrrolide Ligand

MonoAlkoxide Pyrrolide (MAP) catalysts have provided many interesting results in the past few years, especially in the area of *Z* selectivity.[1 - 5] We were interested in synthesizing MAP complexes with the NAr* ligand as well.

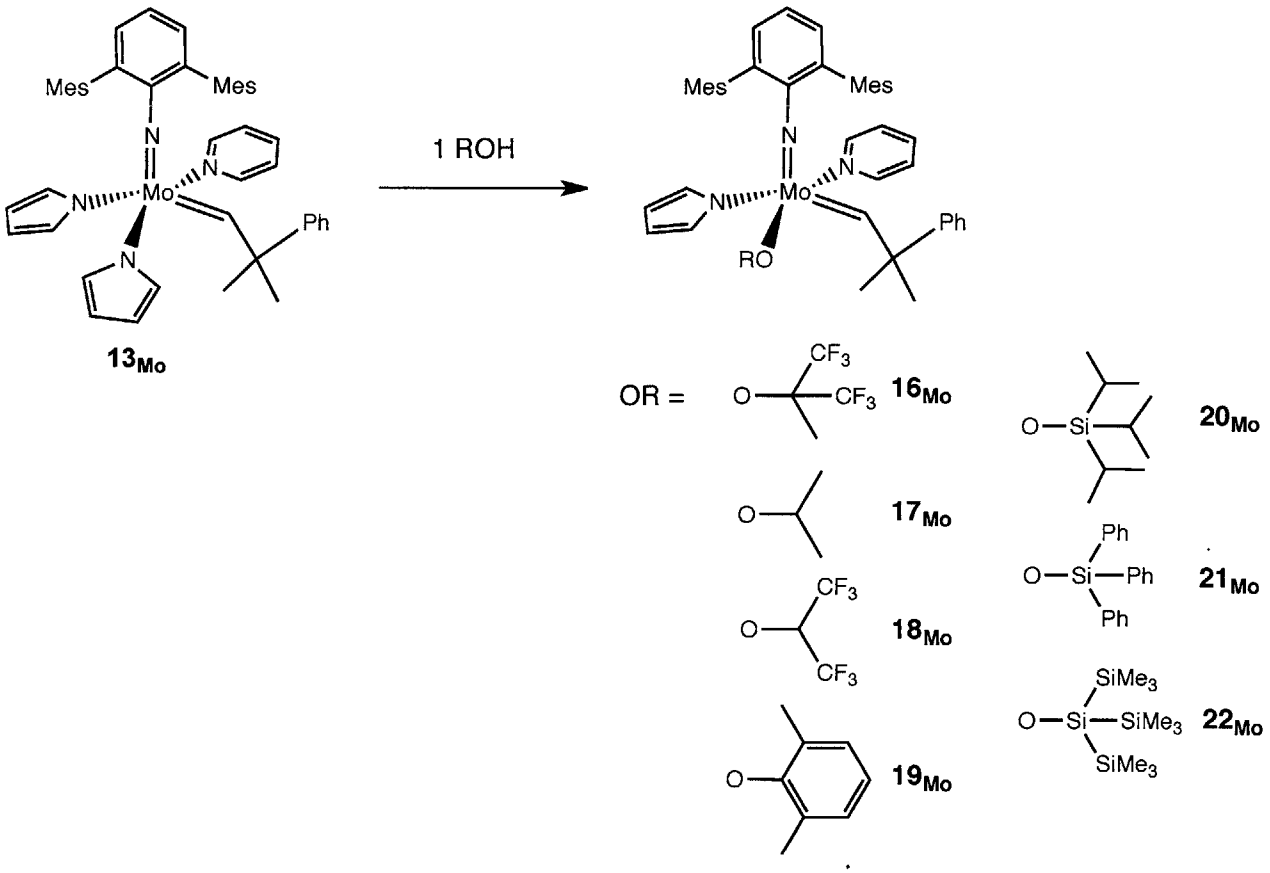

Scheme 3.12. Synthesis of MAP complexes with unsubstituted pyrrolide ligands.

MAP complexes are formed upon addition of one molar equivalent of an alcohol to Mo(NAr*)(CHCMe$_2$Ph)(Pyr)(OR)(Py) (**16$_{Mo}$**, R = CMe(CF$_3$)$_2$; **17$_{Mo}$**, R = ^{i}Pr; **18$_{Mo}$**, R = CH(CF$_3$)$_2$; **19$_{Mo}$**, R = 2,6-Me$_2$C$_6$H$_3$; **20$_{Mo}$**, R = Si^{i}Pr$_3$; **21$_{Mo}$**, R = SiPh$_3$; **22$_{Mo}$**, R = Si(SiMe$_3$)$_3$). The pyridine ligand remains bound in all cases. Compounds **16$_{Mo}$** – **20$_{Mo}$** all show *anti* alkylidenes in solution, as determined by observation of the $^1J_{CH}$ value by ^{1}H NMR spectroscopy. Although it is unusual for the *anti* alkylidene isomer to the major isomer in 4-coordinate group 6 imido alkylidene complexes it has been observed previously for other 5-coordinate, base-stabilized species.[17]

Synthesis of MAP complexes that contain more sterically demanding alkoxide ligands was attempted as well. Although reaction of HOAr* with **13$_{Mo}$** showed a new alkylidene species in the ^{1}H NMR spectrum, both starting materials remained in solution after heating to 80 °C for 5 d. Reaction of one equivalent of Ph$_3$COH with **13$_{Mo}$** provides Mo(NAr*)(CHCMe$_2$Ph)(Pyr)(OCPh$_3$), which can be observed by ^{1}H NMR spectroscopy, but attempts to isolate it were unsuccessful. Mo(NAr*)(CHCMe$_2$Ph)(Pyr)(OCPh$_3$) is not a pyridine adduct. It is interesting to compare **21$_{Mo}$**, which is a pyridine adduct, and Mo(NAr*)(CHCMe$_2$Ph)(Pyr)(OCPh$_3$) since the only difference between the two is the atom bonded to oxygen. The pK_a of HOCPh$_3$ is 12.7 and the pK_a of HOSiPh$_3$ is 10.8.[18] Based on these values, the OSiPh$_3$ ligand should be more electron-withdrawing than the OCPh$_3$ ligand, making it more favorable for pyridine to bind to the complex. The O-C bond length in HOCPh$_3$ is 1.437 Å,[19] while the O-Si bond length is 1.640 Å,[20] making the metal in **21$_{Mo}$** more sterically accessible for pyridine to bind. Thus, both steric and electron influences facilitate the binding of pyridine to **21$_{Mo}$** over Mo(NAr*)(CHCMe$_2$Ph)(Pyr)(OCPh$_3$).

The pyridine ligand stabilizes the alkylidene complexes and brings the electron count to 16. Thus, in pyridine adducts the electrophilicity of the metal is decreased and an open coordination site is blocked, which hinders the reactivity toward olefins both for electronic and steric reasons. Therefore, pyridine-bound compounds are not desirable as olefin metathesis catalysts (unless pyridine dissociates). Lewis acids were employed towards the goal of removing pyridine and isolating base-free alkylidene complexes. Of Lewis acids BF$_3$, BPh$_3$, and B(C$_6$F$_5$)$_3$, it was found that although BF$_3$ and BPh$_3$ sometimes cause decomposition, B(C$_6$F$_5$)$_3$ could be used to abstract pyridine with causing further decomposition. Because of this, B(C$_6$F$_5$)$_3$ was employed generally towards the removal of pyridine. Upon addition of one equivalent of

$B(C_6F_5)_3$ to pyridine adducts, the Lewis pair $B(C_6F_5)_3NC_5H_5$ formed immediately, which can be identified by its ^1H and ^{19}F NMR spectrum. Unfortunately, the similar solubilities of the pyridine-free 14e species and $B(C_6F_5)_3NC_5H_5$ prevented separation and isolation of pyridine-free alkylidene complexes. Clean conversion to one pyridine-free alkylidene species was not observed when $B(C_6F_5)_3$ was added to $\mathbf{16_{Mo}} - \mathbf{20_{Mo}}$, so further characterization of the target MAP species *in situ* was not feasible. However, there were only two alkylidene resonances in ^1H NMR spectra of base-free $\mathbf{21_{Mo}}$ and $\mathbf{22_{Mo}}$ ($\mathbf{21_{Mo}}$' and $\mathbf{22_{Mo}}$', respectively). In each case the two resonances were confirmed as being those of *syn* and *anti* alkylidenes on the basis of the $^1J_{CH}$ values. For $\mathbf{21_{Mo}}$' $K_{eq} = 2.0$ and for $\mathbf{22_{Mo}}$' $K_{eq} = 2.3$ ($K_{eq} = [syn]/[anti]$).

B. Synthesis of MAP Complexes Containing a 2,5-Dimethylpyrrolide Ligand

Since pyridine is not bound to $\mathbf{14_{Mo}}$ and $\mathbf{14_W}$, focus shifted towards their use as a starting material for the synthesis of four-coordinate MAP complexes. MAP complexes M(NAr*)(CHCMe$_2$Ph)(Me$_2$pyr)(O^{t}Bu) ($\mathbf{23_{Mo}}$, M = Mo; $\mathbf{23_W}$, M = W), M(NAr*)(CHCMe$_2$Ph)(Me$_2$pyr)[OCMe(CF$_3$)$_2$] ($\mathbf{24_{Mo}}$, M = Mo; $\mathbf{24_W}$, M = W), M(NAr*)(CHCMe$_2$Ph)(Me$_2$pyr)(OSiPh$_3$) ($\mathbf{25_{Mo}}$, M = Mo; $\mathbf{25_W}$, M = W), and M(NAr*)(CHCMe$_2$Ph)(Me$_2$pyr)(OAr') ($\mathbf{26_{Mo}}$, M = Mo; $\mathbf{26_W}$, M = W) were synthesized by addition of one equivalent of alcohol to $\mathbf{14_{Mo}}$ or $\mathbf{14_W}$. Compounds **23** – **26** were extremely soluble in non-polar organic solvents, but could be recrystallized from MeCN. There is no evidence for any reaction or coordination of MeCN with compounds **23** – **26** at ambient temperature. Compounds **23** – **26** are all mixtures of *syn* and *anti* alkylidene isomers in solution at ambient temperature: both isomers are detected in ^1H NMR spectra.

W(NAr*)(CHCMe$_2$Ph)(Me$_2$pyr)(O^{t}Bu) ($\mathbf{23_W}$) has been studied by X-ray crystallography (Figure 3.13). The crystal exhibited whole molecule disorder, with the major component representing 90 % of the electron density. Discussion of the structure will refer to only the major component. The alkylidene ligand is in the *syn* orientation with the substituents pointed toward the imido ligand. The W1-C1 bond length is 1.875(2) Å, the W1-N1-C21 angle is 173.4(3) °, and the C2-C1-W1 angle is 147.33(19) °, all typical of Group 6 MAP complexes. When viewed along the C21-N1-W1 axis, one mesityl group covers the alkoxide and one mesityl group falls between the pyrrolide and alkylidene ligands. The N1-W1-C1-C2 torsion angle is 12.25 °.

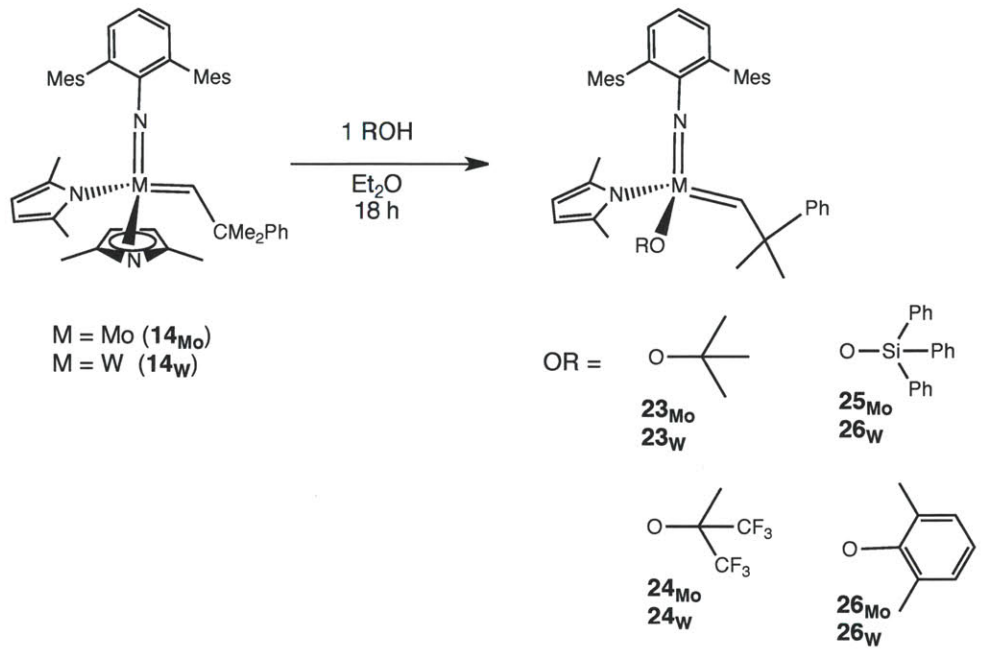

Scheme 3.13. Synthesis of MAP complexes with 2,5-dimethylpyrrolide ligands.

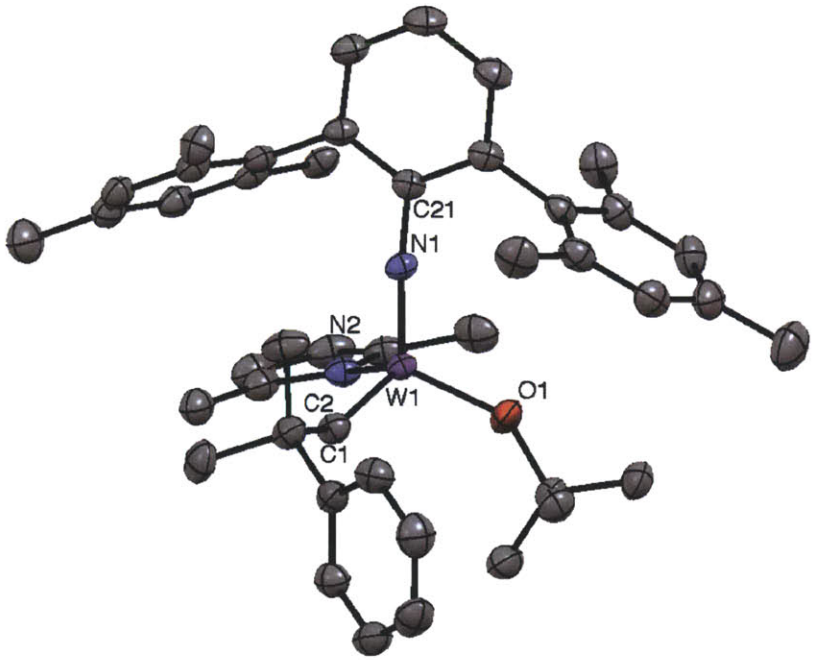

Figure 3.13. Crystal structure of W(NAr*)(CHCMe$_2$Ph)(Me$_2$pyr)(O^{t}Bu), 23$_w$, in thermal ellipsoid representation at the 50 % probability level. Hydrogen atoms and minor disorder component are omitted for clarity. Selected bond lengths (Å): C1-W1 = 1.875(2), W1-N1 = 1.750(2), W1-O1 = 1.8682(19), W1-N2 = 2.033(2). Selected bond angles (°): C2-C1-W1 = 147.33(19), N1-W1-O1 = 115.59(14), N1-W1-C1 = 106.04(16), O1-W1-C1 = 109.35(10), N1-W1-N2 = 111.05(13), O1-W1-N2 = 110.03(10), C1-W1-N2 = 104.07(11), C21-N1-W1 = 173.4(3).

CONCLUSIONS

A new synthetic route was developed in order to install the NAr* ligand at Mo and W. This strategy takes advantage of mixed-imido compounds that contain both t-butylimido and Ar* imido ligands. The more basic t-butylimido ligand can be selectively protonated with HCl-based acids during the alkylidene formation synthetic step, which avoids sacrificing an NAr* ligand and the difficult purification from triflate salts that are characteristic of the traditional route to alkylidene complexes. Use of HCl-based acids, especially pyridine hydrochloride, is more economical, and more convenient for dry box use. Use of pyridine hydrochloride as an acid source for alkylidene synthesis has been expanded by other Schrock group members to allow the synthesis of long-sought tungsten alkyl imido alkylidene complexes.

Many types of alkylidene complexes containing the Ar*imido ligand have been synthesized including dichlorides, monoalkoxide monochlorides, bispyrrolides, and MAP complexes. Complexes containing chloride ligands or unsubstituted pyrrolides are pyridine adducts. Attempts towards removing pyridine with a Lewis acid were unsuccessful. Complexes containing the 2,5-dimethylpyrrolide ligand are pyridine-free and a variety of MAP complexes were synthesized.

These compounds provide a starting point to understanding how steric hindrance at different places in the molecule affect olefin metathesis catalysts. Understanding how steric hindrance at the imido ligand contrasts to steric hindering ligands at the alkoxide in terms of catalyst structure, reactivity, and selectivity is important to the development of new olefin metathesis catalysts. Deeper understanding of structure-function relationships is key to expanding the boundaries of what is possible with olefin metathesis catalysis.

EXPERIMENTAL

General Considerations

All air-sensitive manipulations were performed under nitrogen atmosphere in a drybox or an air-free dual-manifold Schlenk line. All glassware was oven-dried and allowed to cool under vacuum before use. NMR spectra were obtained on Varian 300 MHz, Varian 500 MHz, Bruker 400 MHz, or Bruker 600 MHz spectrometers. ^{1}H and ^{13}C NMR spectra are reported in ppm (parts per million) relative to tetramethylsilane, and referenced to residual $^{1}H/^{13}C$ signals of the deuterated solvent (^{1}H, benzene 7.16, dichloromethane 5.32; ^{13}C, benzene 128.39, dichloromethane 54.00). ^{19}F NMR spectra are reported in ppm relative to trichlorofluoromethane and referenced using an external standard of fluorobenzene (-113.15 ppm). Diethyl ether, toluene, tetrahydrofuran, pentane, benzene, MeCN, DME, and dichloromethane were sparged with nitrogen and passed through activated alumina. Alternatively, dimethoxyethane was dried over Na/benzophenone. All solvents were stored over 4 Å molecular sieves. Pyridiniumchloride derivatives were prepared by addition of excess 2.0 M HCl in diethyl ether to a hexane solution of the pyridine derivative, followed by isolation of the precipitate on a fritted filter. HCl solution in Et_2O was prepared by bubbling gaseous HCl through Et_2O at atmospheric pressure. LiPyr and $LiMe_2Pyr$ were prepared by addition of one equivalent of n-Butyllithium to a cold pentane solution of pyrrole or 2,5-dimethylpyrrole, and the solids were collected on a frit, washed with pentane and dried *in vacuo*. HOAr*,[21] 2,6-dimesitylaniline,[8b] $Mo(N^tBu)_2Cl_2(DME)$,[22] and $W(N^tBu)_2Cl_2(py)_2$[23] were prepared according to literature procedures. All other reagents were used as received.

$Mo(NAr^*)(N^tBu)Cl(NH^tBu)$ (1_{Mo}). A 1.6 M n-Butyllithium solution (2.7 mL, 4.4 mmol) was added to a solution of Ar^*NH_2 (1.45 g, 4.41 mmol) in 15 mL pentane. The mixture was stirred for 45 m after which time it was added to a −20 °C solution of $Mo(N\text{-}t\text{-}Bu)_2Cl_2(DME)$ (1.76 g, 4.42 mmol) in 50 mL of 2:1 Et_2O/pentane and the mixture was stirred for 30 m. The mixture became yellow and precipitate formed. Triethylamine (2 mL, 14 mmol) was added and the mixture stirred for 14 h. The volatiles were removed *in vacuo* and the solid was extracted with pentane. The extract was filtered through a glass-frit covered with a pad of Celite. The volatiles

were removed from the filtrate *in vacuo* and the yellow solid was washed with cold pentane and collected on a filter. The filtrate was concentrated and stored at −20 °C to afford a second crop; total yield 1.83 g (69 %): ^{1}H NMR (C_6D_6) δ 7.274 (s, 1H, N*H*), 6.916 – 6.899 (overlapping signals, 7H, Ar*H*), 2.267 (s, 6H, MesCH_3), 2.258 (s, 6H, MesCH_3), 2.188 (s, 6H, MesCH_3), 1.075 (s, 9H, C(CH_3)), 1.052 (s, 9H, C(CH_3)); ^{13}C{^{1}H} NMR (C_6D_6) δ 154.7, 137.6, 137.4, 137.0, 136.8, 136.4, 129.8, 129.6, 129.1, 128.7, 125.8 (Ar*C*), 71.2 (Mo=N*C*Me$_3$), 57.6 (Mo-NH*C*Me$_3$), 32.3, 31.8, 21.59, 21.56, 21.3 (*C*H$_3$). Anal. Calcd for $C_{32}H_{44}ClMoN_3$: C, 63.83; H, 7.37; N, 6.98. Found: C, 63.56; H, 7.11; N, 6.61.

W(NAr*)(N^{t}Bu)Cl(NH^{t}Bu) ($\mathbf{1_W}$). A solution of n-butyllithium in hexane (2.8 M, 4.5 mL, 12.6 mmol) was added to a stirred solution of H_2NAr* (4.16 g, 12.6 mmol) in 15 mL Et_2O; the resulting solution immediately became yellow. After 15 minutes, the solution of LiNHAr* was added to a stirred solution of W(N^{t}Bu)$_2$Cl$_2$(py)$_2$ (7.01 g, 12.6 mmol) in 100 mL Et_2O at −25 °C. After 30 m, NEt_3 was added (10 mL, 70 mmol). After stirring the mixture for 16 h, the volatiles were removed *in vacuo*. The resulting solid was extracted with pentane and the mixture was filtered through a frit containing a layer of Celite. The volume of the filtrate was reduced *in vacuo* and a beige precipitate formed. The beige solid was collected on a frit and washed with 3 x 1 mL cold pentane. The filtrate was concentrated, cooled to −25 °C, a second crop of beige precipitate formed and was collected in the same manner. Four crops of beige solid were collected for a total yield of 6.701 g, 77 %: ^{1}H NMR (C_6D_6) δ 6.992 (d, 2H, J_{HH} = 7.5 Hz, meta aniline), 6.919 – 6.890 (overlapping signals, 5H, para aniline and aromatic mesityl), 6.299 (s, 1H, N*H*^{t}Bu), 2.254 (s, 12H, Mes*Me*-ortho), 2.194 (s, 6H, Mes*Me*-para), 1.113 (s, 9H, N^{t}Bu), 1.038 (s, 9H, N^{t}Bu); ^{13}C {^{1}H} NMR (C_6D_6) δ 137.7, 137.5, 136.7, 136.6, 129.4, 129.3, 128.9, 125.1 (Aromatic), 68.3, 56.6 (tertiary), 33.0, 32.6 (tBu), 21.6, 21.2 (Mesityl Me). Anal. Calcd for $C_{32}H_{44}ClN_3W$: C, 55.70; H, 6.43; N, 6.09. Experimental: C, 55.78; H, 6.42; N, 6.08.

^{1}H NMR spectrum of $\mathbf{1_W}$ in C_6D_6:

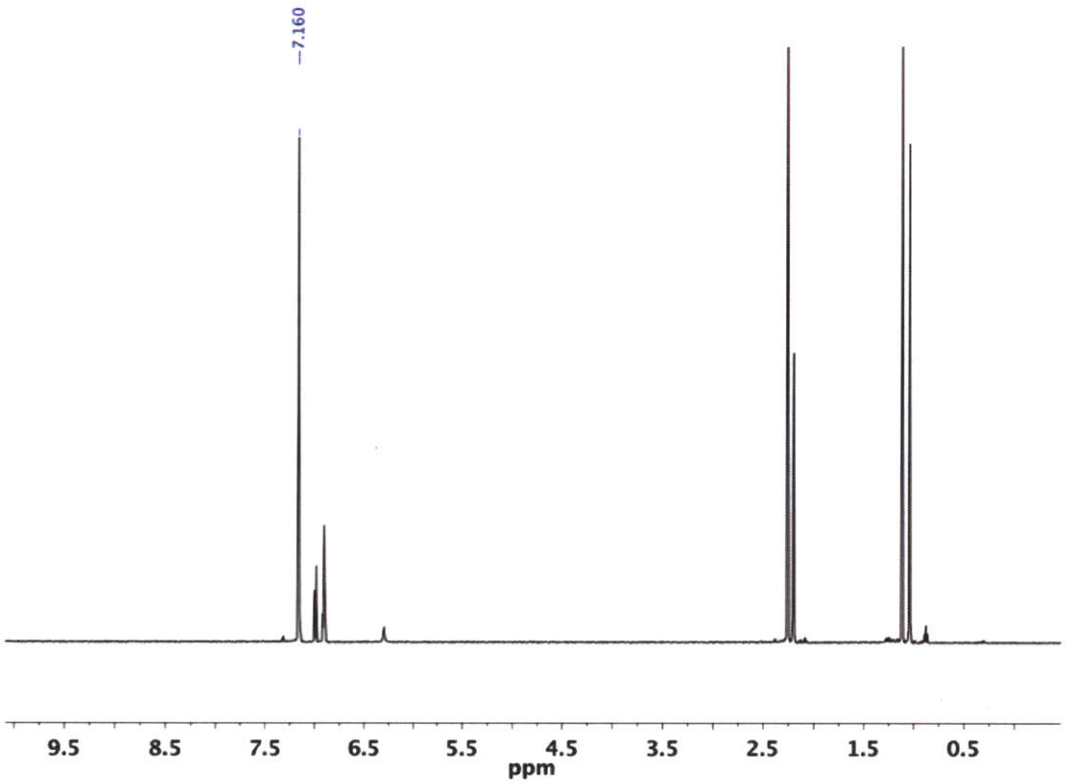

Mo(NAr*)(N^{t}Bu)Cl$_2$(NH$_2$^{t}Bu) ($\mathbf{2_{Mo}}$). Solid 2,6-lutidinium chloride (0.485 g, 3.38 mmol), was added to a −20 °C solution Mo(NAr*)(N^{t}Bu)Cl(NH^{t}Bu) (561 mg, 0.931 mmol) in 60 mL of a 3:1 pentane:toluene solution. The mixture was stirred 16 h and became orange. The reaction mixture was filtered through a fritted glass filter with a pad of Celite. The volatiles were removed *in vacuo* to leave an analytically pure orange powder; yield 1.746 g (90 %): ^{1}H NMR (C_6D_6) δ 6.940 – 6.874 (overlapping signals, 7H, Ar*H*), 2.690 (s, 2H, N*H*$_2$), 2.326 (s, 12H, $C_{ortho}(CH_3)$), 2.171 (s, 6H, $C_{para}(CH_3)$), 1.209 (s, 9H, C(C*H*)$_3$), 0.993 (s, 9H, C(C*H*)$_3$); ^{13}C{^{1}H} NMR (C_6D_6) δ 155.3, 143.0, 138.2, 136.9, 130.2, 129.0, 128.7 (Ar-*C*), 52.9 (Mo=N*C*Me$_3$), 31.6 (Ar-*C*H$_3$), 30.4 (NH$_2$*C*Me$_3$), 29.7 (Ar-*C*H$_3$), 22.4 (C(*C*H$_3$)$_3$), 21.1 (C(*C*H$_3$)$_3$). Anal. Calcd for $C_{32}H_{45}Cl_2MoN_3$: C, 60.19; H, 7.10; N, 6.58. Found: C, 60.06; H, 6.92; N, 6.49.

W(NAr*)(N^{t}Bu)Cl$_2$(NH$_2$^{t}Bu) ($\mathbf{2_W}$). 2,6-LutidineHCl (0.427 g, 2.97 mmol) was added in one portion to a −25 °C solution of W(NAr*)(N^{t}Bu)Cl(NH-t-Bu), **5** (2.035 g, 2.95 mmol), in 50 mL Et$_2$O. The mixture was stirred 16 h, and the volatiles were removed *in vacuo*. The residue was

extracted with benzene and filtered through a layer of Celite on a frit. The volatiles were removed *in vacuo* from the filtrate. The remaining solid was used directly for the synthesis of W(NAr*)(N^{t}Bu)(CH_2CMe_2Ph)$_2$ without further purification (2.110 g): ^{1}H NMR (C_6D_6) δ 7.010 – 6.995 (overlapping signals, 3H), 2.652 (br s, 2H, NH_2^tBu), 2.328 (s, 12H, mesityl ortho CH_3), 2.182 (s, 6H, mesityl para, CH_3), 1.146 (s, 9H, CMe_3), 1.018 (s, 9H, CMe_3).

Mo(NAr*)(N^{t}Bu)(CH_2CMe_2Ph)$_2$ (3_{Mo}). A 0.5 M solution Me_2PhCCH_2MgCl in diethylether (11 mL, 5.5 mmol) was added to a −20 °C solution of Mo(NAr*)(N^{t}Bu)Cl_2(NH_2^tBu) (1.76 g, 2.75 mmol) in 100 mL Et_2O. Over a period of 16 h, a precipitate formed and the orange solution became yellow. The volatiles were removed *in vacuo*. The solids were extracted with pentane and filtered through a glass-fritted filter with a pad of Celite. The filtrate volume was reduced *in vacuo* and put into a freezer at −20 °C. Four crops of yellow microcrystalline product were collected; total yield 2.31 g (81 %): ^{1}H NMR (C_6D_6) δ 7.229, 7.222 (overlapping s, 8H, Ar-H), 7.097 (sextet, 2H, J_{HH} = 4Hz, Ar-H), 6.916 (s, 3H, Ar-H), 6.872 (s, 4H, Ar-H), 3.306 (d, $^2J_{HH}$ = 13 Hz, 2H, MoCH_2), 2.277 (s, 12H, C_{ortho}(CH_3)), 2.189 (s, 6H, C_{para}(CH_3)), 1.307 (s, 6H, CMe_2Ph), 1.156 (s, 9H, C(CH_3)$_3$), 1.095 (s, 6H, CMe_2Ph), 0.578 (d, $^2J_{HH}$ = 13 Hz, 2H, MoCH_2); ^{13}C{^{1}H} NMR (C_6D_6) δ 155.4, 153.9, 138.3, 136.9, 136.7, 136.5, 130.4, 129.2, 128.7, 128.6, 126.3, 125.9, 124.9 (Ar), 79.8, 70.0, 40.1, 33.7, 32.6, 32.5, 21.7, 21.5. Anal. Calcd for $C_{48}H_{60}MoN_2$: C, 75.76; H, 7.95; N, 3.68. Found: C, 75.38; H, 7.73; N, 3.70.

W(NAr*)(N^{t}Bu)(CH_2CMe_2Ph)$_2$ (3_W). A 0.5 M solution of $ClMgCH_2CMe_2Ph$ in hexane (11.6 mL, 5.80 mmol) was added to a stirring solution of W(NAr*)(N^{t}Bu)Cl_2(NH_2^tBu), **2$_W$** (2.110 g, 2.90 mmol), in 100 mL Et_2O at −25 °C. The mixture was warmed to room temperature and stirred for 16 h. The volatiles were removed *in vacuo*. The remaining solids were extracted with pentane and filtered through Celite on a frit. The filtrate volume was reduce *in vacuo* and cooled to −25 °C. A yellow precipitate formed and was collected on a frit. The filtrate volume was reduced *in vacuo* to collect three crops in a similar manner; total yield 1.666 mg, 68 %: ^{1}H NMR (C_6D_6) δ 7.238 - 7.185 (overlapping signals, 8H), 7.103 – 7.069 (m, 2H), 6.983 – 6.966 (overlapping signals, 2H), 6.931 – 6.902 (overlapping signals, 1H), 6.877 (s, 4H, mesityl Ar*H*), 2.267 (s, 12H, mesityl ortho CH_3), 2.187 (s, mesityl para, CH_3) and 2.159 (one half a doublet visible, MoCH_2, 8H integrated together with previous signal), 1.281 (s, 6H, $MoCH_2C$*Me*$_2$Ph),

1.192 (s, 9H, NCMe_3), 1.085 (s, 6H, $MoCH_2CMe_2Ph$), 0.332 (d, 2H, $MoCH_2$); ^{13}C {^1H} NMR (CD_2Cl_2) δ 125.2, 138.2, 137.1, 136.6, 136.4, 129.9, 128.7, 128.4, 126.1, 125.7, 123.8, 89.5, 68.2, 40.4, 33.9, 33.2, 32.4, 21.4, 21.3. Anal. Calcd for $C_{48}H_{60}WN_2$: C, 67.92; H, 7.12; N, 3.30. Found: C, 68.22; H, 7.06; N, 3.21.

^1H NMR spectrum of $\mathbf{3_W}$ in C_6D_6:

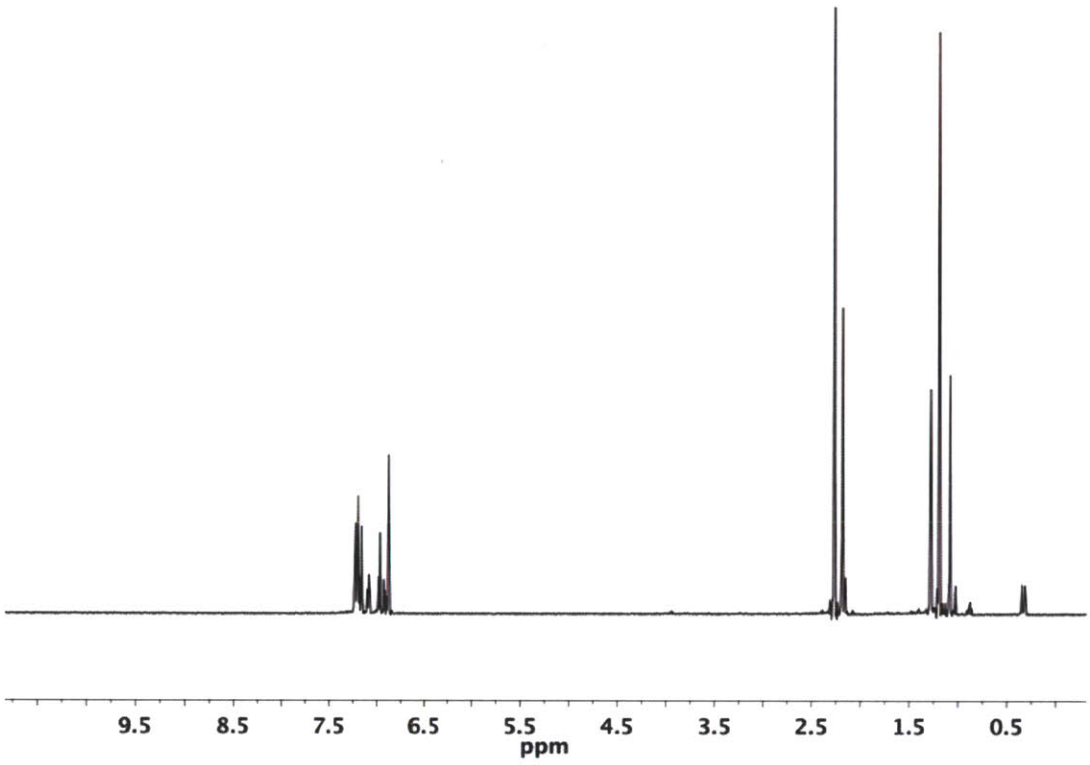

Mo(NAr*)(CHCMe$_2$Ph)Cl$_2$(py) (4_{Mo}). PyridineHCl (500 mg, 3.08 mmol) was added as a solid to a cold (−20 °C) suspension of Mo(NAr*)(N^{t}Bu)(CH_2CMe_2Ph)$_2$ (483 mg, 0.635 mmol) in 30 mL of a 2:1 mixture of pentane:dimethoxyethane. The mixture was stirred 16 h at room temperature over which time a light yellow precipitate formed. The volatiles were removed *in vacuo*. The mixture was extracted with benzene and filtered through a pad of Celite on a glass-fritted filter. The benzene was removed *in vacuo* from the filtrate. The yellow solid was washed with cold pentane and collected on a frit; yield 775 mg (78 %). Crystals for X-ray diffraction were grown by slow diffusion of pentane into a toluene solution: ^1H NMR (CD_2Cl_2, 20 °C) δ 12.606 (s, 1H, Mo=CH, $^1J_{CH}$=151 Hz), 8.149 (d, 2H, J_{HH} = 5 Hz, py-H(2,6)), 7.749 (t, 1H, J_{HH} = 7.5 Hz), 7.348 (t, 1H, J_{HH} = 7.5 Hz, Ar—H), 7.150 – 7.085 (overlapping signals, 6H, Ar-H),

7.009 (s, 2H, MesAr-H), 6.960 – 6.944 (overlapping signals, 3H, Ar-H), 6.755 (s, 2H, MesAr-H), 2.281 (s, 6H, $MesCH_3$), 2.055 (s, 6H, $MesCH_3$), 1.663 (br s, 6H, $MesCH_3$), 1.443 (s, 3H, $MoCHCMe_2Ph$), 1.357 (s, 3H, $MoCHCMe_2Ph$); $^{13}C\{^1H\}$ NMR (CD_2Cl_2, 20 °C) δ 329.4 (Mo=C), 154.8, 148.3, 139.6, 138.2, 137.4, 136.7, 136.2, 129.5, 129.4, 129.1, 129.1, 128.8, 128.5, 126.6, 126.3, 125.1, 118.5 (Aryl), 51.7 ($MoCHCMe_2Ph$), 27.8, 27.0 ($MoCHCMe_2Ph$), 21.5, 21.4, 20.7, 20.3 (MesMe). Anal. Calcd for $C_{39}H_{42}Cl_2MoN_2$: C, 66.38; H, 6.00; N, 3.97. Found: C, 66.08; H, 5.96; N, 3.85.

Mo(NAr*)(CHCMe$_2$Ph)Cl$_2$(3,5-Lut) (5_{Mo}). Solid 3,5-Lutidinium chloride (57 mg, 0.40 mmol) was added to a solution of Mo(NAr*)(N^{t}Bu)(CH_2CMe_2Ph)$_2$ (99 mg, 0.13 mmol) in 8 mL benzene in a 50 mL Schlenk bomb. The mixture was heated to 75 °C for 16 h. The reaction mixture was cooled to room temperature and filtered through a fritted filter with a pad of Celite. The volatiles were removed *in vacuo* from the filtrate to leave a yellow oil. The oil was stirred with 5 mL pentane for 4 h over which time a yellow solid formed. The pentane volume was reduced *in vacuo* and the suspension was cooled to –20 °C. The yellow solid was collected on a frit and washed with cold pentane. The filtrate was concentrated and returned to the freezer and a second crop was collected; total yield 59 mg (61 %): ^1H NMR (CD_2Cl_2, 20 °C) δ 12.582 (s, 1H, Mo=CH), 6.674 (s, 2H), 7.355 – 7.324 (m, 2H), 7.170 – 7.122 (m, 3H), 7.075 (d, 2H, J_{HH} = 8 Hz) 7.021(s, 2H), 6.965 (d, 2H, J_{HH} = 7Hz), 6.825 (s, 2H), 2.346 (s, 6H), 2.112 (s, 6H), 2.026 (s, 6H), 1.689 (br s, 6H), 1.595 (s, 3H), 1.294 (s, 3H); $^{13}C\{^1H\}$ NMR (CD_2Cl_2, 20 °C) δ 328.4 (d, J = 13 Hz, Mo=C), 155.0, 152.4, 150.8, 147.8, 140.6, 137.8, 136.8, 136.6, 136.1, 134.2, 130.3, 129.7, 129.3, 129.1, 128.9, 128.5, 128.2, 126.4, 126.2, 125.8 , 51.3 ($Mo=CHCMe_2Ph$), 26.89, 26.85, 21.3, 21.2, 20.5, 18.5. Anal. Calcd for $C_{41}H_{46}Cl_2MoN_2$: C, 67.12; H, 6.32; N, 3.82. Found: C, 66.81; H, 6.15; N, 3.63.

W(NAr*)(CHCMe$_2$Ph)Cl$_2$(py) (4_W). A solution of pyridine (0.227 g, 2,87 mmol) in 2 mL Et_2O was added to a solution of W(NAr*)(N^{t}Bu)(CH_2CMe_2Ph)$_2$, **3_W** (2.418 g, 2.85 mmol), in 50 mL Et_2O and a pale yellow precipitate formed. The mixture was chilled to −25 °C and HCl (1.1 M in Et_2O, 7.8 mL) was added and the mixture was stirred for 16 h over which time it became orange. The volatiles were removed *in vacuo*. The residue was washed with pentane and then extracted with toluene and benzene and filtered through a pad of Celite on a frit. The volatiles were

removed *in vacuo* to give a yellow powder. The pentane wash was concentrated and cooled to −25 °C. A yellow precipitate formed which was collected on a frit and washed with cold pentane to give a combined yield of 1.565 g (69 %): ^{1}H NMR (C_6D_6) δ 10.732 (s, 1H, $^1J_{CH}$ = 144 Hz, W=C*H*), 8.379 (d, 2H, J_{HH} = 5 Hz), 7.123 (d, 2H, J_{HH} = 8 Hz), 7.075 (t, 2H, J_{HH} = 8 Hz), 7.016 – 6.988 (overlapping signals, 3H), 6.770 (s, 2H), 6.649 (t, 1H, J_{HH} = 8 Hz), 6.282 (t, 2H, J_{HH} = 7 Hz), 2.245 (s, 6H, Mes CH_3), 2.191 (s, 6H, Mes CH_3), 1.861 (br s, 6H, Mes CH_3), 1.662 (s, 3H, Mo=CHCMe_2Ph), 1.603 (s, 3H, Mo=CHCMe_2Ph); ^{13}C NMR (C_6D_6) δ 298.0 (Mo=*C*H), 155.6, 154.4, 152.9, 139.9, 138.6, 137.8, 137.0, 136.9, 129.5, 129.2, 128.9, 128.7, 128.5, 127.7, 126.6, 126.2, 124.7, 47.7 (Mo=CH*C*Me$_2$Ph), 30.8, 29.5, 21.9, 21.6, 21.2. Anal. Calcd for $C_{39}H_{42}Cl_2N_2W$: C, 59.03; H, 5.33; N, 3.53. Found: C, 58.92; H, 5.38; N, 3.47.

^{1}H NMR spectrum of **4$_W$** in C_6D_6:

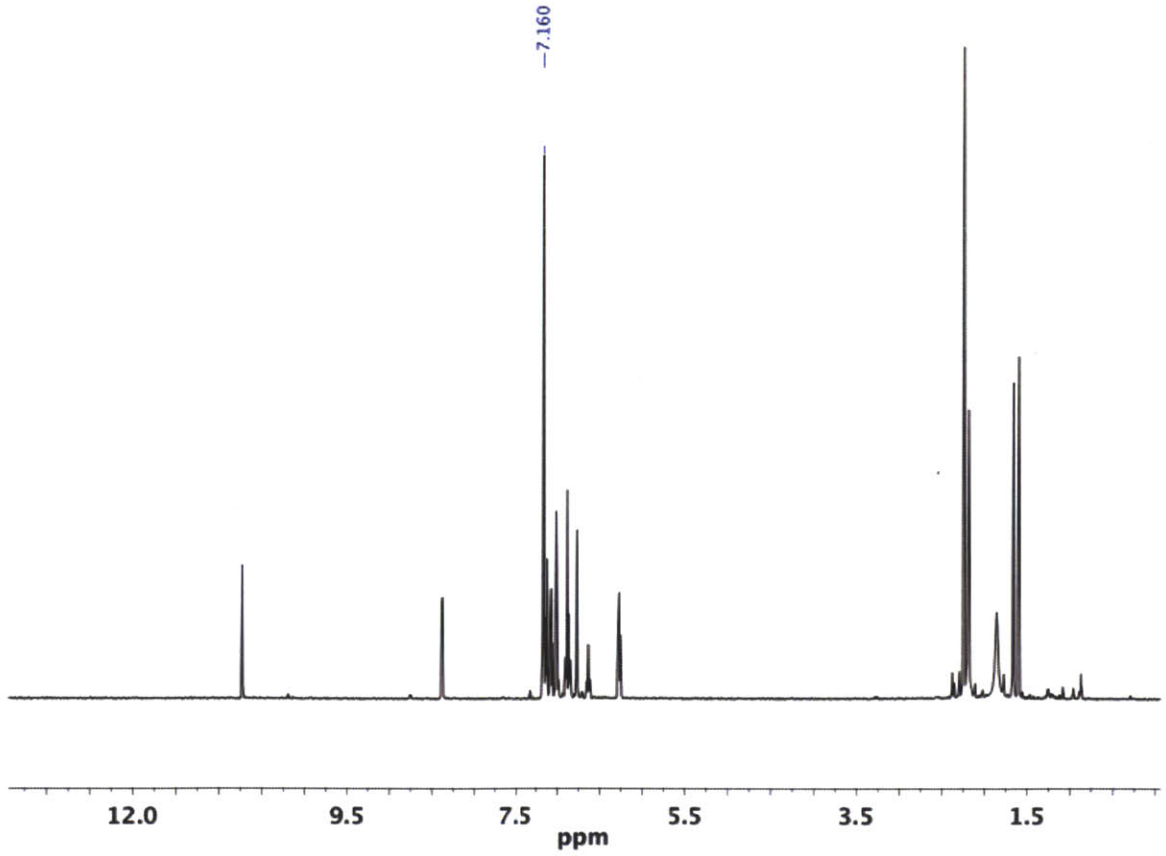

W(NAr*)(CHCMe$_2$Ph)Cl$_2$(bipy) (6$_w$). Method A: A 1.1 M solution of HCl in Et_2O (0.324 mL, 0.356 mmol) was added to a −25 °C solution of bipyridine (19.1 mg, 0.122 mmol) and W(NAr*)(N^{t}Bu)(CH$_2$CMe$_2$Ph)$_2$, **3$_W$** (101 mg, 0.119 mmol), in 4 mL Et_2O. A precipitate formed

immediately and the yellow mixture became orange. After stirring 16 h at room temperature, the volatiles were removed *in vacuo* and the orange solid was extracted with 30 mL CH_2Cl_2 and filtered through a pad of Celite on a frit. The volatiles were removed *in vacuo* from the filtrate to leave 85 mg (82 %) of orange solid.

Method B: Solid 2,2'-bipyridine (25.7 mg, 0.165 mmol) was added to a stirring solution of W(NAr*)(CHCMe$_2$Ph)Cl$_2$(py) (129.8 mg, 0.164 mmol) in 4 mL toluene. The yellow solution became orange and orange precipitate formed. After 1.5 h, the orange solid was collected on a frit, washed with 5 x 1 mL toluene, and dried *in vacuo* to give 110 mg (77 %). ^{1}H NMR (CD_2Cl_2) δ 10.164 (s, 1H, Mo=C*H*), 8.428 (d, 1H, J_{HH} = 4 Hz), 8.043 (s, 3H), 7.973 (m, 2H), 7.338 – 7.220 (overlapping signals, 5H), 7.162 and 7.121 (overlapping br s, 2H), 6.991 (t, 1H, J_{HH} = 7 Hz), 6.756 (s, 4H), 6.396 (s, 2H), 2.309 (s, 6H, mesitylCH_3), 1.774 (s, 6H, mesitylCH_3), 1.654 (s, 3H, Mo=CHCMe_2Ph), 1.609 (s, 6H, mesitylCH_3), 1.548 (s, 3H, Mo=CHCMe_2Ph). Anal. Calcd for $C_{44}H_{45}Cl_2N_3W$: C, 60.70; H, 5.21; N, 4.83. Found: C, 60.91; H, 5.24; N, 4.62.

^{1}H NMR spectrum of $\mathbf{6_W}$ in CD_2Cl_2:

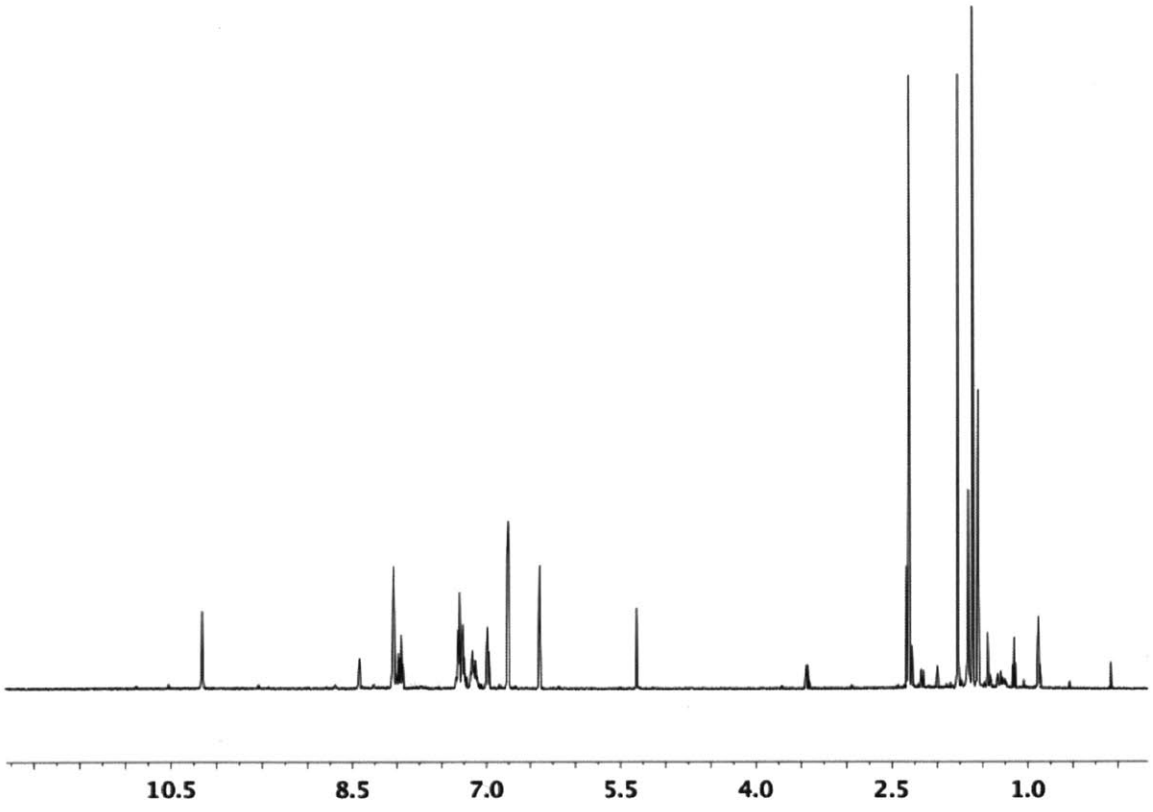

[W(NAr*)(CHCMe$_2$Ph)Cl(bipy)][Zn$_2$Cl$_6$]$_{0.5}$ (7$_w$). Solid $ZnCl_2$(1,4-dioxane) (12.6 mg, 51.6 μmol) was added to a suspension of W(NAr*)(CHCMe$_2$Ph)Cl$_2$(bipy) (44.2 mg, 50.8 μmol) in 4 mL CH_2Cl_2 in a 20 mL scintillation vial. The orange suspension became a clear orange solution. After stirring 1.5 h the volatiles were removed *in vacuo*, and orange solid was extracted with benzene and filtered through a pipette filter. The volatiles were removed *in vacuo*. The orange oil was dissolved in minimal toluene and cooled to −25 °C and orange crystals formed. The mother liquor was removed by pipette, the crystals were washed with cold toluene, and dried *in vacuo* to give 22.8 mg (45 % yield). ^{1}H NMR (CD_2Cl_2) δ 10.707 (s, 1H, Mo=C*H*), 8.890 – 8.852 (overlapping signals, 2H, bpy*H*), 8.699 (d, 1H, J_{HH} = 8 Hz, bpy*H*), 8.583 (t, 1H, J_{HH} = 8 Hz, bpy*H*), 8.479 – 8.434 (overlapping signals, 2H bpy*H*), 7.581 (q, 2H, J_{HH} = 8 Hz), 7.330 (t, 1H, J_{HH} = 8 Hz), 7.129 (d, 2H, J_{HH} = 8 Hz), 6.973 (d, 2H, J_{HH} = 8 Hz), 6.760 (s, 2H, mes*H*), 6.670 (t, 2H, J_{HH} = 8 Hz), 6.612 (s, 2H, mes*H*), 6.417 (t, 1H, J_{HH} = 8 Hz), 2.078 (s, 6H, mesitylCH_3), 2.031 (s, 6H, mesitylCH_3), 1.601 (s, 6H, mesitylCH_3), 1.296 (s, 3H, Mo=CHCMe_2Ph), 0.979 (s, 3H, Mo=CHCMe_2Ph); ^{13}C NMR (CD_2Cl_2) δ 297.1 (Mo=*C*H), 156.7, 154.3, 153.4, 151.5, 145.3, 144.9, 140.7, 140.4, 139.9, 137.8, 137.4, 137.2, 136.7, 136.7, 136.4, 136.2, 130.4, 129.7, 129.7, 129.4, 129.1, 129.0, 128.9, 128.8, 128.7, 128.1, 127.6, 127.5, 126.8, 126.6, 126.2, 125.0, 47.6, 30.4, 26.6, 21.7, 21.2, 20.4.

^{1}H NMR spectrum of **7$_W$** in C_6D_6:

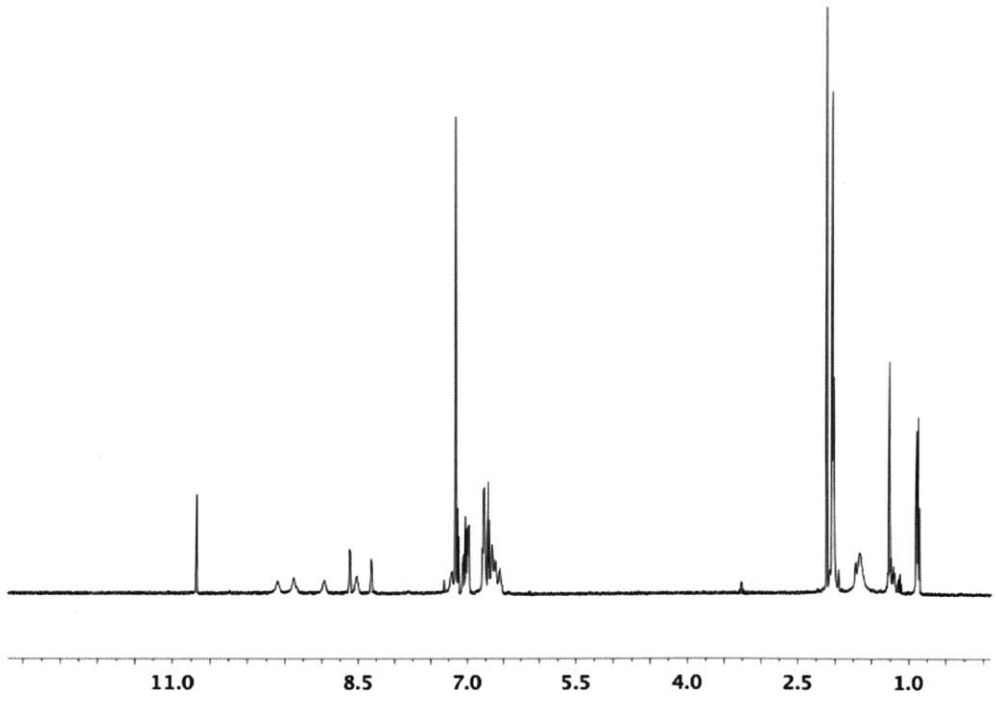

Mo(NAr*)(CHCMe$_2$Ph)Cl(O^{t}Bu)(py) ($\mathbf{8_{Mo}}$). A solution of LiO^{t}Bu (12.0 mg, 150 μmol) in 1 mL Et_2O was added to a suspension of Mo(NAr*)(CHCMe$_2$Ph)Cl$_2$(py), $\mathbf{4_{Mo}}$ (106 mg, 150 μmol), in 5 mL Et_2O at -25 °C. The mixture became green and then yellow. After 2 h, the volatiles were removed *in vacuo*. The remaining solids were extracted with a 1:1 pentane:toluene mixture and filtered through a pipette filter. The solvent volume was removed *in vacuo*, 1 mL pentane was added, and the mixture was cooled to −25 °C. A yellow precipitate formed and was collected on a frit. The solvent was removed from the filtrate, pentane added, and the mixture was cooled to −25 °C to collect two more crops; total yield 84.0 mg (75%): ^{1}H NMR (CD_2Cl_2, 20 °C) δ 12.677 (s, 1H, $^1J_{CH}$ = 148 Hz, Mo=C*H*), 8.10 (d, 2H, J_{HH} = 5Hz), 7.71 (t, 1H, J_{HH} = 7.5 Hz), 7.17 – 7.07 (overlapping m, 6H), 6.96 - 6.95 (overlapping m, 4H), 6.88 (s, 2H, Mesityl-Ar*H*), 6.58 (s, 2H, Mesityl-Ar*H*), 2.16 – 2.12 (overlapping br s, 18 H, MesitylC*H*$_3$), 1.37 (s, 3H, MoCHC*Me*$_2$Ph), 1.23 (s, 3H, MoCHC*Me*$_2$Ph), 1.20 (s, 9H, ^{t}Bu); ^{13}C{^{1}H} NMR (CD_2Cl_2, 20 °C) δ 323.2 (Mo=CH), 153.8, 152.6, 150.4, 138.9, 137.6, 137.0, 129.2, 128.8 (br s), 128.1, 126.4, 126.3, 125.9, 124.6, 80.9 (O*C*Me$_3$), 51.3 (MoCH*C*Me$_2$Ph), 32.9, 30.9, 28.2, 21.6, 21.3, 20.6 (br s). Anal Calcd for $C_{43}H_{51}ClMoN_2O$: C, 69.48; H, 6.79; N, 3.77. Found: C, 69.21; H, 6.79; N, 3.77.

Mo(NAr*)(CHCMe$_2$Ph)Cl[OCMe(CF$_3$)$_2$](py) ($\mathbf{9_{Mo}}$). Solid LiOCMe(CF$_3$)$_2$ (24.0 mg, 0.128 mmol) was added to a suspension of Mo(NAr*)(CHCMe$_2$Ph)Cl$_2$(py) (91.9 mg, 0.130 mmol) in 3 mL Et_2O and the mixture was stirred 1 h at room temperature. The volatiles were removed *in vacuo* and the yellow solid was extracted with a 1:1 pentane:benzene mixture and filtered through a pipette filter. The volatiles were removed *in vacuo* and the yellow solid was washed with cold pentane; yield 59.7 mg (73 %): ^{1}H NMR (C_6D_6, 20 °C) δ 12.782 (s, 1H, $^1J_{CH}$ = 150 Hz, Mo=CH), 8.121 (d, 2H, J_{HH} = 5 Hz), 7.108 – 7.050 (m, 4H), 7.022 – 6.994 (m 1H), 6.904 – 6.883 (m, 3H), 6.798 (d, 2H, J_{HH} = 8Hz), 6.711 (t, 1H, J_{HH} = 7 Hz) 6.635 (s, 2H), 6.377 (t, 2H, J_{HH} = 7 Hz), 2.234 (br s, 6H), 2.124 (s, 6H), 2.000 (br s, 6H), 1.836 (s, 3H), 1.617 (s, 3H), 1.526 (s, 3H); ^{13}C{^{1}H} NMR (C_6D_6, 20 °C) *δ* 326.6 (Mo=CH), 154.2, 152.1, 150.0, 138.3, 137.3, 136.6, 129.6, 129.2, 128.3, 126.2, 126.1, 124.0, 82.6 (q, $^1J_{CF}$ = 30 Hz), 52.4, 29.2, 27.4, 21.6, 21.1, 20.9, 18.3; ^{19}F{^{1}H} NMR (C_6D_6, 20 °C) δ -76.79 (q, J_{FF} = 10 Hz), -77.46 (q, J_{FF} = 10 Hz). Anal. Calcd for $C_{43}H_{45}ClF_6MoN_2O$: C, 60.67; H, 5.33; N, 3.29. Found: C, 60.91; H, 5.47; N, 3.28.

Mo(NAr*)(CHCMe$_2$Ph)Cl[O(2,6-Me$_2$C$_3$H$_6$)](py) (10$_{Mo}$). A solution of LiOAr′ (13.8 mg, 108 μmol) in 2 mL Et_2O was added to a vial containing a suspension of Mo(NAr*)(CHCMe$_2$Ph)Cl$_2$(py) (75 mg, 107 μmol) in 5 mL Et_2O. The reaction mixture was stirred at room temperature for 2 h. The volatiles were removed *in vacuo* and the remaining oil was extracted with benzene and the extract was filtered through a pipette filter. The volatiles were removed *in vacuo* from the filtrate. The remaining solid was dissolved in a minimal amount of a 1:1 pentane/toluene mixture and cooled to −20 °C. A yellow precipitate formed and was collected on a fritted filter by vacuum filtration. The solvent was removed *in vacuo* from the filtrate to which pentane was added and the mixture cooled to −20 °C. In this way, two more crops were collected; yield 60.0 mg (71 %). ^{1}H NMR (CD_2Cl_2, 20 °C) δ 12.762 (s, 1H, $^1J_{CH}$ = 151 Hz, Mo=C*H*), 7.714 (t, 1H, J_{HH} = 7.5 Hz), 7.555 (d, 2H, J_{HH} = 5 Hz), 7.256 (d, 2H, J_{HH} = 7.5 Hz), 7.216 – 7.179 (overlapping signals (4H), 7.081 (t, 2H, J_{HH} = 7.0 Hz), 6.696 (s, 2H, mesityl Ar*H*), 6.935 (d, 2H, J_{HH} = 8.0 Hz), 6.761 (d, 2H, J_{HH} = 7.0 Hz), 6.554 – 6.519 (overlapping signals, 3H), 2.197 (s, 6H, mesitylCH_3), 2.074 (s, 6H, mesitylCH_3), 1.764 (s, 6H, mesitylCH_3), 1.607 (s, 6 H, OPh(CH_3)$_2$), 1.562 (s, 3H, MoCHCMe_2Ph) 1.444 (s, 3H, MoCHCMe_2Ph); ^{13}C{^{1}H} NMR (CD_2Cl_2, 20 °C) δ 326.6 (Mo=*C*H), 160.8, 154.8, 154.1, 152.3, 151.3, 140.1, 139.2, 137.5, 137.3, 137.1, 129.9, 129.2, 129.1, 128.4, 128.4, 127.5, 127.3, 126.4, 126.3, 125.3, 119.3, 53.1, 30.5, 27.0, 21.7, 21.4, 21.0, 19.1. Anal. Calcd for $C_{47}H_{51}ClMoN_2O$: C, 71.34; H, 6.50; N, 3.54. Found: C, 71.06; H, 6.57; N, 3.43.

Mo(NAr*)(CHCMe$_2$Ph)Cl(O^{i}Pr)(py) (11$_{Mo}$). A 1.6 M solution of n-butyllithium in hexanes (18 μL, 29 μmol) was added to a solution of ^{i}PrOH (2.7 μL, 29 μmol) in 1 mL Et_2O and stirred 1.5 h. The LiO^{i}Pr solution was added to a −20 °C suspension of Mo(NAr*)(CHCMe$_2$Ph)Cl$_2$(py) (20 mg, 28 μmol) in 3 mL Et_2O. After 3.5 h the volatiles were removed *in vacuo*. The residue was extracted with pentane and filtered through a pipette filter. The volume of the filtrate was reduced *in vacuo* and cooled to −20 °C. The supernatant was removed from the yellow crystals by pipette and the crystals were dried *in vacuo* to give 18 mg, 87 %. ^{1}H NMR (C_6D_6) δ 12.943 (s, 1H, Mo=C*H*), 8.365 (m, 2H), 7.181 (m, 4H), 7.083 (t, J_{HH} = 8 Hz), 7.021 – 6.978 (overlapping signals, 4H), 6.946 – 6.898 (overlapping signals, 4H), 6.718 (t, J_{HH} = 8 Hz, 1H), 6.644 (br s, 2H), 6.393 (t, J_{HH} = 7 Hz, 2H), 5.182 (septet, 1H, J_{HH} = 6 Hz, OC*H*Me$_2$), 2.343 (br s), 2.166 (br s, 18 H integrated together with the previous signal, Mes C$_6$H$_2$*Me*$_3$), 1.693 (s, 3H, Mo=CHC*Me*$_2$Ph),

1.416 (d, 3H, J_{HH} = 6 Hz, OCHMe_2), 1.352 (s, 3H, Mo=CHCMe_2Ph), 1.225 (d, 3H, J_{HH} = 6 Hz, OCHMe_2). Anal. Calcd for $C_{42}H_{49}ClMoN_2O$: C, 69.17; H, 6.77; N, 3.84. Found: C, 69.14; H, 6.90; N, 3.75.

Mo(NAr*)(CHCMe$_2$Ph)Cl(OAr*)(py) (12_{Mo}). A 1.6 M solution of n-Butyllithium in hexanes (56 μL, 90 μmol) was added to a stirring solution of Ar*OH in 2 mL pentane. White precipitate formed. Analysis of an aliquot by ^{1}H NMR after 1 h showed complete conversion to LiOAr*. The volatiles were removed *in vacuo*. The white solid was dissolved in benzene and added to a stirring solution of Mo(NAr*)(CHCMe$_2$Ph)Cl$_2$(py) in 3 mL benzene in a 25 mL Teflon-stoppered Schlenk tube. The mixture was heated to 80 °C for 16 h. The mixture was cooled to room temperature and the volatiles were removed *in vacuo*. The resulting brown oil was extracted with pentane and the extract was filtered through a frit with a pad of Celite. The volume of the filtrate was reduced *in vacuo* and stored in the freezer at –20 °C. The yellow precipitate was collected on a frit; total yield 47 mg (54 %). Crystals for X-ray diffraction were grown from a concentrated Et$_2$O solution at –20 °C: ^{1}H NMR (CD_2Cl_2, 20 °C) δ 11.308 (s, 1H, Mo=CH, $^1J_{CH}$ = 127 Hz), 7.647 (t, 1H, J_{HH} = 7.5 Hz, Ar-H), 7.459 (d, 2H, J_{HH} = 5Hz, Ar-H), 7.160 - 7.148 (overlapping signals, 3H, Ar-H), 7.071 – 6.975 (overlapping signals, 3H, Ar-H), 6.902 (t, 2H, J_{HH} = 7 Hz), 6.834 – 6.818 (overlapping signals, 5H, Ar-H), 6.756 – 6.728 (overlapping signals, 3H, Ar-H), 6.538 (br s, 1H), 6.389 (br s, 1H), 6.191 (br s, 1H), 6.082 (br s, 1H), 5.950 (br s, 1H), 2.447 and 2.419 (overlapping s, 6H), 2.341 – 2.276 (overlapping signals, 6H), 2.040 – 1.912 (overlapping signals, 12 H), 1.811 (br s, 6H), 1.623 (s, 6H), 1.126 (s, 6H); ^{13}C{^{1}H} NMR (CD_2Cl_2, 20 °C) δ 309.8 (Mo=C), 162.8, 154.5, 153.4, 148.5, 139.4, 138.9, 138.7, 138.4, 137.9, 137.6, 137.2, 137.0, 136.7, 136.5, 136.2, 135.4, 135.0, 132.1, 131.4, 130.7, 130.5, 130.0, 129.5, 129.3, 128.5, 127.9, 127.6, 127.5, 126.1, 125.6, 124.3, 118.5 (ArylC), 55.0 (Mo=CHCMe$_2$Ph), 33.3 (Mo=CHCMe_2Ph), 27.2 (Mo=CHCMe_2Ph), 22.5, 21.7, 21.4, 21.3, 20.4, 19.9(MesMe). Anal. Calcd for $C_{63}H_{67}ClMoN_2O$: C, 75.70; H, 6.76; N, 2.80. Found: C, 75.40; H, 6.84; N, 2.81.

Mo(NAr*)(CHCMe$_2$Ph)(Pyr)$_2$(py) (13_{Mo}). Solid LiPyr (56 mg, 0.77 mmol) was added to a –25 °C stirred suspension of Mo(NAr*)(CHCMe$_2$Ph)Cl$_2$(py) (269 mg, 0.38 mmol) in 8 ml Et$_2$O. The solution became brown and a yellow precipitate formed. After 2 h, the volatiles were

removed *in vacuo*. The yellow solid was extracted with benzene and the mixture was filtered through a pipette filter. The volatiles were removed from the filtrate to leave a brown oil. The oil was triturated by adding 3 mL pentane and stirring until a yellow powder formed. The mixture was chilled to −25 °C and then the yellow solid was collected on a frit and washed with 3 x 1 mL cold pentane and then dried *in vacuo*; yield 280 mg, 96 %: ^{1}H NMR (C_6D_6) δ 12.910 (s, 1H, $^1J_{CH}$ = 145 Hz, Mo=C*H*), 7.355 (d, 1H, J_{HH} = 5 Hz, py*H*), 6.946 – 6.826 (overlapping signals, 7H, Ar*H*), 6.714 – 6.664 (overlapping signals, 3H, Ar*H*), 6.628 (s, 2H), 6.584 (s, 2H), 6.517 (d, 2H, J_{HH} = 7 Hz), 6.471 (t, 1H, J_{HH} = 7 Hz), 6.423 (s, 2H), 6.204 (s, 2H), 5.977 (t, 2H, J_{HH} = 7 Hz) 2.255 (s, 6H, MesCH_3), 2.058 (br s, 6H, MesCH_3), 1.971 (br s, 6H, MesCH_3), 1.903 (s, 3H, Mo=CHCMe_2Ph), 1.223 (s, 3H, Mo=CHCMe_2Ph); ^{13}C {^{1}H} NMR (C_6D_6) δ 319.1 (Mo=*C*), 155.5, 152.5, 146.5, 138.0, 137.7, 137.2, 135.5, 130.1,129.8, 129.6, 128.9, 128.7, 128.5, 128.3, 128.0, 127.5, 125.9, 125.8, 124.1, 108.6, 108.1, 52.0 (Mo=CHCMe_2Ph), 32.0 (Mo=CHCMe_2Ph), 26.8 (Mo=CHCMe_2Ph), 21.7 (Mes*Me*), 21.6 (Mes*Me*), 21.5 (Mes*Me*). Anal. Calcd for $C_{47}H_{50}MoN_4$: C, 73.61; H, 6.57; N, 7.31. Found: C, 73.46; H, 6.52; N, 7.30.

^{1}H NMR spectrum of **13$_{Mo}$** in C_6D_6:

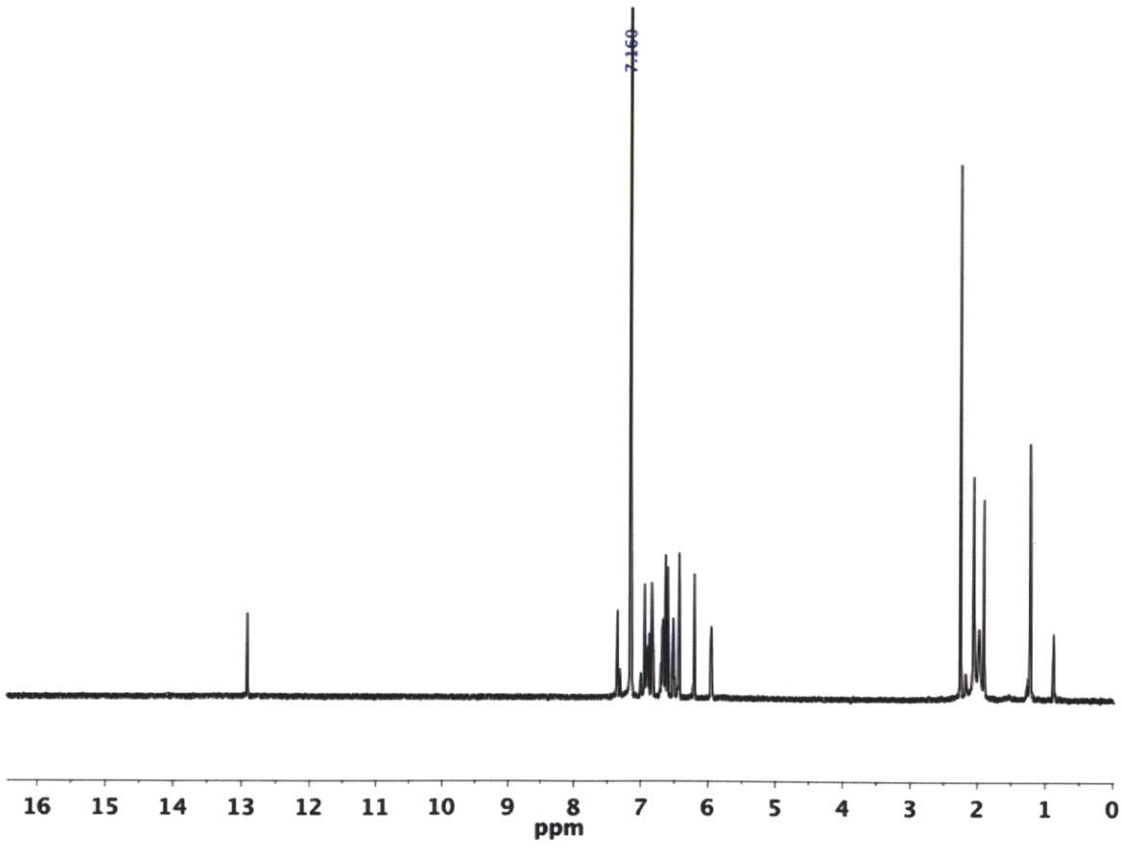

W(NAr*)(CHCMe$_2$Ph)(Pyr)$_2$(py) (13$_W$). Solid LiPyr (49.3 mg, 0.675 mmol) was added to a solution of W(NAr*)(CHCMe$_2$Ph)Cl$_2$(py), 8, (90.0 mg, 0.113 mmol) in Et$_2$O and stirred 8 h at ambient temperature. The volatiles were removed *in vacuo*. The brown oil was extracted with toluene and benzene and filtered through a pipette filter. The volatiles were removed *in vacuo* from the filtrate to leave a yellow oil, which was triturated with pentane (2 mL) by stirring for 16 h. The mixture was cooled to −25 °C, and the yellow power was collected on a fritted filter and washed with cold pentane to give 75.3 mg, 78 %. ^{1}H NMR (C$_6$D$_6$) δ 10.579 (s, 1H, W=C*H*), 7.654 (s, 2H), 7.298 (d, 2H, J_{HH} = 8 Hz), 7.175 (t, 2H, J_{HH} = 8 Hz), 7.072 (t, 1H, J_{HH} = 8 Hz), 7.007 (s, 4H), 6.948 (s, 2H), 6.763 (t, 1H, J_{HH} = 8 Hz), 6.725 (s, 4H), 6.389 (t, 1H, J_{HH} = 6 Hz), 6.230 (s, 2H), 5.924 (s, 2H), 5.565 (s, 2H), 2.196 (18 H, C$_6$H$_2$*Me*$_3$), 1.656 (s, 6H, W=CHC*Me*$_2$Ph); ^{13}C{^{1}H} NMR (CD$_2$Cl$_2$) δ 284.6 (W=*C*H), 154.6, 152.4, 149.6, 139.1, 137.9, 137.7, 137.1, 133.1, 129.6, 129.1, 128.3, 127.1, 126.0, 125.7, 125.6, 124.8, 107.9, 49.0, 31.8, 21.4, 20.8. Anal. calcd for C$_{47}$H$_{50}$N$_4$W: C, 66.04; H, 5.90; N, 6.55. Found: C, 66.14; H, 5.88; N, 6.22.

^{1}H NMR spectrum of **13$_W$** in C$_6$D$_6$:

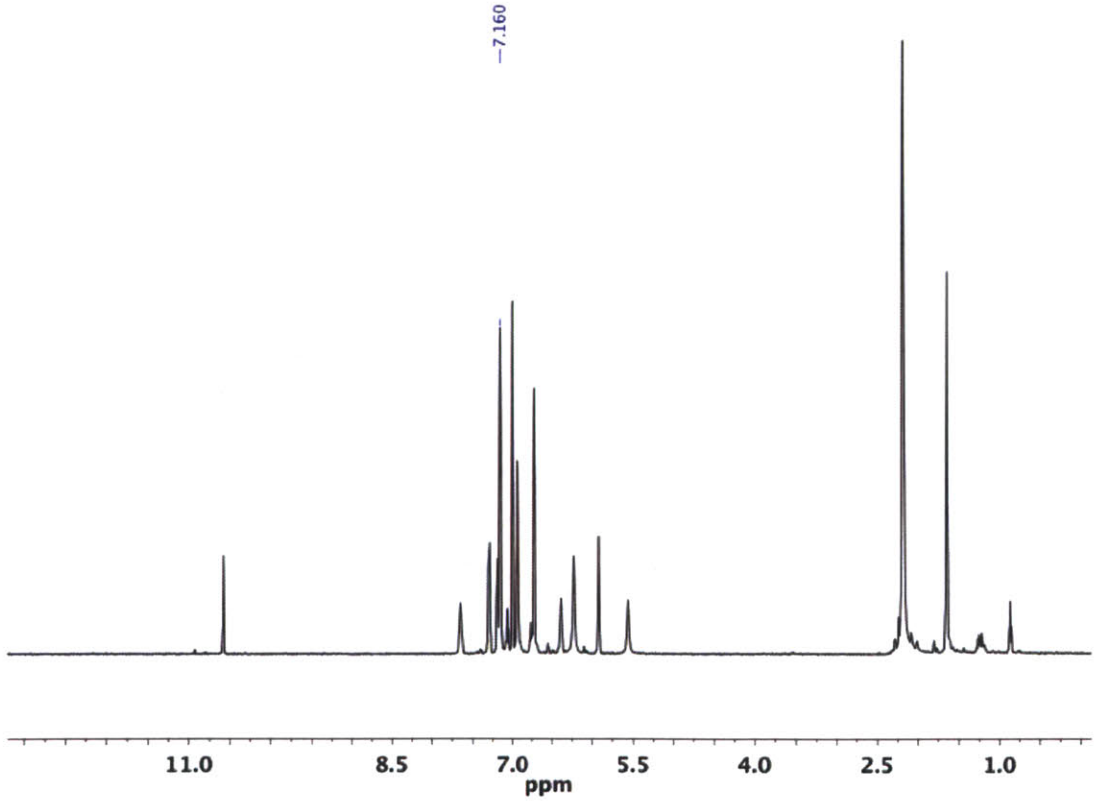

Mo(NAr*)(CHCMe$_2$Ph)(Me$_2$Pyr)$_2$ (14$_{Mo}$). Et_2O (5 mL) was added to a vial containing solid Mo(NAr*)(CHCMe$_2$Ph)Cl$_2$(py) (84.9 mg, 0.120 mmol) and LiMe$_2$Pyr (25.4 mg, 0.251 mmol). The mixture was stirred 16 h, over which time it became brown. The volatiles were removed *in vacuo*. The brown solid was extracted with pentane and the extract was filtered through a pipette filter. The volatiles were removed *in vacuo* from the filtrate to leave analytically pure brown solid; yield 68.6 mg, (77 %): ^{1}H NMR (C_6D_6, 20 °C) δ 13.58 (s, 1H, Mo=C*H*), 7.35 (d, 2H, J_{HH} = 8.0 Hz), 7.12 (d, 2H, J_{HH} = 7.5 Hz), 7.03 – 7.00 (m, 1H), 6.84 – 6.79 (overlapping signals, 4H), 6.70 (d, 2H, J_{HH} = 7.5 Hz), 6.6 – 5.4 (br s, pyr*H*), 2.53 – 1.00 (overlapping broad signals), 2.12 (s), 1.94 (s); ^{1}H NMR (CD_2Cl_2, −40 °C): δ 13.15 (s, 1H, Mo=C*H*), 7.20 (s, 5H, Ar*H*), 7.11 (s, 2H, Ar*H*), 7.01 (s, 1H, Ar*H*), 6.89 (d, 1H, J_{HH} = 7.5 Hz, Ar*H*), 6.86 (d, 1H, , J_{HH} = 7.5 Hz, Ar*H*), 6.82 (s, 1H, Ar*H*), 6.65 (s, 1H, Ar*H*), 5.79 (s, 1H, pyr*H*), 5.71 (s, 1H, pyr*H*), 5.40 (s, 1H, pyr*H*), 3.68 (s, 1H, pyr*H*), 2.29 (s, 3H, CH_3), 2.26 (s, 3H, CH_3), 2.15, 2.14 (overlapping s, 6H, CH_3), 2.02 (s, 3H, CH_3), 1.91 (s, 3H, CH_3), 1.77, 1.75 (overlapping s, 9H, CH_3), 1.49 (s, 3H, CH_3), 1.27 (s, 3H, CH_3), 0.58 (s, 3H, CH_3); ^{13}C{^{1}H} NMR (CD_2Cl_2, −40 °C) δ 317.0 (Mo=CH), 157.3, 152.6, 151.9, 139.8, 138.3, 138.0, 137.9, 137.7, 137.7, 137.4, 137.3, 137.0, 136.7, 136.5, 135.6, 135.0, 131.8, 130.6, 129.4, 128.4, 128.1, 127.4, 126.3, 126.0, 125.7, 125.6, 108.3, 108.2, 105.3, 100.2, 100.2, 53.4, 32.1, 31.3, 22.1, 21.1, 21.0, 20.7, 20.4, 20.0, 19.9, 18.9, 18.3, 13.4, 12.9. Anal. Calcd for $C_{46}H_{53}MoN_3$: C, 74.12; H, 7.18; N, 5.65. Found: C, 74.06; H, 7.06; N, 5.68.

W(NAr*)(CHCMe$_2$Ph)(Me$_2$Pyr)$_2$ (14$_W$). Solid LiMe$_2$Pyr (235 mg, 2.33 mmol) was added in one portion to a −25 °C, stirring solution of W(NAr*)(CHCMe$_2$Ph)Cl$_2$(py), 8 (922 mg, 1.16 mmol) in 25 mL Et_2O. The mixture was stirred 16 h at ambient temperature. The volatiles were removed *in vacuo*. The dark yellow oil was extracted with pentane and filtered through frit with a pad of Celite. The pentane volume was reduced *in vacuo*, and a yellow precipitate formed. The mixture was cooled to −25 °C for 2 h. The yellow solid was collected on a frit and washed with cold pentane (760 mg, 79 %). ^{1}H NMR (CD_2Cl_2, 20 °C) δ 10.528 (br s, 1H, W=C*H*), 7.222 – 7.189 (overlapping signals, Ar*H*, 5H), 7.104 (m, 1H, Ar*H*), 6.945 (d, J_{HH} = 8 Hz), 6.856 (br s, 4H, Ar*H*), 6.4 – 4.4 (br s, NC$_4H_2$Me$_2$), 2.227 (s, 6H, *p*-Mes CH_3), 2.008 (br s, 12H), 1.835 (br s, 12H), 1.5 – 0.9 (br s, 6H, CHC*Me*$_2$Ph); ^{1}H NMR (CD_2Cl_2, −40 °C) δ 10.799 (s, 1H, W=C*H*, $^1J_{CH}$ = 126 Hz), 7.179 (s, 5H, Ar*H*), 7.080 (s, 2H, Ar*H*), 6.906 (d, 1H, $^1J_{HH}$ = 8 Hz, Ar*H*), 6.868 (d, 1H, $^1J_{HH}$ = 8 Hz, Ar*H*), 6.774 (s, 1H, Ar*H*), 6.620 (s, 1H, Ar*H*), 5.797 (s, 1H, Me$_2$pyr*H*), 5.696 (s, 1H,

Me_2pyrH), 5.510 (s, 1H, Me_2pyrH), 3.558 (s, 1H, Me_2pyrH), 2.266 (s, 3H), 2.228 (s, 3H), 2.123 (s, 3H), 2.088 (s, 6H), 2.020 (s, 3H), 1.870 (s, 3H), 1.726 (s, 3H), 1.582 (s, 3H), 1.479 (s, 3H), 1.328 (s, 3H), 0.558 (s, 3H); $^{13}C\{^1H\}$ NMR (CD_2Cl_2, −40 °C) δ 285.3 (Mo=*C*H), 158.1, 153.6, 139.8, 138.3, 138.0, 137.9, 137.6, 137.6, 137.1, 136.8, 136.6, 136.5, 131.8, 130.3, 129.4, 128.4, 128.1, 128.0, 127.3, 125.7, 125.5, 125.4, 109.5, 108.6, 105.4, 99.4, 98.1 (Aromatic), 51.5 (W=CH*C*Me_2Ph), 33.9, 32.5, 22.2, 21.2, 21.0, 21.0, 20.8, 20.4, 20.1, 19.1, 19.0, 13.0 (*C*H_3). Anal. Calcd for $C_{46}H_{53}N_3W$ C, 66.42; H, 6.42; N, 5.05; Found: C, 66.26; H, 6.47; N, 4.98.

Mo(NAr*)(CHCMe$_2$Ph)(OAr′)$_2$ (15$_{Mo}$). Solid LiOAr′ (8.4 mg, 66 μmol) was added to a stirring suspension of Mo(NAr*)(CHCMe$_2$Ph)Cl$_2$(py) (22 mg, 31 μmol) and the mixture was stirred for 16 h. The volatiles were removed *in vacuo*, and the remaining residue was extracted with pentane and filtered through a pipette filter with Celite. The volume of the filtrate was reduced *in vacuo* and then cooled to −25 °C. Crystals were collected by removing the supernatant by pipette and drying *in vacuo*, 12.5 mg, 51 %. ^1H NMR (C_6D_6) δ 11.430 (s, 1H, Mo=C*H*), 7.421 (s, 1H), 7.026 (s), 7.001 (s, 2H integrated with previous signal), 6.964 – 6.898 (overlapping signals, 8H), 6.859 – 6.793 (overlapping signals, 3H), 6.754 (s, 4H), 2.181 (s, 6H, ArCH_3), 2.079 and 2.070 (overlapping s, 24H, ArCH_3), 1.274 (s, 6H, Mo=CHCMe_2Ph); $^{13}C\{^1H\}$ NMR (CD_2Cl_2) 291.4 (Mo=*C*H), 161.3, 155.8, 149.2, 137.4, 136.7, 136.3, 136.0, 129.4, 128.9, 128.6, 128.1, 126.3, 126.3, 126.0, 126.0, 120.6, 50.5, 28.0, 21.4, 20.9, 17.8.

Mo(NAr*)(CHCMe$_2$Ph)(Pyr)[OCMe(CF$_3$)$_2$](py) (16$_{Mo}$). HOCMe(CF$_3$)$_2$ (6.4 μL, 0.052 mmol) was added to Mo(NAr*)(CHCMe$_2$Ph)(Pyr)$_2$(py), **13$_{Mo}$**, (40 mg, 52 μmol) in 2 mL C_6H_6. After 45 m, the reaction mixture was filtered through a pipette filter. The volatiles were removed from the filtrate. To the resulting brown oil, 2 mL pentane was added and a yellow solid formed. The mixture was cooled to −25 °C, after which the yellow solid was collected on a frit and washed with 2 x 0.5 mL cold pentane, and dried *in vacuo*; yield 31 mg, 68 %: ^1H NMR (C_6D_6) δ 12.919 (s, 1H, Mo=C*H*) 7.767 (d, J_{HH} = 6 Hz, 2H, Pyridine), 7.060 (s, 2H), 6.923 – 6.619 (overlapping signals, 15H), 6.241 (t, J_{HH} = 6 Hz, 2H), 2.309 (s), 2.207 (br s), 2.002 (s), 1.882 (br s, 18 H integrated over previous 4 signals), 1.273 (s), 1.172 (s), 1.049 (br s, 9 H integrated over previous 3 signals); ^1H NMR (CD_2Cl_2, alkylidene) δ 12.739 ($^1J_{CH}$ = 148 Hz); ^{13}C NMR (CD_2Cl_2) δ 326.8 (Mo=*C*H), 153.8, 152.4, 146.4, 138.5, 132.1, 129.9, 128.4, 127.5, 126.4, 126.3, 124.4, 106.5,

82.9 (m, only 3 lines visible above baseline, J_{CF} = 27 Hz), 52.5, 31.1, 27.8, 21.5 (br s), 19.9, 16.0; $^{19}F\{^1H\}$ NMR (C_6D_6) δ -76.12 (quartet, J_{FF} = 9 Hz), 77.06 (quartet, J_{FF} = 9 Hz). Anal. Calcd for $C_{47}H_{49}F_6MoN_3O$: C, 64.01; H, 5.60; N, 4.76. Found: C, 63.97; H, 5.63; N, 4.54.

^1H NMR spectrum of $\mathbf{16_{Mo}}$ in C_6D_6:

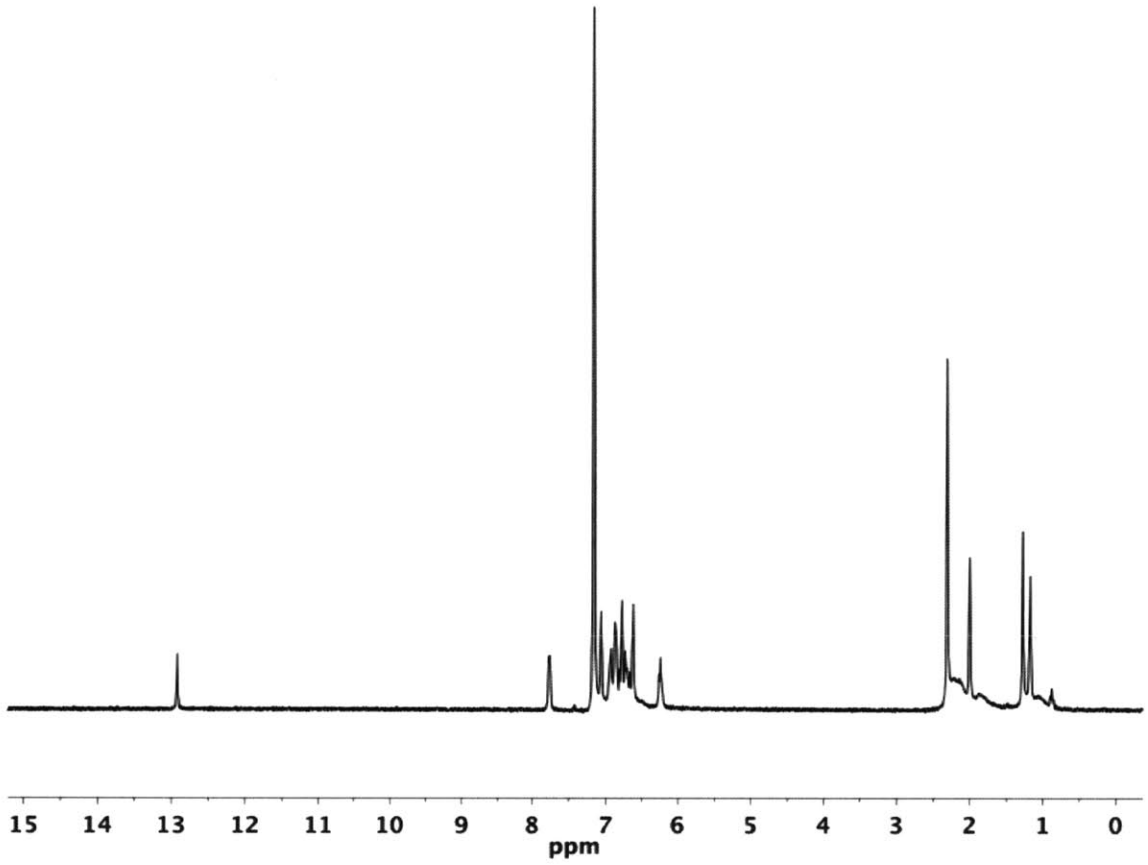

Mo(NAr*)(CHCMe$_2$Ph)(pyr)(O^{i}Pr)(py) ($\mathbf{17_{Mo}}$). HO^{i}Pr was added to a stirred solution of Mo(NAr*)(CHCMe$_2$Ph)(Pyr)$_2$(py), $\mathbf{13_{Mo}}$ (45.4 mg, 59.2 μmol), in 2 mL benzene. After 1.5 h, the reaction mixture was filtered through a pipette filter and the volatiles removed *in vacuo* from the filtrate. Pentane (1 mL) was added and the mixture was stirred at ambient temperature for 1 h and then cooled to −25 °C. The resulting yellow solid was collected on a frit and dried *in vacuo*; yield 24.2 mg, 70 %: ^1H NMR (C_6D_6) δ 12.996 (s, 1H), 8.090 (br s, 2H, pyridine), 7.060 (s, 2H), 6.889 – 6.573 (overlapping signals, 15 H), 6.270 (br s, 2H), 4.520 (septet, J_{HH} = 6 Hz, 1H, OC*H*Me$_2$), 2.292, 2.205, 2.144 (overlapping br s, 18H, Mes*Me*), 1.881 (s, 3H, Mo=CHC*Me*$_2$Ph), 1.375 (s, 3H, Mo=CHC*Me*$_2$Ph), 1.116 (d, J_{HH} = 6 Hz), 1.107 (d, J_{HH} = 6 Hz, 6H integrated together with previous signal); $^{13}C\{^1H\}$ NMR (C_6D_6) δ 319.0 (Mo=*C*H), 153.9, 152.0, 147.8,

137.6, 132.1, 129.3, 128.9, 128.7, 128.1, 126.3, 126.3, 125.6, 123.8, 107.8, 74.3, 51.2, 31.3, 29.4,27.3, 21.7. Anal. Calcd for $C_{46}H_{53}MoN_3O$: C, 72.71; H, 7.03; N, 5.53. Found: C, 72.47; H, 6.91; N, 5.36.

^{1}H NMR spectrum of $\mathbf{17_{Mo}}$ in C_6D_6:

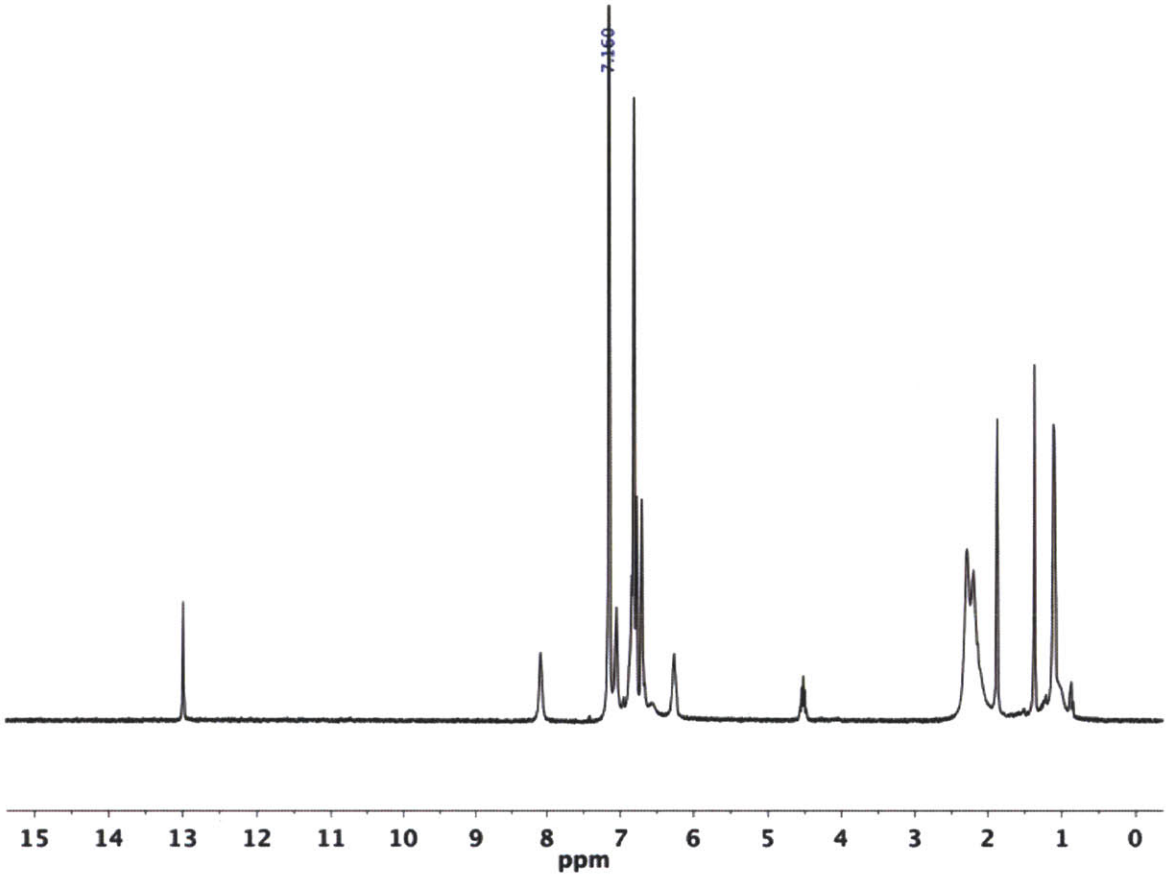

Mo(NAr*)(CHCMe$_2$Ph)(Pyr)[OCH(CF$_3$)$_2$](py) ($\mathbf{18_{Mo}}$). Hexafluoroisopropanol (4.9 μL, 0.047 mmol) was added to a solution of Mo(NAr*)(CHCMe$_2$Ph)(Pyr)$_2$(py), $\mathbf{13_{Mo}}$ (35.6 mg, 0.051 mmol), in 1.5 mL benzene. The reaction mixture was stirred for 1.5 h and then filtered through a fritted filter. The volatiles were removed *in vacuo* from the filtrate. Pentane (2 mL) was added to the remaining oil. The mixture was cooled to −25 °C, and the yellow solid was collected on a fritted filter and dried *in vacuo*; yield 27 mg, 76 %: ^{1}H NMR (C_6D_6) δ 13.069 (s, 1H, Mo=C*H*), 7.888 (d, 2H, J_{HH} = 5 Hz), 7.021 (s, 2H, Mes $C_6H_2Me_3$), 6.897 – 6.754 (overlapping signals, 13 H), 6.655 (s, 2H, Mes $C_6H_2Me_3$), 6.200 (t, 2H, J_{HH} = 7 Hz), 4.220 (septet, J_{CF} = 7 Hz, 1H, OC*H*(CF$_3$)$_2$), 2.264 (s, 6H, MesC*H*$_3$), 2.219 (s, 6H, MesC*H*$_3$), 1.890 (s, 3H, Mo=CHC*Me*$_2$Ph), 1.455 (br s, 6H, MesC*H*$_3$), 1.242 (s, 3H, Mo=CHC*Me*$_2$Ph)); ^{1}H NMR (CD_2Cl_2, alkylidene) δ

12.887 ($^1J_{CH}$ = 148 Hz); ^{13}C NMR (CD_2Cl_2) δ 324.4 (Mo=*C*H), 153.8, 153.2, 152.3, 146.5, 139.0, 137.4, 136.3, 130.2, 129.9, 128.9, 127.9, 126.2, 124.8, 75.8 (m, 5 lines visible above baseline, J_{CF} = 30 Hz), 52.2, 30.8, 27.7, 21.4, 21.4, 20.0; ^{19}F{^{1}H} NMR (C_6D_6) δ -73.34 (apparent quintet, J = 9 Hz, 3F), -74.41 (apparent quintet, J = 9 Hz, 3F). Anal. Calcd for $C_{46}H_{47}F_6MoN_3O$: C, 63.66; H, 5.46; N, 4.84. Found: C, 63.46; H, 5.51; N, 4.72.

^{1}H NMR spectrum of **18$_{Mo}$** in C_6D_6:

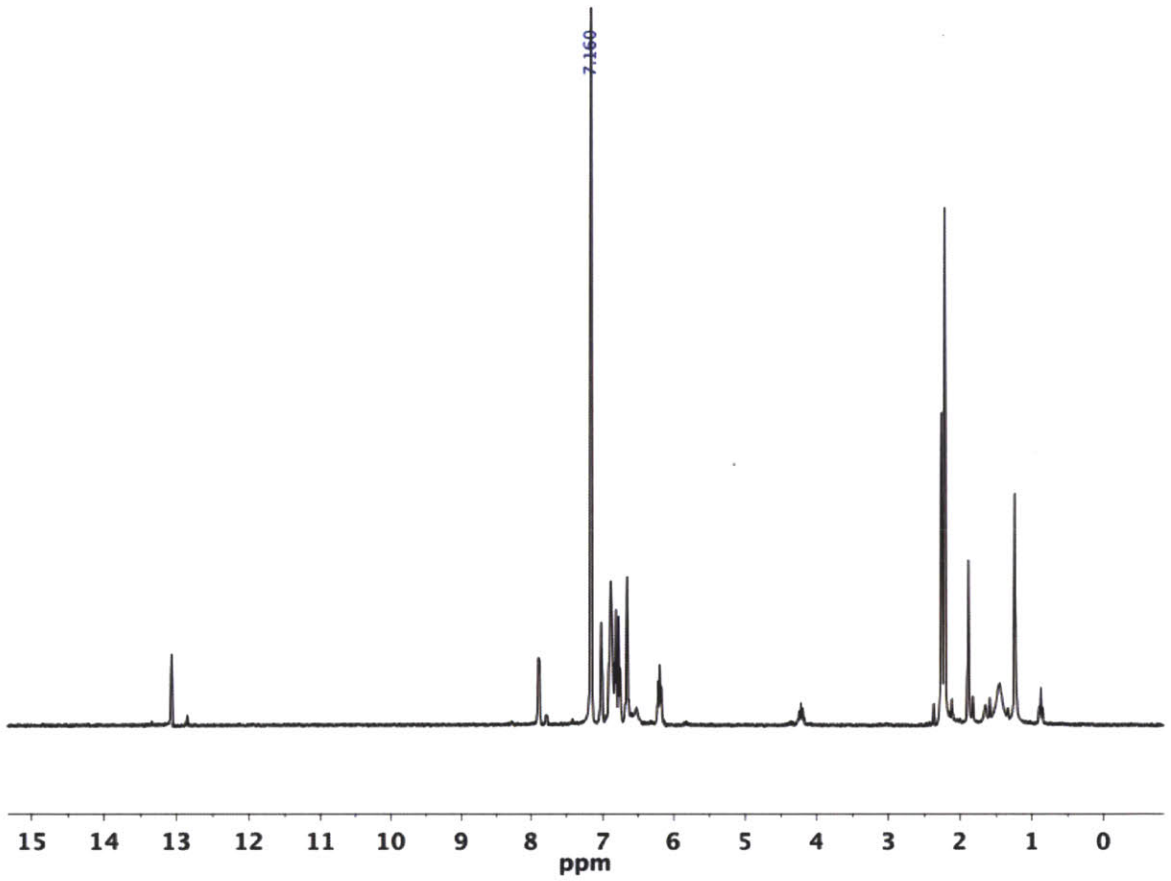

Mo(NAr*)(CHCMe$_2$Ph)(Pyr)(O-2,6-Me$_2$C$_6$H$_3$)(py) (19$_{Mo}$). Solutions of Mo(NAr*)(CHCMe$_2$Ph)(Pyr)$_2$(py), **13$_{Mo}$**, (34 mg, 0.044 mmol) and 2,6-Me$_2$C$_6$H$_3$OH (5.4 mg, 0.044 mmol) each in 0.5 mL C_6D_6 were combined in a Teflon-stoppered NMR tube. After 2 h, the reaction mixture was filtered through a pipette filter with Celite. The volatiles were removed *in vacuo* from the filtrate. Two mL of pentane were added to the residue and the mixture was cooled to −25 °C. A yellow solid formed and was collected on a frit and washed with cold pentane; yield 27 mg, 76 %: ^{1}H NMR (C_6D_6) δ 13.982 (s, 1H, Mo=C*H*), 8.026 (d, 2H, J_{HH} = 5 Hz), 6.955 (d, 2H, J_{HH} = 7 Hz), 6.901 – 6.873 (overlapping signals, 4H), 6.836 (s, 1H), 6.822 (s

1H), 6.787 – 6.763 (overlapping signals, 5H), 6.740 (s, 2H), 6.635 (s, 4H), 6.590 (t, J_{HH} = 8 Hz,1H), 6.143 (t, 2H, J_{HH} = 7 Hz), 2.133 (s, 6H, MesCH_3), 2.080 (s, 6H, MesCH_3), 2.010 (s, 6H, MesCH_3), 1.947 (s, 3H, Mo=CHCMe_2Ph), 1.627 (s, 6H, $C_6H_3Me_2OH$), 1.423 (s, 3H, Mo=CHCMe_2Ph); ^{1}H NMR (CD_2Cl_2, alkylidene) δ 12.768 ($^1J_{CH}$ = 148 Hz); ^{13}C NMR (CD_2Cl_2) δ 321.2 (Mo=*C*H), 161.0, 154.2, 151.9, 149.3, 140.5, 139.0, 137.4, 137.4, 137.0, 131.4, 130.5, 129.3, 129.2, 128.3, 128.2, 127.5, 127.3, 126.1, 126.0, 124.9, 119.4, 106.5, 52.2, 31.5, 29.3, 21.4, 21.3, 21.2, 19.0. Anal. Calcd for $C_{51}H_{55}MoN_3O$: C, 74.52; H, 6.74; N, 5.11. Found: C, 74.22; H, 6.56; N, 4.97.

^{1}H NMR spectrum of **19$_{Mo}$** in C_6D_6:

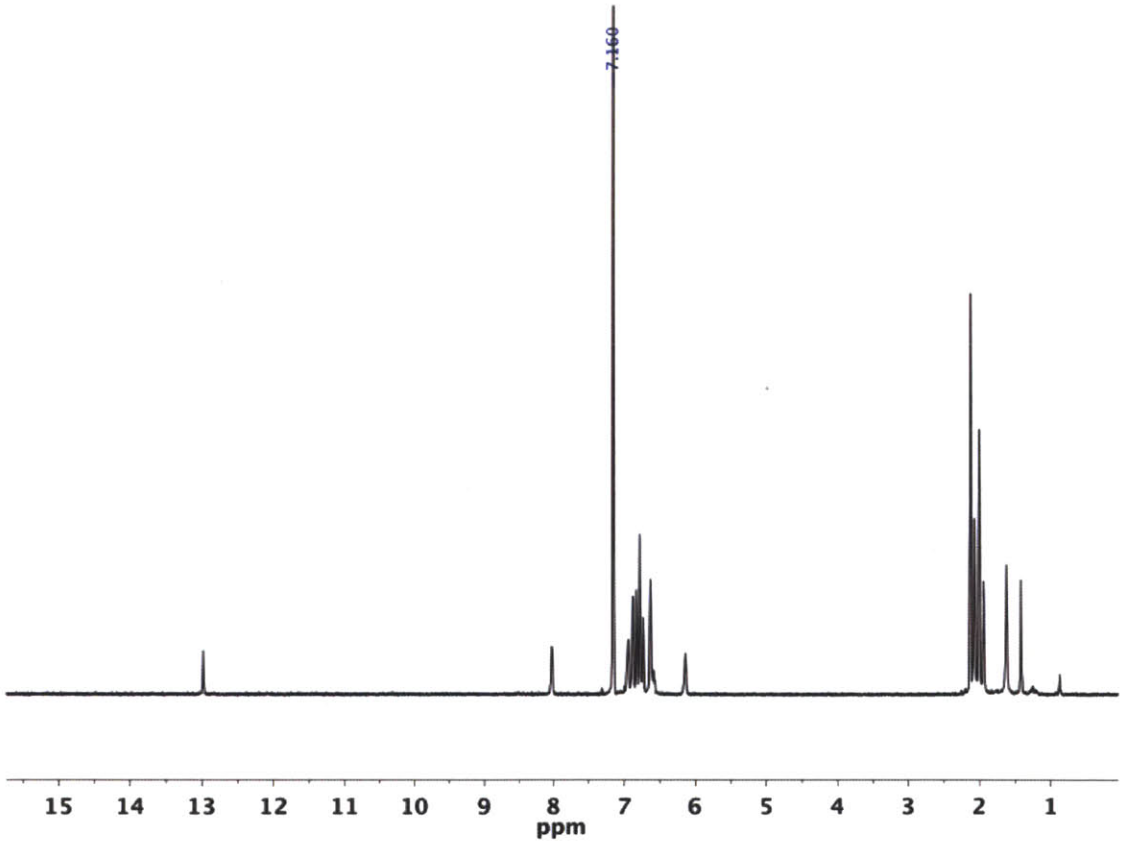

Mo(NAr*)(CHCMe$_2$Ph)(Pyr)[OSi(^{i}Pr)$_3$](py) (20$_{Mo}$). HOSi(i-Pr)$_3$ (8.8 μL, 44 μmol) was added to a suspension of Mo(NAr*)(CHCMe$_2$Ph)(Pyr)$_2$(py), **13$_{Mo}$**, (34 mg, 44 μmol) in 0.7 mL C_6D_6 in a Telfon-stoppered NMR tube. A ^{1}H NMR spectrum obtained after 1 h shows complete consumption of starting materials. The reaction mixture was filtered through a pipette filter with Celite, and the volatiles removed *in vacuo* from the filtrate to leave a brown oil. Pentane (1 mL)

was added to the residue and the mixture was cooled to −25 °C. The orange solid was collected on a fritted filter and washed with cold pentane; yield 30 mg, 77 %: ^{1}H NMR (C_6D_6) δ 13.204 (br s, 1H, Mo=C*H*), 7.456 (br s, 2H), 7.094 (t, 2H, J_{HH} = 8 Hz), 7.019 (m, 4H), 6.774 (s, 3H), 6.727 (m, 2H), 6.623 (s, 2H), 6.373 (s, 2H), 6.332 (s, 2H), 6.253 (br s, 2H), 2.318 (s, 6H, MesC*H*$_3$), 2.131 (br s, MesC*H*$_3$), 1.900 (br s, MesC*H*$_3$, 12 H integrated with previous signal), 1.351 (s, 3H, Mo=CHC*Me*$_2$Ph), 1.298 – 1.137 (overlapping m, 3H, C*H*Me$_2$), 1.107 (s, 3H, Mo=CHC*Me*$_2$Ph), 0.995 (br m, CH*Me*$_2$), 0.969 (br m, CH*Me*$_2$, 18 H integrated together with previous signal); ^{13}C{^{1}H} NMR (CD_2Cl_2, –30 °C) δ 321.5 (Mo=*C*H), 152.9, 151.6, 147.2, 139.4, 138.4, 138.3, 138.0, 137.8, 137.4, 136.7, 136.7, 136.2, 135.7, 135.1, 131.7, 129.7, 129.4, 129.2, 129.0, 128.5, 128.4, 128.1, 126.3, 126.1, 125.9, 124.1, 105.4, 51.1 (Mo=CH*C*Me$_2$Ph), 31.5, 28.3, 21.4, 21.4, 20.7, 20.6, 20.6, 20.4, 18.6, 18.6, 14.0. Anal. Calcd for $C_{52}H_{67}MoN_3OSi$: C, 71.45; H, 7.73; N, 4.81. Found: C, 71.19; H, 7.54; N, 4.86.

^{1}H NMR spectrum of **20$_{Mo}$** in C_6D_6:

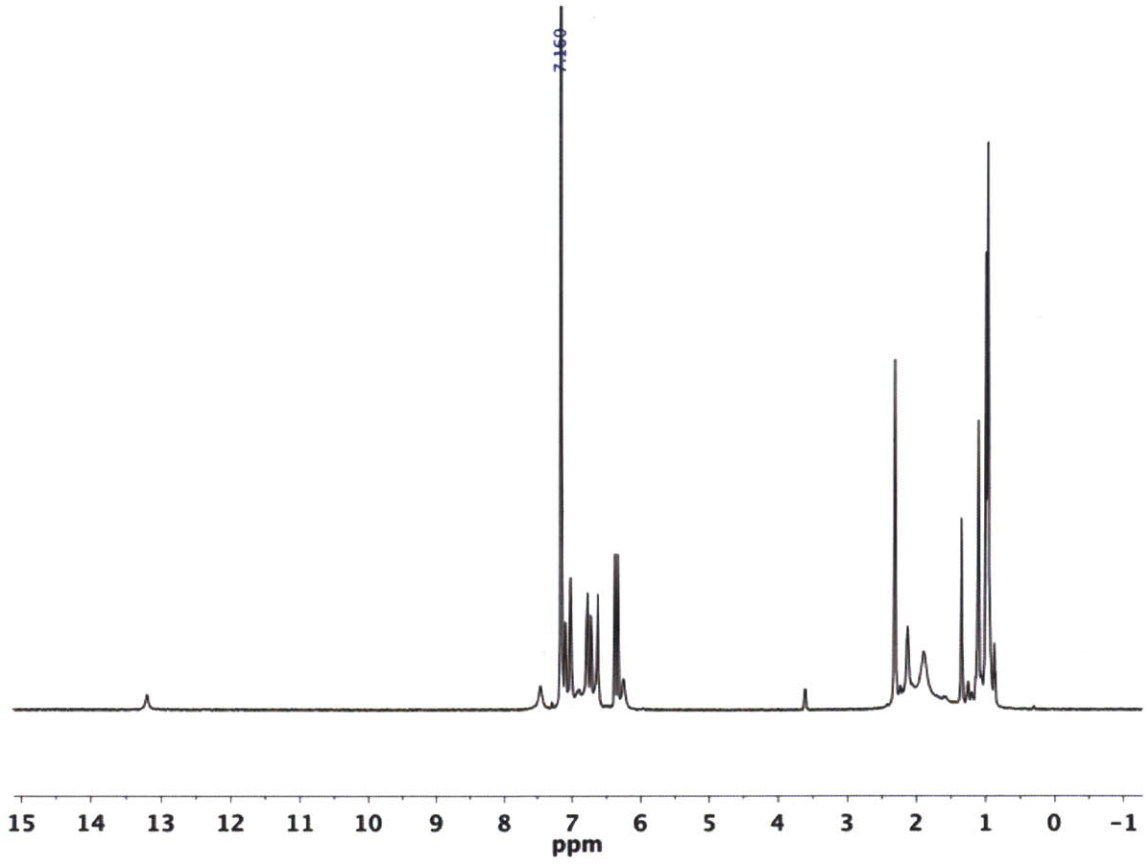

Mo(NAr*)(CHCMe$_2$Ph)(Pyr)(OSiPh$_3$)(py) ($\mathbf{21_{Mo}}$). A solution of triphenylsilanol (14.8 mg, 0.054 mmol) in 1 mL toluene was added to a solution of Mo(NAr*)(CHCMe$_2$Ph)(Pyr)$_2$(py), $\mathbf{13_{Mo}}$ (41 mg, 0.054 mmol), in 3 mL toluene and the reaction mixture was stirred for 5 h. The reaction mixture was filtered through a pipette filter with Celite, and the volatiles removed *in vacuo* from the filtrate. The residue was dissolved in a 1:1 toluene:pentane mixture and the solution was cooled to −25 °C. The solid was collected on a frit, washed with cold pentane, and dried *in vacuo*. The filtrate was concentrated to collect a second crop in the same manner; total yield 26.1 mg, 50 %: ^{1}H NMR (C_6D_6) δ 13.320 (s, 1H, $^1J_{CH}$ = 148 Hz, Mo=C*H*), 7.375 (dd, 6H, J_{HH} = 8 Hz, J_{HH} = 2 Hz), 7.290 (d, 2H, J_{HH} = 5 Hz), 7.197 and 7.183 (overlapping s, 7 H), 7.049 – 6.931 (overlapping signals, 9 H), 6.796 – 6.703 (overlapping signals, 7 H), 6.584 – 6.548 (overlapping signals, 3H), 6.021 (t, 2H, J_{HH} = 7 Hz), 2.246 (s, 6H, Mes $C_6H_2Me_3$), 2.045 (s, 6H Mes $C_6H_2Me_3$), 1.756 (s, 3H, Mo=CHCMe_2Ph), 2.0 – 1.4 (very br s, 6H, Mes $C_6H_2Me_3$), 1.250 (s, 3H, Mo=CHCMe_2Ph). ^{1}H NMR (CD_2Cl_2, alkylidene) δ 13.089 ($^1J_{CH}$ = 147 Hz); ^{13}C NMR (CD_2Cl_2) δ 323.2, 152.6, 147.8, 138.8, 137.9, 137.0, 136.1, 132.2, 129.7, 129.3, 129.2, 128.8, 128.5, 127.8, 126.8, 126.7, 126.3, 124.3, 106.6, 52.5, 31.2, 28.8, 21.6, 21.1, 20.8. Anal. Calcd for $C_{52}H_{67}MoN_3OSi$: C, 75.05; H, 6.30; N, 4.30. Experimental: C, 74.64; H, 6.04; N, 4.34.

^{1}H NMR spectrum of $\mathbf{21_{Mo}}$ in CD_2Cl_2:

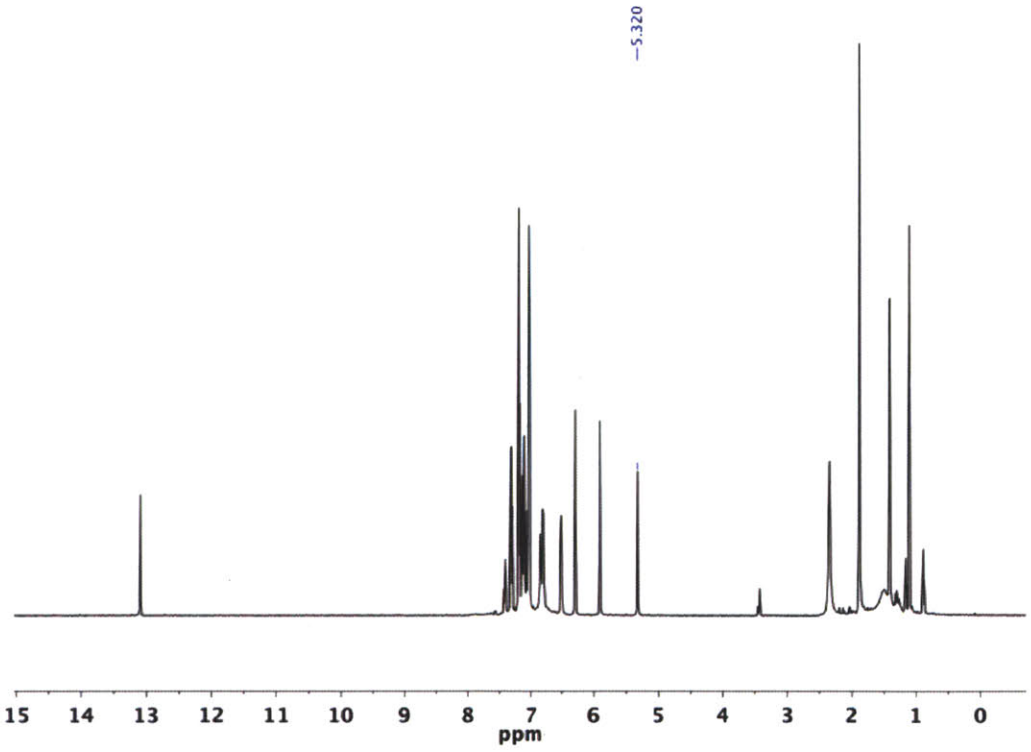

Mo(NAr*)(CHCMe$_2$Ph)(Pyr)[OSi(SiMe$_3$)$_3$](py) ($\mathbf{22_{Mo}}$). A solution of HOSi(SiMe$_3$)$_3$ (14 mg, 0.053 mmol) in 0.3 mL C_6D_6 was added to a suspension of Mo(NAr*)(CHCMe$_2$Ph)(Pyr)$_2$(py), $\mathbf{13_{Mo}}$ (40 mg, 0.052 mmol), in 0.3 mL C_6D_6 in a Teflon-stoppered NMR tube. A ^{1}H NMR spectrum obtained after 1 h shows that consumption of starting materials was complete. The reaction mixture was filtered through a pipette filter with Celite, and the volatiles were removed *in vacuo* from the filtrate. Pentane (1 mL) was added to the residue and the mixture was cooled to −25 °C. The dark yellow crystals were collected by decantation of the supernatant, and dried *in vacuo*; yield 31 mg, 61 %: ^{1}H NMR (C_6D_6) δ 13.303 (s, 1H, Mo=C*H*), 7.371 (d, 2H, J_{HH} = 5 Hz), 7.250 (d, 2H, J_{HH} = 8 Hz), 7.135 (d, 2H, J_{HH} = 8 Hz), 7.053 (d, 1H, J_{HH} = 7 Hz), 7.023 (s, 2H), 6.866 – 6.691 (overlapping signals, 4H), 6.653 – 6.621 (overlapping signals, 4H), 6.576 (s, 2H), 6.352 (t, 2H, J_{HH} = 7 Hz), 2.322 (s, 6H, Mes C$_6$H$_2$*Me*$_3$), 2.072 (s, 9H), 1.3 – 2.0 (br s, 6H, Mes C$_6$H$_2$*Me*$_3$), 1.364 (s, 3H, Mo=CHC*Me*$_2$Ph), 0.209 (s, 27 H, OSi(SiMe$_3$)$_3$). ^{1}H NMR (CD_2Cl_2, alkylidene) δ 13.096 ($^1J_{CH}$ = 147 Hz); ^{13}C NMR (CD_2Cl_2) δ 322.5 (Mo=*C*H), 153.6, 152.5, 148.3, 138.1, 136.8, 131.3, 130.0, 129.3, 128.6, 126.9, 126.4, 126.2, 125.0, 106.8, 52.3, 31.4, 30.8, 21.7, 21.0, 20.9, 1.5. Anal. Calcd for $C_{52}H_{73}MoN_3OSi_4$: C, 64.76; H, 7.63; N, 4.36; Experimental: C, 64.84; H, 7.75; N, 4.32.

^{1}H NMR spectrum of $\mathbf{22_{Mo}}$ in C_6D_6:

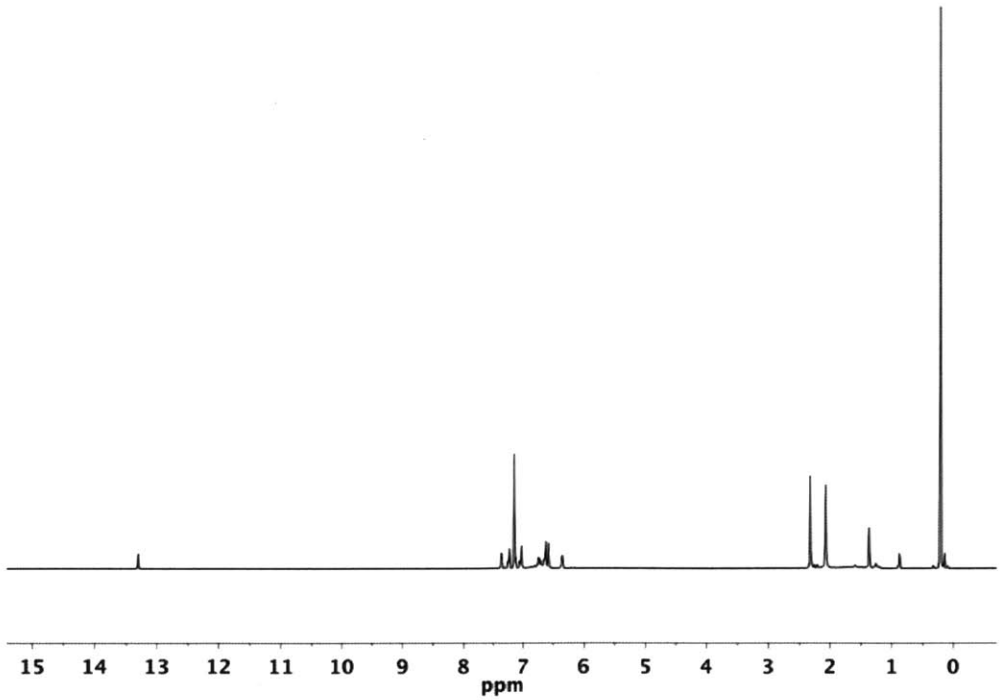

***In situ* observation of Mo(NAr*)(CHCMe$_2$Ph)(Pyr)(OCPh$_3$).** A solution of Ph_3COH (12 mg, 0.046 mmol) in 0.3 mL C_6D_6 was added to a suspension of Mo(NAr*)(CHCMe$_2$Ph)(Pyr)$_2$(py) (35 mg, 0.047 mmol) in 0.3 mL C_6D_6 in a teflon stoppered NMR tube which was heated to 60 °C 2 h. The reaction mixture was filtered through a pipette filter with Celite. The volatiles were removed *in vacuo* from the filtrate. ^{1}H NMR (C_6D_6) δ 10.840 (s, 1H, Mo=C*H*), 7.304 (d), 7.090 – 6.862 (overlapping signals), 6.749 (s), 6.517 (s), 6.377 (s), 6.246 (s), 2.331 (s, 6H, Mes C_6H_2*Me*$_3$), 2.095 (s, 6H, Mes C_6H_2*Me*$_3$), 2.008 (s, 6H, Mes C_6H_2*Me*$_3$), 1.421 (s, 3H, Mo=CHC*Me*$_2$Ph), 1.351 (s, 3H, Mo=CHC*Me*$_2$Ph).

General procedure for addition of B(C$_6$F$_5$)$_3$ to 21$_{Mo}$ and 22$_{Mo}$. A solution of $B(C_6F_5)_3$ in ~0.2 mL C_6D_6 was added to a solution of Mo complex in ~0.4 mL C_6D_6 in a teflon-stoppered NMR tube. The tube was inverted to mix and ^{1}H and ^{19}F NMR spectra were obtained.

21$_{Mo}$': 14.3 mg (0.0146 mmol) **21$_{Mo}$** and 7.0 mg (0.0137 mmmol) $B(C_6F_5)_3$. ^{1}H NMR (C_6D_6, alkylidene resonances): δ 12.234 (W=C*H*, *anti*, $^1J_{CH}$ = 154 Hz, integration 51), 11.799 (W=C*H*, *syn*, $^1J_{CH}$ = 121 Hz, integration 100).

22$_{Mo}$': 21.2 mg (0.0220 mmol) **22$_{Mo}$** and 11.0 mg (0.0215 mmol) $B(C_6F_5)_3$. ^{1}H NMR spectra were obtained at 400 MHz, 500 MHz, and 600 MHz to distinguish the ^{13}C satellites from resonances due to trace impurities. ^{1}H NMR (C_6D_6, alkylidene resonances): δ 12.995 (W=C*H*, *anti*, $^1J_{CH}$ = 149 Hz, integration 44), 12.386 (W=C*H*, *syn*, $^1J_{CH}$ = 118 Hz, integration 100).

Mo(NAr*)(CHCMe$_2$Ph)(Me$_2$Pyr)(O^{t}Bu) (23$_{Mo}$). From 8$_{Mo}$. A suspension of **8$_{Mo}$** (31 mg, 42 μmol) in 3 mL Et_2O was added to a vial containing solid LiMe$_2$Pyr (4.2 mg, 42 μmol). The mixture was stirred 2h over which time the solution changed from yellow to orange. The volatiles were removed *in vacuo* and the resulting oil was extracted with pentane and the extract was filtered through a pipette filter. The pentane was removed *in vacuo* to leave a dark orange solid; yield 30 mg (99 %). Compound **23$_{Mo}$** can be recrystallized from MeCN.

From 14$_{Mo}$. HO^{t}Bu (7 μL, 73 μmol) was added to a solution of **12** (55 mg, 74 μmol) in 3 mL Et_2O in a 20 mL vial and stirred 18 h. The volatiles were removed *in vacuo*, and the solid was extracted with pentane and filtered through a pipette filter. The volatiles were removed *in vacuo* from the filtrate to leave a dark orange solid; yield 41 mg (77 %).

Compound **23_{Mo}** was observed as a 1:1 mixture of *syn* and *anti* alkylidene species. The spectral features are reported together since they cannot be distinguished except the alkylidene resonances: ^{1}H NMR (C_6D_6, 20 °C) δ 11.861 (s, 1H, $^1J_{CH}$ = 118 Hz, Mo=C*H*, syn), 11.696 (s, 1H, $^1J_{CH}$ = 153 Hz, Mo=C*H*, anti), 7.174 – 7.099 (overlapping signals, Ar*H*), 7.056 – 6.849 (overlapping signals, Ar*H*), 6.730 (s, 2H, Ar*H*), 6.259 (s, 2H, pyr*H*), 6.075 (s, 2H, pyr*H*), 2.279 (s, 6H, mesitylCH_3), 2.225 (s, 6H, mesitylCH_3), 2.186, 2.180 (overlapping s, 12H, mesitylCH_3), 2.088 (s, 6H, mesitylCH_3), 2.032 (s, 6H, mesitylCH_3), 1.904 (br s, 6H, pyrCH_3), 1.709 (s, 3H, MoCHCMe_2Ph), 1.563 (s, 3H, MoCHCMe_2Ph), 1.433 (s, 3H, MoCHCMe_2Ph), 1.270 (s, 3H, MoCHCMe_2Ph), 0.954 (s, 9H, OCMe_3), 0.845 (s, 9H, OCMe_3);); ^{13}C{^{1}H} NMR (C_6D_6, 20 °C) δ 295.9, 283.4 (Mo=*C*H), 155.0, 154.9, 150.4, 149.4, 140.2, 138.1, 138.0, 137.4, 137.3, 137.3, 137.0, 136.9, 136.8, 136.5, 136.2, 136.1, 130.6, 130.0, 129.8, 129.4, 129.3, 129.3, 128.9, 128.9, 128.7, 128.4, 127.6, 127.3, 127.2, 126.7, 126.7, 126.6, 126.6, 126.4, 126.4, 126.3, 126.3, 126.2, 124.1, 124.0, 119.0, 109.4, 109.1, 83.4, 80.9, 53.1, 51.9, 51.6, 50.9, 33.4, 33.1, 32.9, 31.8, 31.5, 31.2, 30.8, 30.1, 21.8, 21.8, 21.6, 21.6, 21.4, 20.7, 20.6, 20 – 18 (br s). Anal. Calcd for $C_{44}H_{54}MoN_2O$: C, 73.11; H, 7.53; N, 3.88. Found: C, 73.22; H, 7.58; N, 3.91.

W(NAr*)(CHCMe$_2$Ph)(Me$_2$Pyr)(O^{t}Bu) (23_W) HO^{t}Bu (6.4 μL, 66.9 μmol) was added to a −25 °C, stirring solution of W(NAr*)(CHCMe$_2$Ph)(Me$_2$Pyr)$_2$, **14_W** (55.3 mg, 66.5 μmol), in 2 mL Et_2O. The solution was stirred at ambient temperature for 16 h. The volatiles were removed *in vacuo*. The orange oil was extracted with pentane and the extract was filtered through a pipette filter. The volatiles were removed *in vacuo* from the filtrate. The orange oil was dissolved in minimal MeCN/Et_2O and stored at −25 °C for 16 h over which time crystals formed. The mother liquor was removed by pipette and the crystals were washed with cold MeCN and dried under vacuum to give 42.0 mg, 78 % yield. ^{1}H NMR (C_6D_6, *Anti* isomer, 38 %, selected resonances) *δ* 9.663 (s, $^1J_{CH}$ = 150 Hz, W=C*H*), 6.246 (s, 2H, pyr*H*), 2.203 (s, 6H, MesCH_3), 2.179 (s, 6H, MesCH_3), 2.046 (s, 6H, MesCH_3), 1.417 (s, 3H, W=CHCMe_2Ph), 1.297 (s, 3H, W=CHCMe_2Ph), 0.907 (s, 9H, OCMe_3); ^{1}H NMR (C_6D_6, *Syn* isomer, 62 %, selected resonances) *δ* 8.582 (s, $^1J_{CH}$ = 110 Hz, J_{HW} = 14 Hz, W=C*H*), 6.052 (s, 2H, Pyr*H*), 2.277 (s, 6H, MesCH_3), 2.228 (s, 6H, MesCH_3), 2.107 (s, 6H, MesCH_3), 1.685 (s, 3H, W=CHCMe_2Ph), 1.566 (s, 3H, W=CHCMe_2Ph), 0.823 (s, 9H, OCMe_3); ^{1}H NMR (C_6D_6, remaining resonances reported together) *δ* 7.224 (d, J_{HH} = 8 Hz), 7.174 – 7.132 (signals overlapping solvent), 7.034 (t, J_{HH} = 8 Hz), 6.997 (s), 6.931 (s),

6.873 (d, J_{HH} = 4 Hz), 6.844 (s), 6.737(s),1.937 (br s, *Me*$_2$pyr); $^{13}C\{^1H\}$ NMR (C_6D_6) δ 265.0, 256.0 (W=*C*H), 154.0, 152.8, 152.0, 139.8, 137.2, 137.2, 137.1, 137.0, 136.6, 136.5, 136.3, 136.2, 130.3, 129.9, 129.6, 129.2, 128.8, 127.3, 126.6, 126.2, 126.1, 125.4, 110.1, 85.4, 82.0, 51.4, 47.7, 34.5, 33.7, 33.6, 32.7, 31.6, 31.6, 21.8, 21.7, 21.6, 21.6, 21.4, 20.6. Anal. calcd for $C_{44}H_{54}N_2OW$: C, 65.18; H, 6.71; N, 3.46. Found: C, 65.02; H, 6.76; N, 3.59.

^1H NMR spectrum of **23$_W$** in C_6D_6:

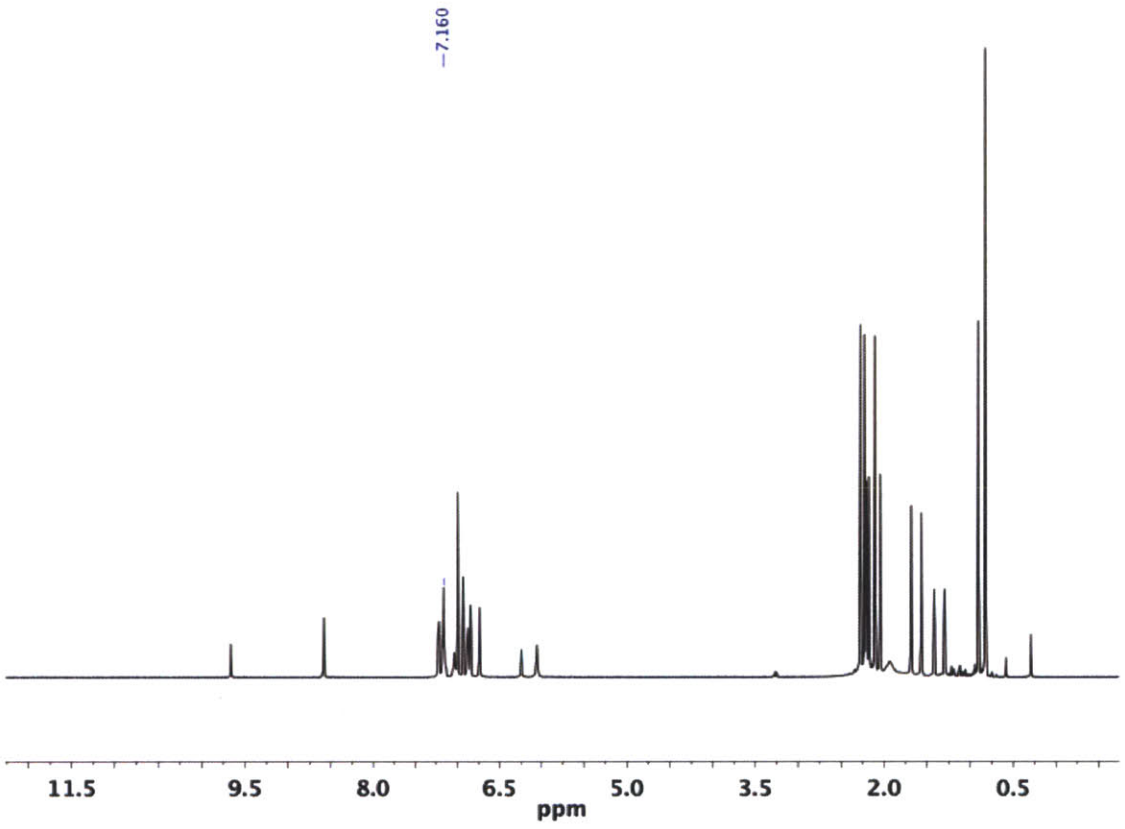

Mo(NAr*)(CHCMe$_2$Ph)(Me$_2$Pyr)[OCMe(CF$_3$)$_2$] (24$_{Mo}$) HOCMe(CF$_3$)$_2$ (9.8 μL, 80 μmol) was added by microsyringe to a −25 °C, stirred solution of Mo(NAr*)(CHCMe$_2$Ph)(Me$_2$Pyr)$_2$, **14$_{Mo}$** (59.5 mg, 80.0 μmol), in 2 mL Et$_2$O. The solution was stirred at ambient temperature for 16 h. The volatiles were removed *in vacuo*. The oil was extracted with pentane and the extract was filtered through a pipette filter. The volatiles were removed *in vacuo* from the filtrate. The dark yellow oil was dissolved in minimal acetonitrile and the solution was stored at −25 °C for 16 h. The mother liquor was removed from the crystals by pipette and the crystals were washed with cold acetonitrile and dried under vacuum; yield 45 mg, 68 %; ^1H NMR (C_6D_6, *syn* isomer, 70 %,

selected resonances) δ 12.073 (s, 1H, Mo=C*H*, $^1J_{CH}$ = 120 Hz), 5.910 (s, 1H, $Me_2C_4H_2N$), 5.786 (s, 1H, $Me_2C_4H_2N$), 2.251 (s, 6H, MesCH_3), 2.170 (s, 6H, MesCH_3), 1.948 (s, 3H, Methyl), 1.692 (s, 3H, Methyl), 1.566 (s, 3H, Methyl), 1.521 (s, 3H, Methyl), 0.678 (s, 3H, Methyl); ^{1}H NMR (C_6D_6, *anti* isomer, 30 %, selected resonances) δ 11.896 (s, 1H, Mo=C*H*), 6.143 (s, 2H, $Me_2C_4H_2N$), 2.369 (s, 6H, MesCH_3), 2.185 (s, 6H, MesCH_3), 1.718 (s, 6H, $Me_2C_4H_2N$), 1.390 (s, 3H, Methyl), 1.284 (s, 3H, Methyl), 1.089 (s, 3H, Methyl); ^{1}H NMR (C_6D_6, remaining resonances reported together) δ 7.143 – 7.206 (overlapping signals, Ar*H*), 6.996 – 6.925 (overlapping signals, Ar*H*), 6.883 (s, Ar*H*), 6.868 (s, Ar*H*), 6.804 (s, Ar*H*), 6.776 (m, Ar*H*), 6.706 (s, Ar*H*), 2.108 (s, MesCH_3, coincident signal from both isomers; ^{13}C {^{1}H} NMR (CD_2Cl_2, both isomers reported together) δ 293.0, 155.3, 148.0, 140.6, 137.8, 137.2, 136.5, 136.0, 135.9, 135.8, 135.7, 132.4, 130.9, 130.2, 129.6, 129.1, 128.8, 128.7, 128.6, 128.5, 128.5, 128.3, 128.3, 128.2, 127.5, 126.8, 126.6, 126.5, 126.3, 108.9, 108.2, 54.8, 51.3, 31.7, 29.9, 29.2, 27.6, 21.7, 21.4, 21.3, 21.3, 20.1, 18.8, 18.3, 15.8; ^{19}F NMR (C_6D_6) δ -77.00 (quartet, J_{FF} = 9 Hz), -77.287 (quartet, J_{FF} = 9 Hz).

^{1}H NMR spectrum of **24$_{Mo}$** in C_6D_6:

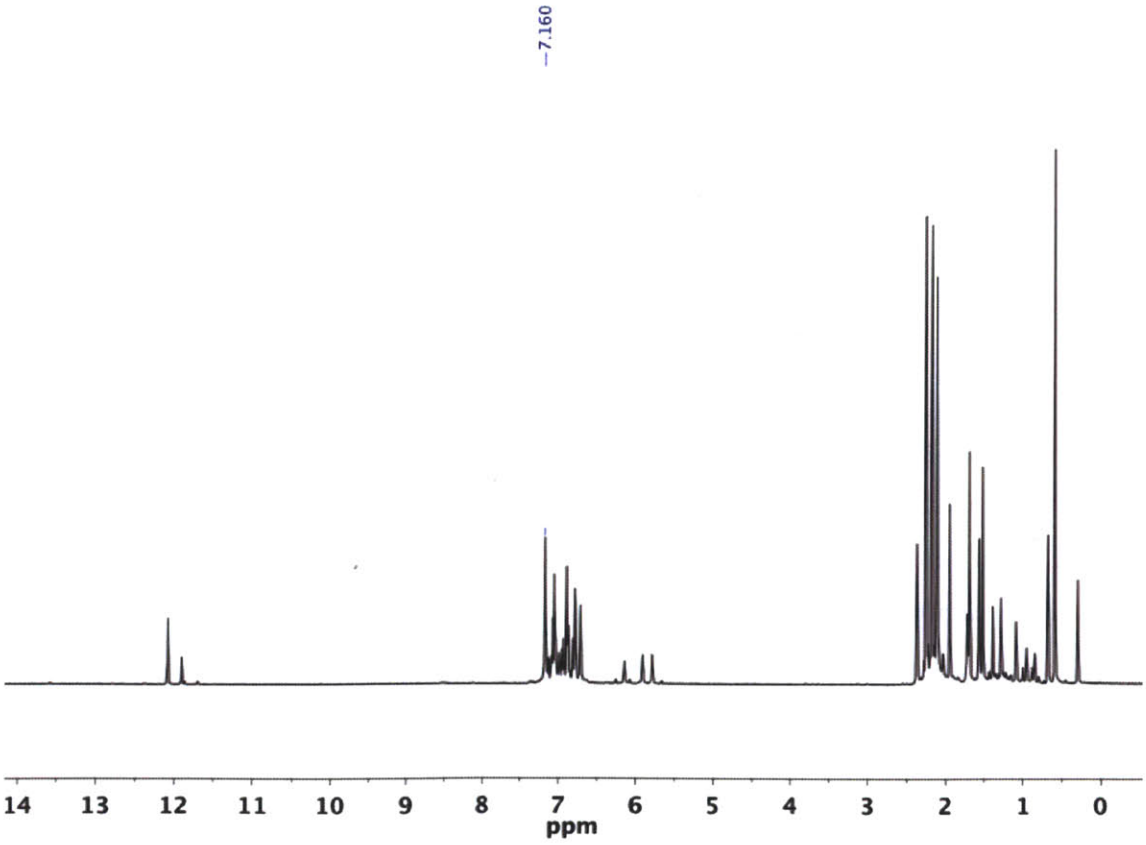

W(NAr*)(CHCMe$_2$Ph)(Me$_2$Pyr)[OCMe(CF$_3$)$_2$] (24$_W$) HOCMe(CF$_3$)$_2$ (8.5 μL, 69 μmol) was added by microsyringe to a −25 °C, stirring solution of W(NAr*)(CHCMe$_2$Ph)(Me$_2$Pyr)$_2$, **14$_W$** (57.9 mg, 69.6 μmol), in 2 mL Et$_2$O. The solution was stirred at ambient temperature for 16 h. The volatiles were removed *in vacuo*. The oil was extracted with pentane and the extract was filtered through a pipette filter. The volatiles were removed *in vacuo* from the filtrate. The dark yellow oil was dissolved in minimal MeCN and stored at −25 °C for 16 h over which time crystals formed. The mother liquor was removed by pipette and the crystals were washed with cold MeCN and dried under vacuum to give 43 mg, 68 % yield. ^{1}H NMR (C$_6$D$_6$) δ 8.846 (s, 1H, $^1J_{CH}$ = 113 Hz, W=C*H*), 7.114 – 7.067 (overlapping signals, 4H, Ar*H*), 6.999 (d, J_{HH} = 7 Hz, 1H), 6.964 (s, 3H), 6.764 (s, 2H), 6.724 (s, 2H), 5.927 (s, 1H, pyr*H*), 5.718 (s, 1H, pyr*H*), 2.315 (s, 3H, C*H*$_3$), 2.260 (s, 6H, MesC*H*$_3$), 2.171 (s, 6H, MesC*H*$_3$), 2.129 (s, 6H, MesC*H*$_3$), 1.727 (s, 3H, C*H*$_3$), 1.677 (s, 3H, C*H*$_3$), 1.522 (s, 3H, C*H*$_3$), 0.692 (s, 3H, OC(CF$_3$)$_2$C*H*$_3$); ^{13}C{^{1}H} NMR (C$_6$D$_6$) δ 263.1 (W=*C*H), 153.9, 150.9, 140.2, 137.0, 136.6, 136.2, 135.9, 130.6, 129.3, 128.9, 128.7, 128.7, 126.9, 126.7, 126.5, 111.1, 110.3 (Ar*C*), 52.6 (W=CH*C*Me$_2$Ph), 33.1, 31.0, 22.0, 21.6, 21.5, 19.6, 18.6, 16.0, 1.8, 0.4. ^{19}F NMR (C$_6$D$_6$) δ −76.98 (quartet, J_{FF} = 9 Hz), −77.22 (quartet, J_{FF} = 9 Hz). Anal. Calcd for C$_{44}$H$_{48}$F$_6$N$_2$OW: C, 57.52; H, 5.27; N, 3.05. Found: C, 57.34; H, 5.36; N, 3.22.

^{1}H NMR spectrum of **24$_W$** in C_6D_6:

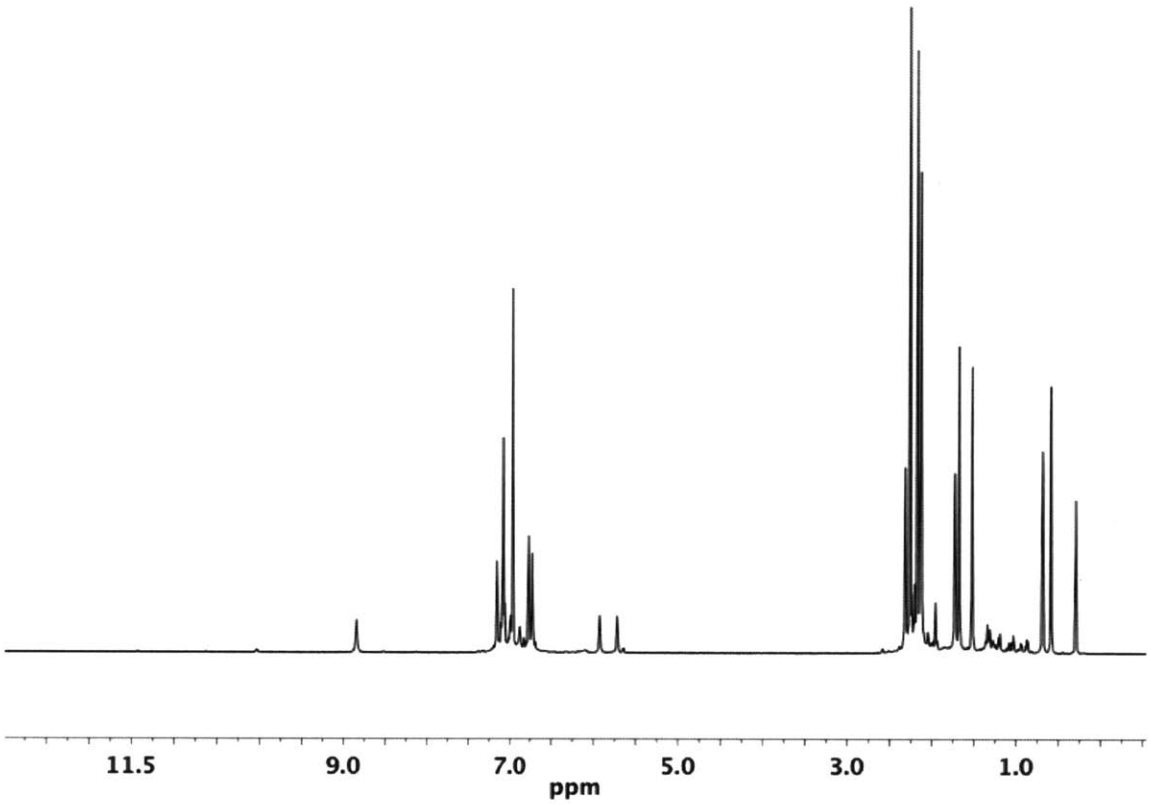

Mo(NAr*)(CHCMe$_2$Ph)(Me$_2$Pyr)(OSiPh$_3$) (25$_{Mo}$). Solid HOSiPh$_3$ (18.9 mg, 68.4 μmol) was added to a −25 °C, stirred solution of Mo(NAr*)(CHCMe$_2$Ph)(Me$_2$Pyr)$_2$, **14$_{Mo}$** (49.5 mg, 66.5 μmol), and the mixture was stirred at ambient temperature for 16 h. The volatiles were removed *in vacuo*. The brown oil was extracted with pentane, the extract was filtered through a pipette filter, and the volatiles removed *in vacuo* from the filtrate. The brown oil was dissolved in minimal acetonitrile and the solution was stored at −25 °C for 16 h. The mother liquor was removed from the orange precipitate by pipette and the precipitate was washed with cold MeCN and dried under vacuum; yield 51 mg, 82 % yield: ^{1}H NMR (C_6D_6) δ 11.479 (s, 1H, Mo=C*H*), 7.357 (t, 3H, Ar*H*), 7.348 (d, 3H, Ar*H*), 7.212 – 7.17 (overlapping signals, 3H, Ar*H*), 7.158 (overlapping with solvent), 7.144 – 7.125 (overlapping signals, 4H), 7.049 – 6.945 (overlapping signals, 6H), 6.891 (m, 1H, Ar*H*), 6.877 (m, 1H), 6.858 (s, 2H, $C_6H_2Me_3$), 6.472 (s, 2H, $C_6H_2Me_3$) 5.990 and 5.905 (overlapping br s, 2H, Me$_2$*pyr*), 2.392 (br s, 3H, *Me*$_2$pyr), 2.274 (s, 6H, $C_6H_2Me_3$), 2.059 (s, 6H, $C_6H_2Me_3$), 2.007 (s, 6H, $C_6H_2Me_3$), 1.525 (s, Mo=CHC*Me*$_2$Ph),

1.481 (s, Mo=CHC*Me*$_2$Ph), 1.203 (br s, 3H, *Me*$_2$pyr); ^{13}C{^{1}H} NMR (CD_2Cl_2) δ 288.0 (Mo=*C*H), 154.9, 148.4, 139.9, 137.1, 136.6, 136.3, 136.1, 135.9, 135.7, 130.6, 130.3, 129.0, 128.7, 128.5, 128.2, 127.4, 126.3, 126.0, 108.4, 53.0, 32.0, 30.7, 21.8, 21.2, 20.7. Anal. Calcd for $C_{58}H_{60}MoN_2OSi$: C, 75.30; H, 6.54; N, 3.03. Found: C, 75.09; H, 6.49; N, 3.07.

^{1}H NMR spectrum of **25$_{Mo}$** in C_6D_6:

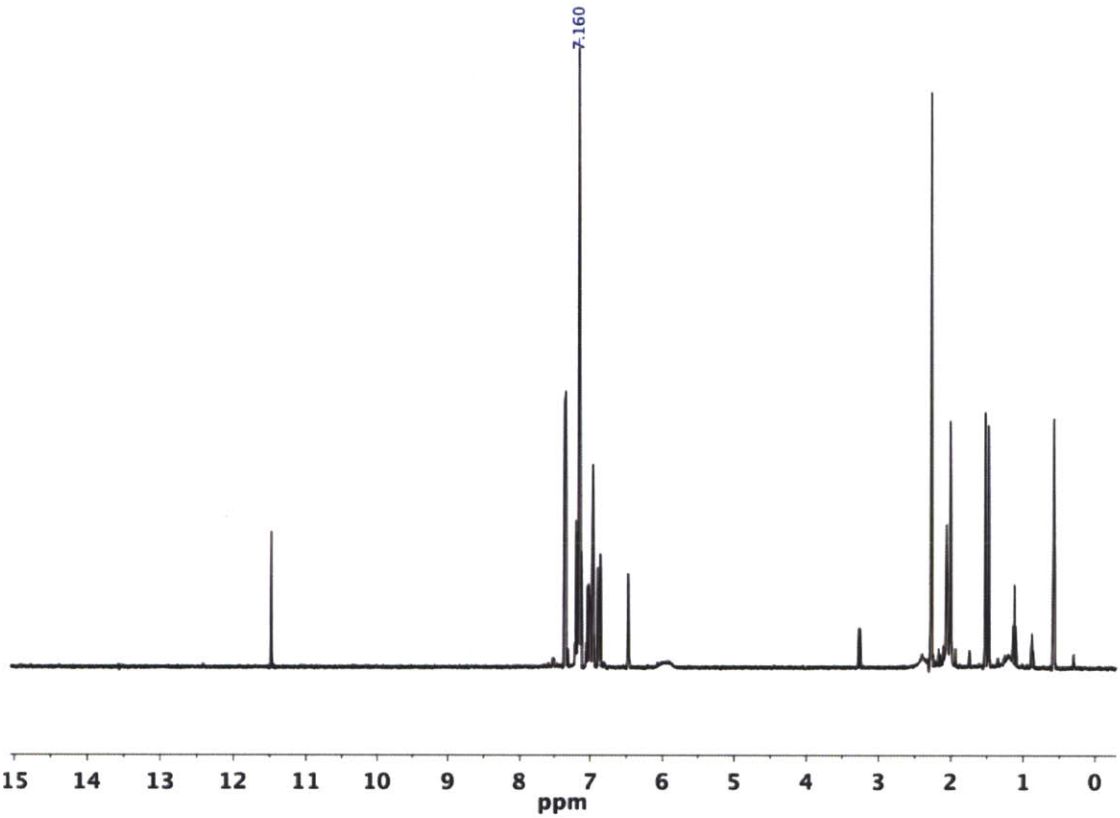

W(NAr*)(CHCMe$_2$Ph)(Me$_2$Pyr)(OSiPh$_3$) (25$_W$) Solid $HOSiPh_3$ (22.7 mg, 82.1 μmol) was added to a −25 °C, stirring solution of W(NAr*)(CHCMe$_2$Ph)(Me$_2$Pyr)$_2$, **14$_W$** (75.7 mg, 91.0 μmol), and the mixture was allowed to stir at ambient temperature for 16 h. The volatiles were removed *in vacuo*. The yellow oil was extracted with pentane, the extract was filtered through a pipette filter, and the volatiles removed *in vacuo* from the filtrate. The yellow oil was dissolved in 1 mL MeCN/0.1 mL Et_2O and stored at −25 °C for 16 h over which time yellow precipitate formed. The mother liquor was removed by pipette and the solid was washed with cold MeCN and dried under vacuum. The mother liquor was concentrated and cooled to −25 °C to collect a second crop for a combined yield of 81.6 mg, 89 %. ^{1}H NMR (C_6D_6) δ 8.286 (s, 1H, W=C*H*,

$^1J_{HW}$ = 15 Hz), 7.309 (dd, 4H, J_{HH} = 8 Hz, J_{HH} = 1 Hz), 7.204 – 7.172 (overlapping signals, 3H), 7.141 (s, 2H), 7.126 (s, 3H), 7.112 (m, 1H), 7.084 – 6.992 (overlapping signals, 6H), 6.955 (m, 1H), 6.940 (s, 1H), 6.875 (s, 2H, $C_6H_2Me_3$), 6.446 (s, 2H, $C_6H_2Me_3$), 6.023 and 5.844 (overlapping br s, 2H, $Me_2C_4H_2N$), 2.343 (br s, 3H, $Me_2C_4H_2N$), 2.282 (s, 6H, $C_6H_2Me_3$), 2.082 (s, 6H, $C_6H_2Me_3$), 2.011 (s, 6H, $C_6H_2Me_3$), 1.563 (s, 3H, Mo=CHCMe_2Ph), 1.431 (s, 3H, Mo=CHCMe_2Ph), 1.334 (br s, 3H, $Me_2C_4H_2N$). $^{13}C\{^1H\}$ NMR (CD_2Cl_2) δ 258.0, 153.7, 151.0, 139.4, 136.8, 136.7, 136.6, 136.2, 136.0, 135.8, 135.4, 130.6, 130.2, 128.9, 128.6, 128.4, 128.3, 126.1, 126.0, 126.0, 109.6, 51.1, 33.8, 32.3, 21.8, 21.3, 20.7. Anal. Calcd for $C_{58}H_{60}N_2OSiW$: C, 68.77; H, 5.97; N, 2.77. Found: C, 68.48; H, 5.78; N, 2.86.

^{1}H NMR spectrum of **25$_W$** in C_6D_6:

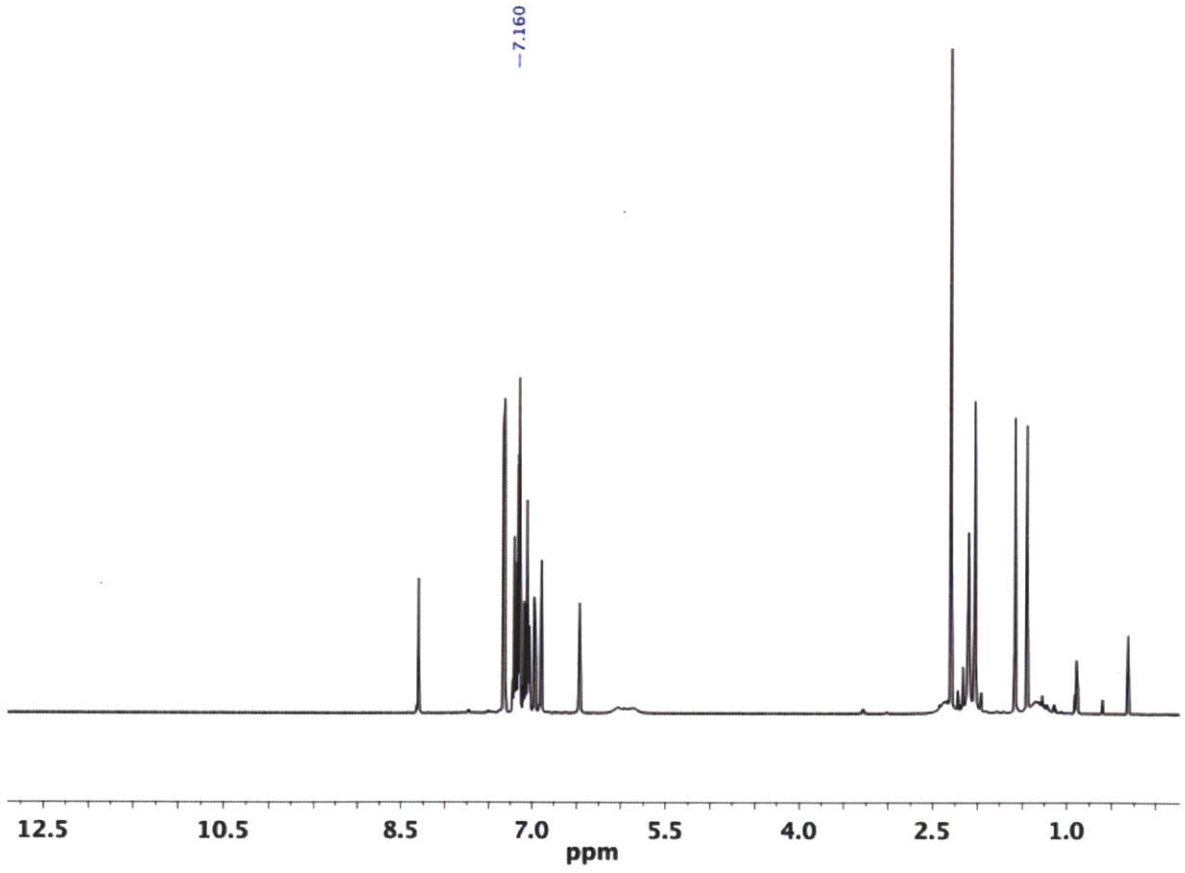

Mo(NAr*)(CHCMe$_2$Ph)(Me$_2$Pyr)(O-2,6-Me$_2$C$_6$H$_3$) (26$_{Mo}$). Solid 2,6-$Me_2C_6H_3OH$ (6.9 mg, 56 μmol) was added to a −25 °C stirred solution of Mo(NAr*)(CHCMe$_2$Ph)(Me$_2$Pyr)$_2$, **14$_{Mo}$** (40.9 mg, 55.0 μmol), and the brown mixture was stirred 16 h at ambient temperature. The volatiles

were removed *in vacuo* and the brown oil was extracted with pentane and the extract was filtered through a pipette filter with Celite. The volatiles were removed under reduced pressure from the filtrate. The remaining oil was dissolved in 1 mL MeCN/0.1 mL Et_2O and the mixture was cooled to −25 °C. The supernatant was removed from the orange precipitate by pipette and the orange solid was washed with cold MeCN and dried *in vacuo*; yield 21.5 mg, 51 %: ^{1}H NMR (C_6D_6, *syn* and *anti* reported together with the *anti* alkylidene proton integrated as 1H) δ 12.191 (s, 1H, $^1J_{CH}$ = 155 Hz, anti Mo=C*H*), 11.635 (s, 2H, $^1J_{CH}$ = 118 Hz, syn Mo=C*H*), 7.004 – 6.860 (overlapping signals, Ar*H*, 21H), 6.803 – 6.767 (overlapping signals, 16H, Ar*H*), 6.723 – 6.665 (overlapping signals, 8H, Ar*H*), 6.224 (s, 2H, anti $NC_4H_2Me_2$), 6.026 s, 4H, syn $NC_4H_2Me_2$), 2.291 (s, 12H, syn MesCH_3), 2.165 (s, 6H, anti MesCH_3), 2.110 (s, 18 H), 2.100 (s, 12H), 2.041 (br s, 12H), 2.013 (s, 6H), 1.903 (s, 6H), 1.871 (s, 6H), 1.695 (s, 6H), 1.613 (s, 12H), 1.561 (s, 3H, anti Mo=CHCMe_2Ph), 1.335 (s, 6H), 1.242 (s, 3H, anti Mo=CHCMe_2Ph); ^{13}C {^{1}H} NMR (C_6D_6, syn and anti isomers reported together) δ 310.4 (Mo=*C*H), 291.2 (Mo=*C*H), 165.4, 160.8, 155.6, 148.7, 148.6, 140.6, 137.6, 137.4, 137.1, 136.8, 136.6, 136.5, 135.9, 134.3, 131.0, 130.0, 129.9, 129.5, 129.2, 129.0, 129.0, 128.8, 128.7, 127.9, 126.8, 126.6, 126.5, 126.4, 126.4, 125.9, 121.9, 121.5, 109.9, 109.6, 54.0, 51.9, 32.8, 30.9, 29.4, 22.0, 21.5, 21.5, 21.4, 21.4, 20.9, 18.4, 18.2, 17.9, 17.8, 17.2. Anal. Calcd for $C_{48}H_{54}MoN_2O$: C, 74.78; H, 7.06; N, 3.63. Found: C, 74.56; H, 6.78; N, 3.10.

^{1}H NMR spectrum of **26$_{Mo}$** in C_6D_6:

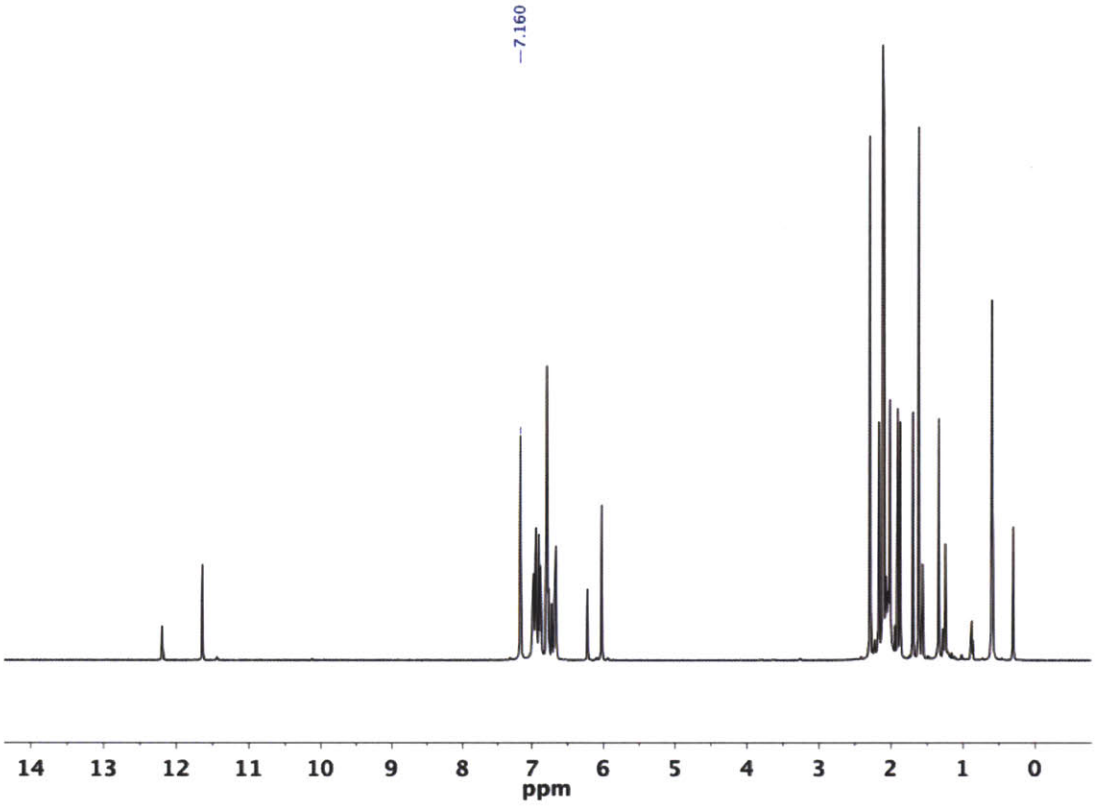

W(NAr*)(CHCMe$_2$Ph)(Me$_2$Pyr)(O-2,6-Me$_2$C$_6$H$_3$) (26$_W$) Solid Ar'OH (13.2 mg, 0.108 mmol) was added to a −25 °C, stirring solution of W(NAr*)(CHCMe$_2$Ph)(Me$_2$Pyr)$_2$, **14$_W$** (88.5 mg, 0.106 mmol), and allowed to stir at ambient temperature for 16 h. The volatiles were removed *in vacuo*. The yellow oil was extracted with pentane, the extract was filtered through a pipette filter, and the volatiles removed *in vacuo* from the filtrate. The yellow oil was dissolved in 1 mL MeCN and stored at −25 °C for 16 h over which time yellow precipitate formed. The mother liquor was removed by pipette and the solid was washed with cold MeCN and dried under vacuum. The mother liquor was concentrated and cooled to −25 °C to collect three crops in the same manner, 65.0 mg, 71 %. ^{1}H NMR (C_6D_6, resonances reported for major isomer, about 85 %) δ 8.501 (s, 1H, $^1J_{HW}$ = 14 Hz, W=C*H*), 7.030 – 6.961 (overlapping signals, Ar*H*, 6H), 6.859 – 6.842 (overlapping signals, 2H, Ar*H*), 6.796 – 6.768 (overlapping signals, 4H, Ar*H*), 6.681 – 6.651 (overlapping signals, 3H, Ar*H*), 6.007 (s, 2H, pyr*H*), 2.294 (s, 6H, MesC*H*$_3$), 2.127 (s, 6H, MesC*H*$_3$), 2.095 (s, 6H, MesC*H*$_3$), 1.682 (s, 3H, W=CHC*Me*$_2$Ph), 1.627(s, 6H), 1.342 (s, 3H, W=CHC*Me*$_2$Ph). ^{13}C{^{1}H} NMR (CD_2Cl_2, all visible peaks (both isomers) reported)

δ 261.5 (W=*C*H), 162.8, 153.9, 151.0, 139.8, 137.1, 136.9, 136.0, 130.6, 129.0, 128.6, 128.6, 128.4, 126.7, 126.4, 126.1, 125.8, 122.2, 110.3, 51.8, 34.0, 32.6, 21.7, 21.4, 21.2, 21.1, 20.6, 18.1, 16.6. Anal. Calcd for $C_{48}H_{54}N_2OW$: C, 67.13; H, 6.34; N, 3.26. Found: C, 66.99; H, 6.47; N, 3.51.

^{1}H NMR spectrum of **26$_W$** in C_6D_6:

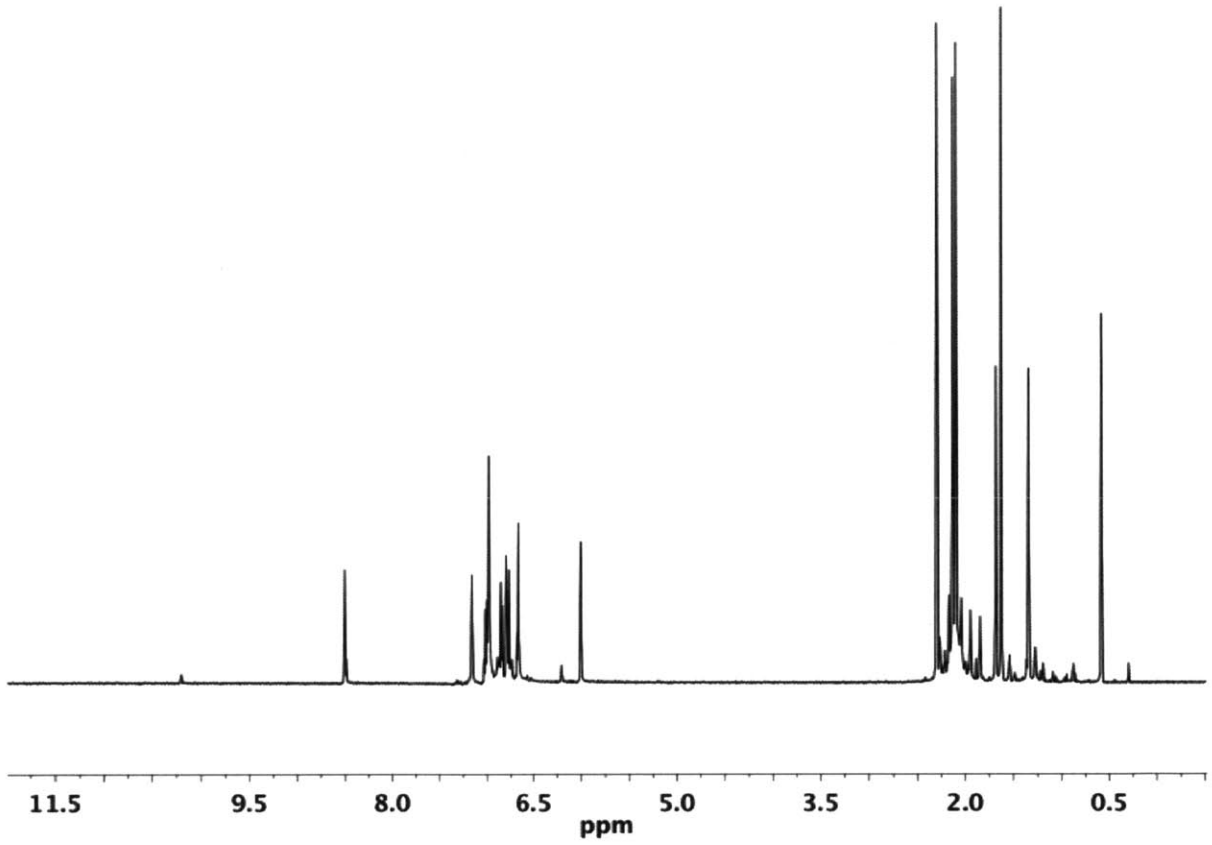

X-ray structure determination

Low-temperature diffraction data (φ- and ω-scans) were collected on a Bruker-AXS X8 Kappa Duo diffractometer coupled to a Smart Apex2 CCD detector with Mo K_a radiation (λ = 0.71073 Å). Structures were solved by direct methods using SHELXS[24] and refined against F^2 on all data by full-matrix least squares with SHELXL-97,[25] following established refinement strategies.[26] All non-hydrogen atoms were refined anisotropically. All hydrogen atoms were included in the model at geometrically calculated positions and refined using a riding model unless specified below. The isotropic displacement parameters of all hydrogen atoms were fixed to 1.2 times the U value of the atoms they are linked to (1.5 times for methyl groups). All disordered atoms were refined with the help of similarity restraints on the 1,2- and 1,3- distances and displacement parameters as well as rigid bond restraints for anisotropic displacement parameters.

Mo(NAr*)(N^{t}Bu)Cl(NH^{t}Bu) ($\mathbf{1_{Mo}}$) crystallizes in the monoclinic space group *Cc* with one molecule per asymmetric unit. Coordinates for the hydrogen atom on N2 were taken from the difference Fourier synthesis and the hydrogen atom was subsequently refined semi-freely with the help of a distance restraint on the 1,2-distance.

Mo(NAr*)(N^{t}Bu)(CH$_2$CMe$_2$Ph) ($\mathbf{3_{Mo}}$) crystallizes in the monoclinic space group $P2_1/c$ with one target molecule of per asymmetric unit. The structure determination was straightforward and without complications.

Mo(NAr*)(CHCMe$_2$Ph)Cl$_2$(py) ($\mathbf{4_{Mo}}$) crystallizes in the triclinic space group $P\bar{1}$ with one molecule per asymmetric unit. The alkylidene ligand (C25 to C34) is disordered over two positions. The ratio between the two components was refined freely and converged at 0.867(3). The coordinates for the hydrogen atom on alkylidene carbon, C25, were taken from the difference Fourier synthesis and the hydrogen atom was subsequently refined semi-freely with the help of a distance restraint.

[W(NAr*)(CHCMe$_2$Ph)Cl(bipy)][Zn$_2$Cl$_3$]$_{0.5}$ ($\mathbf{7_w}$) crystallizes in the triclinic space group $P\bar{1}$ with one molecule of 10, one molecule of toluene and one-half molecule of Zn_2Cl_6 per asymmetric unit. The second half of the Zn_2Cl_6 is generated by the crystallographic inversion

center. The tungsten-bound chlorine, the bipyridine ligand as well as the tungsten atom itself were treated as disordered over two positions. The ratio between the two components was refined freely and converged at 0.6824(15). The disorder was refined with the help of similarity restraints on 1-2 and 1-3 distances and displacement parameters as well as rigid bond restraints for anisotropic displacement parameters for all atoms. Coordinates for the hydrogen atom on C1, which is the carbon atom directly binding to the tungsten, were taken from the difference Fourier synthesis. The hydrogen atom was subsequently refined semi-freely with the help of a distance restraint on the C—H-distance (target 0.95(2) Å). All bond lengths and angles specified and discussed throughout this publication are those of the major component of the disorder.

Mo(NAr*)(CHCMe$_2$Ph)Cl(OAr*)(py) (12$_{Mo}$) crystallizes in the triclinic space group $P\bar{1}$ with two molecules in the asymmetric unit along with two molecules of Et_2O, and half a molecule of benzene. One of the Et_2O molecules (C5 to C8, O2) is disordered over two mutually exclusive positions, and the occupancy ratio of the two components was refined freely and converged at 0.506(12). The benzene molecule is located near a crystallographic inversion center and disordered over four positions, two of which are pairwise related to the other two by the inversion center. The occupancy ratio of the two mutually exclusive components was refined freely and converged at 0.755(8). The first of the two crystallographically independent molecules of **12$_{Mo}$** contains independent disorders over two positions for a mesityl group (C116 to C124), the alkylidene ligand (C150 to C158), and the pyridine ligand (N12, C159 to C163). The second independent molecule of **12$_{Mo}$** contains independent disorders over two positions for a mesityl group (C216 to C224) and part of the alkylidene ligand (C253 to C258). The respective ratios between the two components for each disorder were refined freely and converged at 0.536(7), 0.552(6), and 0.545(11), respectively, for the first independent molecule and at 0.58(3) and 0.70(2), respectively, for the second one. The hydrogen atoms on the alkylidene carbons, C149 and C249, while visible in the difference Fourier synthesis, were included into the model at geometrically calculated positions and refined using a riding model because of the disorder of the alkylidene ligand. During data collection, ice formed on the crystal and affected several reflections, the worst twelve of which were omitted for refinement.

Mo(NAr*)(CHCMe$_2$Ph)(OAr')$_2$ (15$_{Mo}$) crystallizes in the space group $P2_1/c$ with one molecule per asymmetric unit. Alkylidene ligand (C25 to C34) is disordered over two positions. The ratio between the two components was refined freely and converged at 0.74846. The disorder was refined with the help of similarity restraints on 1-2 and 1-3 distances and displacement parameters as well as rigid bond restraints for anisotropic displacement parameters.

W(NAr*)(CHCMe$_2$Ph)(Me$_2$Pyr)(O^{t}Bu) (23$_W$) crystallizes in the monoclinic space group $P2_1/c$ with one molecule per asymmetric unit and shows whole-molecule disorder. The ratio between the two components was refined freely and converged at 0.8979(13). The disorder was refined with the help of similarity restraints on 1-2 and 1-3 distances and displacement parameters as well as rigid bond restraints for anisotropic displacement parameters for all atoms. The following pairs of almost overlapping atoms were constrained to show identical anisotropic displacement parameters: C1/C1A, C42/C42A, C43/C43A, C44/C44A, C33/C33A, C34/C34A, C35/C35A. Coordinates for the hydrogen atom on C1, which is the carbon atom directly binding to the tungsten, were taken from the difference Fourier synthesis. The hydrogen atom was subsequently refined semi-freely with the help of a distance restraint on the C–H-distance (target 0.95(2) Å). This approach did not work for the minor component of the whole-molecule disorder and H1A was introduced in its geometrically calculated position and refined using a riding model. All bond lengths and angles specified and discussed throughout this publication are those of the major component of the disorder.

Table 3.1. Crystal data and structure refinement for Mo(NAr*)(N^tBu)Cl(NH^tBu), (1_{Mo}).

Identification code	x10070
Empirical formula	C_{32} H_{44} Cl Mo N_3
Formula weight	602.09
Temperature	100(2) K
Wavelength	0.71073 Å
Crystal system	Monoclinic
Space group	*Cc*
Unit cell dimensions	a = 22.2063(11) Å α = 90°
	b = 8.6597(5) Å β = 112.9120(10)°
	c = 17.7277(9) Å γ = 90°
Volume	3140.1(3) $Å^3$
Z	4
Density (calculated)	1.274 Mg/m^3
Absorption coefficient	0.526 mm^{-1}
F(000)	1264
Crystal size	0.30 x 0.25 x 0.20 mm^3
Theta range for data collection	2.49 to 32.91°
Index ranges	-33<=*h*<=33, -13<=*k*<=13, -27<=*l*<=27
Reflections collected	66929
Independent reflections	11745 [R_{int} = 0.0267]
Completeness to theta = 32.91°	100.0 %
Absorption correction	Semi-empirical from equivalents
Max. and min. transmission	0.9020 and 0.8581
Refinement method	Full-matrix least-squares on F^2
Data / restraints / parameters	11745 / 3 / 349
Goodness-of-fit on F^2	1.051
Final *R* indices [$I>2\sigma(I)$]	*R*1 = 0.0169, *wR*2 = 0.0431
R indices (all data)	*R*1 = 0.0175, *wR*2 = 0.0434
Absolute structure parameter	-0.011(10)
Largest diff. peak and hole	0.294 and -0.182 $e.Å^{-3}$

Table 3.2. Crystal data and structure refinement for Mo(NAr*)(N^{t}Bu)(CH_2CMe_2Ph)$_2$ (3_W).

Identification code	10079	
Empirical formula	C48 H60 Mo N2	
Formula weight	760.92	
Temperature	100(2) K	
Wavelength	0.71073 Å	
Crystal system	Monoclinic	
Space group	$P2_1/c$	
Unit cell dimensions	a = 16.1681(8) Å	a= 90°
	b = 12.1635(6) Å	b= 110.4790(10)°
	c = 22.4671(11) Å	g = 90°
Volume	4139.2(4) Å^3	
Z	4	
Density (calculated)	1.221 Mg/m^3	
Absorption coefficient	0.351 mm^{-1}	
F(000)	1616	
Crystal size	0.15 x 0.10 x 0.05 mm^3	
Theta range for data collection	1.34 to 30.03°	
Index ranges	-22<=h<=22, -17<=k<=17, -31<=l<=31	
Reflections collected	120028	
Independent reflections	12105 [R(int) = 0.0621]	
Completeness to theta = 30.03°	100.0 %	
Absorption correction	Semi-empirical from equivalents	
Max. and min. transmission	0.9827 and 0.9493	
Refinement method	Full-matrix least-squares on F^2	
Data / restraints / parameters	12105 / 0 / 473	
Goodness-of-fit on F^2	1.026	
Final R indices [I>2sigma(I)]	R1 = 0.0346, wR2 = 0.0835	
R indices (all data)	R1 = 0.0496, wR2 = 0.0913	
Largest diff. peak and hole	0.839 and -0.402 e.Å^{-3}	

Table 3.3. Crystal data and structure refinement for Mo(NAr*)(CHCMe$_2$Ph)Cl$_2$(py), (4_{Mo}).

Identification code	x11036	
Empirical formula	C_{39} H_{42} Cl_2 Mo N_2	
Formula weight	705.59	
Temperature	100(2) K	
Wavelength	0.71073 Å	
Crystal system	Triclinic	
Space group	$P\bar{1}$	
Unit cell dimensions	a = 8.5068(12) Å	α = 91.532(3)°
	b = 10.2626(14) Å	β = 96.714(3)°
	c = 21.510(3) Å	γ = 110.575(3)°
Volume	1741.4(4) Å^3	
Z	2	
Density (calculated)	1.346 Mg/m^3	
Absorption coefficient	0.559 mm^{-1}	
F(000)	732	
Crystal size	0.25 x 0.15 x 0.05 mm^3	
Theta range for data collection	1.91 to 30.31°	
Index ranges	-12<=h<=12, -14<=k<=14, -30<=l<=30	
Reflections collected	75423	
Independent reflections	10446 [R_{int} = 0.0527]	
Completeness to theta = 30.31°	99.9 %	
Absorption correction	Semi-empirical from equivalents	
Max. and min. transmission	0.9726 and 0.8728	
Refinement method	Full-matrix least-squares on F^2	
Data / restraints / parameters	10446 / 389 / 501	
Goodness-of-fit on F^2	1.069	
Final R indices [I>2σ(I)]	R1 = 0.0349, wR2 = 0.0791	
R indices (all data)	R1 = 0.0443, wR2 = 0.0837	
Largest diff. peak and hole	1.317 and -1.287 e.Å^{-3}	

Table 3.4. Crystal data and structure refinement for [W(NAr*)(CHCMe2Ph)Cl(bpy)][Zn2Cl6]$_{0.5}$ (7w).

Identification code	x12001	
Empirical formula	C_{51} H_{53} Cl_4 N_3 W Zn	
Formula weight	1098.98	
Temperature	100(2) K	
Wavelength	0.71073 Å	
Crystal system	Triclinic	
Space group	$P\bar{1}$	
Unit cell dimensions	a = 9.8830(7) Å	a = 79.475(2)°
	b = 11.6031(8) Å	b = 83.2370(10)°
	c = 20.9756(15) Å	g = 83.253(2)°
Volume	2337.0(3) Å^3	
Z	2	
Density (calculated)	1.562 Mg/m^3	
Absorption coefficient	3.239 mm^{-1}	
F(000)	1104	
Crystal size	0.10 x 0.10 x 0.05 mm^3	
Theta range for data collection	1.79 to 30.31°	
Index ranges	-14<=h<=14, -16<=k<=16, -29<=l<=29	
Reflections collected	100713	
Independent reflections	14002 [R_{int} = 0.0518]	
Completeness to theta = 30.31°	99.8 %	
Absorption correction	Semi-empirical from equivalents	
Max. and min. transmission	0.8548 and 0.7377	
Refinement method	Full-matrix least-squares on F^2	
Data / restraints / parameters	14002 / 552 / 680	
Goodness-of-fit on F^2	1.039	
Final R indices [I>2σ(I)]	R1 = 0.0261, wR2 = 0.0630	
R indices (all data)	R1 = 0.0307, wR2 = 0.0644	
Largest diff. peak and hole	0.911 and -0.869 e.Å^{-3}	

Table 3.5. Crystal data and structure refinement for Mo(NAr*)(CHCMe$_2$Ph)Cl(OAr*)(py) (12_{Mo}).

Identification code	X11073	
Empirical formula	$C_{68.50}$ $H_{78.50}$ Cl Mo N_2 O_2	
Formula weight	1093.22	
Temperature	100(2) K	
Wavelength	0.71073 Å	
Crystal system	Triclinic	
Space group	$P\bar{1}$	
Unit cell dimensions	a = 16.251(3) Å	α = 71.259(5)°
	b = 16.403(4) Å	β = 87.158(5)°
	c = 24.476(5) Å	γ = 68.692(5)°
Volume	5740(2) Å^3	
Z	4	
Density (calculated)	1.265 Mg/m^3	
Absorption coefficient	0.322 mm^{-1}	
F(000)	2314	
Crystal size	0.15 x 0.10 x 0.10 mm^3	
Theta range for data collection	1.35 to 30.32°	
Index ranges	-23<=h<=23, -22<=k<=23, -34<=l<=34	
Reflections collected	248510	
Independent reflections	34398 [R(int) = 0.0783]	
Completeness to theta = 30.32°	99.9 %	
Absorption correction	Semi-empirical from equivalents	
Max. and min. transmission	0.9685 and 0.9533	
Refinement method	Full-matrix least-squares on F^2	
Data / restraints / parameters	34398 / 2819 / 1848	
Goodness-of-fit on F^2	1.016	
Final R indices [I>2sigma(I)]	R1 = 0.0445, wR2 = 0.0931	
R indices (all data)	R1 = 0.0803, wR2 = 0.1095	
Largest diff. peak and hole	0.956 and -0.912 e.Å^{-3}	

Table 3.6. Crystal data and Structure refinement for $Mo(NAr^*)(CHCMe_2Ph)(OAr')_2$ (15_{Mo}).

Identification code	11160	
Empirical formula	C50H55MoNO2	
Formula weight	797.89	
Temperature	100(2) K	
Wavelength	0.71073 Å	
Crystal system	Monoclinic	
Space group	P2(1)/c	
Unit cell dimensions	a = 15.6872(19)	alpha = 90 °
	b = 12.0416(14)	beta = 96.176(2) °
	c = 22.224(3)	gamma = 90 °
Volume	4173.7(9)	
Z	4	
Density (calculated)	1.270 Mg/m^3	
Absorption coefficient	0.354 mm^{-1}	
F(000)	1680	
Crystal size	0.15 x 0.15 x 0.05 mm	
Theta range for data collection	1.84 to 30.03 °	
Limiting indices	$-22 < h < 22, -16 < k < 16, -31 < l < 31$	
Reflections collected	99345	
Independent reflections	12201 (R_{int} = 0.0677)	
Completeness to Theta = 30.03°	100.0 %	
Absorption correction	Semi-empirical from equivalents	
Max. and min. transmission	0.9825 and 0.9488	
Refinement method	Full-matrix least-squares on F^2	
Data / restraints / parameters	12201 / 348 / 592	
Goodness-of-fit on F^2	1.084	
Final R indices [$I>2\sigma(I)$]	R1 = 0.0412, wR2 = 0.0878	
R indices (all data)	R1 = 0.0521, wR2 = 0.0921	
Largest diff. peak and hole	1.000 and -1.297 e $Å^{-3}$	

Table 3.7. Crystal data and structure refinement for W(NAr*)(CHCMe$_2$Ph)(Me$_2$pyr)(O^{t}Bu) (23_W).

Identification code	x12104	
Empirical formula	C_{44} H_{54} N_2 O W	
Formula weight	810.74	
Temperature	100(2) K	
Wavelength	0.71073 Å	
Crystal system	Monoclinic	
Space group	$P2_1/c$	
Unit cell dimensions	a = 11.6685(8) Å	a = 90°
	b = 14.3088(9) Å	b = 91.113(2)°
	c = 22.9645(16) Å	g = 90°
Volume	3833.5(4) Å^3	
Z	4	
Density (calculated)	1.405 Mg/m^3	
Absorption coefficient	3.048 mm^{-1}	
F(000)	1656	
Crystal size	0.05 x 0.04 x 0.03 mm^3	
Theta range for data collection	1.68 to 31.51°	
Index ranges	-17<=h<=17, -21<=k<=21, -33<=l<=33	
Reflections collected	186081	
Independent reflections	12749 [R_{int} = 0.0546]	
Completeness to theta = 31.51°	99.9 %	
Absorption correction	Semi-empirical from equivalents	
Max. and min. transmission	0.9141 and 0.8625	
Refinement method	Full-matrix least-squares on F^2	
Data / restraints / parameters	12749 / 1946 / 840	
Goodness-of-fit on F^2	1.066	
Final R indices [I>2σ(I)]	R1 = 0.0273, wR2 = 0.0597	
R indices (all data)	R1 = 0.0395, wR2 = 0.0640	
Largest diff. peak and hole	1.028 and -0.570 e.Å^{-3}	

REFERENCES

[1] (a) Flook, M. M.; Jiang, A. J.; Schrock, R. R.; Müller, P.; Hoveyda, A. H. *J. Am. Chem. Soc.* **2009**, *131*, 7962. (b) Flook, M. M.; Gerber, L. C. H.; Debelouchina, G. T.; Schrock, R. R. *Macromolecules* **2010**, *43*, 7515. (c) Flook, M. M.; Ng, V. W. L.; Schrock, R. R. *J. Am. Chem. Soc.* **2011**, *133*, 1784. (d) Flook, M. M.; Börner, J.; Kilyanek, S.; Gerber, L. C. H.; Schrock, R. R. *Organometallics* **2012**, *31*, 6231.

[2] (a) Jiang, A. J.; Zhao, Y.; Schrock, R. R.; Hoveyda, A. H. *J. Am. Chem. Soc.* **2009**, *131*, 16630. (b) Marinescu, S. C.; Schrock, R. R.; Müller, P.; Takase, M. K.; Hoveyda, A. H. *Organometallics* **2011**, *30*, 1780. (c) Townsend, E. M.; Schrock, R. R.; Hoveyda, A. H. *J. Am. Chem. Soc.* **2012**, *134*, 11334. (d) Peryshkov, D. V.; Schrock, R. R.; Takase, M. K.; Müller, P.; Hoveyda, A. H. *J. Am. Chem. Soc.* **2011**, *133*, 20754.

[3] (a) Ibrahem, I; Yu, M.; Schrock, R. R.; Hoveyda, A. H. *J. Am. Chem. Soc.* **2009**, *131*, 3844. (b) Yu, M.; Ibrahem, I.; Hasegawa, M.; Schrock, R. R.; Hoveyda, A. H. *J. Am. Chem. Soc.* **2012**, *134*, 2788.

[4] (a) Marinescu, S. C.; Schrock, R. R.; Müller, P.; Hoveyda, A. H. *J. Am. Chem. Soc.* **2009**, *131*, 10840. (b) Marinescu, S. C.; Levine, D.; Zhao, Y.; Schrock, R. R.; Hoveyda, A. H. *J. Am. Chem. Soc.* **2011**, *133*, 11512.

[5] (a) Wang, C.; Yu, M.; Kyle, A. F.; Jacubec, P.; Dixon, D. J.; Schrock, R. R.; Hoveyda, A. H. *Chem. Eur. J.* **2013**, *19*, 2726. (b) Wang, C.; Haeffner, F.; Schrock, R. R.; Hoveyda, A. H. *Angew. Chem., Int. Ed.* **2013**, *52*, 1939.

[6] For a terminal Ar*imido of Ga see (a) Wright, R. J.; Brynda, M.; Fettinger, J. C.; Betzer, A. R.; Power, P. P. *J. Am. Chem. Soc.* **2006**, *128*, 12498. For bridging Ar* imido of Group 14 metals see: (b) Merrill, W. A.; Wright, R. J.; Stanciu, C. S.; Olmstead, M. M.; Fettinger, J. C.; Power, P. P. *Inorg. Chem.* **2010**, *49*, 2010. For bridging Ar* imido of As and Bi see: (c) Schulz, A.; Villinger, A. *Inorg. Chem.* **2009**, *48*, 7359. (d) Michalik, D.; Schulz, A.; Villinger, A. *Angew. Chem., Int. Ed.* **2010**, *49*, 7575.

[7] (a) Iluc, V. M.; Hillhouse, G. L. *J. Am. Chem. Soc.* **2010**, *132*, 15148. (b) Laskowski, C. A.; Miller, A. J. M.; Hillhouse, G. L.; Cundari, T. R. *J. Am. Chem. Soc.* **2011**, *133*, 771. (c) Iluc, V. M.; Miller, A. J. M.; Anderson, J. S.; Monreal, M. J.; Mehn, M. P.; Hillhouse, G. L. *J. Am. Chem. Soc.* **2011**, *133*, 13055.

[8] (a) Gavenonis, J.; Tilley, T. D. *J. Am. Chem. Soc.* **2002**, *124*, 8536. (b) Gavenonis, J.; Tilley, T. D. *Organometallics* **2002**, *21*, 5549. (c) Gavenonis, J.; Tilley, T. D. *Organometallics* **2004**, *23*, 31.

[9] Wampler, K. M.; Schrock, R. R. Unpublished results.

[10] Bell, A.; Clegg, W.; Dyer, P. W.; Elsegood, M. R. J.; Gibson, V. C.; Marshall, E. L. *J. Chem. Soc., Chem. Commun.* **1994**, 2547.

[11] (a) Schrock, R. R.; Murdzek, J. S.; Bazan, G. C.; Robbins, J.; DiMare, M.; O'Regan, M. *J. Am. Chem. Soc.* **1990**, *112*, 3875. (b) Oskam, J. H.; Fox, H. H.; Yap, K. B.; McConville, D. H.; O'Dell, R.; Lichtenstein, B. J.; Schrock, R. R. *J. Organomet. Chem.* **1993**, *459*, 185.

[12] Addison, A. W.; Rao, T. N.; Van Rijn, J. J.; Veschoor, G. C. *J. Chem. Soc. Dalton Trans.* **1984**, 1349.

[13] Jeong, H.; Axtell, J. C.; Török, B.; Schrock, R. R.; Müller, P. *Organometallics* **2012**, *31*, 6522.

[14] Heppekausen, J.; Fürstner, A.; *Angew. Chem., Int. Ed.* **2011**, *50*, 7829.

[15] (a) Lichtscheidl, A. G.; Ng, V. W. L.; Müller, P.; Takase, M. K.; Schrock R. R.; Malcolmson, S. J.; Meek, S. J.; Li. B.; Kiesewetter, E. T.; Hoveyda, A. H. *Organometallics* **2012**, *31* (12), 4558.

[16] Singh, R.; Czekelius, C.; Schrock, R. R.; Müller, P.; Hoveyda, A. H. *Organometallics* **2007**, *26*, 2528.

[17] Schrock, R. R.; Crowe, W. E.; Bazan, G. C.; DiMare, M.; O'Regan, M. B.; Schofield, M. H. *Organometallics* **1991**, *10*, 1832.

[18] Duchateau, R.; Cremer, U.; Harmsen, R. J.; Mohamud, S. I.; Abbenhuis, H. C. L.; van Santen, R. A.; Meetsma, A.; Thiele, S. K.-H.; van Tol, M. F. J.; Kranenburg, M. *Organometallics* **1999**, *18*, 5447.

[19] Fonari, M. S.; Simonov, Y. A.; Wang, W.-J.; Tang, S.-W.; Ganin, W. V. *Cryst. Eng. Comm.* **2009**, *11*, 94.

[20] Goeta, A. E.; Lawrence, S. E.; Meehan, M. M.; O'Dowd, A.; Spalding, T. R. *Polyhedron* **2002**, *21*, 1689.

[21] Dickie, D. A.; MacIntosh, I. S.; Ino, D. D.; He, Q.; Labeodan, O. A.; Jennings, M. C.; Schatte, G.; Walsby, C. J.; Clyburne, J. A. C. *Can. J. Chem.* **2008**, *86*, 20.

[22] Dyer, P. W.; Gibson, V. C.; Howard, J. A. K.; Whittle, B.; Wilson, C. *J. Chem. Soc., Chem. Commun.* **1992**, 1666.

[23] Rische, D.; Baunemann, A.; Winter, M.; Fischer, R. A. *Inorg. Chem.* **2006**, *45*, 269.

[24] Sheldrick, G. M. *Acta Cryst.* **1990**, *A46*, 467.

[25] Sheldrick, G. M. *Acta Cryst.* **2008**, *A64*, 112.

[26] Müller, P. *Crystallography Reviews* **2009**, *15*, 57.

Chapter 4

Fundamental Reactivity of Alkylidene Complexes Containing a 2,6-Dimesitylphenylimido Ligand

Portions of this chapter have appeared in print:

Gerber, L. C. H.; Schrock, R. R.; Müller, P.; Takase, M. K. Synthesis of Molybdenum Alkylidene Complexes That Contain the 2,6-Dimesitylphenylimido Ligand. *J. Am. Chem. Soc.* **2011**, *133,* 18142.

Gerber, L. C. H.; Schrock, R. R.; Müller, P. Molybdenum and Tungsten Monoalkoxide Pyrrolide (MAP) Alkylidene Complexes That Contain a 2,6-Dimesitylphenylimido Ligand. *Organometallics* **2013**, *32*, 2373.

INTRODUCTION

Molybdenum and tungsten alkylidene compounds containing a 2,6-dimesitylphenylimido (NAr*) ligand have been synthesized (Chapter 3). This work is motivated by the success of MAP (MonoAlkoxide Pyrrolide) complexes that contain a bulky alkoxide ligand, which have been successfully used for *Z*-selective olefin metathesis reactions including ring-opening metathesis polymerization (ROMP),[1] homocoupling,[2] ring-opening/cross-metathesis,[3] ethenolysis,[4] and formation of natural products through ring-closing reactions.[5] Catalysts for these *Z*-selective reactions all contain a sterically demanding alkoxide ligand and a comparatively small imido ligand. We were interested in exploring the reactivity of compounds where this steric bias is reversed, specifically compounds that contain a bulky imido ligand and a comparatively small alkoxide ligand. A 2,6-dimesitylphenylimido ligand was chosen as the basis for these studies.

To fully understand the effects of the NAr* ligand, we were interested in studying NAr*-bearing MAP complexes and their fundamental reactivity. Many complexes containing the NAr* ligand are a mixture of *syn* and *anti* alkylidenes in solution or the solid state (see Chapter 3; substituents point towards the imido ligand in the *syn* and away in the *anti* alkylidene isomer). Understanding the nature of this unusual isomerism is important to understanding the effects of the NAr* ligand. Kinetic studies were conducted to obtain the rates of interconversion between the two alkylidene isomers.

Reactions with ethylene are important, as ethylene is a byproduct of any reaction in which terminal olefins are metathesized. Understanding the identity and stability of compounds that form in the presence of ethylene is important to discovering how catalysts decompose and how to develop longer-lived catalysts. The NAr* ligand is able to stabilize several unsubstituted metallacycle complexes as well as methylidene complexes. Additionally, study of neophylidene and methylidene complexes with stoichiometric amounts of monomers provide a better understanding of polymerization initiation as well as a way to compare the differing reactivity between substituted and unsubstituted alkylidene species. This chapter explores these types of fundamental reactivity to provide a deeper understanding of the NAr* system and how its properties differ from those of other alkylidene complexes.

RESULTS AND DISCUSSION

I. Study of Alkylidene Isomers

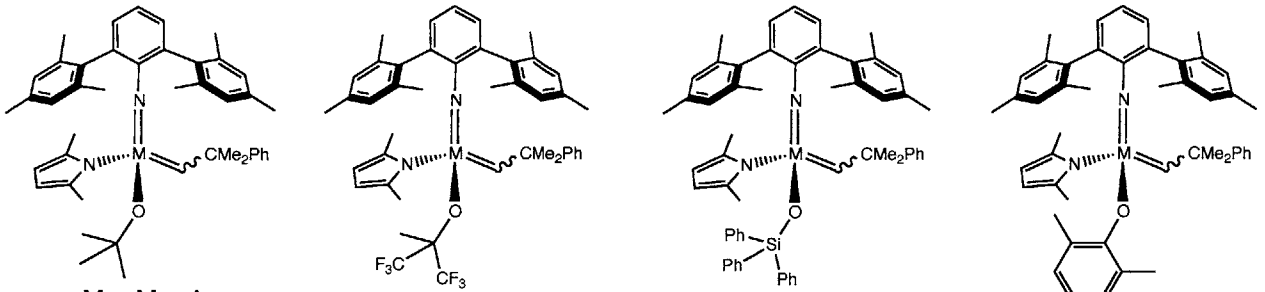

Figure 4.1. Labeling scheme for MAP complexes.

The four-coordinate MAP species shown in Figure 4.1, **1** – **4**, are a mixture of *syn* and *anti* alkylidene isomers in C_6D_6 solution as observed by ^{1}H NMR spectroscopy. In the *syn* alkylidene isomer the substituents on the alkylidene ligand point towards the imido ligand, whereas in the *anti* alkylidene ligand the substituents on the alkylidene ligand point away from the imido ligand (Scheme 4.1). The *syn* alkylidene isomer has an α-agostic interaction, while the *anti* alkylidene isomer does not, allowing these two species to be distinguished by the coupling constants between the α-carbon and proton ($^1J_{CH}$), which are typically in the range of 110 – 125 Hz for *syn* alkylidenes and 140 – 155 Hz for *anti* alkylidenes.[6] Equilibrium constants for compounds **1** – **4** were determined by integration of the alkylidene resonances in the ^{1}H NMR spectra (Table 4.1). This equilibrium typically lies heavily towards the *syn* alkylidene in 4-coordinate Mo or W imido alkylidene species, and such low equilibrium constants have not been observed previously.[6] Values observed previously are of the 10^2 – 10^3 order of magnitude. We attribute the relative stability of the *anti* isomer to the presence of the bulky NAr* ligand since Mo(NAr)(CHCMe$_2$Ph)(Me$_2$pyr)(OCMe$_3$) and Mo(NAr)(CHCMe$_2$Ph)(Me$_2$pyr)[OCMe(CF$_3$)$_2$] (Ar = 2,6-dimesitylphenyl) only show the *syn* isomer in solution by ^{1}H NMR spectroscopy, and these compounds have the same ligand set (except for the imido substituent) as $\mathbf{1_{Mo}}$ and $\mathbf{2_{Mo}}$.[7] The significantly larger K_{eq} values for $\mathbf{3_{Mo}}$ and $\mathbf{3_W}$, compared to compounds **1**, **2**, and **4**, can be attributed to the greater steric demand of the triphenylsiloxide ligand. Equilibrium constants that

are orders of magnitude smaller than those observed previously signify only small changes in stability of the *anti* isomer relative to the *syn*. Analysis using the equation $\Delta G° = -RTln(K_{eq})$ shows that when $K_{eq} = 1$, the *syn* and *anti* isomers are equal in free energy, but when $K_{eq} = 1000$ the *syn* is only 4.1 kcal mol^{-1} more stable than the *anti* isomer. This relationship indicates how great of an effect even small changes in the dynamics of a system can have.

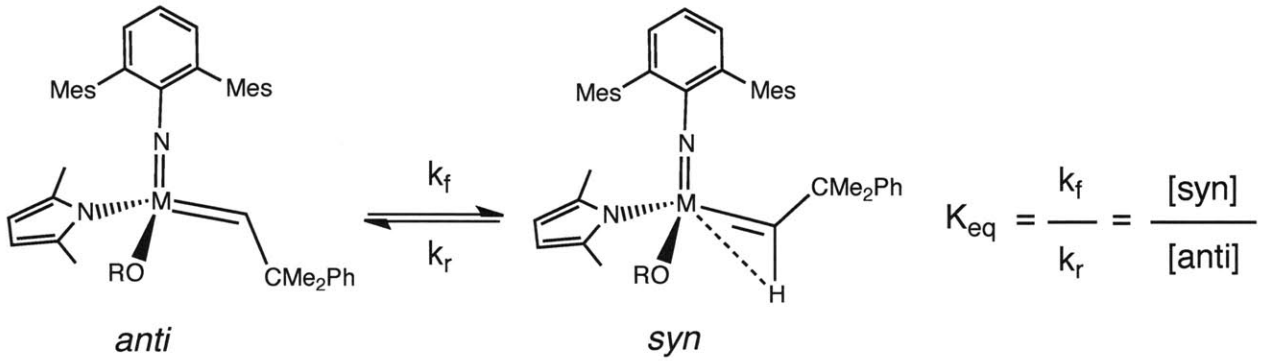

Scheme 4.1. *Syn* and *anti* alkylidene species.

Table 4.1. Rate and equilibrium constants for 4-coordinate Mo and W MAP species measured at 21 °C.

Compound	K_{eq}	$k_f (s^{-1})$	$k_r (s^{-1})$
Mo(NAr*)(CHCMe$_2$Ph)(Me$_2$pyr)(O^{t}Bu), **1$_{Mo}$**	0.9	0.05 ± 0.01	0.06 ± 0.01
Mo(NAr*)(CHCMe$_2$Ph)(Me$_2$pyr)[OCMe(CF$_3$)$_2$], **2$_{Mo}$**	2.7	(2.9 ± 0.6) x 10^{-2}	(1.1 ± 0.04) x 10^{-2}
Mo(NAr*)(CHCMe$_2$Ph)(Me$_2$pyr)(OSiPh$_3$), **3$_{Mo}$**	26	~ 0.5	~ 0.02
Mo(NAr*)(CHCMe$_2$Ph)(Me$_2$pyr)(OAr'), **4$_{Mo}$**	2.2	0.1 ± 0.02	0.05 ± 0.01
W(NAr*)(CHCMe$_2$Ph)(Me$_2$pyr)(O^{t}Bu), **1$_W$**	1.8	1.4 ± 0.6	0.8 ± 0.4
W(NAr*)(CHCMe$_2$Ph)(Me$_2$pyr)[OCMe(CF$_3$)$_2$], **2$_W$**	12	1.8 ± 1.1	0.15 ± 0.2
W(NAr*)(CHCMe$_2$Ph)(Me$_2$pyr)(OSiPh$_3$), **3$_W$**	100	~ 50	~ 0.5
W(NAr*)(CHCMe$_2$Ph)(Me$_2$pyr)(OAr'), **4$_W$**	5.6	2 ± 2	0.4 ± 0.4

2D ^{1}H-^{1}H EXSY was used to determine the kinetics of exchange between the two alkylidene isomers when K_{eq} was close to 1.[8] From EXSY experiments, k can be determined by integration of the cross peaks, where $k = k_f + k_r$. With k in hand, k_f and k_r are determined by

using K_{eq}. Table 4.1 shows rate and equilibrium constants as determined from NMR spectroscopic studies. The rate constants for compounds **1**, **2**, and **4** were determined using EXSY. Due to higher equilibrium constants for compounds **3**, rate constants for $\mathbf{3_{Mo}}$ and $\mathbf{3_W}$ were determined after generation of additional *anti* alkylidene isomer by irradiation at low temperature. The compounds were irradiated at 350 nm at −78 °C to generate additional *anti* alkylidene isomer, and the decay of the mixture back to equilibrium was followed at various temperatures. Rate constants k_f were determined at −20 °C, −30 °C, and −40 °C for $\mathbf{3_{Mo}}$, and −40 °C, −50 °C, and −60 °C for $\mathbf{3_W}$ these values were used to extrapolate to 21 °C.

In all cases, the rate of rotation is at least an order of magnitude faster for W complexes than for their Mo congeners. These results are consistent with reported data for k_f for both W and Mo complexes of $M(NAr)(CHCMe_3)[OCMe(CF_3)_2]_2$, which also show that k_f is much faster for W than Mo: k_f was measured over a range of temperatures for $W(NAr)(CHCMe_3)[OCMe(CF_3)_2]_2$ and when extrapolated to −27.4 °C, $k_f = 153 \times 10^{-4}$ s^{-1} while k_f for $Mo(NAr)(CHCMe_3)[OCMe(CF_3)_2]_2$ was measured to be 2.26×10^{-4} s^{-1} at −27.4 °C.[6] Furthermore, for alkylidene rotation of MAP methylidene complexes studied by EXSY, the rate constants for the Mo complexes $Mo(NAr)(CH_2)(OHIPT)(Pyr)$ ($k = < 0.2$ s^{-1}) and $Mo(NAr)(CH_2)(OBitet)(Pyr)$ ($k = < 0.2$ s^{-1}) are smaller than those for any of the W complexes $W(NAr)(CH_2)(OTPP)(Me_2Pyr)$ ($k = 90$ s^{-1}), *R*-$W(NAr)(CH_2)(OBitet)(Me_2Pyr)$ ($k = 3.6$ s^{-1}), and *S*-$W(NAr)(CH_2)(OBitet)(Me_2Pyr)$ ($k = 5.1$ s^{-1}) (OHIPT = 2,6-bis(2,4,6-triisopropylphenyl)phenoxide, OTPP = 2,3,5,6-tetraphenylphenoxide, and OBitet = the phenoxide derived from the deprotonation of 3,3'-dibromo-2'-(t-butyldimethylsilyloxy)-5,5',6,6',7,7',8,8'-octahydro-[1,1'-binaphthalen]-2-ol).[9]

Interconversion of alkylidene isomers for W, Mo, and Re complexes has previously been studied computationally.[10] The $\Delta G^{\ddagger}$ of rotation has been calculated for the Mo and W complexes $M(NMe)(CHCH_3)(OMe)_2$, $M(NPh)(CHCH_3)(OMe)_2$, $M(NMe)(CHCH_3)(OEt)_2$, and $M(NPh)(CHCH_3)(OEt)_2$. For these compounds, the $\Delta G^{\ddagger}$ values for alkylidene rotation are about the same for equivalent Mo and W complexes, indicating that they would have similar rotation rates. The same study calculates that for the complexes $M(NMe)(CHCH_3)(OMe)_2$ and $M(NMe)(CHCH_3)(OEt)_2$ the more electropositive W (compared with Mo) increases the ionic character of the metal ligand bonds.[10] More ionic character of the metal ligand bonds should make reaching the transition state easier, since rotation requires breaking the M–C π bond. If this

is the case, the more accessible transition state for W over Mo complexes should result in faster bond rotation.

II. Reaction of NAr* Alkylidene Complexes with Ethylene

Ethylene is the simplest olefin, and is also a product of metathesis reactions anytime a terminal olefin substrate is used (Scheme 4.2). Thus, the reaction of olefin metathesis catalysts with ethylene can provide important information about how a catalyst works and how it decomposes. Both methylidenes and unsubstituted metallacycles can form upon reaction of an alkylidene with ethylene. Methylidenes, although part of the catalytic cycle whenever terminal olefins are a substrate, can be unstable and have been shown to decompose bimolecularly,[11] which is a probable route of catalyst deactivation. Stabilization of methylidenes is a strategy to provide longer-lived metathesis catalysts. Unsubstituted metallacycles can form during catalysis through the reaction of a methylidene with ethylene and are not part of the productive catalytic cycle. An unsubstituted metallacycle that cannot readily lose ethylene to reform the methylidene can be a thermodynamic sink for the catalyst and slow the rate of reaction. Additionally, unsubstituted metallacycles have been shown to rearrange to give Mo(IV) or W(IV) olefin complexes.[11, 12]

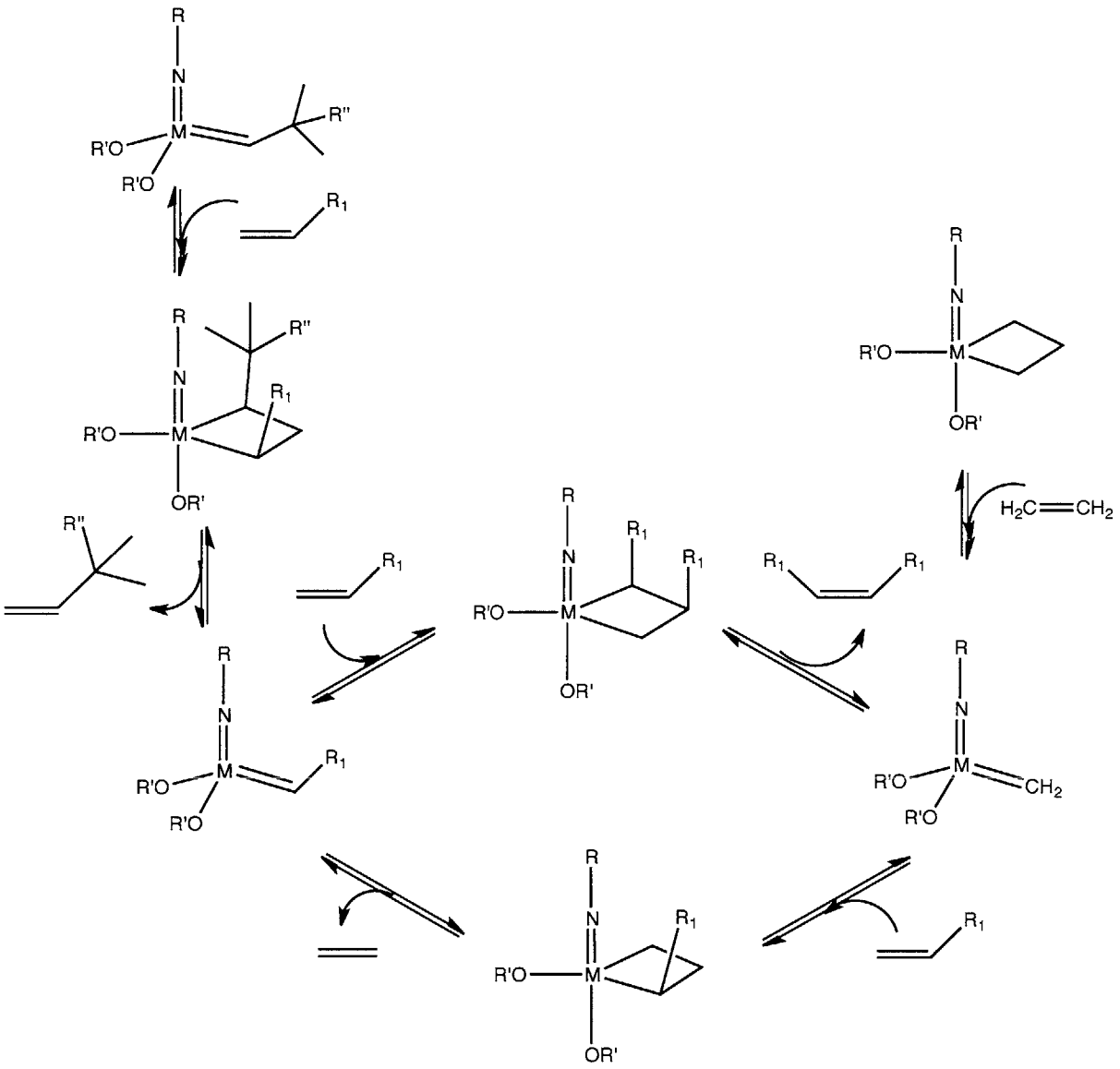

Scheme 4.2. Catalytic cycle for the homocoupling of terminal olefins.

There are only a few reported examples of four-coordinate methylidene compounds of group six metals that have been isolated,[13] shown in Figure 4.2. All isolated methylidene compounds contain sterically demanding aryloxide ligands. Based on this precedent, the NAr* ligand seems well-poised as a supporting ligand for stable methylidene species.

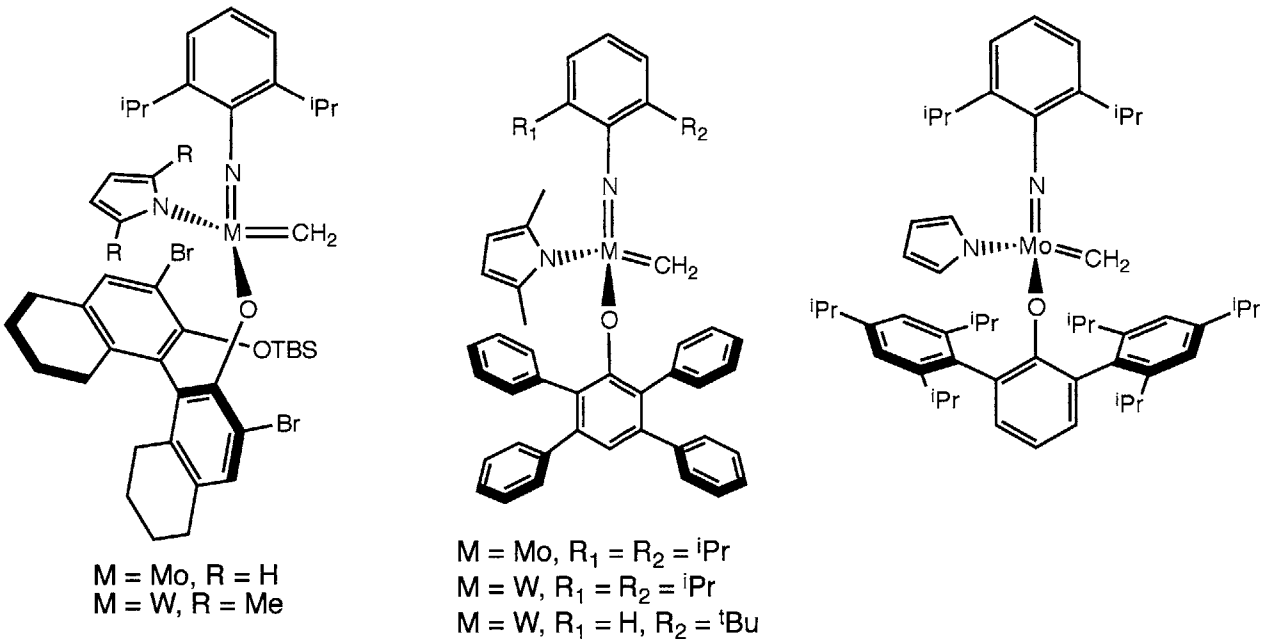

Figure 4.2. Previously isolated four-coordinate methylidenes of W or Mo.

Addition of 1 atm ethylene to a degassed solution of W(NAr*)(CHCMe$_2$Ph)(Me$_2$Pyr)(OSiPh$_3$) (**3$_W$**) in C_6D_6 resulted in complete conversion of **3$_W$** to metallacycle W(NAr*)(C_3H_6)(Me$_2$Pyr)(OSiPh$_3$) (**5$_W$**) (Scheme 4.3). Application of vacuum to the solution of **5$_W$** led to the isolation of the methylidene compound, W(NAr*)(CH_2)(Me$_2$pyr)(OSiPh$_3$) (**6$_W$**). Compounds **5$_W$** and **6$_W$** were isolated by conducting the reaction in a pentane/Et_2O solvent mixture and cooling the reaction mixture to −25 °C overnight, upon which **5$_W$** crystallizes. Compound **5$_W$** was dissolved in excess toluene and the volatiles were removed *in vacuo* to isolate **6$_W$**. Solutions of **5$_W$** in C_6D_6 solution always show about 10 % **6$_W$** and ethylene in their ^{1}H NMR spectra. Application of vacuum to **5$_W$** in the solid state does not change the ratio of **5$_W$**:**6$_W$**, and dissolved ethylene is still observed by ^{1}H NMR spectroscopy upon dissolution in C_6D_6, indicating an equilibrium between **5$_W$** and **6$_W$** in solution.

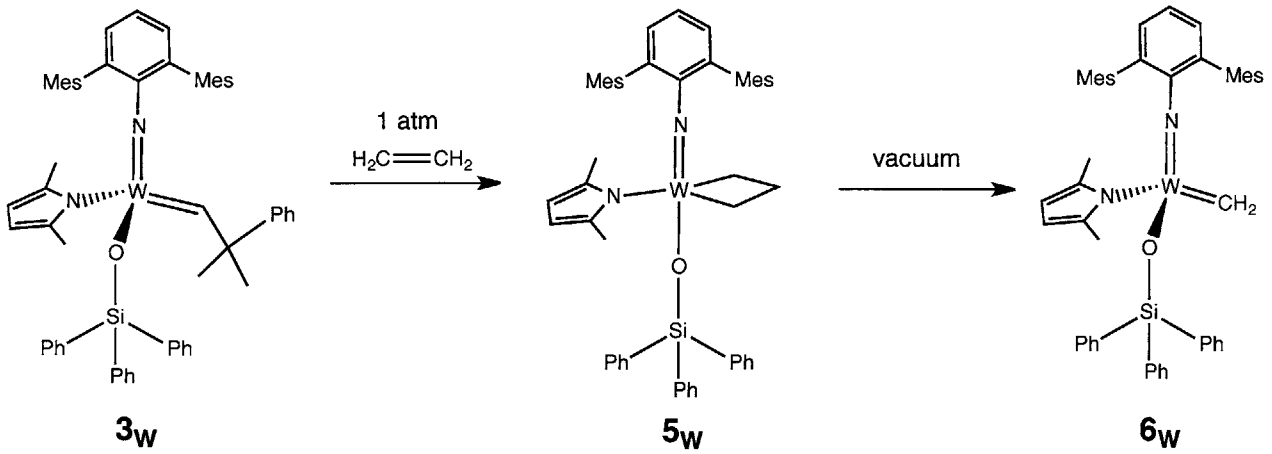

3W **5W** **6W**

Scheme 4.3 Synthesis of metallacycle 5_W and methylidene 6_W.

The structure of $\mathbf{5_W}$ was determined by X-ray crystallography (Figure 4.3). Compound $\mathbf{5_W}$ crystallizes in the space group $P2_1/n$ with two independent molecules in the asymmetric unit. Compound $\mathbf{5_W}$ is about midway between a trigonal bipyramid and a square pyramid: the τ value is 0.60 (where $\tau = 0$ for a square pyramid and $\tau = 1$ for a trigonal bipyramid).[14] Within the trigonal bipyramidal framework, the imido and siloxide ligands are in the apical sites, while the pyrrolide and metallacycle are in the equatorial plane. The N2 – W1 – C1 angle is 141.31(7)° and the N2 – W1 – C3 angle is 133.35(7)°, meaning the pyrrolide ligand is bent slightly towards C1. The space-filling model shows the steric protection of the metallacycle by the NAr* ligand.

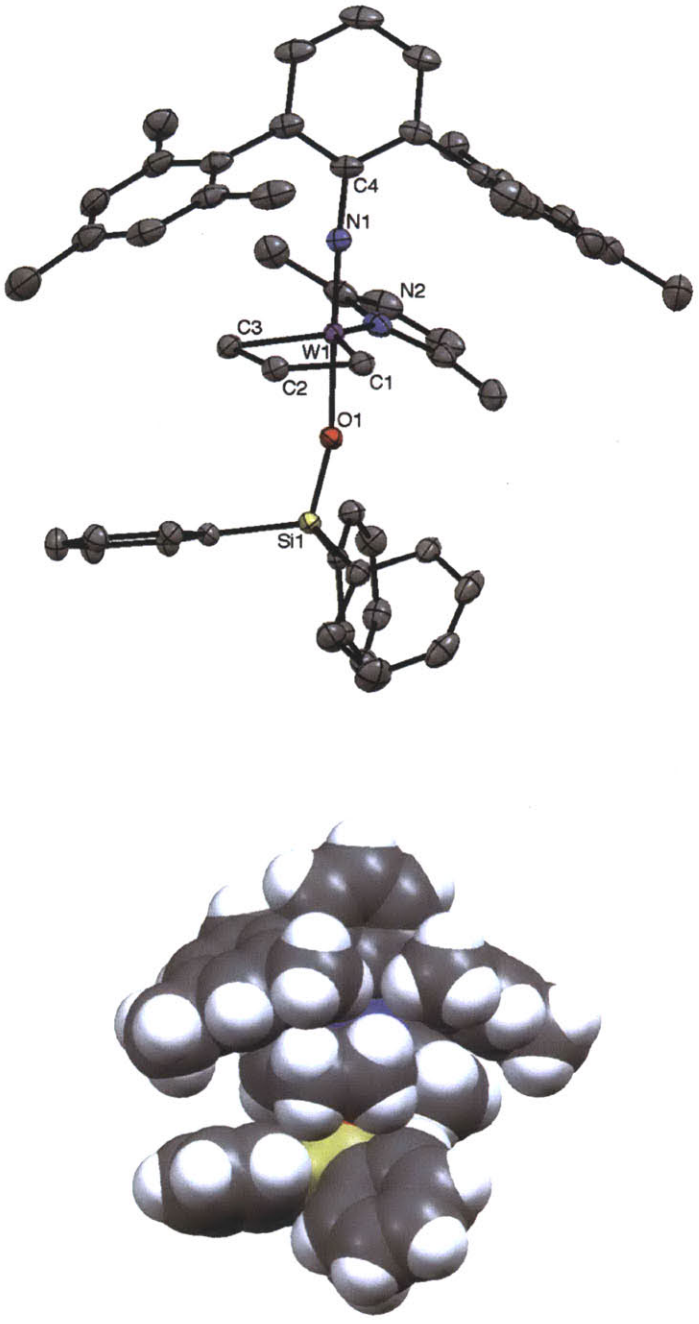

Figure 4.3. Crystal structure of 5_W. The top picture shows the thermal ellipsoids drawn at the 50 % probability level with hydrogen atoms omitted for clarity. The bottom picture shows the space-filling diagram. Selected bond lengths (Å) and angles (°): W1-N1 = 1.7711(16), W1-O1 = 1.9613(13), W1-C3 = 2.0500(19), W1-N2 = 2.0597(17), W1-C1 = 2.0628(19), W1-C2 = 2.3658(19), C1-C2 = 1.593(3), C2-C3 = 1.600(3), N1-W1-O1 = 177.45(6), N1-W1-C3 = 94.93(8), O1-W1-C3 = 85.84(7), N1-W1-N2 = 95.78(7), O1-W1-N2 = 85.43(6), C3-W1-N2 = 133.35(7), N1-W1-C1 = 92.44(8), O1-W1-C1 = 85.23(7), C3-W1-C1 = 83.15(8), N2-W1-C1 = 141.31(7), C2-C1-W1 = 79.52(10), C2-C3-W1 = 79.77(10), C1-C2-C3 = 117.49(15), C4-N1-W1 = 177.10(15), Si1-O1-W1 = 165.48(8).

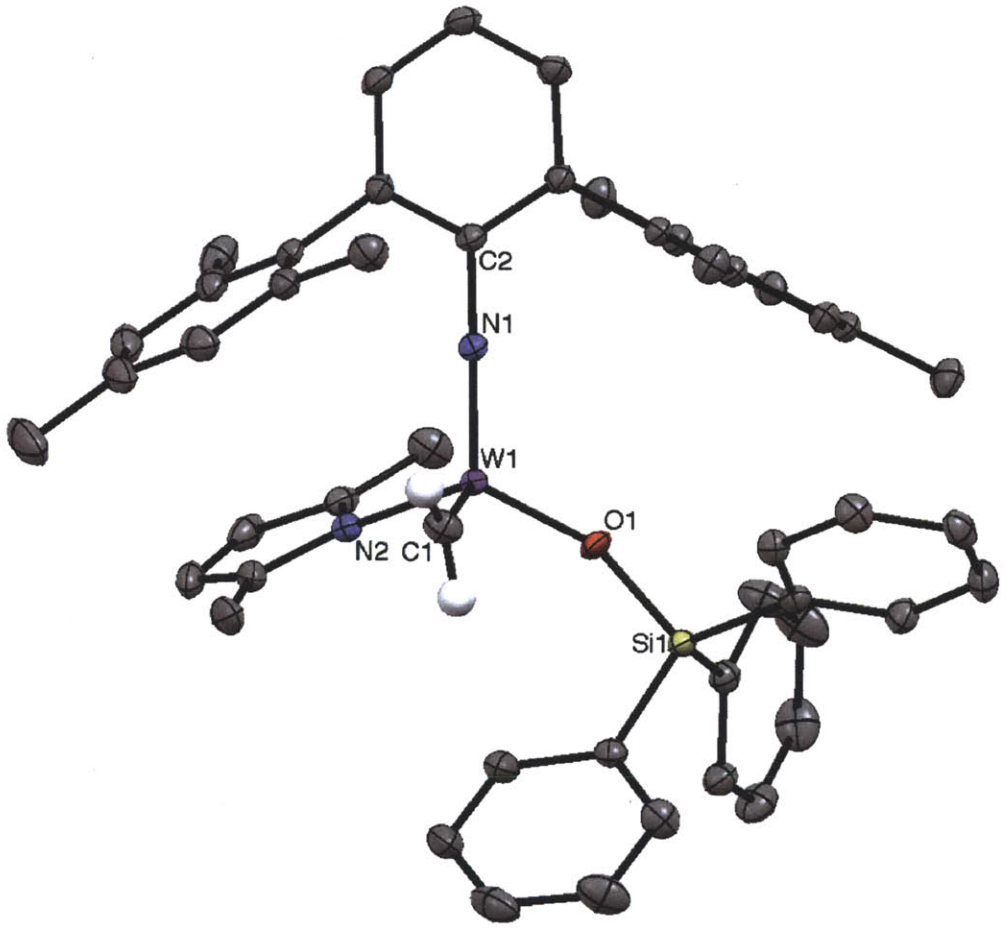

Figure 4.4. Thermal ellipsoid (50 %) representation of 6_W. The minor component of disorder and hydrogen atoms except those on C1 and are omitted for clarity. Selected bond lengths (Å) and angles (°): W1-N1 = 1.7404(15), W1-O1 = 1.853(4), W1-C1 = 1.892(2), W1-N2 = 2.0092(19), N1-C2 = 1.403(2), N1-W1-O1 = 118.41(17), N1-W1-C1 = 102.09(8), O1-W1-C1 = 111.66(17), N1-W1-N2 = 109.55(8), O1-W1-N2 = 111.15(18), C1-W1-N2 = 102.51(8), C2-N1-W1 = 175.38(14), Si1-O1-W1 = 147.9(3).

The structure of $\mathbf{6_W}$ was determined by X-ray crystallography. Compound $\mathbf{6_W}$ crystallizes in space group $P2_1/c$ with one molecule per asymmetric unit. The tungsten atom, pyrrolide ligand, methylidene ligand, N1 and O1 are disordered over two positions with the major component representing 90 % of the electron density. The two components of the disorder are two different enantiomers at tungsten. The geometry at tungsten is distorted tetrahedral. When looking down the N1 – W1 axis, one mesityl group is above the siloxide ligand and the other is between the methylidene and pyrrolide ligands.

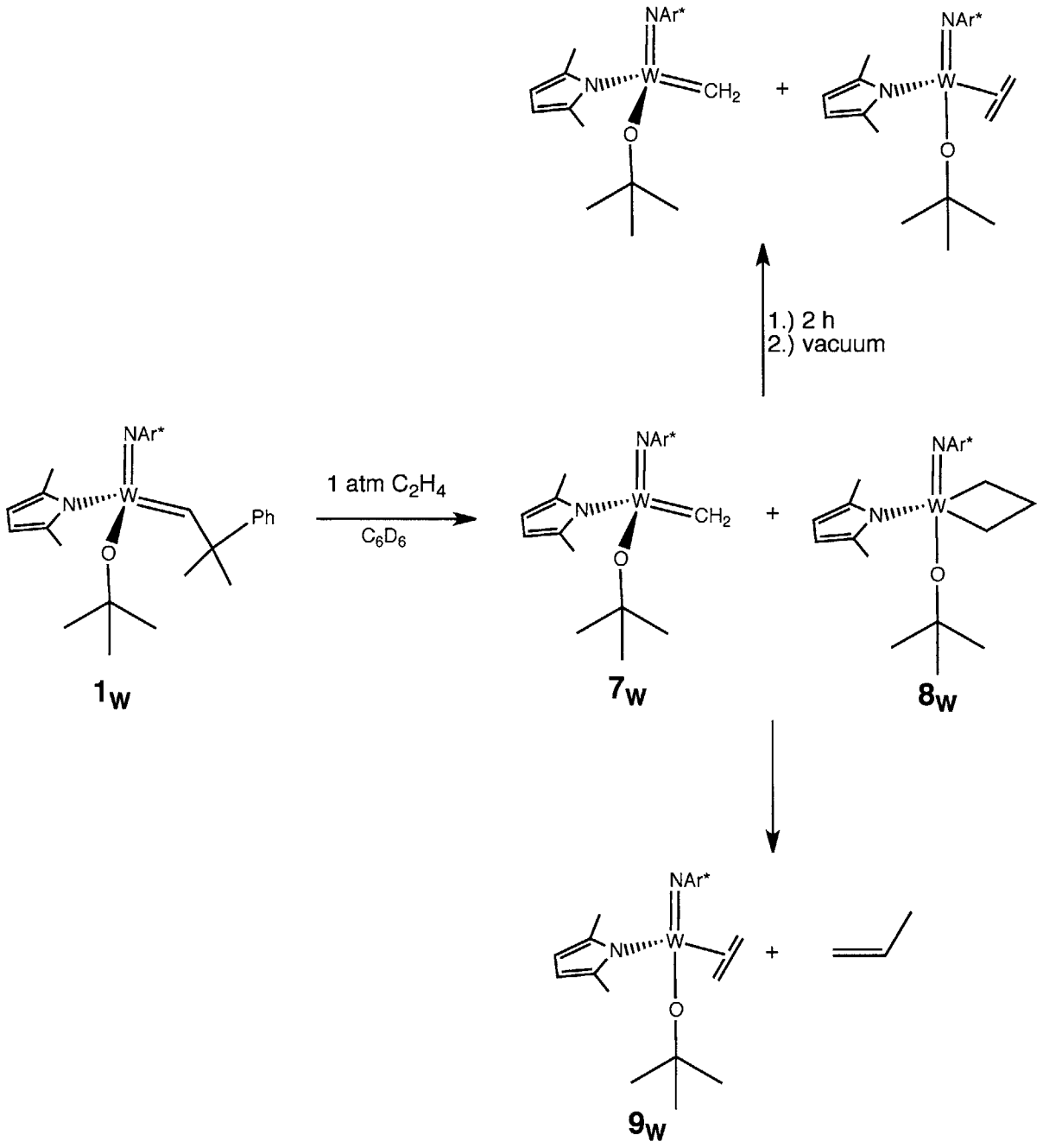

Scheme 4.4. Reaction of $\mathbf{1_W}$ with ethylene.

Upon addition of ethylene (1 atm) to a degassed C_6D_6 solution of W(NAr*)(CHCMe$_2$Ph)(Me$_2$pyr)(O^{t}Bu) (**1$_W$**), a 1:1 mixture of methylidene W(NAr*)(CH$_2$)(Me$_2$pyr)(O^{t}Bu) (**7$_W$**) and metallacycle W(NAr*)(C$_3$H$_6$)(Me$_2$pyr)(O^{t}Bu) (**8$_W$**) is generated (Scheme 4.4). When this mixture was allowed to sit for 2 h under an ethylene

atmosphere, followed by removal of the volatiles *in vacuo*, the ^{1}H NMR spectrum in C_6D_6 under an N_2 atmosphere showed a 2:1 mixture of $\mathbf{7_W}$ to the ethylene complex ($\mathbf{9_W}$), and the ratio did not change over 24 h. When 1 atm ethylene is added to a degassed C_6D_6 solution of $\mathbf{1_W}$ and the reaction monitored over time, complete conversion to the ethylene complex is observed, and propylene is observed in solution as well. These experiments indicate that there is an equilibrium in solution between metallacycle $\mathbf{8_W}$ and methylidene $\mathbf{7_W}$, that metallacycle $\mathbf{8_W}$ rearranges to the ethylene complex with concomitant extrusion of propylene, and that without ethylene present methylidene $\mathbf{7_W}$ does not decompose to the ethylene complex.

Methylidene complex $\mathbf{7_W}$ is isolated by exposure of a degassed solution of $\mathbf{1_W}$ in toluene to 1 atm ethylene for 20 m, followed by removal of the volatiles *in vacuo* (Scheme 4.5). The short reaction time prevents any significant formation of the ethylene complex. Compound $\mathbf{7_W}$ is recrystallized from a mixture of acetonitrile and diethyl ether. The ^{1}H NMR spectrum of $\mathbf{7_W}$ in C_6D_6 shows two methylidene resonances at 9.60 and 9.51 ppm ($^2J_{HH}$ = 9 Hz). The downfield resonance shows a J_{WH} of 15 Hz and the upfield resonance shows a J_{WH} of 6 Hz (Figure 4.5). The two different coupling constants are indicative of an agostic interaction of one methylidene proton with tungsten.

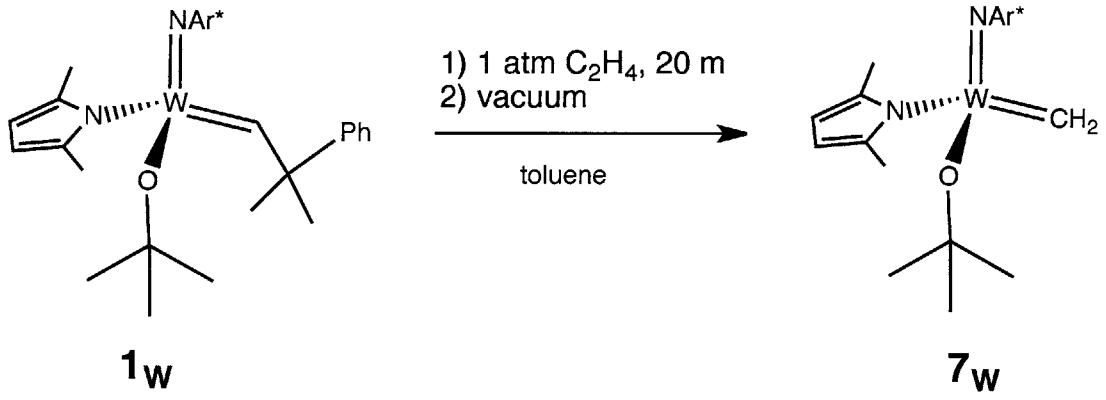

1W **7W**

Scheme 4.5. Synthesis of W(NAr*)(CH_2)(Me_2Pyr)(O^{t}Bu), 7_W.

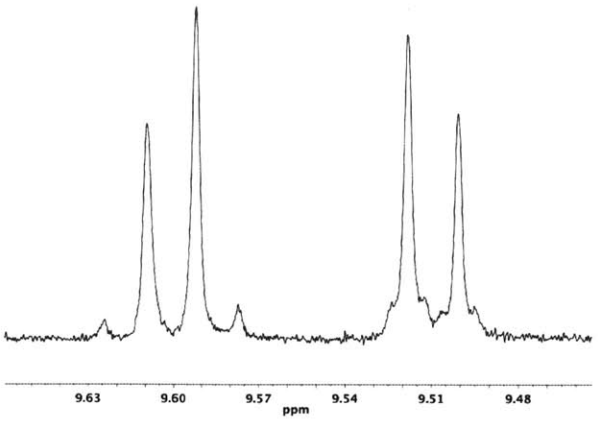

Figure 4.5. Methylidene region of the ^{1}H NMR spectrum of W(NAr*)(CH_2)(Me_2Pyr)(O^{t}Bu), 7_W.

Addition of 1 atm ethylene to a degassed solution of $\mathbf{4_W}$ in C_6D_6 results in complete conversion of $\mathbf{4_W}$ to metallacycle complex W(NAr*)(C_3H_6)(Me_2Pyr)(OAr') ($\mathbf{10_W}$) and a small amount of methylidene W(NAr*)(CH_2)(Me_2Pyr)(OAr') ($\mathbf{11_W}$), shown in Scheme 4.6. Application of vacuum to the mixture completely converts $\mathbf{10_W}$ to $\mathbf{11_W}$. Compound $\mathbf{10_W}$ is isolated by performing the reaction in pentane and cooling to –25 °C upon which yellow crystals are isolated in 57 % yield. Dissolution of the crystals in toluene and removal of the volatiles *in vacuo* provides $\mathbf{11_W}$.

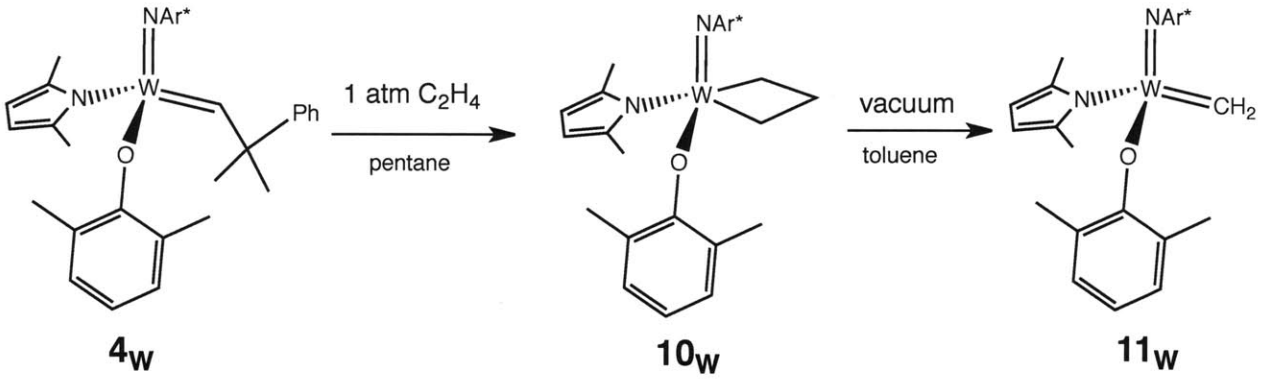

Scheme 4.6. Synthesis of Mo(NAr*)(C_3H_6)(Me_2Pyr)(OAr') (10_W) and Mo(NAr*)(CH_2)(Me_2Pyr)(OAr') (11_W).

Compound $\mathbf{11_W}$ shows only one methylidene resonance in the ^{1}H NMR spectrum in C_6D_6. Initially, observation of one methylidene resonance was attributed to rapid rotation of the methylidene. In order to observe decoalescence at low temperature, a sample of $\mathbf{11_W}$ was prepared in toluene-d_8. The ^{1}H NMR spectrum in toluene-d_8 shows two methylidene resonances,

which become even further separated in CD_2Cl_2 solution (Figure 4.6), indicating that the two resonances are coincident in C_6D_6, rather than being equivalent through rapid rotation of the methylidene.

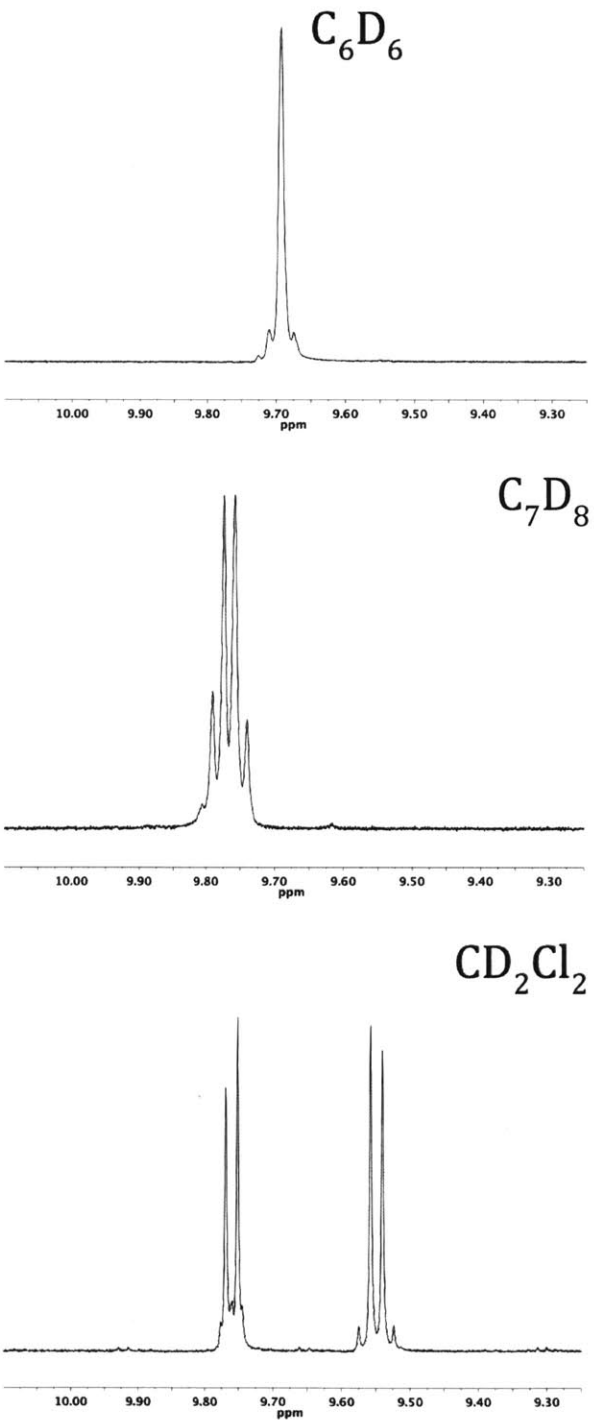

Figure 4.6. Alkylidene region of the ^{1}H NMR spectra 11_W in various solvents.

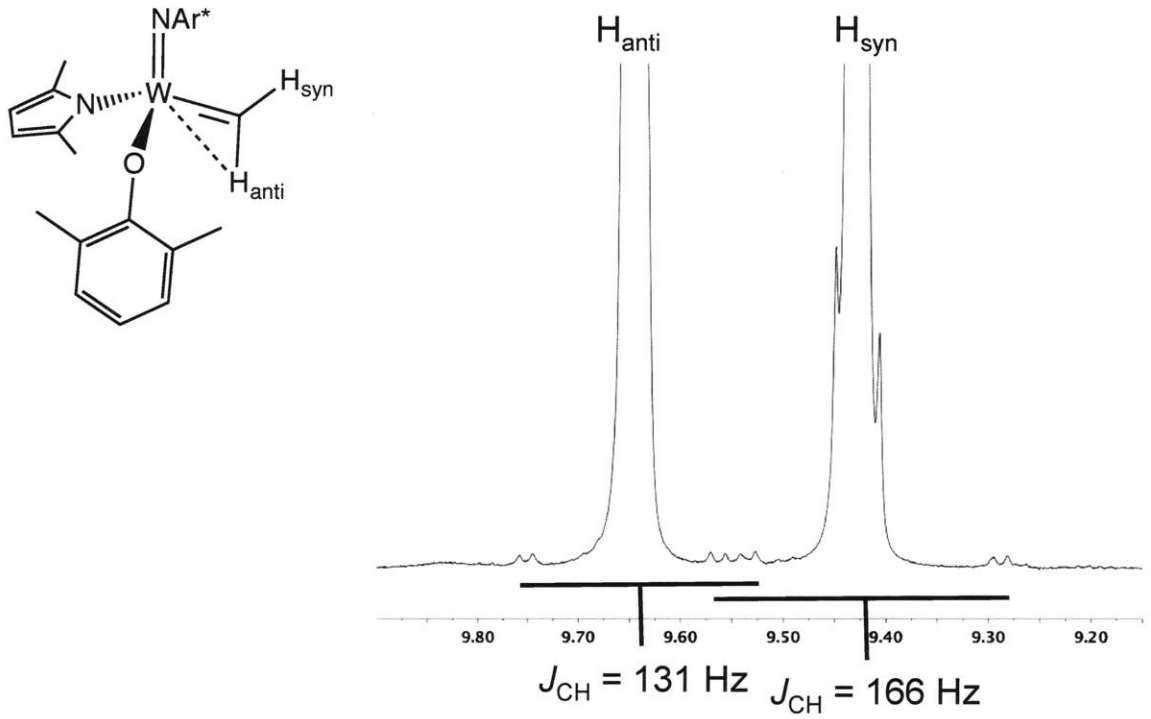

Figure 4.7. Vertically expanded alkylidene region of the ^{1}H NMR spectrum of $\mathbf{11_W}$.

The two methylidene resonances in the ^{1}H NMR spectrum of $\mathbf{11_W}$ obtained in CD_2Cl_2 each show different coupling to tungsten and carbon (Figure 4.7). One methylidene proton couples to tungsten with a J_{WH} value of 17 Hz, while the other methylidene proton couples to tungsten with a J_{WH} value of 7 Hz (coupling is not visible in Figure 4.7, but is in Figure 4.6). The methylidene proton that gives rise to the upfield resonance couples to carbon with a $^1J_{CH}$ value of 166 Hz and the proton providing the downfield resonance has a $^1J_{CH}$ value of 131 Hz. These coupling constants allow the upfield resonance to be assigned as the *syn* proton and the downfield resonance as the *anti* proton. The larger proton-tungsten coupling of the *syn* proton is consistent with the higher s-character of the C–H bond due to the larger W–C–H angle because of the agostic interaction between H_{anti} and W.

The rate of methylidene rotation of $\mathbf{6_W}$ and $\mathbf{11_W}$ was studied by EXSY. The rate constant is 0.3 s^{-1} for $\mathbf{6_W}$ and 0.1 s^{-1} for $\mathbf{11_W}$. In both cases, these are smaller than the rate constants for neophylidene compounds $\mathbf{3_W}$ and $\mathbf{4_W}$. Additionally, the rate constants for $\mathbf{6_W}$ and $\mathbf{11_W}$ are smaller than observed previously for W methylidene compounds W(NAr)(CH_2)(OTPP)(Me_2Pyr) (k = 90 s^{-1}), *R*-W(NAr)(CH_2)(OBitet)(Me_2Pyr) (k = 3.6 s^{-1}), and *S*-W(NAr)(CH_2)(OBitet)(Me_2Pyr) (k =

5.1 s^{-1}), but possibly in the same range as Mo methylidene complexes Mo(NAr)(CH_2)(OHIPT)(Pyr) (k = < 0.2 s^{-1}) and Mo(NAr)(CH_2)(OBitet)(Pyr) (k = < 0.2 s^{-1}).[9]

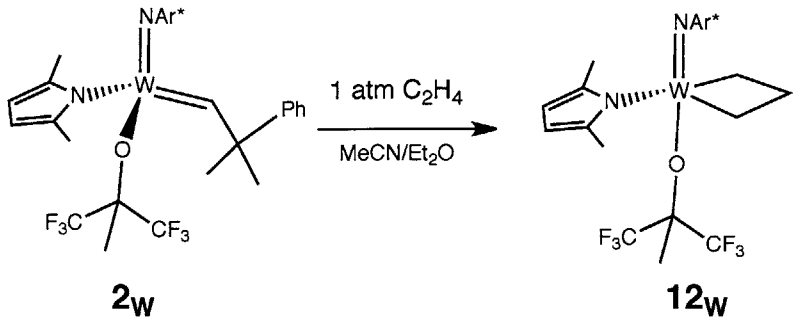

2W **12W**

Scheme 4.7. Synthesis of W(NAr*)(C_3H_6)(Me_2Pyr)[OCMe(CF_3)$_2$] (12_W).

Addition of 1 atm ethylene to a C_6D_6 solution of $\mathbf{2_W}$ results in complete conversion to W(NAr*)(C_3H_6)(Me_2Pyr)[OCMe(CF_3)$_2$] ($\mathbf{12_W}$). Compound $\mathbf{12_w}$ can be isolated by performing the reaction in MeCN and cooling the solution to –25 °C, upon which $\mathbf{12_W}$ crystallizes. When vacuum is applied to $\mathbf{12_W}$ clean conversion to a methylidene species is not observed: several alkylidene resonances are observed in the ^{1}H NMR spectrum.

Addition of 1 atm of ethylene to a solution of $\mathbf{1_{Mo}}$ results in complete consumption of $\mathbf{1_{Mo}}$ after 10 m, as observed by ^{1}H NMR spectroscopy. A methylidene species is present, but a major component of the reaction mixture is an ethylene complex. After 16 h, complete conversion to Mo(NAr*)(CH_2CH_2)(Me_2Pyr)(O^{t}Bu), propylene, and 3-methyl-3-phenyl-1-butene is observed. Attempts to isolate Mo(NAr*)(CH_2CH_2)(Me_2Pyr)(O^{t}Bu) have been unsuccessful. Reaction of $\mathbf{2_{Mo}}$ with 1 atm ethylene shows a mixture of metallacycle and methylidene species by ^{1}H NMR spectroscopy after 10 m. After application of vacuum, complete conversion to the methylidene is observed, but attempts to isolate the methylidene have been unsuccessful. After addition of 1 atm of ethylene to a degassed solution of $\mathbf{3_{Mo}}$, broad methylidene resonances are observed by ^{1}H NMR spectroscopy. This compound cannot be isolated though, because upon concentration of the solution, the methylidene reacts with the 3-methyl-3-phenyl-1-butene byproduct to regenerate $\mathbf{3_{Mo}}$. Reaction of $\mathbf{4_{Mo}}$ with 1 atm ethylene led to no resonances consistent with formation of methylidene or metallacycle species in the ^{1}H NMR spectrum.

For NAr* compounds, isolation of Mo methylidene and metallacycle species has been much more difficult than isolation of the W congeners. For specific ligand sets, the W

metallacycles are much more stable. Metallacycle complexes can be isolated for W with O[CMe$(CF_3)_2$], $OSiPh_3$, and OAr' ligands, while in the case of Mo clean conversion to the metallacycle is not observed without decomposition to the methylidene or olefin complex. In the case of the O^{t}Bu ligand, decomposition of the unsubstituted metallacycle to the M(IV) ethylene complex is observed for both Mo and W. Since this rearrangement is proposed to be an intramolecular process, increased steric protection against bimolecular reaction is unlikely to prevent this process. The O^{t}Bu ligand is much less electron-withdrawing than the other three alkoxide ligand that have been studied. The pK_a values of HO^{t}Bu, HOCMe$(CF_3)_2$, $HOSiPh_3$, and 2,6-$Me_2C_6H_3OH$ are 17.6,[15] 9.6,[15] 10.8,[16] and 10.6,[15] respectively. The more electron-rich metal center in the O^{t}Bu complexes likely makes reductive processes more facile. Tungsten methylidene species can be isolated for O^{t}Bu, $OSiPh_3$, and OAr' ligands. Although molybdenum methylidene species can be observed *in situ* for O^{t}Bu, OCMe$(CF_3)_2$, and $OSiPh_3$, these compounds are not stable enough for isolation.

The steric protection of the NAr* ligand stabilizes methylidene and unsubstituted metallacycle complexes against bimolecular decomposition so that they can be isolated. Four-coordinate 14e$^-$ methylidene complexes that have been isolated previously employ sterically demanding aryloxide ligands. The NAr* system takes advantage of the same strategy to isolate these typically unstable species, but adds diversity to the set of isolated methylidene complexes and expands its numbers greatly.

III. Stoichiometric Reactions of NAr* Complexes with Cyclic Olefins

Reaction of $\mathbf{3_W}$ with one equivalent of 2,3-dicarbomethoxynorbornadiene (**DCMNBD**) shows slow consumption of **DCMNBD** at 50 °C along with appearance of several broad olefinic resonances and alkylidene resonances as well as much remaining $\mathbf{3_W}$ in the ^{1}H NMR spectra. This result indicates that the rate of propagation is significantly faster than the rate of initiation for the polymerization of **DCMNBD** by $\mathbf{3_W}$.

Reaction of $\mathbf{6_W}$ with **DCMNBD** results in clean conversion of $\mathbf{6_W}$ to the first-insertion product, $\mathbf{12_W}$ (Scheme 4.8). The resonances in the ^{1}H NMR spectrum can be assigned (Figure 4.8) with the help of a 2D gCOSY NMR spectrum (Figure 4.9).

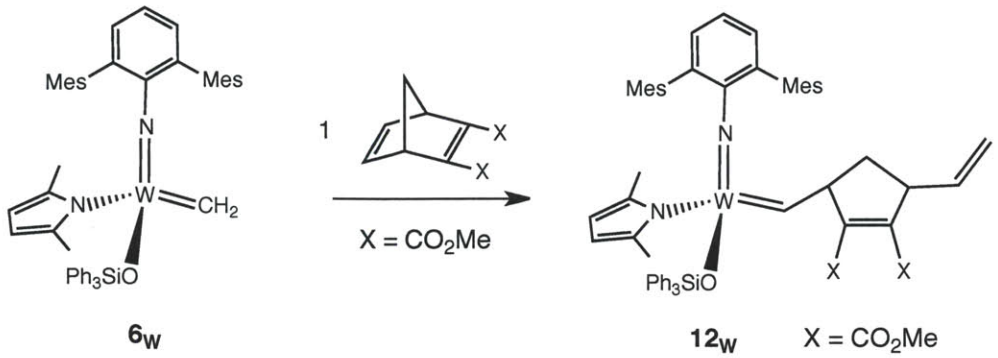

6_W 12_W X = CO_2Me

Scheme 4.8. Reaction of W(NAr*)(CH_2)(Me_2Pyr)(OSiPh_3) (6_W) with DCMNBD to form 12_W.

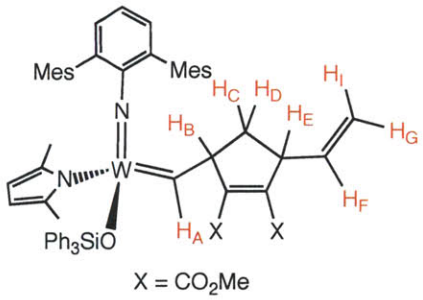

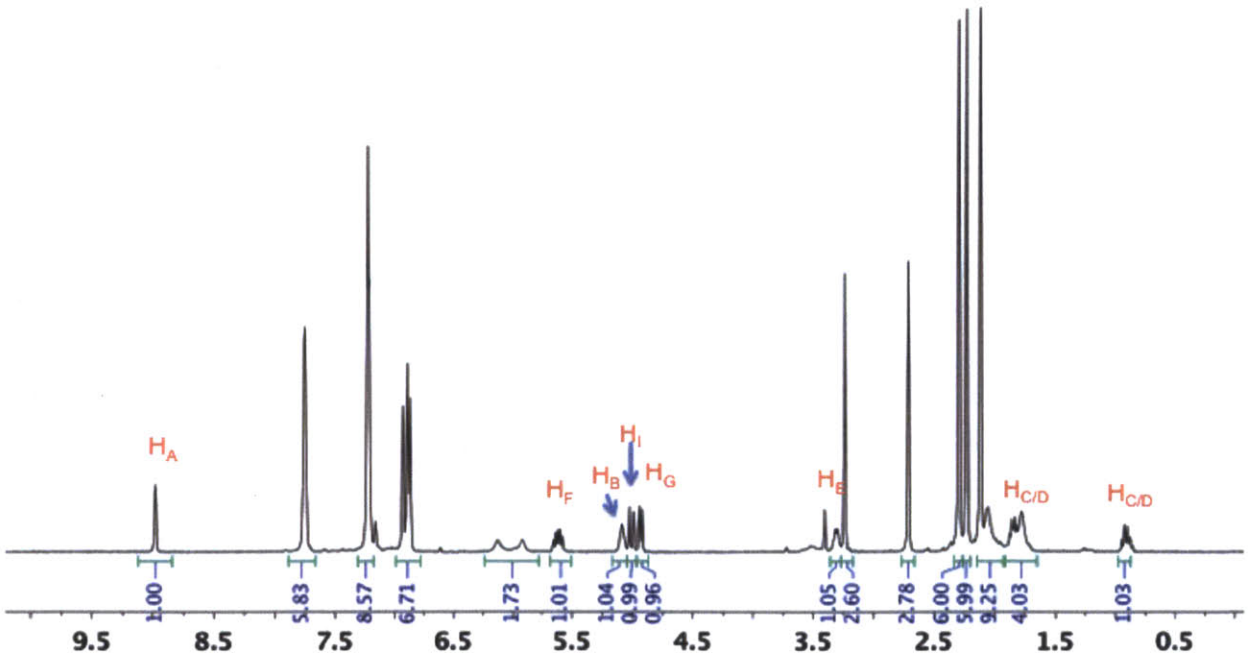

Figure 4.8. ^{1}H NMR spectrum of 12_W with proton assignments.

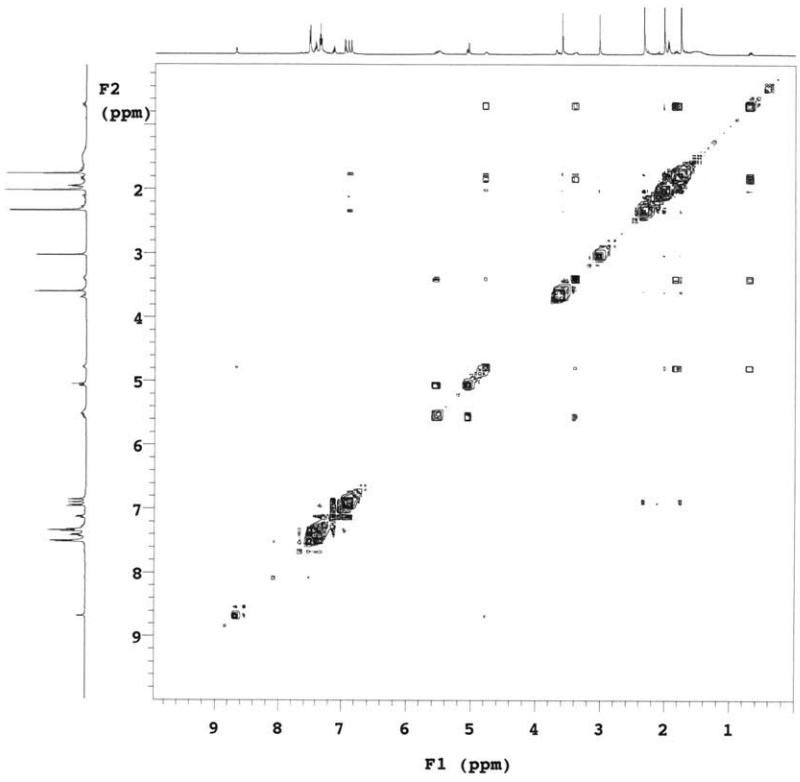

Figure 4.9. gCOSY of 12_W.

Attempts to recrystallize $\mathbf{12_W}$ from acetonitrile at −25 °C led to the crystallization of a species that is an acetonitrile adduct and has also undergone a 1,3-hydrogen shift ($\mathbf{13_W}$), see Figure 4.10. Compound $\mathbf{13_W}$ crystallizes in space group $P\bar{1}$ along with disordered acetonitrile and diethyl ether solvent molecules. It is a distorted square pyramid with the alkylidene ligand at the apical site. The τ value is 0.22 (where $\tau = 0$ for a square pyramid and $\tau = 1$ for a trigonal bipyramid). The W1–N1–C13 bond angle is relatively bent, at 165.2(2)°. The shift of the hydrogen atom from C6 in $\mathbf{12_W}$ to C4 in $\mathbf{13_W}$ is evident by the essentially tetrahedral geometry at C4, and the planar geometry at C6. Additionally, the C4–C5 bond length is 1.519(4), which indicates a C–C single bond, while the C5–C6 bond length is 1.351(4), characteristic of a C=C double bond. Although similar hydrogen shifts have not been observed before in polymers of **DCMNBD**, this phenomenon is not surprising because H_E in $\mathbf{12_W}$ is a doubly allylic position, rendering it more acidic.

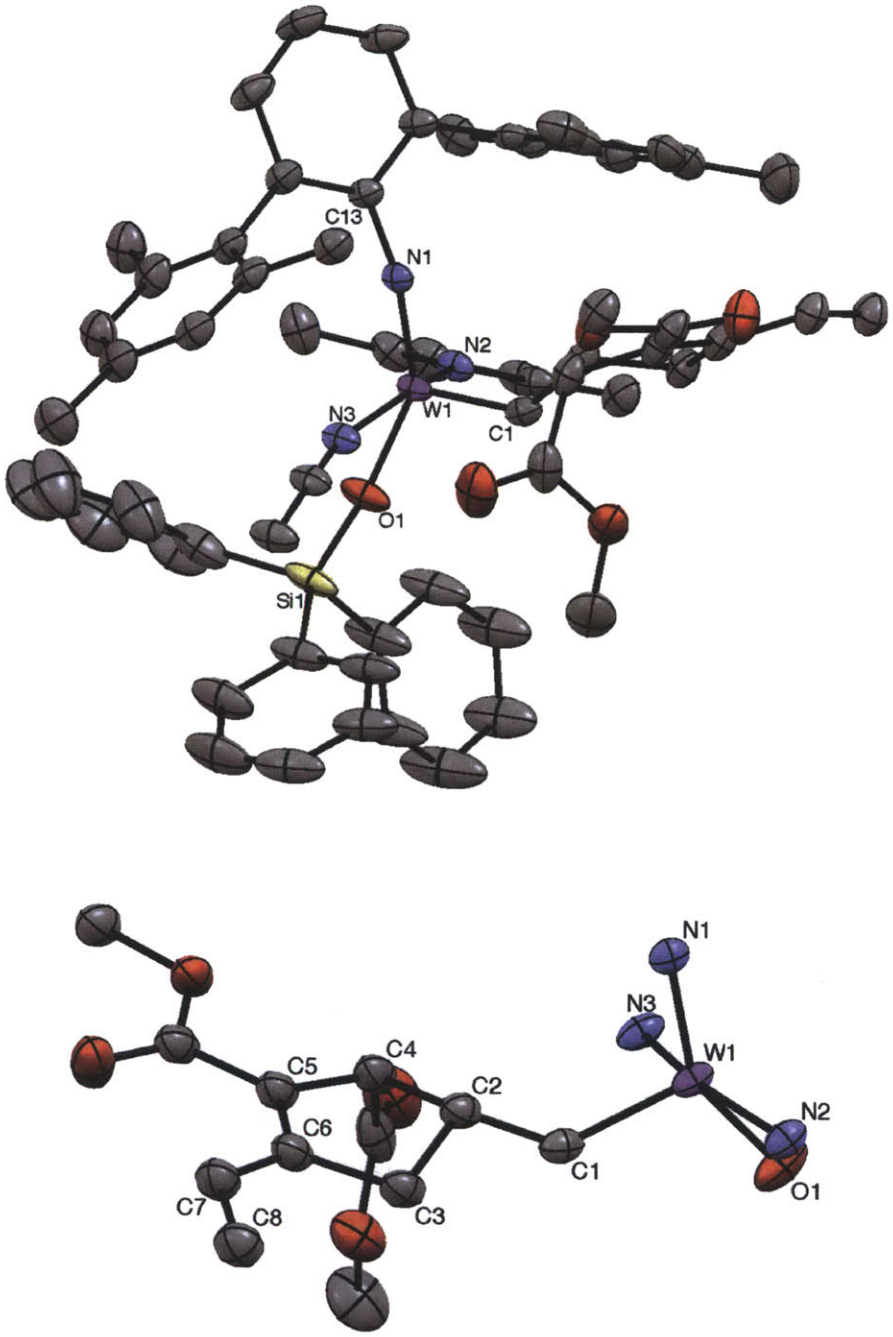

Figure 4.10. X-ray crystal structure of 13_W shown with 50 % probability ellipsoids. Hydrogen atoms, solvent molecules, and minor components of disorder are omitted for clarity. The bottom shows the alkylidene ligand and first coordination sphere of W. Selected bond lengths (Å) and angles (°): W1-N1 = 1.769(2), W1-C1 = 1.895(3), W1-O1 = 1.942(6), W1-N2 = 2.088(2), W1-N3 = 2.189(2), C4-C5 = 1.519(4), C5-C6 = 1.351(4), N1-W1-C1 = 101.00(11), N1-W1-O1 = 147.7(4), C1-W1-O1 = 110.3(3), N1-W1-N2 = 97.39(9), C1-W1-N2 = 102.03(10), O1-W1-N2 = 84.0(4), N1-W1-N3 = 93.70(9), C1-W1-N3 = 90.81(10), O1-W1-N3 = 78.5(4), N2-W1-N3 = 161.05(9), C9-C4-C5 = 113.1(3), C9-C4-C2 = 114.0(3), C5-C6-C7 = 127.3(3), C7-C6-C3 = 122.2(3).

An independent synthesis of $\mathbf{13_W}$ was sought. Dissolution of $\mathbf{12_W}$ in CD_3CN, similar to crystallization conditions, did not induce the hydrogen shift. Addition of one equivalent of NEt_3 to a CD_3CN solution of $\mathbf{12_W}$ provided a new species whose spectra are consistent with $\mathbf{13_W}$ (Scheme 4.9). The gCOSY shows a different coupling pattern than $\mathbf{12_W}$ and it is consistent with having undergone the 1,3-hydrogen shift (Figure 4.11). The compound observed by NMR is consistent with being a 5-coordinate MeCN adduct due to the downfield shift of the alkylidene proton compared to $\mathbf{12_W}$. Determination of the crystal structure of $\mathbf{13_W}$ synthesized as shown in Scheme 4.9 confirms that the $\mathbf{13_W}$ is the same species observed in the previous crystal structure determination.

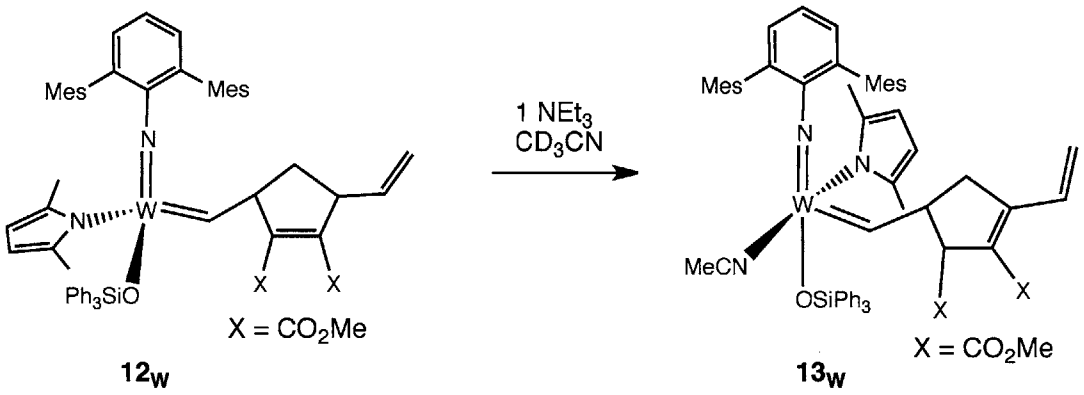

Scheme 4.9. Alternate synthesis of 13_W.

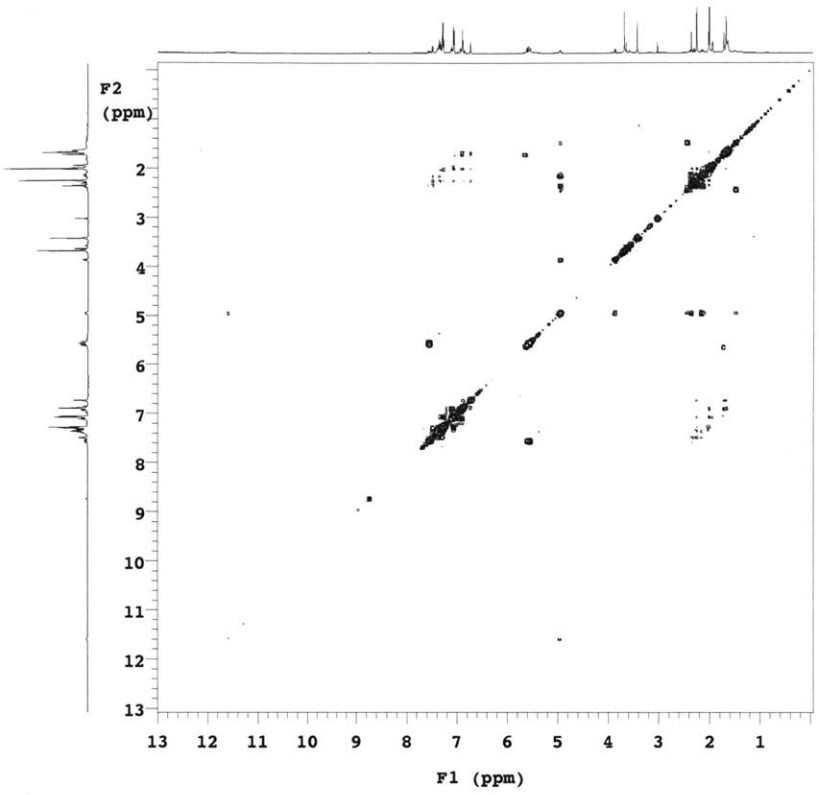

Figure 4.11. gCOSY of 13_W.

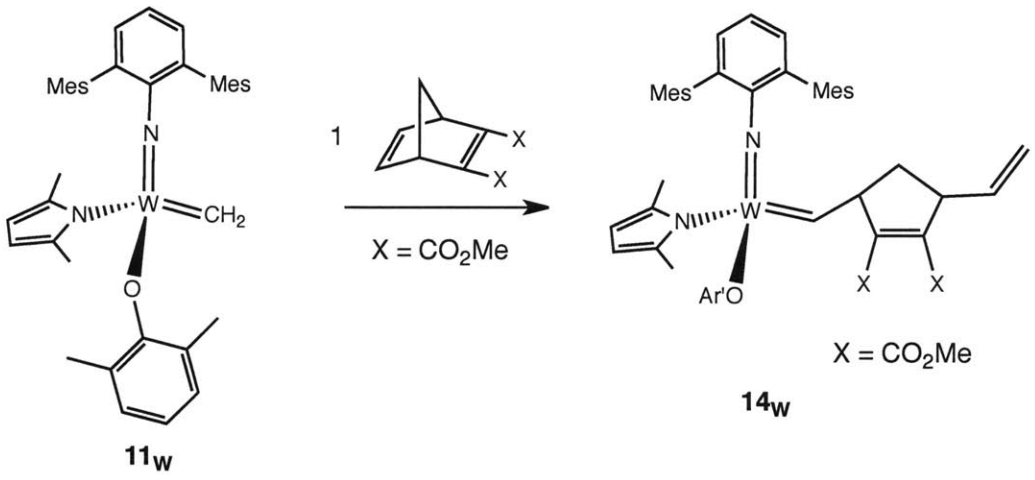

Scheme 4.10. Synthesis of 14_W.

Similar to the reaction of $\mathbf{6_W}$, reaction of $\mathbf{11_W}$ with one equivalent of **DCMNBD** shows clean conversion to a first-insertion product ($\mathbf{14_W}$), indicating that the rate of initiation is much greater than the rate of polymer propagation of **DCMNBD** by $\mathbf{11_W}$.

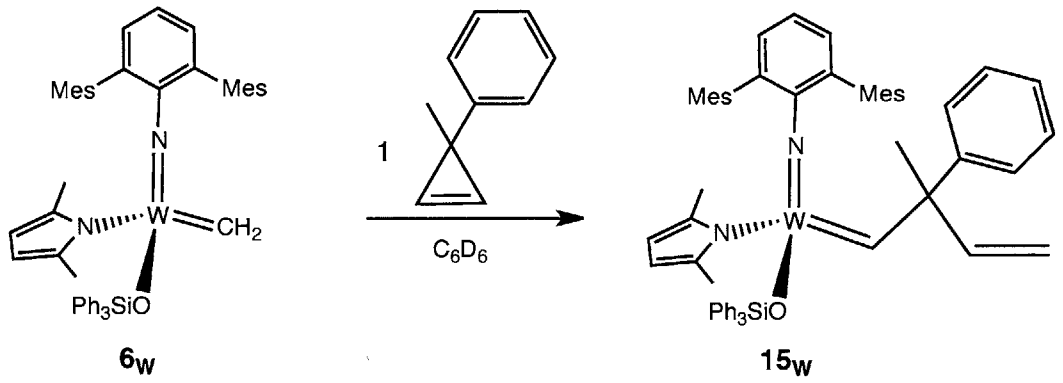

6W **15W**

Scheme 4.11. Synthesis of 15_W.

Clean conversion to a first-insertion product is observed in the reaction of **6_W** with one equivalent of 3-methyl-3-phenylcyclopropene (**MPCP**), shown in Scheme 4.11. **MPCP** is a very strained olefin and thus more reactive than **DCMNBD**. The fact that clean initiation is observed even with this reactive substrate indicates how much more reactive the methylidene species is than a substituted alkylidene, since all methylidene is consumed before any **15_W** continues to propagate.

These reactions indicate that the methylidene species are much more reactive with olefins than their neophylidene counterparts. In Chapter 5 this is used to develop new metathesis reactivity where norbornene and norbornadiene substrates are ring-opened using ethylene.

CONCLUSIONS

Kinetic studies of the alkylidene rotation were conducted. The equilibrium constants for the NAr* neophylidene complexes are much lower than those observed for previous four-coordinate alkylidene complexes of Mo and W. The destabilization of the *syn* alkylidene and thus lower equilibrium constants are attributed to the steric hindrance of the NAr* ligand. Additionally, the W alkylidene isomers interconvert approximately an order of magnitude faster than the Mo congeners, consistent with what has been observed previously for methylidene complexes.

Reaction of NAr* complexes with ethylene produces unsubstituted metallacycle and methylidene complexes. Methylidene complexes can be isolated for W with O^{t}Bu, OSiPh$_3$, and OAr' ligands. The steric protection afforded by the NAr* ligand prevents bimolecular

decomposition of the methylidene species, adding stability and allowing for isolation. Mo methylidene complexes can be observed *in situ* within mixture of products, but no Mo methylidene species were isolated. Unsubstituted metallacycles are isolated for W compounds with $OCMe(CF_3)_2$, $OSiPh_3$, and OAr' ligands. The unsubstituted metallacycle decomposes reductively to M(IV) ethylene complexes for both Mo and W, likely because of the less electron-withdrawing alkoxide ligand, which makes reduction more facile. The only Mo complex for which an unsubstituted metallacycle can be observed *in situ* is the complex with the $OCMe(CF_3)_2$ ligand; in this case the unsubstituted metallacycle is in equilibrium with the methylidene. These data indicate that the unsubstituted metallacycles are less stable for Mo than W (compared to the methylidenes). The stability provided by the NAr* ligand allows for the isolation of these types of species that are intermediates during olefin metathesis.

NAr* neophylidene complexes do not show clean conversion to first-insertion products upon reaction with strained olefins. However, the methylidene complexes are much more reactive, and clean conversion of these to first-insertion products is observed in several cases. The much lower reactivity of the neophylidene is likely exacerbated by the steric hindrance of the NAr* ligand. The disparate reactivity between substituted and unsubstituted alkylidene ligands is utilized to develop new catalytic activity in Chapter 5.

EXPERIMENTAL

General Considerations All air-sensitive manipulations were performed under nitrogen atmosphere in a glovebox or an air-free dual-manifold Schlenk line. All glassware was oven-dried and allowed to cool under vacuum before use. NMR spectra were obtained on Varian 300 MHz, Varian 500 MHz, or Bruker 600 MHz spectrometers. ^{1}H and ^{13}C NMR spectra are reported in δ (parts per million) relative to tetramethylsilane, and referenced to residual $^{1}H/^{13}C$ signals of the deuterated solvent (^{1}H (δ) benzene 7.16, chloroform 7.27, methylene chloride 5.32, toluene 2.09, acetonitrile 1.94; ^{13}C (δ) benzene 128.39, chloroform 77.23, methylene chloride 54.00, toluene 20.40). ^{19}F NMR spectra are reported in δ (parts per million) relative to trichlorofluoromethane and referenced using an external standard of fluorobenzene (δ −113.15). Diethyl ether, toluene, tetrahydrofuran, pentane, benzene, dichloromethane, and dimethoxyethane were sparged with nitrogen and passed through activated alumina. All solvents

were stored over 4 Å molecular sieves. Liquid reagents were degassed, brought into the glovebox, and stored over 4 Å molecular sieves. Mo(NAr*)(CHCMe$_2$Ph)(Me$_2$pyr)(O^{t}Bu) (**1$_{Mo}$**),[17] W(NAr*)(CHCMe$_2$Ph)(Me$_2$pyr)(O^{t}Bu) (**1$_W$**),[18] Mo(NAr*)(CHCMe$_2$Ph)(Me$_2$pyr)[OCMe(CF$_3$)$_2$] (**2$_{Mo}$**),[18] W(NAr*)(CHCMe$_2$Ph)(Me$_2$pyr)[OCMe(CF$_3$)$_2$] (**2$_W$**),[18] Mo(NAr*)(CHCMe$_2$Ph)(Me$_2$pyr)(OSiPh$_3$) (**3$_{Mo}$**),[18] W(NAr*)(CHCMe$_2$Ph)(Me$_2$pyr)(OSiPh$_3$) (**3$_W$**),[18] Mo(NAr*)(CHCMe$_2$Ph)(Me$_2$pyr)(OAr') (**4$_{Mo}$**),[18] and W(NAr*)(CHCMe$_2$Ph)(Me$_2$pyr)(OAr') (**4$_W$**)[18] were prepared according to literature procedures. All other reagents were used as received.

EXSY experiments Samples were prepared in C_6D_6 in teflon-stoppered NMR tubes. EXSY experiments were run at 21 °C with a mixing time of 1 s.

Irradiation experiments Samples were prepared in toluene-*d*$_8$ in teflon-stoppered NMR tubes and irradiated at –78 °C in a Rayonet photolysis apparatus at 350 nm. The samples were kept at –78 °C until placed in a 500 MHz NMR spectrometer preequilibrated at the desired temperature. Data were collected over at least two half lives by observing the decay of the *anti* resonance with respect to an internal standard of poly(dimethylsiloxane).

W(NAr*)(C$_3$H$_6$)(Me$_2$Pyr)(OSiPh$_3$) (5$_W$). W(NAr*)(CHCMe$_2$Ph)(Me$_2$Pyr)(OSiPh$_3$) (**3$_W$**) (36.9 mg, 0.0364 mmol) was dissolved in 10 mL of 10:1 pentane:Et$_2$O in a 50 mL Schlenk bomb. The solution was degassed by applying vacuum for several seconds. The flask was refilled with 1 atm ethylene and the mixture was stirred for 2 h. The flask was brought into the dry box and cooled to –25 °C for 16 h over which time yellow crystals formed. The mother liquor was removed by pipette and the crystals were collected on a frit and washed with 0.5 mL cold pentane to yield 12.0 mg (36 %). ^{1}H NMR (C_6D_6): δ 7.389 (d, 6H, Ar*H*), 7.136 – 7.071 (overlapping signals, 9H, Ar*H*), 6.768 (s, 4H, Mes*H*), 6.742 – 6.701 (overlapping signals, 3H, Ar*H*), 6.082 (s, 2H, NMe$_2$C$_4$*H*$_2$), 3.998 (dt, J_{HH} (d) = 11 Hz, J_{HH} (t) = 4 Hz, 2H, C$_\alpha$*H*), 3.999 (dt, J_{HH} (d) = 11 Hz, J_{HH} (t) = 4 Hz, 2H, C$_\alpha$*H*), 2.158 (s, 6H, *Me*), 2.150 (s, 6H, *Me*), 1.990 (s, 12H, Mes*Me*), -1.117 (m, 1H, C$_\beta$*H*), -1.270 (m, 1H, C$_\beta$*H*); ^{13}C NMR (C_6D_6): δ 142.3, 137.9, 137.4, 137.3, 136.6, 135.9, 135.8, 132.6, 129.9, 129.7, 129.2, 128.7, 128.3, 126.9, 108.9, 99.3 (*C$_\alpha$*), 21.5, 21.4, 16.5, 4.4

(C_β). Anal. Calcd for $C_{51}H_{54}N_2OSiW$: C, 66.37; H, 5.90; N, 3.04; Experimental: C, 66.12; H, 6.10; N, 2.90.

W(NAr*)(CH_2)(Me_2Pyr)($OSiPh_3$) (6_W). W(NAr*)(CHCMe$_2$Ph)(Me$_2$Pyr)($OSiPh_3$) (3_W) (55.0 mg, 54.3 μmol) was suspended in 6 mL of 5:1 pentane:Et_2O. The solution was degassed by applying vacuum for several seconds. The flask was refilled with 1 atm ethylene and the mixture was stirred for 2 h. The flask was brought into the dry box and cooled to –25 °C for 16 h over which time yellow crystals formed. The mother liquor was removed by pipette and the crystals were washed with 3 x 0.5 mL cold pentane. The crystals were dissolved in 10 mL toluene and the volatiles were removed *in vacuo* to yield 30.4 mg of yellow powder (63 %). Crystals for X-ray diffraction were grown by slow diffusion of pentane into a concentrated benzene solution of 6_W at ambient temperature. ^{1}H NMR (C_6D_6): δ 9.557 (d, 1H, W=CH_2, $^2J_{HH}$ = 9 Hz), 8.998 (d, 1H, W=CH_2, $^2J_{HH}$ = 9 Hz), 7.458 (d, 7Hz, Ar*H*), 7.189 – 7.175 (overlapping signals, 2H, Ar*H*), 7.152 – 7.123 (overlapping signals, 5H, Ar*H*), 6.988 (m, 4H, Ar*H*), 6.841 (s, 2H, Ar*H*), 6.530 (s, 2H, Ar*H*), 5.982 (s, 2H, Ar*H*), 2.209 (s, 6H, CH_3), 2.103 (s, 6H, CH_3), 1.998 (s, 6H, CH_3), 1.885 (s, 6H, CH_3); ^{13}C NMR (C_6D_6): δ 237.8 (W=*C*H_2, $^1J_{CW}$ = 180 Hz), 154.0, 138.6, 137.0, 136.9, 136.5, 135.8, 135.7, 134.9, 130.9, 129.2, 129.1, 110.2, 21.7, 21.4, 20.7, 17.0. Anal. Calcd for $C_{49}H_{50}N_2OSiW$: C, 65.77; H, 5.63; N, 3.13; Experimental: C, 65.48; H, 5.48; N, 3.07.

W(NAr*)(CH_2)(Me_2Pyr)(O^{t}Bu) (7_W). W(NAr*)(CHCMe$_2$Ph)(Me$_2$Pyr)(O^{t}Bu), 1_W (51 mg, 73 μmol) was dissolved in 10 mL toluene in a 50 mL Schlenk bomb. The solution was degassed by applying vacuum for 5 s. The flask was filled with 1 atm ethylene and stirred for 10 m. The volatiles were removed *in vacuo* to leave an orange oil. The oil was extracted with pentane, filtered through a pipette filter, and the pentane removed *in vacuo*. The oil was dissolved in MeCN/Et_2O and cooled to –25 °C, and orange crystals formed. The mother liquor was removed by pipette, the crystals were washed with 3 x 0.3 mL cold MeCN and dried under vacuum; yield 30 mg, 68 %. ^{1}H NMR (C_6D_6): δ 9.601 (d, $^2J_{HH}$ = 9 Hz, $^1J_{HW}$ = 15 Hz, 1H, W=CH_2), 9.510 (d, $^2J_{HH}$ = 9 Hz, $^1J_{HW}$ = 6 Hz, 1H, W=CH_2), 6.964 (overlapping signals, 3H, Ar*H*), 6.843 (s, 2H, Mes*H*), 6.794 (s, 2H, Mes*H*), 6.083 (s, 2H, NMe$_2$C$_4H_2$), 2.204 (s, 6H, CH_3), 2.193 (s, 6H, CH_3), 2.121 (s, 6H, CH_3), 1.970 (s, 6H, CH_3), 0.934 (s, 9H, OC(CH_3); ^{13}C{^{1}H} NMR (C_6D_6): δ 235.1 (W=*C*H_2), 157.9, 153.9, 138.2, 137.5, 137.5, 137.1, 136.8, 136.8, 136.6, 136.6, 136.3, 136.2,

134.8, 129.4, 129.2, 129.0, 128.8, 126.1, 124.8, 110.0, 109.8, 105.8, 83.5, 31.8, 31.7, 24.9, 21.6, 21.6, 21.4, 21.4, 21.3, 21.0, 17.8, 17.7.

Observation of W(NAr*)(C_3H_6)(Me_2Pyr)(O^tBu) *in situ* W(NAr*)(CH_2)(Me_2Pyr)(O^tBu), **1a$_W$** (10.2 mg, 12.6 μmol), was dissolved in 0.5 mL C_6D_6 in a J.Young-style NMR tube. The solution was freeze-pump-thawed two times. The tube was refilled with ethylene and a ^{1}H NMR spectrum was obtained which showed a 1:1 mixture of W(NAr*)(C_3H_6)(Me_2Pyr)(O^tBu): W(NAr*)(CH_2)(Me_2pyr)(O^tBu) and 3-methyl-3-phenyl-1-butene. The resonances belonging to W(NAr*)(C_3H_6)(Me_2Pyr)(O^tBu) are reported. ^{1}H NMR (C_6D_6): δ 6.898 (overlapping signals, 3H, Ar*H*), 6.790 (s, 4H, Mes*H*), 6.050 (s, 2H, Pyr*H*), 3.826 (m, 4H, $C_\alpha H$), 2.273 (s, 6H, CH_3), 2.127 (s, 6H, CH_3), 2.067 (s, 12H, Mes$(CH_3)_{ortho}$), 0.752 (s, 9H, $OC(CH_3)_3$), −1.110 (m, 2H, $C_\beta H$).

Observation of W(NAr*)(CH_2CH_2)(Me_2Pyr)(O^tBu) *in situ* W(NAr*)(CH_2)(Me_2Pyr)(O^tBu), **1a$_W$** (10.9 mg, 13.4 μmol), was dissolved in 0.5 mL C_6D_6 in a J.Young-style NMR tube. The solution was freeze-pump-thawed two times. The tube was refilled with ethylene and a ^{1}H NMR spectrum was obtained after 4 h. A 3:1:1 mixture of W(NAr*)(CH_2CH_2)(Me_2Pyr)(O^tBu): W(NAr*)(C_3H_6)(Me_2Pyr)(O^tBu): W(NAr*)(CH_2)(Me_2pyr)(O^tBu) along with 3-methyl-3-phenyl-1-butene and propylene was observed. The resonances belonging to W(NAr*)(CH_2CH_2)(Me_2Pyr)(O^tBu) are reported. ^{1}H NMR (C_6D_6): δ 6.882 (overlapping signals, Ar*H*, 3H), 6.853 (s, 1H, Ar*H*), 6.809 (s, 1H, Ar*H*), 6.749 (s, 2H, Ar*H*), 6.006 (s, 2H, Pyr*H*), 3.514 (m, 1H, $H_2C{=}CH_2$), 3.452 (m, 1H, $H_2C{=}CH_2$), 3.046 (m, 1H, $H_2C{=}CH_2$), 3.526 (m, 1H, $H_2C{=}CH_2$), 2.297 (s, 6H, CH_3), 2.244 (s, 6H, CH_3), 2.210 (s, 6H, CH_3), 2.173 (s, 6H, CH_3), 0.846 (s, 9H, $OC(CH_3)_3$).

W(NAr*)(C_3H_6)(Me_2Pyr)(OAr') (10$_W$). W(NAr*)(CHCMe_2Ph)(Me_2Pyr)(OAr'), **4$_W$** (78 mg, 0.091 mmol) was dissolved in pentane in Schlenk bomb. The solution was degassed by applying vacuum for a few seconds. The flask was refilled with 1 atm ethylene and stirred for 5 m. The flask was cooled to –25 °C and orange crystals formed over 16 h. The supernatant was removed by pipette and the crystals washed with cold pentane and dried *in vacuo*; yield 40 mg, 57 %. ^{1}H NMR (C_6D_6): δ 6.828 – 6.806 (overlapping signals, 9H, Ar*H*), 6.621 (t, J_{HH} = 7 Hz, 1H, ArH_{para}), 5.901 (s, 2H, $NMe_2C_4H_2$), 3.920 (m, 4H, $C_\alpha H$), 2.217 (s, 6H, CH_3), 2.210 (s, 6H, CH_3), 2.040 (s,

12H, Mes$(CH_3)_{ortho}$), 1.769 (s, 6H, CH_3), -1.219 (m, 2H, C$_\alpha H$). ^{13}C NMR (C_6D_6): δ 160.2, 150.9, 142.4, 137.3, 137.0, 136.4, 132.8, 129.6, 129.1, 129.0, 127.5, 127.0, 120.3, 109.0, 99.1 (C_α, $^1J_{CW}$ = 250 Hz), 21.5, 21.4, 18.7, 16.8, 3.6 (C_β). Anal. Calcd for $C_{41}H_{48}N_2OW$: C, 64.06; H, 6.29; N, 3.64; Experimental: C, 64.32; H, 6.46; N, 3.58.

W(NAr*)(CH$_2$)(Me$_2$Pyr)(OAr') (11$_W$). W(NAr*)(CHCMe$_2$Ph)(Me$_2$Pyr)(OAr'), **4$_W$** (135 mg, 0.158 mmol), was dissolved in pentane in Schlenk bomb. The solution was degassed by reducing the pentane volume to ~ 3 mL under vacuum. The flask was refilled with 1 atm ethylene, stirred for 10 m, and orange precipitate formed. The flask was cooled to –25 °C for 16 h. The solid was collected on a frit and washed with cold pentane. The solid was dissolved in 10 mL toluene and the volatiles removed *in vacuo*. The resulting oil was stirred with pentane and the volatiles removed *in vacuo* to yield a yellow solid, 82 mg (70 %). ^{1}H NMR (C_6D_6): δ 9.693 (s, 2H, W=CH_2), 6.963 (s, 3H, Ar*H*), 6.839 (d, 2H, Ar*H*), 6.748 (overlapping signals, 3H, Ar*H*), 6.562 (s, 2H, Ar*H*), 6.602 (NMe$_2$C$_4H_2$), 2.157 (s, 6H, CH_3), 2.089 (s, 6H, CH_3), 2.044 (s, 6H, CH_3), 1.995 (s, 6H, CH_3), 1.922 (s, 6H, CH_3); ^{1}H NMR (C_7D_8, alkylidene resonance): δ 9.677 (d, $^2J_{HH}$ = 9 Hz, W=CH_2), 9.644 (d, $^2J_{HH}$ = 9 Hz, W=CH_2); ^{1}H NMR (CD_2Cl_2, alkylidene resonance): δ 9.761 (d, $^2J_{HH}$ = 9 Hz, J_{HW} = 7 Hz, $^1J_{CH}$ = 131 Hz, W=CH_2), 9.550 (d, $^2J_{HH}$ = 9 Hz, J_{HW} = 17 Hz, $^1J_{CH}$ = 166 Hz, W=CH_2); ^{13}C NMR (C_6D_6): δ 241.4, 138.5, 137.2, 136.8, 136.7, 136.5, 135.2, 129.7, 129.4, 129.1, 129.0, 128.9, 127.6, 126.7, 126.0, 122.8, 110.4, 21.6, 21.4, 20.8, 17.8, 17.7. Anal. Calcd for $C_{39}H_{44}N_2OW$: C, 63.25; H, 5.99; N, 3.78; Experimental: C, 63.34; H, 6.10; N, 3.44.

W(NAr*)(C$_3$H$_6$)(Me$_2$Pyr)[OCMe(CF$_3$)$_2$] (12$_W$).

W(NAr*)(CHCMe$_2$Ph)(Me$_2$Pyr)[OCMe(CF$_3$)$_2$] (**2$_W$**) (53.6 mg, 58.3 μmol) was dissolved in 3 mL of a 2:1 MeCN:Et$_2$O mixture in a 50 mL Schlenk bomb. The volume of the solution was reduced to 1 mL and the solution degassed by application of vacuum. The flask was refilled with 1 atm of ethylene and the solution stirred for 10 m before the flask was sealed, brought into the dry box, and cooled to –25 °C for 16 h over which time crystals formed. The mother liquor was removed by pipette. The crystals were dissolved in pentane, the solution transferred to a vial, and the volatiles removed *in vacuo* to leave a yellow solid, 26.0 mg (54 %). ^{1}H NMR (C_6D_6): δ 6.832 (s, 4H, Mes*H*), 6.750 (t, 1H, ArH_{para}), 6.675 (d, 2H, ArH_{meta}), 5.916 (s, 2H, Pyr*H*), 4.073 (dt, J_{HH}

= 12 Hz, J_{HH} = 4 Hz, 2H, WCH_α), 3.916 (dt, J_{HH} = 11 Hz, J_{HH} = 4 Hz, 2H, WCH_α), 2.214 (s, 6H, ArCH_3), 2.018 (s, 6H, ArCH_3), 1.958 (s, 12H, Mes(CH_3)$_{meta}$), 0.847 (s, 1H, OC(CH_3)(CF$_3$)$_2$), −0.763 (m, 1H, H$_\beta$), −1.169 (m, 1H, H$_\beta$); ^{13}C NMR (C_6D_6): δ 142.2, 137.8, 137.4, 136.8, 132.0, 130.0, 129.7, 128.7, 127.5, 108.5 (Aryl), 99.6 (C$_\alpha$, J_{CW} = 32 Hz), 28.7, 23.1, 21.5 (Mes*Me*), 21.2 (Mes*Me*), 15.7, 14.7, 3.8 (C$_\beta$); ^{19}F NMR (C_6D_6): δ −77.81. Anal. Calcd for $C_{37}H_{42}F_6N_2OW$: C, 53.63; H, 5.11; N, 3.38; Experimental: C, 53.67; H, 5.04; N, 3.48.

Observation of Mo(NAr*)(CH$_2$CH$_2$)(Me$_2$Pyr)(O^{t}Bu) *in situ*. A solution of Mo(NAr*)(CHCMe$_2$Ph)(Me$_2$Pyr)(O^{t}Bu), **1$_{Mo}$**, in 0.5 mL C_6D_6 in a J.Young-style NMR tube was degassed by freeze-pump-thawing two times. The tube was refilled with 1 atm ethylene, sealed, and inverted to mix. After 16 h, a ^{1}H NMR spectrum shows conversion to Mo(NAr*)(CH$_2$CH$_2$)(Me$_2$Pyr)(O^{t}Bu) as the only Mo-based product. ^{1}H NMR (C_6D_6): δ 6.896 (m, 1H, Ar*H*), 6.833 – 6.808 (overlapping signals, 6H, Ar*H*), 6.127 (s, 2H, pyr*H*), 2.448 – 2.358 (overlapping m, 2H, C*H*$_2$=C*H*$_2$), 2.297 (s, ArCH_3, 6H), 2.227 (s, ArCH_3, 6H), 2.074 (s, ArCH_3, 6H), 2.023 (s, ArCH_3, 6H), 1.921 (m, 1H, C*H*$_2$=C*H*$_2$), 1.752 (m, 1H, C*H*$_2$=C*H*$_2$), 0.880 (s, 9H, OC(CH_3)$_3$).

Observation of Mo(NAr*)(CH$_2$)(Me$_2$Pyr)[OCMe(CF$_3$)$_2$] *in situ*. A solution of Mo(NAr*)(CHCMe$_2$Ph)(Me$_2$Pyr)[OCMe(CF$_3$)$_2$], **2$_{Mo}$**, in 0.5 mL C_6D_6 in a J.Young-style NMR tube was degassed by freeze-pump-thawing two times. The tube was refilled with 1 atm ethylene, sealed, and inverted to mix. After 20 m, the volatiles were removed *in vacuo*. The non-volatile components were dissolved in C_6D_6 and a ^{1}H NMR spectrum was obtained. ^{1}H NMR (C_6D_6): δ 11.672 (d, 1H, $^2J_{HH}$ = 4 Hz, MoC*H*$_2$), 11.603 (d, 1H, $^2J_{HH}$ = 4 Hz, MoC*H*$_2$), 6.919 (s, 2H, Ar*H*), 6.890 (s, 2H, Ar*H*), 6.859 (d, 1H, Ar*H*), 6.778 (d, 1H, Ar*H*), 4.668 (br s, 2H, Pyr*H*), 2.176 (s, 6H, ArCH_3), 2.156 (s, 6H, ArCH_3), 2.115 (s, 6H, ArCH_3), 2.073 (s, 6H, ArCH_3), 1.091 (s, 3H, OC(CF$_3$)$_2$(CH_3)).

Observation of First-Insertion Product 12$_W$. To a solution of W(NAr*)(CH$_2$)(Me2pyr)(OSiPh$_3$), **6$_W$** (27 mg, 30 μmol) in 0.6 mL C_6D_6 in a teflon-stoppered NMR tube was added DCMNBD (5.0 μL, 29 μmol). ^{1}H NMR (C_6D_6): δ 8.988 (d, 1H, $^3J_{HH}$ = 2 Hz, $^1J_{CH}$ = 154 Hz, W=C*H*), 7.757 (d, 6H, Ar*H*), 7.222 and 7.215 (overlapping signals, 8H, Ar*H*),

6.930 (s, 2H, Ar*H*), 8.898 – 8.868 (overlapping signals, 5H, Ar*H*), 6.130 (br s, 1H, ($NMe_2C_4H_2$), 5.918 ($NMe_2C_4H_2$), 5.619 (m, 1H, H_F), 5.085 (m, 1H, H_B), 5.008 (d, $^3J_{HH}$ = 17 Hz, H_I), 4.929 (d, $^3J_{HH}$ = 10 Hz, H_G), 3.310 (m, 1H, H_E), 3.239 (s, 3H, CO_2CH_3), 2.714 (s, 3H, CO_2CH_3), 2.297 (s, 6H, MesCH_3), 2.230 (s, 6H, MesCH_3), 2.119 (s, 6H, MesCH_3), 2.055 (br s, 3H, N$Me_2C_4H_2$), 1.848 (m, $H_{C/D}$), 1.778 (br s, N$Me_2C_4H_2$, 4H integrated with previous peak), 0.914 (m, 1H, $H_{C/D}$); ^{13}C NMR (C_6D_6): δ 251.9, 170.5, 166.1, 153.4, 150.2, 138.5, 138.1, 137.9, 137.7, 137.3, 136.7, 136.3, 135.5, 130.1, 129.8, 129.7, 128.9, 128.7, 128.2, 125.6, 117.7, 108.4 (br), 107.2 (br), 54.7, 52.5, 51.8, 50.7, 41.8, 21.8, 21.7, 21.1, 20.0 (br), 14.5 (br).

Crystallization of 13_W for X-ray diffraction. To a solution of W(NAr*)(CH_2)(Me_2pyr)($OSiPh_3$), $\mathbf{6_W}$ (32.0 mg, 35.8 μmol) in 0.5 mL C_6H_6 and 0.5 mL pentane in 20 mL vial was added DCMNBD (6.2 μL, 35.4 μmol) with stirring. The yellow solution immediately became orange. The volatiles were removed *in vacuo* after 20 m. The remaining oil was extracted with benzene, filtered through a pipette filter, and the volatiles removed under reduced pressure from the filtrate. The remaining orange oil was dissolved in toluene, Et_2O, and pentane and cooled to −25 °C. Crystals formed within 19 days (not quantitative).

Observation of 13_W.

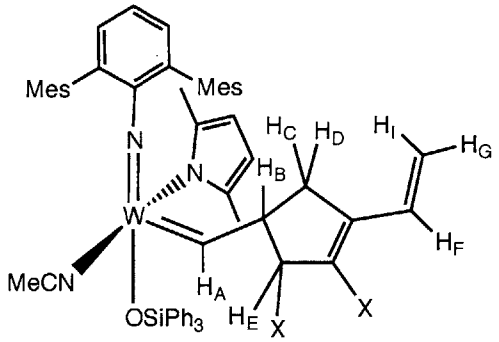

DCMNBD (4.0 μL, 23 μmol) was added to a stirring solution of W(NAr*)(CH_2)(Me_2Pyr)($OSiPh_3$) ($\mathbf{6_w}$) (21.4 mg, 23.9 μmol) in 2 mL benzene. After 5 m, NEt_3 (3.3 μL, 24 μmol) was added. The volatiles were removed *in vacuo* and NMR spectra were obtained in CD_3CN. Crystals for diffraction were obtained from MeCN and Et_2O solution at −25 °C. A short X-ray diffraction data set was collected in order to determine the unit cell, atom connectivity, and geometry. This data confirmed it to be the same as the previous crystal

structure of $\mathbf{13_W}$. ^{1}H NMR (CD_3CN): δ 11.583 (br s, 1H, H_A), 7.559 (dd, 1H, J_{HH} = 11 Hz, J_{HH} = 18 Hz), 7.377 – 7.335 (overlapping m, 6H, Ar*H*), 7.285 (t, 6H, J_{HH} = 7 Hz, Ar*H*), 7.069 (dd, 6H, J_{HH} = 1.5 Hz, J_{HH} = 8 Hz), 6.897 – 6.883 (overlapping signals, 4H), 6.733 (s, 2H, pyr*H*), 5.605 (dd, 1H, , J_{HH} = 11 Hz, J_{HH} = 1 Hz, H_G), 5.554 (dd, 1H, J_{HH} = 18 Hz, J_{HH} = 1 Hz, H_I), 4.955 (pseudo quintet, 1H, J_{HH} = 4 Hz, H_B), 3.866 (dd, 1H, J_{HH} = 9 Hz, J_{HH} = 1 Hz, H_E), 3.683 (s, 3H, CO_2CH_3), 3.427 (s, 3H, CO_2CH_3), 2.360 (m, 1H, $H_{C/D}$), 2.252 (s, 6H, MesCH_3), 2.140 (m, 1H, $H_{C/D}$), 2.008 (s, 6H, MesCH_3), 1.679 (s, 6H, MesCH_3), 1.646 (br s, 6H, Pyr(CH_3)$_2$).

Observation of $\mathbf{14_W}$.

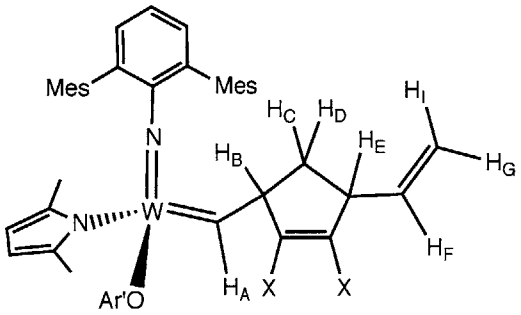

X = CO_2Me

W(NAr*)(CH_2)(Me_2Pyr)(OAr'), $\mathbf{11_W}$ (22.9 mg, 29.8 μmol), was dissolved in 0.5 mL C_6D_6 in a J.Young-style NMR tube, **DCMNBD** (4.2 μL, 24 μmol) was added, and NMR spectra were obtained after 15 m. ^{1}H NMR (C_6D_6): δ 9.394 (d, 1H, J_{HH} = 3 Hz, H_A), 7.010 (d, 2H, J_{HH} = 7 Hz, ArH_{para}), 6.694 (s, 1H, Ar*H*), 6.925 (m, 1H, Ar*H*), 6.879 (s, 2H, Mes*H*), 6.771 (s, 2H, Mes*H*), 6.733 (t, 1H, J_{HH} = 7 Hz, ArH_{meta}), 6.613 (m, 1H, Ar*H*), 6.162 (br s, 1H, Pyr*H*), 6.059 (br s, 1H, Pyr*H*), 5.640 (m, 1H, H_F), 5.472 (m, 1H, H_B), 5.030 (d, 1H, J_{HH} = 19 Hz, H_I), 4.970 (s, 1H, J_{HH} = 10 Hz, H_G), 3.403 (s, 3H, CO_2CH_3), 3.308 (m, 1H, H_E), 3.249 (s, 3H, CO_2CH_3), 2.719 (s, 3H, PyrCH_3), 2.242 (s, 6H, ArCH_3), 2.231 (s, 6H, ArCH_3), 2.181 (s, 6H, ArCH_3), 2.166 (s, 6H, ArCH_3), 1.823 (dt, 1H, J_{HH} = 13 Hz, J_{HH} = 8 Hz, $H_{C/D}$), 1.002 (pseudo q, J_{HH} = 11 Hz).

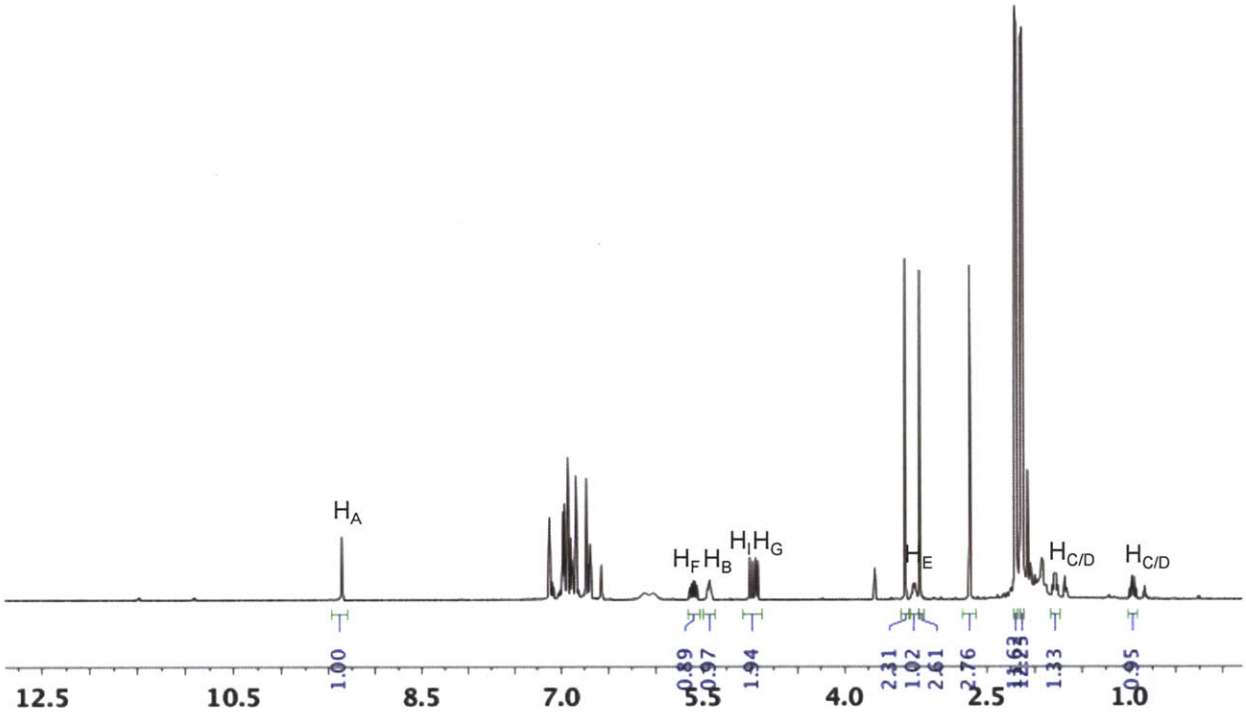
H_A
H_F H_B
H_I H_G
H_E
H_C/D
H_C/D
1.00
0.89
0.97
1.94
2.31
1.02
2.61
2.76
1.33
0.95
12.5
10.5
8.5
7.0
5.5
4.0
2.5
1.0

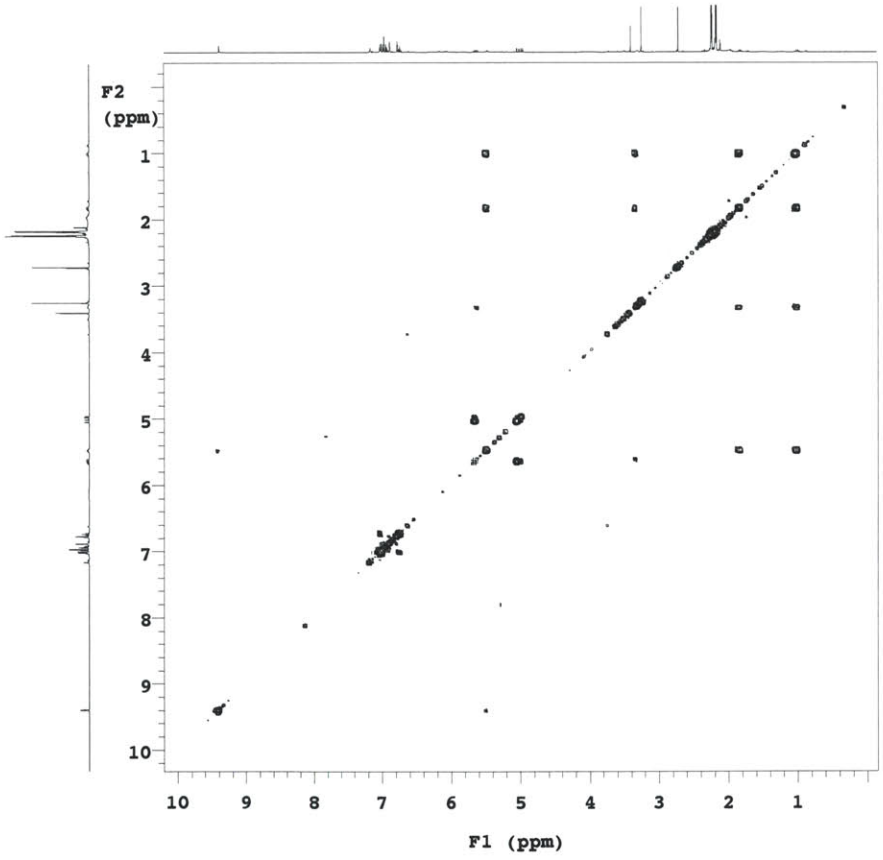
F2 (ppm)
F1 (ppm)
1
2
3
4
5
6
7
8
9
10

Observation of 15_W. MPCP (1.3 μL, 10 μmol) was added by syringe to a J.Young-style NMR tube containing a solution of W(NAr*)(CH_2)(Me_2Pyr)($OSiPh_3$) (**6_W**) (9.7 mg, 11 μmol) in 0.5 mL C_6D_6. A ^{1}H NMR spectrum was obtained. ^{1}H NMR (C_6D_6): δ 8.320 (s, 1H, J_{WH} = 7 Hz, W=C*H*), 7.423 (d, 6H, Ar*H*, J_{WH} = 7 Hz), 7.197 (m, 3H, Ar*H*), 7.146 (t, 6H, J_{WH} = 7 Hz, Ar*H*), 7.055 – 6.983 (overlapping signals, 6H, Ar*H*), 6.874 (overlapping signals, 4H, Ar*H*), 6.491 (s, 2H, Mes*H*), 6.073 (dd, 1H, J_{WH} = 11 Hz, J_{WH} = 18 Hz, W=CHC(Me)(Ph)C*H*CH_2), 5.860 (br s, 2H, Pyr*H*), 4.978 (d, 1H, J_{WH} = 11 Hz, W=CHC(Me)(Ph)CHC(H_{trans})(H_{cis})), 4.776 (d, 1H, J_{WH} = 18 Hz, W=CHC(Me)(Ph)CHC(H_{trans})(H_{cis})), 2.276 (s, 6H, ArCH_3), 2.091 (s, 6H, ArCH_3), 2.003 (s, 6H, ArCH_3), 1.768 (s, 3H, W=CHC(*Me*)(Ph)CHCH_2), 1.013 (br s, PyrCH_3).

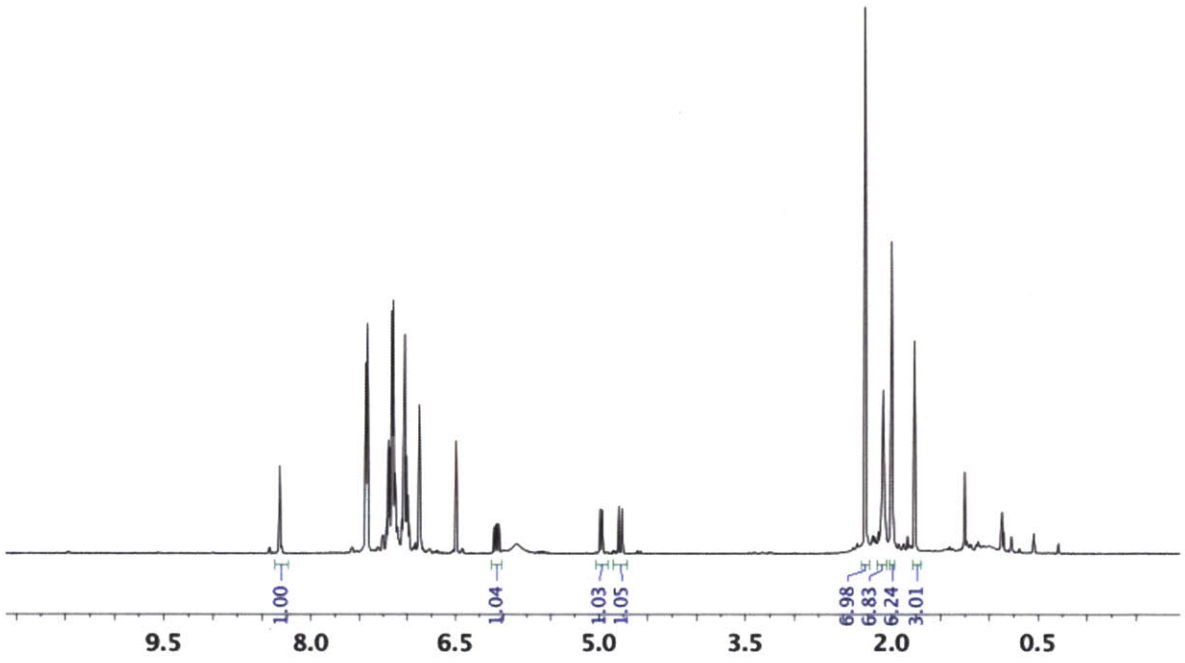

Crystallographic details. Low-temperature diffraction data (ϕ-and ω-scans) were collected on a Bruker-AXS X8 Kappa Duo diffractometer coupled to a Smart Apex2 CCD detector with Mo Kα radiation (λ = 0.71073 Å) from an Incoatec *IμS* micro-source. The structures were solved by direct methods using SHELXS[19] and refined against F2 on all data by full-matrix least squares with SHELXL-97[20] following established refinement strategies[21]. All non-hydrogen atoms were refined anisotropically. All hydrogen atoms were included into the model at geometrically calculated positions and refined using a riding model unless indicated below. The isotropic displacement parameters of all hydrogen atoms were fixed to 1.2 times the *U* value of the atoms

they are linked to (1.5 times for methyl groups). Details of the data quality, a summary of the residual values of the refinements as well as other pertinent parameters are listed in the following tables.

$W(NAr^*)(C_3H_6)(Me_2Pyr)(OSiPh_3)$ ($\mathbf{5_W}$) crystallizes in monoclinic space group $P2_1/n$ with two molecules per asymmetric unit. The refinement was straightforward and without complications. All bond lengths and angles specified and discussed throughout this report are those of the molecule containing W1.

$W(NAr^*)(CH_2)(Me_2Pyr)(OSiPh_3)$ ($\mathbf{6_W}$) crystallizes in monoclinic space group $P2_1/n$ with one molecule per asymmetric unit. The tungsten atom, pyrrolide ligand, methylidene ligand, oxygen (O1), and imido nitrogen (N1) were disordered over two positions. The ratio between the two components was refined freely and converged at 0.9029(3). The disorder was refined with the help of similarity restraints on the 1-2 and 1-3 distances and displacement parameters as well as rigid bond restraints for anisotropic parameters for all atoms. Coordinates for the hydrogen atoms on C1, the carbon atom binding directly to tungsten, were taken from the difference Fourier synthesis. The hydrogen atoms were refined semi-freely with the help of distance restraints on the C-H distance (target 0.95(2) Å) while constraining the U_{iso} value of the hydrogen atoms to 1.2 the U_{eq} value of the carbon atom to which the hydrogen binds. All bond lengths and angles specified and discussed throughout this report are those of the major component of the disorder.

Compound $\mathbf{13_W}$ crystallizes in triclinic space group $P\bar{1}$ with one molecule $\mathbf{13_W}$, 1.5 molecules MeCN, and 1.5 molecules Et_2O per asymmetric unit. The siloxide ligand (O1, Si1, C43 – C60) was disordered over two positions. The ratio between the two components was refined freely and converged at 0.7722. One Et_2O molecule was disordered over three positions. The ratio between the three components was refined freely and converged at 0.4837:0.3041:0.2117. A remaining solvent molecule was modeled as a two-part disorder between a Et_2O and an MeCN molecule. The ratio between the two components was refined freely and converged at 0.5280 for MeCN. All disorder was refined with the help of similarity restraints on 1-2 and 1-3 distances and displacement parameters as well as rigid bond restraints for anisotropic displacement parameters for all atoms. The following pairs of nearly overlapping atoms were constrained to show

identical anisotropic displacement parameters: C49/C49a, C45/C45a, C44/C44a, C46/C46a. Coordinates for the hydrogen atom on C1 (the carbon atom that binds directly to the tungsten) were taken from the difference Fourier synthesis. The hydrogen atom was subsequently refined semi-freely with the help of a distance restraint on the C—H-distance (target 0.95(2) Å).

Table 4.2. Crystal data and structure refinement for 5_W.

Identification code	12191
Empirical formula	C51 H54 N2 O Si W
Formula weight	922.90
Temperature	100(2) K
Wavelength	0.71073 Å
Crystal system	Monoclinic
Space group	$P2_1/n$
Unit cell dimensions	a = 19.6235(16) Å a= 90°
	b = 22.9245(19) Å b= 91.756(2)°
	c = 19.7261(17) Å g = 90°
Volume	8869.8(13) $Å^3$
Z	8
Density (calculated)	1.382 Mg/m^3
Absorption coefficient	2.670 mm^{-1}
F(000)	3760
Crystal size	0.35 x 0.30 x 0.30 mm^3
Theta range for data collection	1.36 to 30.51°
Index ranges	-28<=h<=28, -32<=k<=32, -28<=l<=28
Reflections collected	385055
Independent reflections	27055 [R(int) = 0.0396]
Completeness to theta = 30.51°	100.0 %
Absorption correction	Semi-empirical from equivalents
Max. and min. transmission	0.5014 and 0.4551
Refinement method	Full-matrix least-squares on F^2
Data / restraints / parameters	27055 / 6 / 1025
Goodness-of-fit on F^2	1.023
Final R indices [I>2sigma(I)]	R1 = 0.0220, wR2 = 0.0494
R indices (all data)	R1 = 0.0421, wR2 = 0.0596
Largest diff. peak and hole	1.081 and -0.737 $e.Å^{-3}$

Table 4.3. Crystal data and structure refinement for 6_W.

Identification code	x13095a	
Empirical formula	C49 H50 N2 O Si W	
Formula weight	894.85	
Temperature	100(2) K	
Wavelength	0.71073 Å	
Crystal system	Monoclinic	
Space group	$P2_1/c$	
Unit cell dimensions	a = 10.6649(12) Å	a= 90°
	b = 23.348(3) Å	b= 93.836(3)°
	c = 16.8858(19) Å	g = 90°
Volume	4195.2(8) $Å^3$	
Z	4	
Density (calculated)	1.417 Mg/m^3	
Absorption coefficient	2.820 mm^{-1}	
F(000)	1816	
Crystal size	0.250 x 0.200 x 0.120 mm^3	
Theta range for data collection	1.490 to 30.999°	
Index ranges	-15<=h<=15, -33<=k<=32, -24<=l<=24	
Reflections collected	145022	
Independent reflections	13374 [R(int) = 0.0435]	
Completeness to theta = 25.242°	100.0 %	
Absorption correction	Semi-empirical from equivalents	
Max. and min. transmission	0.4339 and 0.3390	
Refinement method	Full-matrix least-squares on F^2	
Data / restraints / parameters	13374 / 365 / 550	
Goodness-of-fit on F^2	1.058	
Final R indices [I>2sigma(I)]	R1 = 0.0216, wR2 = 0.0451	
R indices (all data)	R1 = 0.0268, wR2 = 0.0465	
Extinction coefficient	n/a	
Largest diff. peak and hole	0.669 and -0.488 $e.Å^{-3}$	

Table 4.4. Crystal data and structure refinement for 13_W.

Identification code	12177p-1
Empirical formula	C70.94 H85.30 N4.53 O6.47 Si W
Formula weight	1316.90
Temperature	100(2) K
Wavelength	0.71073 Å
Crystal system	Triclinic
Space group	$P\bar{1}$
Unit cell dimensions	a = 12.0776(7) Å a= 88.6940(10)°
	b = 12.8509(7) Å b= 83.7240(10)°
	c = 22.2515(13) Å g = 75.0450(10)°
Volume	3316.6(3) $Å^3$
Z	2
Density (calculated)	1.319 Mg/m^3
Absorption coefficient	1.814 mm^{-1}
F(000)	1365
Crystal size	0.25 x 0.15 x 0.07 mm^3
Theta range for data collection	1.64 to 31.55°
Index ranges	-17<=h<=17, -18<=k<=18, -32<=l<=32
Reflections collected	229724
Independent reflections	22121 [R(int) = 0.0401]
Completeness to theta = 31.55°	99.8 %
Absorption correction	Semi-empirical from equivalents
Max. and min. transmission	0.8835 and 0.6598
Refinement method	Full-matrix least-squares on F^2
Data / restraints / parameters	22121 / 606 / 1068
Goodness-of-fit on F^2	1.274
Final R indices [I>2sigma(I)]	R1 = 0.0375, wR2 = 0.0870
R indices (all data)	R1 = 0.0423, wR2 = 0.0887
Largest diff. peak and hole	2.671 and -2.143 $e.Å^{-3}$

REFERENCES

[1] (a) Flook, M. M.; Jiang, A. J.; Schrock, R. R.; Müller, P.; Hoveyda, A. H. *J. Am. Chem. Soc.* **2009**, *131*, 7962. (b) Flook, M. M.; Gerber, L. C. H.; Debelouchina, G. T.; Schrock, R. R. *Macromolecules* **2010**, *43*, 7515. (c) Flook, M. M.; Ng, V. W. L.; Schrock, R. R. *J. Am. Chem. Soc.* **2011**, *133*, 1784. (d) Flook, M. M.; Börner, J.; Kilyanek, S.; Gerber, L. C. H.; Schrock, R. R. *Organometallics* **2012**, *31*, 6231.

[2] (a) Jiang, A. J.; Zhao, Y.; Schrock, R. R.; Hoveyda, A. H. *J. Am. Chem. Soc.* **2009**, *131*, 16630. (b) Marinescu, S. C.; Schrock, R. R.; Müller, P.; Takase, M. K.; Hoveyda, A. H. *Organometallics* **2011**, *30*, 1780. (c) Townsend, E. M.; Schrock, R. R.; Hoveyda, A. H. *J. Am. Chem. Soc.* **2012**, *134*, 11334. (d) Peryshkov, D. V.; Schrock, R. R.; Takase, M. K.; Müller, P.; Hoveyda, A. H. *J. Am. Chem. Soc.* **2011**, *133*, 20754.

[3] (a) Ibrahem, I; Yu, M.; Schrock, R. R.; Hoveyda, A. H. *J. Am. Chem. Soc.* **2009**, *131*, 3844. (b) Yu, M.; Ibrahem, I.; Hasegawa, M.; Schrock, R. R.; Hoveyda, A. H. *J. Am. Chem. Soc.* **2012**, *134*, 2788.

[4] (a) Marinescu, S. C.; Schrock, R. R.; Müller, P.; Hoveyda, A. H. *J. Am. Chem. Soc.* **2009**, *131*, 10840. (b) Marinescu, S. C.; Levine, D.; Zhao, Y.; Schrock, R. R.; Hoveyda, A. H. *J. Am. Chem. Soc.* **2011**, *133*, 11512.

[5] (a) Wang, C.; Yu, M.; Kyle, A. F.; Jacubec, P.; Dixon, D. J.; Schrock, R. R.; Hoveyda, A. H. *Chem. Eur. J.* **2013**, *19*, 2726. (b) Wang, C.; Haeffner, F.; Schrock, R. R.; Hoveyda, A. H. *Angew. Chem., Int. Ed.* **2013**, *52*, 1939.

[6] (a) Oskam, J. H.; Schrock, R. R. *J. Am. Chem. Soc.* ***1992***, *114*, 7588. (b) Oskam, J. H.; Schrock, R. R. *J. Am. Chem. Soc.* **1993**, *115*, 11831.

[7] Singh, R.; Schrock, R. R.; Müller, P.; Hoveyda, A. H. *J. Am. Chem. Soc.* **2007**, *129*, 12654.

[8] Perrin, C. L.; Dwyer, T. J. *Chem. Rev.* **1990,** *90*, 935.

[9] Schrock, R. R., King, A. J.; Marinescu, S. C.; Simpson, J. H.; Müller, P. *Organometallics* **2010**, *29*, 5241.

[10] Poater, A.; Monfort-Solans, X.; Clot, E.; Copéret, C.; Eisenstein, O. *Dalton Trans.* **2006**, 3077.

[11] Arndt, S.; Schrock, R. R.; Müller, P *Organometallics* **2007**, *26*, 1279.

[12] (a) Tsang, W. C. P.; Schrock, R. R.; Hoveyda, A. H. *Organometallics* **2001**, *20*, 5658. (b) Tsang, W. C. P.; Hulzsch, K. C.; Alexander, J. B.; Bonitatebus, P. J, Jr.; Schrock, R. R.;

Hoveyda, A. H. *J. Am. Chem. Soc.* **2003**, *125*, 2652. (c) Tsang, W. C. P.; Jamieson, J. Y.; Aeilts, S. L.; Hultzsch, K. C.; Schrock, R. R.; Hoveyda, A. H. *Organometallics*, **2004**, *23*, 1997. (d) Schrock, R. R.; Murdzek, J. S.; Bazan, G. C.; Robbins, J.; DiMare, M.; O'Regan, M. *J. Am. Chem. Soc.* **1990**, *112*, 3875.

[13] (a) Kreickmann, T; Arndt, S.; Schrock, R. R.; Müller, P *Organometallics* **2007**, *26*, 5702. (b) Jiang, A. J.; Simpson, J. H.; Müller, P; Schrock, R. R. *J. Am. Chem. Soc.* **2009**, *131*, 7770. (c) Schrock, R. R.; Jiang, A. J.; Marinescu, S. C.; Simpson, J. H.; Müller, P *Organometallics* **2010**, *29*, 5241. (d) Townsend, E. M., Kilyanek, S. M.; Schrock, R. R.; Müller, P.; Smith, S. J.; Hoveyda, A. H. *Organometallics* **2013**, ASAP August 7, 2013.

[14] Addison, A. W.; Rao, T. N.; Van Rijn, J. J.; Veschoor, G. C. *J. Chem. Soc. Dalton Trans.* **1984**, 1349.

[15] Serjeant, E. P.; Dempsey, B. *International Union of Pure and Applied Chemistry. Commission on Equilibrium Data. Ionisation Constants of Organic Acids in Aqueous Solution*; Oxford; New York: Pergamon Press, 1979.

[16] Duchateau, R.; Cremer, U.; Harmsen, R. J.; Mohamud, S. I.; Abbenhuis, H. C. L.; van Santen, R. A.; Meetsma, A.; Thiele, S. K.-H.; van Tol, M. F. J.; Kranenburg, M. *Organometallics*, **1999**, *18*, 5447.

[17] Gerber, L. C. H.; Schrock, R. R.; Müller, P.; Takase, M. K. *J. Am. Chem. Soc.*, **2011**, *133*, 18142.

[18] Gerber, L. C. H.; Schrock, R. R.; Müller, P. *Organometallics*, **2013**, *32*, 2373.

[19] Sheldrick, G. M., *Acta Cryst.* **1990**, *A46*, 467.

[20] Sheldrick, G. M., Acta Cryst. **2008**, *A64*, 112.

[21] Müller, P. *Crystallography Reviews* **2009**, *15*, 57.

Chapter 5

Alkylidene Compounds Containing the 2,6-Dimesitylphenylimido Ligand as Catalysts for Olefin Metathesis

INTRODUCTION

In order to provide greater utility for olefin metathesis in chemical synthesis, new catalysts that push the boundaries of current reactivity are sought. The development of olefin metathesis catalysts for selective metathesis has been an ongoing goal, and many important advances have been made over the years.

The emergence of compounds that are stereogenic at the metal center and contain sterically demanding spectator ligands has provided *Z*-selective catalysts for olefin metathesis reactions. *Z*-selective catalysts based on molybdenum and tungsten are MAP (MonoAryloxide Pyrrolide) compounds that possess sterically demanding aryloxide ligands, typically substituted 2,6-terphenoxides or monoprotected Bitet ligands (Figure 5.1). Catalysts have been developed for *cis*-selective ring-opening metathesis polymerization (ROMP),[1] homocoupling,[2] ring-opening cross-metathesis, [3] ethenolysis, [4] and formation of natural products through ring-closing reactions.[5] A similar strategy was also applied for the development of *Z*-selective catalysts based on ruthenium, specifically, the active catalyst species contain a stereogenic metal center and a sterically demanding chelating N-heterocyclic carbene that are proposed to bias the metallacycle intermediates for the formation of *cis* bonds (Figure 5.1).[6]

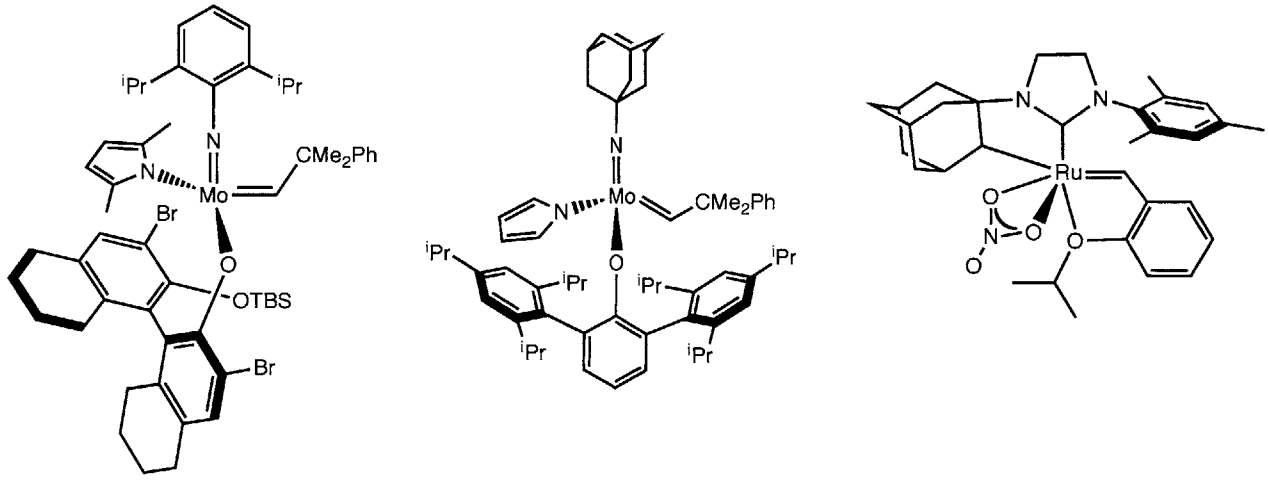

Figure 5.1. Examples of *Z*-selective catalysts for olefin metathesis reactions.

In order to better understand the dynamics at play between sterics and selectivity, MAP complexes were synthesized where the steric bias is switched: compounds that contain a 2,6-

dimesitylphenylimido ligand and comparatively small alkoxide or aryloxide ligand.[7,8] The hypothesis was that the switch in steric bias would provide an entry to *E* selectivity by the mechanism shown in Scheme 5.1. A *syn* alkylidene reacts with substrate or monomer with its substituents pointed away from the imido ligand due to the sterically demanding imido substituent. The metallacycle opens to form a *trans* olefin and an *anti* alkylidene. The electron-donating alkoxide ligand then promotes rotation of the *anti* alkylidene to the *syn* alkylidene[9] before further propagation. Upon synthesizing these compounds though, it was found that the *anti* and *syn* alkylidene isomers are about equal in energy, with equilibrium constants in the range of $10^0 - 10^2$ unlike all previous examples of four-coordinate imido alkylidene compounds where the *syn* alkylidene is more stable than the *anti*.[8] Because both alkylidene isomers are present and they are interconverting readily, *E*-selectivity is unlikely.

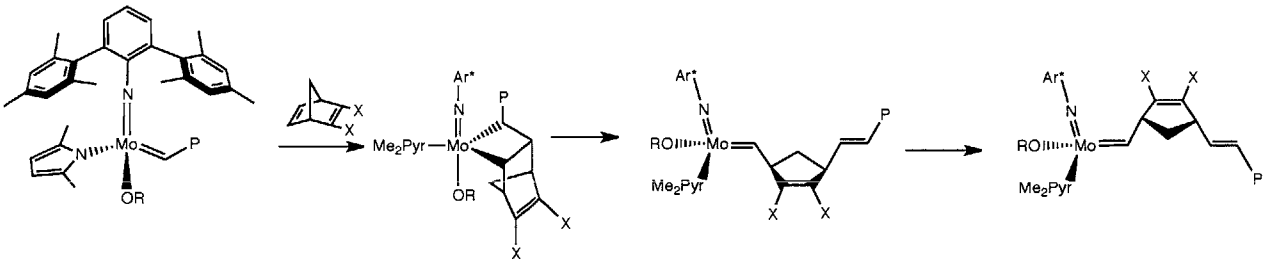

Scheme 5.1. Proposed route to *E*-selective catalysts. Ar* = 2,6-dimesitylphenyl, Me_2Pyr = 2,5-dimethylpyrrolide, P = propagating polymer chain.

Although the unexpected alkylidene isomerism was inconsistent with our hypothesis about *E* selectivity, we were interested in exploring these compounds as catalysts for olefin metathesis. Even if these catalysts are not *cis* or *trans* selective, they may provide new reactivity or selectivity. Additionally, they will provide a deeper understanding of the interplay between the imido and alkoxide ligands, and how sterically demanding ligands affect the catalytic ability of MAP compounds.

RESULTS AND DISCUSSION

I. Ring-Opening Metathesis Polymerization

A. Polymerization of 2,3-Dicarbomethoxynorbornadiene by Five-Coordinate Compounds

Ring-opening metathesis polymerization (ROMP) is a useful reaction to assess the inherent selectivity of metathesis catalysts. When a strained monomer is utilized, the release of ring strain prevents the reverse reaction from occurring, which allows the initial selectivity to be observed without isomerization from the reverse reaction.

Most of the Mo NAr* MAP or monoalkoxide chloride compounds containing the unsubstituted pyrrolide ligand were isolated as pyridine adducts (Figure 5.2). It has been shown in Chapter 3 that $B(C_6F_5)_3$ can be used to remove the pyridine ligand *in situ*, but that the pyridine-free MAP complexes or monoalkoxide chloride complexes could not be isolated from the $B(C_6F_5)_3NC_5H_5$ byproduct.[8] To test these *in situ* generated complexes for ROMP of 2,3-dicarbomethoxynorbornadiene (**DCMNBD**), one equivalent of $B(C_6F_5)_3$ was added to the Mo or W pyridine complex, a ^1H NMR spectrum was obtained to ensure complete formation of $B(C_6F_5)_3NC_5H_5$, and 100 equivalents of **DCMNBD** was added to the resulting mixture.

Reactions were conducted in toluene (0.2 M) at ambient temperature and were run until the conversion was complete, as determined by ^1H NMR spectroscopy. Data are shown in Table 5.1. None of the compounds give a highly regular structure, either in terms of *cis* or *trans* bonds or tacticity. No clear trends are observable between the structure of the initiator and the resulting polymer structure. Although the initial goal of the development of compounds containing the Ar*imido ligand was to find *trans* selective catalysts, no catalysts yet have been found that improve upon the *trans* selectivity of $Mo(NAr)(CHCMe_2Ph)(O^tBu)_2$ (Ar = 2,6-diisopropylphenyl).[10]

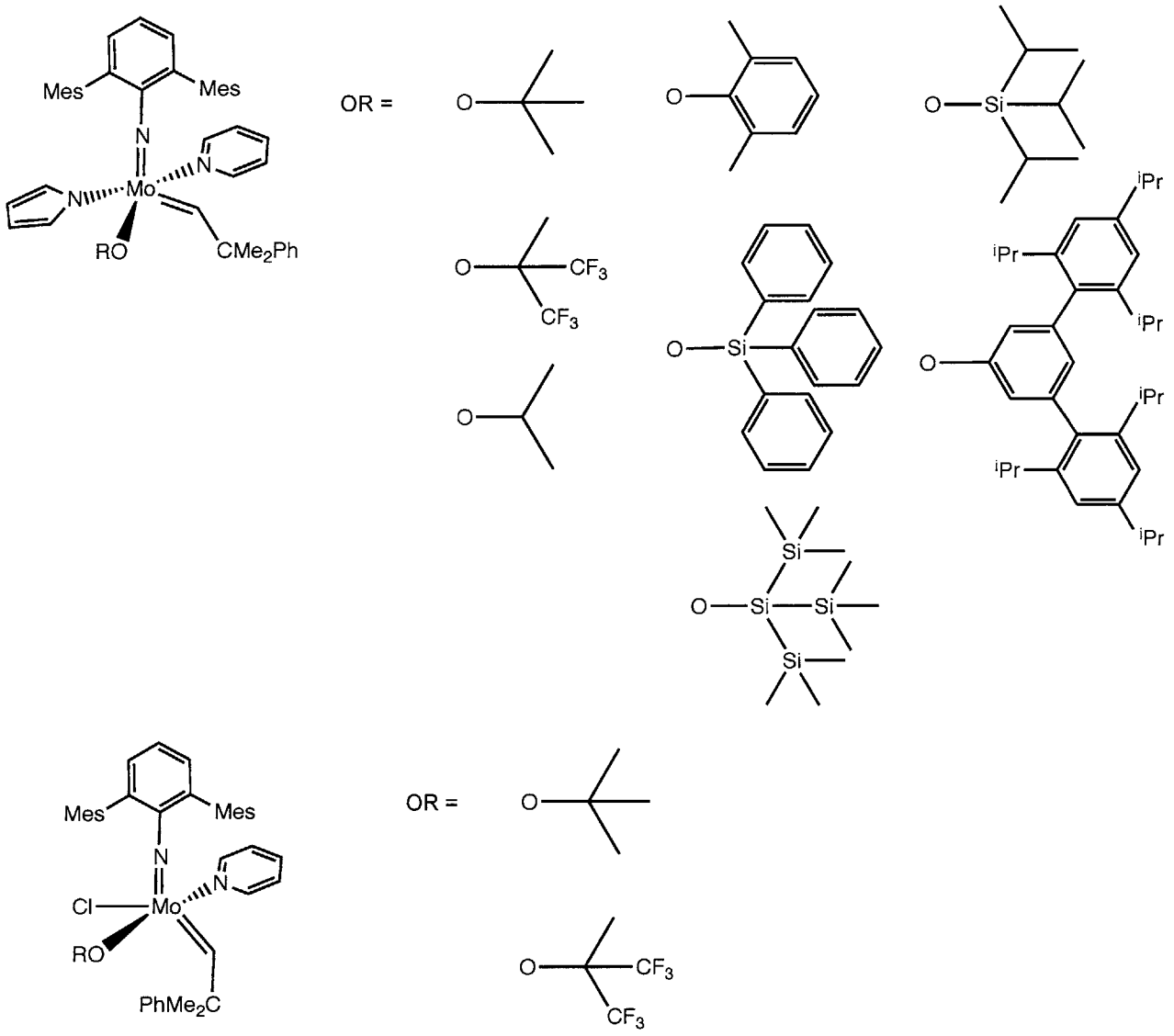

Figure 5.2. Five-coordinate compounds employed for the polymerization of DCMNBD.

Of the *in situ* generated catalysts that have been screened, the most *trans* selective were Mo(NAr*)(CHCMe$_2$Ph)(Pyr)(OSi^{i}Pr$_3$) and Mo(NAr*)(CHCMe$_2$Ph)(Pyr)(OSiPh$_3$). Since temperature can have a drastic effect on the selectivity of a reaction,[11, 1b] the polymerizations were repeated at 0 °C and 60 °C, and in both cases the resulting polymer contained less *trans* content. The reactions conducted at 0 °C were slowed significantly, and gave only very little conversion after 2 h, while the reactions conducted at ambient temperature were complete after the same amount of time.

Table 5.1. Polymerization of DCMNBD by Mo(NAr*)(CHCMe$_2$Ph)(L$_1$)(L$_2$)(pyridine). One equivalent of B(C$_6$F$_5$)$_3$ was added to remove pyridine. Reactions were conducted in toluene (0.2 M) and quenched with benzaldehyde once conversion was complete. Reactions were conducted at ambient temperature unless otherwise indicated. Ar' = 2,6-dimethylphenyl; 3,5-HIPTO = 3,5-(2,4,6-triisopropylphenyl)C$_6$H$_3$; TMS = trimethylsilyl

Ligand 1	Ligand 2	% *trans*	Temperature
Pyr	OAr'	6	
Pyr	3,5-HIPTO	13	
Pyr	O^{i}Pr	31	
Pyr	OCH(CF$_3$)$_2$	35	
Pyr	OSi(TMS)$_3$	52	
Cl	OCMe(CF$_3$)$_2$	60	
Pyr	OSi^{i}Pr$_3$	61	0 °C
Pyr	OSiPh$_3$	62	0 °C
Cl	O^{t}Bu	62	
Pyr	OCMe(CF$_3$)$_2$	75	
Pyr	OSi^{i}Pr$_3$	77	60 °C
Pyr	OSiPh$_3$	81	60 °C
Pyr	OSi^{i}Pr$_3$	83	
Pyr	OSiPh$_3$	88	

B. Polymerization of 2,3-Dicarbomethoxynorbornadiene and by Four-Coordinate Compounds

Mo and W NAr* MAP compounds that contain the 2,5-dimethylpyrrolide ligand are four-coordinate species. To understand the selectivity of these compounds, **DCMNBD** was polymerized by 1 % of compounds **1** – **4** (Figure 5.3). Results are shown in Table 5.2. None of the catalysts provide a polymer with regular structure either in terms of C=C bond isomers or tacticity. *Trans* content of the polymers range between 19 % and 70 %. There are no clear catalyst structure – function trends, either in terms of metal or alkoxide ligand.

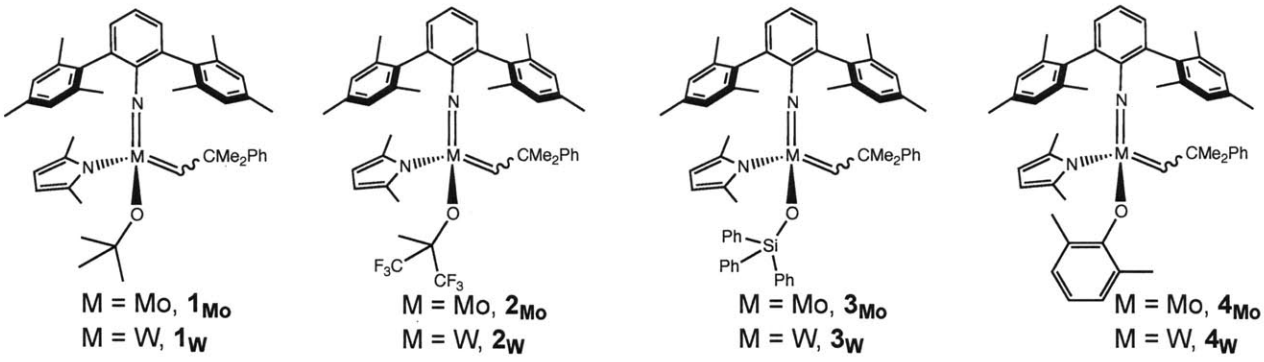

Figure 5.3. Labeling scheme for olefin metathesis catalysts.

Table 5.2. Structures of poly(DCMNBD) obtained with catalysts 1 – 4. Reactions were conducted with 2 % catalyst in 0.25 M toluene solution at ambient temperature and monitored until conversion of DCMNBD was complete.

Catalyst	% *trans*
$\mathbf{1_{Mo}}$	59
$\mathbf{1_W}$	54
$\mathbf{2_{Mo}}$	57
$\mathbf{2_W}$	30
$\mathbf{3_{Mo}}$	70
$\mathbf{3_W}$	19
$\mathbf{4_{Mo}}$	34
$\mathbf{4_W}$	38

C. Polymerization of Other Monomers

DCMNBD is often used as a test substrate to better understand catalysts, but expansion of ROMP to other monomers is important to understanding the structure – function relationships and limitations of the catalysts.

Polymerization of *rac*-2,3-dicarbomethoxynorbornene (**DCMNBE**) was conducted for catalysts **1** – **4**. Reactions were conducted in toluene (0.5 M) at ambient temperature, monitored by ^{1}H NMR spectroscopy until conversion was complete, and quenched with benzaldehyde. Results are shown in Table 5.3. Compounds **1**, **2**, and $\mathbf{3_W}$ produced completely irregular structures: resonances in the ^{13}C and ^{1}H NMR spectra were extremely broad and it was not possible to distinguish between *cis*, *trans*, *isotactic*, or *syndiotactic* resonances. In the case of

poly(**DCMNBE**) synthesized with $\mathbf{3_{Mo}}$ it was possible to distinguish *cis* and *trans* resonances in the NMR spectra. Compounds $\mathbf{4_{Mo}}$ and $\mathbf{4_W}$ produced polymer that was not soluble in chloroform-*d*, acetone-d_6, or benzene-d_6. The low solubility could be due to the inherent nature of the polymer that is formed, or due to poor initiation, in which case very high molecular weight polymers form. Catalyst $\mathbf{2_W}$ catalyzes the reaction very slowly. The polymerization was quenched with benzaldehyde after 7 d despite the fact that it was not complete.

These results are consistent with the results obtained for **DCMNBD** in that for either monomer no regular polymer structures are obtained. It is proposed that the structures are less regular for **DCMNBD** than **DCMNBE** though, as judged by the extremely broad resonances for **DCMNBE** where no fine structure could be determined. There are two enantiomers of **DCMNBE** due to the unsaturation between C2 and C3, which is not true for **DCMNBD**. The additional interactions between the different monomer enantiomers with the two enantiomers of the chiral MAP catalysts may complicate the polymerization more than in the case of **DCMNBD** causing even less regular structures.

Table 5.3. Structures of poly(DCMNBE) obtained with catalysts 1 – 4.

Catalyst	Structure
$\mathbf{1_{Mo}}$	No regular structure
$\mathbf{1_W}$	No regular structure
$\mathbf{2_{Mo}}$	No regular structure
$\mathbf{2_W}$	No regular structure (slow reaction)
$\mathbf{3_{Mo}}$	~ 50 % *trans*
$\mathbf{3_W}$	No regular structure
$\mathbf{4_{Mo}}$	Insoluble polymer
$\mathbf{4_W}$	Insoluble polymer

In order to expand the scope of ROMP with NAr* catalysts, polymerization reactions were conducted with a variety of substituted norbornenes with 2 % of $\mathbf{3_w}$ as catalyst, shown in Figure 5.4. The reactions were quenched after several days (3-10 days), although none was complete. None of the polymers obtained from **A** – **E** have a regular structure. This result is not surprising, because even with the catalyst Mo(NAd)(CHCMe$_2$Ph)(Pyr)(OHMT) (Ad = 1-Adamantyl, OHMT = OAr* = 2,6-bis(2,4,6-trimethylphenyl)phenoxide), which gives a regular *cis,syndiotactic* polymer for several norbornene-based monomers, irregular polymer is obtained

for monomers **A**, **C**, **D**, and **E**.[12] Additionally, no polymer was obtained after 6 days from the monomer 2,3-dicyano-7-oxanorbornene. The lack of polymerization in this case is likely due to the ability of the cyano groups to coordinate to the metal center.

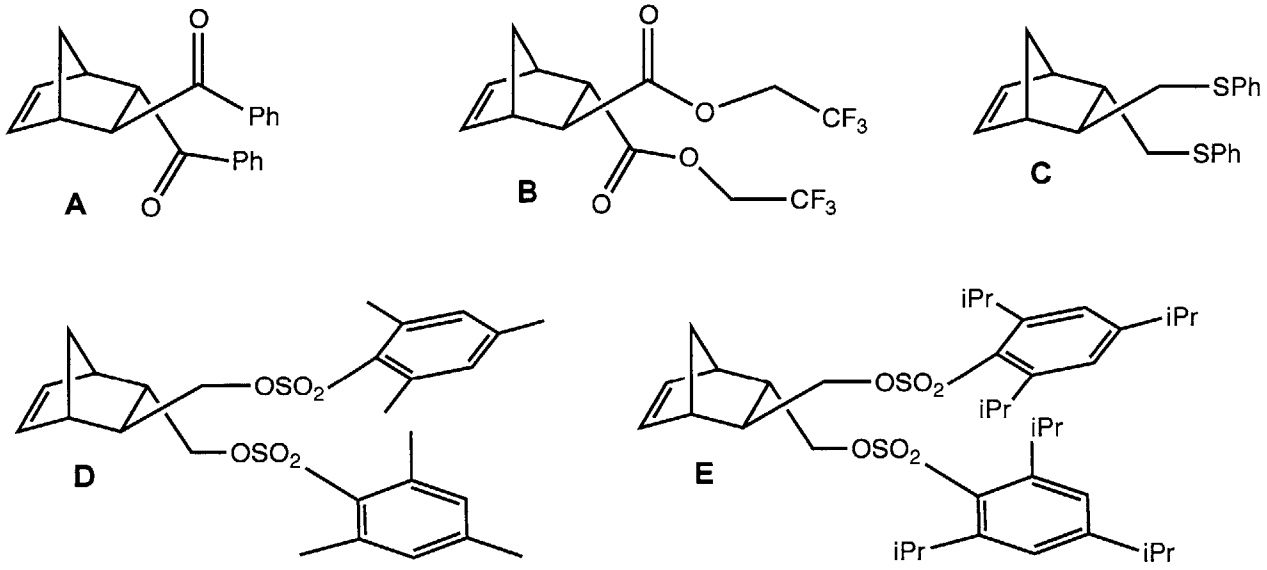

Figure 5.4. Monomers utilized for ROMP reactions catalyzed by 3_W.

II. Homocoupling of Terminal Olefins

A. Homocoupling of 1-Octene

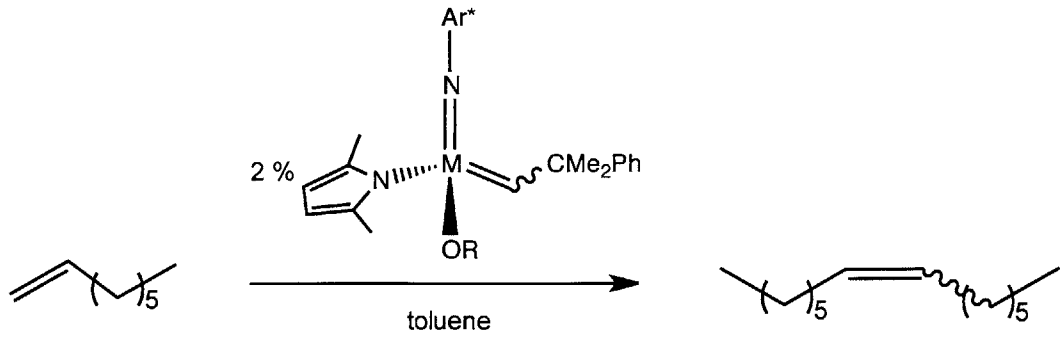

Scheme 5.2. Homocoupling of 1-octene with NAr* catalysts.

Compounds **1** – **4** were tested as catalysts for the homocoupling of 1-octene (Table 5.4). Reactions were conducted in toluene (0.4 M) at ambient temperature and monitored by ^{1}H NMR

spectroscopy. They are metathesis active, although they are relatively slow. Many of the catalysts show conversions that are lower or the same after 24 h as they were at 6 h. These results could indicate that the catalysts have died after 6 h, and the conversions after 24 h are within the error of integration of the peaks in the NMR spectrum. It could also indicate that back reaction of some of the product with ethylene has occurred, and the conversion represents the equilibrium between the forward and reverse reactions without more efficient removal of ethylene (reactions were performed in closed vials).

These catalysts are not *cis* or *trans* selective. In all cases the *trans* content stays fairly consistent throughout the reactions, indicating that the poor selectivity is inherent to the catalysts rather than the result of secondary metathesis. Since both *syn* and *anti* alkylidene species are present in solution during catalysis and there is facile interconversion of the two isomers, it is not surprising that results close to the thermodynamic mixture are obtained.

Table 5.4. Results for the homocoupling of 1-octene by MAP catalysts.

Catalyst	% conversion after 1 h	% conversion after 6 h	% conversion after 24 h	Further % conversion (time)	% trans
$\mathbf{1_{Mo}}$	53	66	69		82
$\mathbf{1_{W}}$	51		57	65 (101 h)	72
$\mathbf{2_{Mo}}$	69	75	70		80
$\mathbf{2_{W}}$	43		57	65 (101 h)	58
$\mathbf{3_{Mo}}$	59	69	64		74
$\mathbf{3_{W}}$	59	65	65		80
$\mathbf{4_{Mo}}$	64	69	71	67 (77 h)	81
$\mathbf{4_{W}}$	36	60	62	67 (77 h)	76

The report by Jiang *et al.*[2a] includes screening results for the homocoupling of 1-octene by many MAP catalysts, all of which contain sterically demanding aryloxide or alkoxide ligands. A large variety of selectivities and conversions are observed depending on the catalyst and the condition. The catalyst that gives both high *cis*-selectivity and conversion for this reaction is W(NAr')(CHCMe$_2$Ph)(Pyr)(Mes$_2$Bitet) (Ar' = 2,6-dimethylphenyl, Pyr = pyrrolide, Mes$_2$Bitet =

the phenoxide derived from deprotonation of 3,3'-dimesityl-2'-methoxy-5,5',6,6',7,7',8,8'-octahydro-[1,1'-binaphthalen]-2-ol), providing 64 % conversion after 2 h with 93 % *cis* product with 4 % catalyst loading. It is clear that the system is very sensitive to small changes in sterics though, as most MAP catalysts tested do not give high selectivites, though all contain sterically demanding alkoxide or aryloxide ligands. Catalysts that give 20 – 30 % *cis* product, as the NAr* catalysts do, are W(NAr)(CHCMe$_2$Ph)(Me$_2$Pyr)(Br$_2$Bitet), W(NAr)(CHCMe$_2$Ph)(Me$_2$Pyr)(OTPP), W(NAr^{Cl})(CHCMe$_3$)(Me$_2$Pyr)(HIPTO), W(NAr')(CHCMe$_2$Ph)(Me$_2$Pyr)(OSi(TMS)$_3$), Mo(NAd)(CHCMe$_2$Ph)(Me$_2$Pyr)(OSi(TMS)$_3$), and Mo(NAr)(CHCMe$_2$Ph)(Pyr)((Trip)$_2$Bitet(TMS)). These results indicate that in order to achieve selectivity, it is not enough to produce a catalyst with a steric bias between the aryloxide or alkoxide and imido ligands, but fine-tuning of all factors is important. In the case of the NAr* catalysts, the sterically demanding imido ligand destabilizes the *syn* alkylidene, and since both alkylidene isomers are available as part of the catalytic cycle, thermodynamic mixtures of product are obtained.

B. Homocoupling of 1,3-Dienes

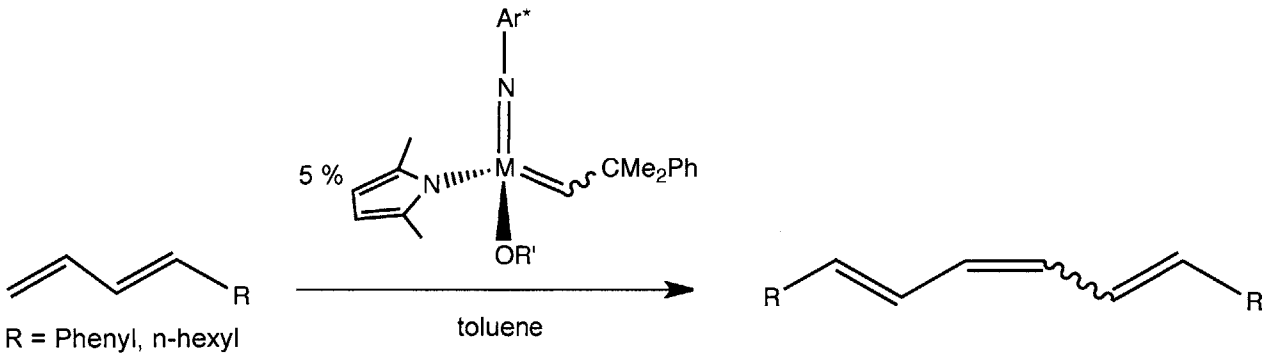

Scheme 5.3. Homocoupling of 1,3-dienes with NAr* catalysts.

In order to understand the chemoselectivity of catalysts **1** – **4**, the homocoupling of 1,3-dienes was conducted. The motivation for these reactions was to determine whether the catalysts show any selectivity towards terminal olefins, or if they react with both internal and terminal olefins.

Table 5.5. Results for the homocoupling of 1,3-decadiene after 24 h. * = *E* olefin and side products integrated together because of overlap in the NMR spectra.

Catalyst	% substrate remaining	% Yield of Z olefin	% Yield of E olefin	% yield of side products
$\mathbf{1_{Mo}}$	53	31	0	15*
$\mathbf{1_{W}}$	20	7	33	40
$\mathbf{2_{Mo}}$	0	80		20*
$\mathbf{2_{W}}$	0	20	25	65
$\mathbf{3_{Mo}}$	20	30	25	25
$\mathbf{3_{W}}$	0	35	20	45
$\mathbf{4_{Mo}}$	20	45	20	15
$\mathbf{4_{W}}$	0	40	25	35

Table 5.6. Homocoupling of 1,3-decadiene by 3_W.

Time	% substrate remaining	% Yield of *Z* olefin	% Yield of *E* olefin	% Yield of Side Products
2 h	35	50	10	5
8 h	10	50	15	25
24 h	0	35	20	45

Results for the homocoupling of *E*-1,3-decadiene are shown in Table 5.5 and Table 5.6. Consistent with the results for the homocoupling of 1-octene, no high *cis* or *trans* selectivity is observed. Table 5.5 shows the yields of products determined by integration of olefin resonances in the ^{1}H NMR spectra after 24 h. Side products are obtained from the reaction of internal olefins. With this linear, unhindered diene, all the catalysts react with both internal and terminal olefins, despite the steric hindrance of the catalyst. In all cases, the tungsten-based catalysts give a higher proportion of side products than their molybdenum congeners, indicating that the Mo-based catalysts have higher selectivity for the terminal olefins. Additionally, the tungsten catalysts are faster than their molybdenum analogs, as determined by the amount of substrate remaining at all time points. Among the alkoxide ligands, the O^{t}Bu compounds are the least reactive. This trend is likely due to electronic variations. The pK_a values of HO^{t}Bu, HOCMe$(CF_3)_2$, HOSiPh$_3$, and

2,6-$Me_2C_6H_3OH$ are 17.6,[13] 9.6,[13] 10.8,[14] and 10.6,[13] respectively. Based on the pK_a values, it follows that the O^tBu ligand is significantly less electron-withdrawing than the other three, and the more eletron-rich metal center in the t-butoxide compounds likely bind olefin substrate less strongly, leading to the slower reactivity.

Table 5.6 shows the results over time for the homocoupling of 1,3-decadiene by $\mathbf{3_W}$. This is intended as a representative example, and results with other catalysts are similar. As expected, conversion becomes higher with time, but these results indicate that product also reacts further with the catalyst. After 2 h, there is a preference for the *Z* olefin, but the ratio of *Z*:*E* olefin decreases with time, indicating isomerization of the initial product, likely by olefin metathesis. The ratio of side products to homocoupled product increases with time, which is additional indication that the catalyst reacts with the internal olefins formed in the homocoupled product.

Table 5.7. Results for the homocoupling of *E*-buta-1,3-dienylbenzene after 24 h.

Catalyst	% substrate remaining	% Yield of Z olefin	% Yield of E olefin	% yield of side products
$\mathbf{1_{Mo}}$	85	0	0	15
$\mathbf{1_W}$	60	15	25	0
$\mathbf{2_{Mo}}$	8	58	33	0
$\mathbf{2_W}$	0	40	60	0
$\mathbf{3_{Mo}}$	50	20	25	5
$\mathbf{3_W}$	0	36	54	9
$\mathbf{4_{Mo}}$	0	31	69	0
$\mathbf{4_W}$	0	30	70	0

Table 5.8. Homocoupling of *E*-buta-1,3-dienylbenzene by $\mathbf{3_W}$.

Time	% substrate remaining	% Yield of *Z* olefin	% Yield of *E* olefin	% Yield of Side Products
2 h	45	30	20	5
8 h	20	35	35	10
24 h	0	36	54	9

Results for the homocoupling of *E*-buta-1,3-dienylbenzene are shown in Table 5.7 and Table 5.8. There is no particular selectivity for *cis* or *trans* olefins, as observed for the homocoupling of 1-octene and 1,3-decadiene. Due to the phenyl substitutent in the vinylic position, the internal olefins are less reactive and less side products are formed than for 1,3-decadiene. Catalyst reactivity is consistent with the results obtained for 1,3-decadiene: the O^{t}Bu catalysts react slower than the catalysts containing the more electron-withdrawing alkoxide ligands and the W catalysts react faster than their Mo congeners. Examination of the time course results shown in Table 5.8 show a decrease in the ratio of *Z*:*E* olefin product, indicating that although the internal olefin moieties near the phenyl substituent do not react much, the center olefin continues to isomerize, likely by both olefin metathesis and by isomerization from light.[2c,15]

Homocoupling of dienes has been studied employing MAP catalysts M(NAr)(CHCMe$_2$Ph)(Pyr)(2,6-R$_2$C$_6$H$_3$) and M(NAr)(C$_3$H$_6$)(Pyr)(2,6-R$_2$C$_6$H$_3$) (M = Mo or W, Ar = 2,6-diisopropylphenyl or 2,6-dimethylphenyl, Pyr = pyrrolide, R = 2,4,6-triisopropylphenyl or 2,4,6-trimethylphenyl).[2c] These results show high *cis* selectivity in many cases. Similar to what was observed here, less side products are produced with the more sterically demanding substrate *E*-buta-1,3-dienylbenzene than linear substrate 1,3-decadiene. Trends observed in the previous study show that the bulkier ligand sets (OHIPT and 2,6-diisopropylphenylimido, where OHIPT = 2,6-di(triisoproylphenyl)phenoxide) give higher *Z* selectivity and chemoselectivity. The interesting comparison is between catalysts **4$_{Mo}$**, **4$_W$**, and M(NAr')(CHCMe$_2$Ph)(Pyr)(OHMT) (M = Mo, W; OHMT = 2,6-dimesitylphenoxide, Ar' = 2,6-dimethylphenyl) because these have the same substituents on the ligands, except with the aryloxide and imido substituents switched. In that study, that was the least sterically hindering ligand set employed, and it gave the lowest *Z*- and chemoselectivity. Catalysts **4$_{Mo}$** and **4$_W$** give similar chemoselectivity as M(NAr')(CHCMe$_2$Ph)(Pyr)(OHMT) (M = Mo, W) for the homocoupling of 1,3-decadiene, but higher chemoselectivity for the homocoupling of *E*-buta-1,3-dienylbenzene. Based on the lower chemoselectivities observed for the OHMT based catalysts observed previously the chemoselectivities observed in these studies are not surprising.

The previous studies of diene homocoupling show that Mo catalysts give higher conversions at comparable reaction times and produce more side products than the W congeners. In these studies the opposite trend is observed: the W catalysts are more reactive as measured by

the same two metrics. Higher reactivity for W catalysts than Mo catalysts has also been observed for polymerization of cyclooctenes.[16] A change in rate determining step between the two catalyst systems could explain this observation. Studies of Mo and W methylidenes and metallacycles show that both the formation and the break-up of the metallacycle is faster for Mo than W.[17] When either of these processes are the rate-limiting step, it would be expected that Mo catalysts are faster than W. In the systems studied here, it has been shown that alkylidene rotation is faster for W than Mo.[8] If instead alkylidene rotation is the rate-limiting step, W catalysts should be faster than Mo.

III. Ring-Opening Metathesis

Strained cyclic olefins typically undergo polymerization processes with Group 6 olefin metathesis catalysts. We were interested in understanding the dynamics of the possibly competing processes of polymerization and ring-opening metathesis under ethylene atmosphere. By using NAr* methylidene complexes as catalyst, the ring-opening of substituted norbornenes and norbornadienes with ethylene has been developed. Scheme 5.4 shows the proposed mechanism for ring-opening metathesis and how polymerization may be a competing reaction pathway. The methylidene catalyst reacts with substrate to form a first-insertion product. If the first-insertion product reacts with ethylene, then ring-opening metathesis occurs. If the first-insertion product reacts with another equivalent of substrate, then polymerization occurs. Reaction of the methylidene with ethylene to form the unsubstituted metallacyclobutane is also a possible competing reaction that could sequester some of the active form of the catalyst.

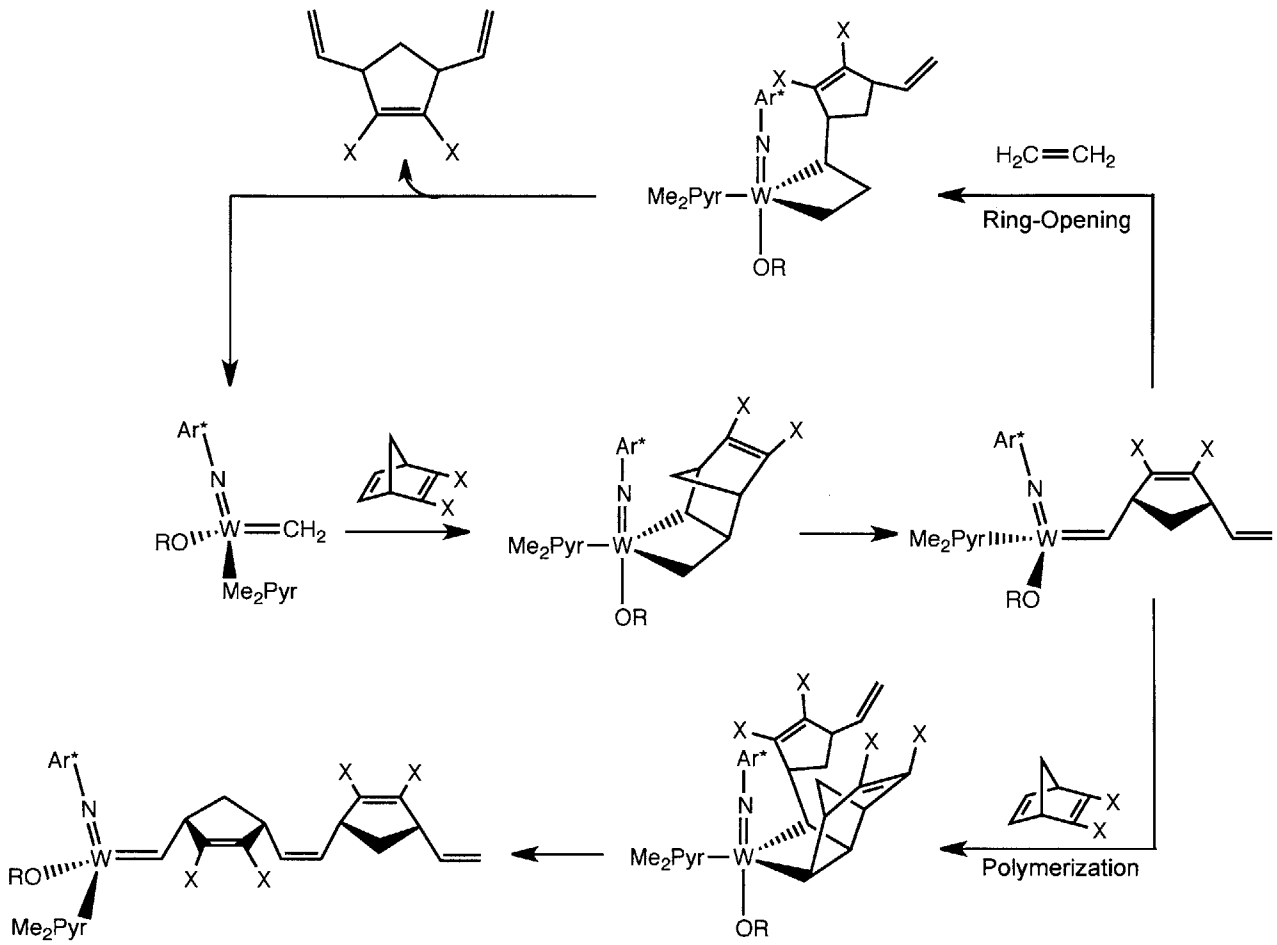

Scheme 5.4. Ring-opening metathesis *versus* ring-opening metathesis polymerization for substituted norbornadienes.

Previously, in order to prevent polymerization and facilitate ring-opening metathesis, sterically hindered norbornenes with substituents in the 7-position were required for ring-opening cross-metathesis (ROCM) reactions.[18] In certain cases, substituted norbornenes can undergo ROCM with excess cross partner with no reported oligomerization with Group 8 metathesis catalysts.[19] Ring-opening metathesis of substituted norbornenes with ethylene has been reported using a Group 8 catalyst.[20]

The tungsten methylidene compounds W(NAr*)(CH_2)(Me_2Pyr)($OSiPh_3$) (**5**) and W(NAr*)(CH_2)(Me_2Pyr)(OAr′) (**6**) (Figure 5.5) react cleanly with one molar equivalent of **DCMNBD** to give a first-insertion product (Chapter 4). This reactivity is in contrast to the neophylidene species $\mathbf{3_W}$ and $\mathbf{4_W}$ that show a complex mixture of products upon addition of one molar equivalent of **DCMNBD**, indicating that the rate of polymer propagation is much faster

than the rate of polymer initiation. Catalysts $\mathbf{3_W}$ and $\mathbf{4_W}$ also polymerize **DCMNBD** at a relatively slow rate, only showing complete conversion with 1 % catalyst after 5 d. Following these observations, it seemed that by using ethylene to cleave the first-insertion products, ring-opening metathesis could be performed on substrates that are typically used as monomers for polymerization.

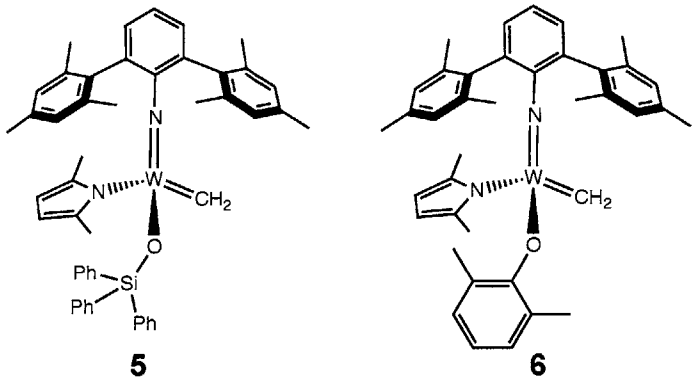

Figure 5.5. Tungsten methylidene compounds.

Reactions were performed by mixing toluene solutions of catalyst and substrate inside the dry box, degassing the solution by application of vacuum through the Schlenk manifold, and refilling the system with ethylene. Slow reaction of the first-insertion product with additional substrate is required for this procedure since a few minutes elapse after the catalyst and substrate are mixed before ethylene is added. The time after mixing of catalyst and substrate is a variable that cannot be easily controlled, and this is likely the cause in some of the variation in the results. Initial reactions were conducted with **DCMNBD** and **5** as catalyst. Although conversions were initially low, ring-opening could be performed catalytically, with no evidence for oligomer or polymer formation by ^{1}H NMR spectroscopy.

Table 5.9. Ring-opening metathesis results for DCMNBD. Reactions performed in toluene with 2 % catalyst in a closed system unless otherwise indicated. Percent yields determined by ^{1}H NMR spectroscopy. a = 1 % catalyst, b = open to ethylene line .

Entry	Catalyst	Time (h)	Temperature (° C)	Pressure (atm)	% Yield Ring Opened	% Yield Polymer
1	**5**[a]	16	20	1	14	0
2	**5**[a]	16	20	1[b]	22	0
3	**6**[a]	16	20	1	25	0
4	**5**	4	20	3.7	16	11
5	**6**	4	20	3.7	10	0
6	**5**	16	20	3.7	24	4
7	**6**	16	20	3.7	41	0
8	**6**	24	20	3.7	41	0
9	**6**	48	20	3.7	53	0
10	**5**	16	20	20	3	2
11	**6**	16	20	20	24	0
12	**6**	18	60	3.7	0	0
13	**6**	22	20	3.7	47	0
14	**6**	22	20	1	45	0
15	**6**	24	20	1	63	5
16	**6**	93	60	1	Quantitative	0
17	**6**	21	60	1	85	0
18	**6**	21	80	1	52	8
19	**6**	48	60	1	70	0

Results for the ring-opening metathesis reactions for **DCMNBD** are listed in Table 5.9. These reactions were used to find optimal conditions for the reaction. One atmosphere of ethylene was found to work as well or better than higher pressures. Comparison of entries 7 and 11 show that higher conversion is achieved with 3.7 atm than 20 atm of ethylene, giving 41 % and 24 % conversion after 16 h, respectively. Comparison of entries 13 and 14 shows that similar

results are obtained with 3.7 and 1 atm of ethylene, giving 47 % and 45 % conversion. Higher ethylene concentrations could give lower conversions for multiple reasons. One possibility is that the catalysts decompose to inactive species more quickly in the presence of ethylene. Additionally, ethylene can act as an inhibitor of this reaction by sequestering some of the catalyst as an unsubstituted tungstacyclobutane when it reacts with the active methylidene species. A combination of these factors could also be at play, especially if the unsubstituted tungstacyclobutane species rearranges reductively to tungsten (IV) olefin complexes, as is observed for $W(NAr^*)(C_3H_6)(Me_2Pyr)(O^tBu)$, see Chapter 4.

The temperature 60 °C works well for this reaction. Entries 14, 17, and 18 in Table 5.9 show results at 20 °C, 60 °C, and 80 °C. After 22 h, the reaction at 20 °C showed 45 % conversion, while the reaction at 60 °C showed 85 % conversion, and the reaction at 80 °C showed 60 % conversions, but 52 % to the ring-opened product and 8 % to polymer.

Catalyst **6** provides higher conversion than **5**. In Table 5.9, entries 4 and 5, entries 6 and 7, and entries 10 and 11 give direct comparisons of the two catalysts. Catalyst **5** consistently provides polymer byproduct in this reaction, while it was rare for catalyst **6**. Additionally, catalyst **5** performs much more poorly than **6** at 20 atm of ethylene, giving only 5 % conversion, and 3 % yield of the desired product.

In order to detect if oligomers are forming, despite not being detected by NMR spectroscopy, GC-MS analysis of the reaction mixture was conducted. No dimer, which would be expected if oligomerization were a competing reaction pathway, was detected.

Table 5.10. Ring-opening metathesis of norbornenes by 2 % of catalyst 6 at 60 °C and 1 atm ethylene. Percent yields determined by ^{1}H NMR spectroscopy.

Entry	Substrate	Time (h)	% Yield of Ring-Opened	% Yield of Polymer
1	**DCMNBE**	48	Quantitative	0
2	**DCMNBE**	25	Quantitative	0
3	**B**	25	Quantitative	0
4	**C**	24	63	37

Once conditions for the ring-opening metathesis were determined for **DCMNBD** the reaction was extended to other substituted norbornenes (Table 5.10). **DCMNBE** and **B** (Figure 5.4) give complete conversion to the ring-opened product. The ^{1}H NMR spectra of the reaction mixtures show no evidence for polymer or oligomer formation, and analysis by GC-MS shows no formation of dimer. The reaction with **C** shows 100 % conversion of monomer, but 37 % yield of polymer. This effect is likely due to electronic factors: **DCMNBE** and **B** both have electron-withdrawing ester groups at the C2 and C3 positions, while **C** has an electron-donating alkyl group, which should render **C** more reactive with the electron-deficient metal center. The more reactive the substrate is in comparison to ethylene, the more oligomers or polymer will form.

A major difference from the reactions of **DCMNBD** and the substituted norbornenes is the shorter reaction times. All the reactions with the substituted norbornenes (Table 5.10) are complete within 25 h (Table 5.10, entry 2), while the reaction of **DCMNBD** under the same conditions only 85% complete after 21 h (Table 5.9, entry 17). The only difference between **DCMNBD** and **DCMNBE** is the unsaturation between C2 and C3, which changes both the geometry at C2 and C3, as well as the electronics of the substrate. Although sterics could contribute to this effect, it is likely more due to electronics. The greater electron-deficiency of **DCMNBD** likely slows the reaction of substrate with the electron-deficient metal center.

Ring-opening metathesis reactions were also attempted with **A**, 3-methyl-3-phenyl-cyclopropane (**MPCP**), and 7-oxa-2,3-bis(trifluoromethyl)norbornadiene (**O-NBDF6**). No conversion was observed for **A** or **O-NBDF6**. Reactions with **MPCP** were indiscriminant and several products were observed. Although yields were difficult to measure, more polymer than ring-opened product was observed at both 20 °C and 80 °C. Based on the complicated NMR spectra, smaller oligomers were likely formed as well. **MPCP** is more reactive than the other substrates tested, due to its higher ring strain as well as more electron-donating substituents, so it is not surprising that **MPCP** is a substrate that is outside the scope of this reaction, since the higher reactivity makes polymerization the dominant process.

The NAr* ligand allows for the development of this new reactivity. Stabilization of methylidene species due to the steric protection provided by the NAr* ligand is important to this reactivity. It allows the required methylidene catalysts to be isolated, and additionally the NAr* ligand prevents bimolecular decomposition of the methylidene intermediates that form during the

catalytic cycle. On one hand, the NAr* ligand provides stability, but additionally the steric hindrance helps prevent polymerization and promote ring-opening metathesis reactions. The NAr* ligand provides the necessary bias to the system so that a first-insertion product will react more quickly with the small ethylene molecule than another substrate molecule.

CONCLUSIONS

Many types of olefin metathesis reactions have been conducted in order to understand the reactivity of compounds containing the 2,6-dimesitylphenylimido ligand as catalysts for olefin metathesis. The catalysts tested are not *cis* or *trans* selective, which is unsurprising in light of the equilibrium between the *syn* and *anti* alkylidene isomers in these compounds. No distinguishable structure-function trends were observed for polymerization reactions, but since ROMP reactions typically do not undergo reverse reactions, we understand the lack of *cis* or *trans* selectivity is inherent to these catalysts and not as a result of isomerization. All NAr* catalysts tested for the homocoupling of 1-octene give *cis/trans* mixtures close to the thermodynamic ratio from early time points, indicating that the lack of *cis/trans* selectivity is inherent to the catalysts, and not as a result of isomerization, consistent with the polymerization results.

To test the chemoselectivity of terminal versus internal olefins, homocoupling of 1,3-dienes was conducted. Consistent with previous results, NAr* catalysts produced more side products from the reaction of internal olefins with linear 1,3-decadiene than the more sterically protected phenyl substituted diene, *E*-buta-1,3-dienylbenzene. Catalysts $\mathbf{4_{Mo}}$ and $\mathbf{4_{W}}$ were more selective for internal olefins for the homocoupling of *E*-buta-1,3-dienylbenzene than M(NAr′)(CHCMe$_2$Ph)(Pyr)(OHMT) (M = Mo, W), compounds with similar sterics, but at different positions in the catalyst, indicative that the Ar* imido ligand provides better steric protection than the 2,6-dimesitylphenoxide. It was interesting to see that in the case of NAr* catalysts, the W compounds were more reactive than the Mo catalysts with the same ligand set. This reactivity difference is contrary to previous MAP catalysts tested for these reactions, where Mo catalysts are more reactive. This effect could be due to a change in rate limiting step between when a terphenyl substituent is on the imido versus the aryloxide ligand. Since alkylidene rotation is faster for W than Mo for the NAr* compounds, bond rotation becoming the rate

limiting step could explain the observed results, which would be an interesting effect of the NAr* ligand.

A NAr* methylidene catalyst has been used to develop new reactivity for Group 6 olefin metathesis catalysts. Although neophylidene compounds do not initiate well for polymerization, it was found that for the methylidene compounds initiation is much faster than propagation. By exploiting this large difference in rates, rather than performing polymerization, ring-opening metathesis could be conducted. In the case of norbornenes and norbornadienes with electron-withdrawing substitutents, conversion to the ring-opened product with no polymer byproduct was observed. The NAr* system allows for the development of this new reactivity because the steric protection of the NAr* ligand stabilizes methylidene species which are required both as the isolated catalyst and as reaction intermediates. Additionally, the steric hindrance provided by the NAr* ligand prevents polymerization by biasing the first-insertion product to react with ethylene rather than another equivalent of substrate. The ring-opening of strained olefins is typically a ROMP process, but we can successfully perform the ring-opening metathesis of strained olefins selectively by utilizing catalysts containing the NAr* ligand.

EXPERIMENTAL

General Considerations

All air-sensitive manipulations were performed under nitrogen atmosphere in a drybox or an air-free dual-manifold Schlenk line. All glassware was oven-dried and allowed to cool under vacuum before use. NMR spectra were obtained on Varian 300 MHz, Varian 500 MHz, Bruker 400 MHz, or Bruker 600 MHz spectrometers. ^{1}H and ^{13}C NMR spectra are reported in δ (parts per million) relative to tetramethylsilane, and referenced to residual $^{1}H/^{13}C$ signals of the deuterated solvent (^{1}H (δ): benzene 7.16, chloroform 7.26, methylene chloride 5.32, toluene 2.09. ^{13}C (δ): benzene 128.39, chloroform 77.23, methylene chloride 54.00, toluene 20.40).). ^{19}F NMR spectra are reported in δ (parts per million) relative to trichlorofluoromethane and referenced using an external standard of fluorobenzene (δ −113.15). Diethyl ether, toluene, tetrahydrofuran, pentane, benzene, dichloromethane, and dimethoxyethane were sparged with nitrogen and passed through activated alumina. All solvents were stored over 4 Å molecular sieves. Liquid reagents were degassed, brought into the drybox, and stored over 4 Å molecular

sieves. **DCMNBD**,[21] **DCMNBE**,[22] **A**,[23] **B**,[24] **C**,[12] **D**,[12] and **E**[12] were prepared according to literature procedures. All other reagents were used as received.

General Procedure for the Polymerization of DCMNBD with Five-Coordinate Compounds

Mo-alkylidene compound (0.0048 mmol) and $B(C_6F_6)_3$ (0.0048 mmol) were each dissolved/suspended in 0.3 mL C_6D_6. The catalyst solution was added to a J.Young style NMR tube followed by the solution of $B(C_6F_6)_3$. ^1H and ^{19}F NMR spectra were recorded after 15 m. The solution was transferred to a vial. A solution of 100 molar equivalents (100 mg, 0.48 mmol) of **DCMNBD** in 1 mL toluene was transferred to the vial with the stirring catalyst solution. The reaction mixture was stirred until conversion of monomer was complete, as determined by ^1H NMR spectroscopy. Once conversion was complete, the vial was removed from the dry box and 0.30 mL of benzaldehyde was added and stirred for 1 h. 20 mL of MeOH was added to precipitate the polymer. The polymer was allowed to settle for 16 h. The polymer was collected by vacuum filtration or centrifugation, washed with MeOH, and dried *in vacuo*.

General Procedure for ROMP Reactions with Catalysts 1 – 4

A solution of monomer (100 mg, 0.48 mmol) in 0.5 mL toluene was added to a stirring solution of catalyst (0.0048 mmol) in 0.5 mL toluene. Reactions were monitored by ^1H NMR spectroscopy by diluting an aliquot with C_6D_6. Once the reaction was complete, the vial was brought out of the dry box, 0.3 mL benzaldehyde was added, and the mixture stirred 1 h. MeOH (20 mL) was added and a white precipitate formed. The precipitate was collected on a fritted filter, washed with MeOH, and dried *in vacuo*.

General Procedure for homocoupling of 1-octene.

A solution of 1-octene (63 μL, 0.40 mmol) in 0.5 mL toluene was added to a stirring solution of catalyst (8.0 μmol) in 0.5 mL toluene. Reactions were monitored by ^1H NMR spectroscopy by removing a drop of the reaction mixture and adding 0.5 mL undried $CDCl_3$.

General Procedure for the Homocoupling of 1,3-Decadiene.

1,3-decadiene (2.13 M, 47 μL, 0.10 mmol), anthracene (internal standard), 0.5 mL C_6D_6, and a stir bar were added to a 4 mL vial. An aliquot was taken and diluted with C_6D_6 in order to

determine the ratio of substrate to internal standard. A solution of catalyst (5.0 μmol) in 0.2 mL C_6D_6 was added and the cap was placed loosely on the vial. Aliquots were taken after 2 h, 8 h, and 24 h. The amounts of remaining substrate, *Z* olefin, *E* olefin were determined by integration versus the internal standard. The amount of side products was determined by subtraction.

Table 5.11. Homocoupling of 1,3-decadiene by 1_{Mo}. *Combined % yield of *E* olefin and side products due to overlapping resonances.

Time	% substrate remaining	% Yield of *Z* olefin	% Yield of *E* olefin	% Yield of Side Products
2 h	100	0	0	0
8 h	60	15		25*
24 h	54	31		15*

Table 5.12. Homocoupling of 1,3-decadiene by 1_W.

Time	% substrate remaining	% Yield of *Z* olefin	% Yield of *E* olefin	% Yield of Side Products
2 h	75	0	20	5
8 h	40	8	32	20
24 h	20	7	33	40

Table 5.13. Homocoupling of 1,3-decadiene by 2_{Mo}. *Combined % yield of *E* olefin and side products due to overlapping resonances.

Time	% substrate remaining	% Yield of *Z* olefin	% Yield of *E* olefin	% Yield of Side Products
2 h	25	30	10	35
8 h	10	70		20*
24 h	0	80		20*

Table 5.14. Homocoupling of 1,3-decadiene by 2_W. *Combined % yield of *E* olefin and side products due to overlapping resonances.

Time	% substrate remaining	% Yield of *Z* olefin	% Yield of *E* olefin	% Yield of Side Products
2 h	30	60		10*
8 h	5	40	20	35
24 h	0	20	25	65

Table 5.15. Homocoupling of 1,3-decadiene by 3_{Mo}.

Time	% substrate remaining	% Yield of *Z* olefin	% Yield of *E* olefin	% Yield of Side Products
2 h	70	0	5	25
8 h	45	25	15	15
24 h	20	30	25	25

Table 5.16. Homocoupling of 1,3-decadiene by 4_{Mo}.

Time	% substrate remaining	% Yield of *Z* olefin	% Yield of *E* olefin	% Yield of Side Products
2 h	50	30	10	10
8 h	20	40	18	22
24 h	20	45	20	15

Table 5.17. Homocoupling of 1,3-decadiene by 4_W. *Combined % yield of *E* olefin and side products due to overlapping resonances.

Time	% substrate remaining	% Yield of *Z* olefin	% Yield of *E* olefin	% Yield of Side Products
2 h	30	55		15*
8 h	5	45	20	30
24 h	0	40	25	35

General Procedure for the Homocoupling of *E*-buta-1,3-dienylbenzene.

E-buta-1,3-dienylbenzene (3.0 M, 33 μL, 0.10 mmol), hexamethylbenzene (internal standard), 0.5 mL C_6D_6, and a stir bar were added to a 4 mL vial. An aliquot was taken and diluted with C_6D_6 in order to determine the ratio of substrate to internal standard. A solution of catalyst (5.0 μmol) in 0.2 mL C_6D_6 was added. Aliquots were taken after 2 h, 8 h, and 24 h. The amounts of remaining substrate, *Z* olefin, *E* olefin were determined by integration versus the internal standard. The amount of side products was determined by subtraction.

Table 5.18. Homocoupling of *E*-buta-1,3-dienylbenzene by 1_{Mo}.

Time	% substrate remaining	% Yield of *Z* olefin	% Yield of *E* olefin	% Yield of Side Products
2 h	100	0	0	0
8 h	90	0	0	10
24 h	85	0	0	15

Table 5.19. Homocoupling of *E*-buta-1,3-dienylbenzene by 1_W.

Time	% substrate remaining	% Yield of *Z* olefin	% Yield of *E* olefin	% Yield of Side Products
2 h	90	0	10	0
8 h	75	0	25	0
24 h	60	15	25	0

Table 5.20. Homocoupling of *E*-buta-1,3-dienylbenzene by 2_{Mo}. *Combined % yield of *E* olefin and side products due to overlapping resonances.

Time	% substrate remaining	% Yield of *Z* olefin	% Yield of *E* olefin	% Yield of Side Products
2 h	65	25		10*
8 h	30	65		5*
24 h	8	58		33*

Table 5.21. Homocoupling of *E*-buta-1,3-dienylbenzene by 2_W.

Time	% substrate remaining	% Yield of *Z* olefin	% Yield of *E* olefin	% Yield of Side Products
2 h	35	65	0	0
8 h	0	60	40	0
24 h	0	40	60	0

Table 5.22. Homocoupling of *E*-buta-1,3-dienylbenzene by 3_{Mo}.

Time	% substrate remaining	% Yield of *Z* olefin	% Yield of *E* olefin	% Yield of Side Products
2 h	90	0	10	0
8 h	70	0	30	0
24 h	50	20	25	5

Table 5.23. Homocoupling of *E*-buta-1,3-dienylbenzene by 4_{Mo}.

Time	% substrate remaining	% Yield of *Z* olefin	% Yield of *E* olefin	% Yield of Side Products
2 h	40	35	40	0
8 h	0	39	61	0
24 h	0	31	69	0

Table 5.24. Homocoupling of *E*-buta-1,3-dienylbenzene by 4_W.

Time	% substrate remaining	% Yield of *Z* olefin	% Yield of *E* olefin	% Yield of Side Products
2 h	20	50	30	0
8 h	0	40	60	0
24 h	0	30	70	0

General Procedure for Ring-Opening Metathesis with 1 atm Ethylene

A solution of substrate (50 mg) in 0.5 mL toluene was added to a solution of catalyst in 0.5 mL toluene in a 100 mL, teflon-stoppered Schlenk flask. The solution was brought out of the dry box, attached to a Schlenk line, and degassed by applying vacuum for 5 s. The flask was refilled with ethylene and sealed. The reaction was heated to the temperature listed in Table 5.9 or Table 5.10. After the reaction time, a few drops of water were added to quench the reaction. An aliquot was taken, the volatiles were removed *in vacuo* and an NMR spectrum was obtained in $CDCl_3$.

Dimethyl 3,5-divinylcyclopent-1-ene-1,2-dicarboxylate

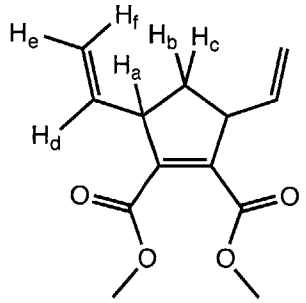

A solution of **DCMNBD** (51.5 mg, 0.247 mmol) in 0.5 mL toluene was added to a stirring solution of W(NAr*)(CH_2)(Me_2Pyr)(OAr'), **6** (208 μL of a 0.1 M solution in C_6H_6, 20.8 μmol) in 0.5 mL toluene in a 100 mL teflon-stoppered Schlenk flask. The solution was degassed by applying vacuum for 5 s. The flask was refilled with 1 atm ethylene, sealed, and heated to 60 °C. After 5 d a few drops of water was added. The aqueous and organic layers were separated. The aqueous layer was extracted with 3 x 1 mL Et_2O. The combined organic fractions were washed with 2 x 1 mL water and 1 x 1 mL brine. The solution was dried with $MgSO_4$ and filtered. The filtrated was eluted through a plug of silica gel and dried *in vacuo* to give 36 mg of a yellow oil (62 %).^{1}H NMR ($CDCl_3$) δ 5.815 (m, 2H, H_d), 5.106 (d, J_{HH} = 17 Hz, 2H, H_f), 5.050 (d, J_{HH} = 11 Hz, 2H, H_e), 3.752 (s, 6H, CH_3), 3.619 (m, 2H, H_a), 2.502 (dt, J_{HH} = 9 Hz, J_{HH} = 14 Hz, 1H, H_b/H_c), 1.665 (dt, J_{HH} = 7 Hz, J_{HH} = 14 Hz, 1H, H_b/H_c); ^{13}C NMR ($CDCl_3$) δ 165.7 (CO_2Me), 142.3, 138.9, 116.2 (olefinic), 52.2, 50.4, 37.0 (aliphatic); HRMS (ESI) *m/z* calc'd for $C_{13}H_{17}O_4$ (MH^+): 237.1121, found: 237.1111.

Dimethyl 3,5-divinylcyclopentane-1,2-dicarboxylate

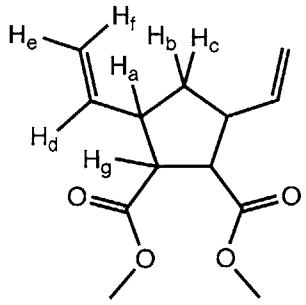

A solution of **DCMNBE** (54.8 mg, 0.261 mmol) in 0.5 mL toluene was added to a stirring solution of W(NAr*)(CH_2)(Me_2Pyr)(OAr'), **6** (4.8 μL of a 0.1 M solution in C_6H_6, 48 μmol) in 0.5 mL toluene in a 100 mL teflon-stoppered Schlenk flask. The solution was degassed by applying vacuum for 5 s. The flask was refilled with 1 atm ethylene, sealed, and heated to 60 °C. After 25 h a few drops of water was added. The aqueous and organic layers were separated. The aqueous layer was extracted with 3 x 1 mL Et_2O. The combined organic fractions were washed with 2 x 1 mL water and 1 x 1 mL brine. The solution was dried with $MgSO_4$, filtered, and the volatiles were removed *in vacuo*. The oil was dissolved in hexanes with 1 % ethylacetate, and eluted through a plug of silica gel and dried *in vacuo* to give 27 mg of a colorless oil (43 %). ^{1}H NMR ($CDCl_3$) δ 5.853 (m, 1H, H_d), 5.667 (m, 1H, H_d), 5.075 (pseudo t, J_{HH} = 17 Hz, 2H, H_f), 5.013 (pseudo t, J_{HH} = 10 Hz, 2H, H_e), 3.679 (s, 3H, CH_3), 3.644 (s, 3H, CH_3), 3.331 (dd, J_{HH} = 8 Hz, J_{HH} = 10 Hz, 1H, H_g), 3.074 (dd, J_{HH} = 9 Hz, J_{HH} = 10 Hz, 1H, H_g), 3.025 (m, 1H, H_a), 2.772 (m, 1H, H_a), 2.077 (dt, J_{HH} = 7 Hz, J_{HH} = 13 Hz, 1H, H_b/H_c), 1.639 (dt, J_{HH} = 11 Hz, J_{HH} = 13 Hz, 1H, H_b/H_c); ^{13}C NMR ($CDCl_3$) δ 174.6 (CO_2Me), 173.5 (CO_2Me), 139.6, 137.6, 116.3, 115.5 (olefinic), 52.1, 52.1, 52.0, 51.8, 48.0, 45.7, 38.3; HRMS (ESI) *m/z* calc'd for $C_{13}H_{18}O_4Na$ (MNa^+): 261.1097, found: 261.1104.

Bis(2,2,2-trifluoroethyl) 3,5-divinylcyclopentane-1,2-dicarboxylate

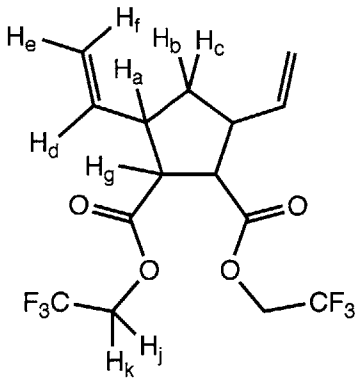

A solution of **B** (48.3 mg, 0.140 mmol) in 0.5 mL toluene was added to a stirring solution of W(NAr*)(CH_2)(Me_2Pyr)(OAr'), **6** (2.9 μL of a 0.1 M solution in C_6H_6, 29 μmol) in 0.5 mL toluene in a 100 mL teflon-stoppered Schlenk flask. The solution was degassed by applying vacuum for 5 s. The flask was refilled with 1 atm ethylene, sealed, and heated to 60 °C. After 25 h a few drops of water was added. The aqueous and organic layers were separated. The aqueous layer was extracted with 3 x 1 mL Et_2O. The combined organic fractions were washed with 2 x 1 mL water and 1 x 1 mL brine. The solution was dried with $MgSO_4$, filtered, and the volatiles were removed *in vacuo*. The oil was dissolved in hexanes with 1 % ethylacetate, and eluted through a plug of silica gel and dried *in vacuo* to give 32 mg of a colorless oil (61 %). ^{1}H NMR ($CDCl_3$) δ 5.833 (m, 1H, H_d), 5.666 (m, 1H, H_d), 5.133 – 5.039 (overlapping d, 4H, H_e and H_f), 4.563 – 4.347 (overlapping m, 4H, H_j and H_k), 3.456 (pseudo t, J_{HH} = 9 Hz, 1H, H_g), 3.164 (pseudo t, J_{HH} = 9 Hz, 1H, H_g), 3.105 (m, 1H, H_a), 2.802 (m, 1H, H_a), 2.167 (dt, J_{HH} = 7 Hz, J_{HH} = 13 Hz, 1H, H_b/H_c), 1.664 (dt, J_{HH} = 10 Hz, J_{HH} = 13 Hz, 1H, H_b/H_c); ^{19}F NMR ($CDCl_3$) δ -73.44 (t, $^3J_{HF}$ = 8 Hz), -73.74 (t, $^3J_{HF}$ = 8 Hz); ^{13}C NMR ($CDCl_3$) δ 172.1, 171.1 ($CO_2CH_2CF_3$), 138.6, 136.7 (olefinic), 123.0 (quartet, J_{CF} = 275, CF_3), 122.9 (quartet, J_{CF} = 275, CF_3), 117.3, 116.4 (olefinic), 60.8 (quartet, J_{CF} = 37 Hz, CH_2CF_3), 60.6 (quartet, J_{CF} = 37 Hz, CH_2CF_3), 51.6, 51.6, 47.9, 45.4, 38.1; HRMS (ESI) *m/z* calc'd for $C_{15}H_{16}F_6O_4Na$ (MNa^+): 397.0845, found: 397.0860.

((3,5-Divinylcyclopentane-1,2-diyl)bis(methylene))bis(phenylsulfane)

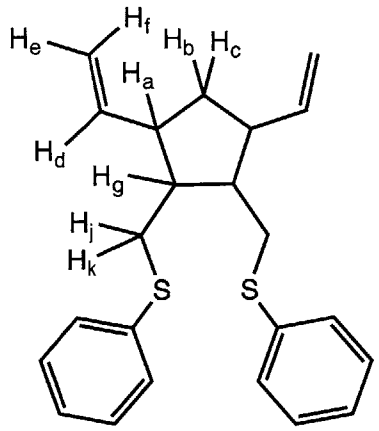

A solution of **C** (51.7 mg, 0.152 mmol) in 0.5 mL toluene was added to a stirring solution of W(NAr*)(CH_2)(Me_2Pyr)(OAr'), **6** (3.0 μL of a 0.1 M solution in C_6H_6, 30 μmol) in 0.5 mL toluene in a 100 mL teflon-stoppered Schlenk flask. The solution was degassed by applying vacuum for 5 s. The flask was refilled with 1 atm ethylene, sealed, and heated to 60 °C. After 25 h a few drops of water was added. The aqueous and organic layers were separated. The aqueous layer was extracted with 3 x 1 mL Et_2O. The combined organic fractions were washed with 2 x 1 mL water and 1 x 1 mL brine. The volatiles were removed *in vacuo*, the resulting oil was extracted with MeOH, and filtered through a pipette filter to remove polymer byproduct. The oil was dissolved in hexanes with 1 % ethylacetate, and eluted through a plug of silica gel and dried *in vacuo* to give 18 mg of a colorless oil (32 %). ^{1}H NMR ($CDCl_3$) δ 7.308 – 7.272 (overlapping signals, 4H, Ar*H*), 7.254 – 7.228 (overlapping signals, 4H, Ar*H*), 7.143 (tt, J_{HH} = 7 Hz, J_{HH} = 2 Hz, 2H, Ar*H*), 5.856 (ddd, 1H, H_d), 5.737 (ddd, 1H, H_d), 5.102 – 5.059 (overlapping signals, 2H, H_e and H_f), 4.991 – 4.943 (overlapping signals, 2H, H_e and H_f), 3.168 – 2.999 (overlapping m, 3H), 2.871 – 2.808 (overlapping m, 2H), 2.450 (m, 1H), 2.279 (m, 1H), 2.040 – 1.968 (overlapping m, 2H), 1.514 (dt, J_{HH} = 10 Hz, J_{HH} = 13 Hz, 1H, H_b/H_c); ^{13}C NMR ($CDCl_3$) δ 141.83, 138.66 (*C*O_2CH_2SPh), 137.45, 137.25, 129.14, 129.04, 129.03, 128.96 (Aromatic), 125.91, 125.81, 116.03, 114.79 (Olefinic), 49.42, 48.74, 46.56, 46.08, 37.92, 37.16, 35.96; HRMS (ESI) *m/z* calc'd for $C_{23}H_{27}S_2$ (MH^+): 367.1549, found: 367.1563.

General Procedure for Ring-Opening Metathesis of DCMNBD with >1 atm Ethylene.

A solution of **DCMNBD** (50 mg, 0.24 mmol) in 0.5 mL toluene was added to a solution of catalyst (0.0048 mmol) in 0.5 mL toluene in a 4 mL vial. The vial was placed inside a pressure

reactor and sealed. The apparatus was removed from the dry box, pressurized to the desired ethylene pressure (3.7 atm or 20 atm), and allowed to stir for the desired reaction time. After the reaction time, a few drops of water were added to quench the reaction. An aliquot was taken, the volatiles were removed *in vacuo* and an NMR spectrum was obtained in $CDCl_3$.

REFERENCES

[1] (a) Flook, M. M.; Jiang, A. J.; Schrock, R. R.; Müller, P.; Hoveyda, A. H. *J. Am. Chem. Soc.* **2009**, *131*, 7962. (b) Flook, M. M.; Gerber, L. C. H.; Debelouchina, G. T.; Schrock, R. R. *Macromolecules* **2010**, *43*, 7515. (c) Flook, M. M.; Ng, V. W. L.; Schrock, R. R. *J. Am. Chem. Soc.* **2011**, *133*, 1784. (d) Flook, M. M.; Börner, J.; Kilyanek, S.; Gerber, L. C. H.; Schrock, R. R. *Organometallics* **2012**, *31*, 6231.

[2] (a) Jiang, A. J.; Zhao, Y.; Schrock, R. R.; Hoveyda, A. H. *J. Am. Chem. Soc.* **2009**, *131*, 16630. (b) Marinescu, S. C.; Schrock, R. R.; Müller, P.; Takase, M. K.; Hoveyda, A. H. *Organometallics* **2011**, *30*, 1780. (c) Townsend, E. M.; Schrock, R. R.; Hoveyda, A. H. *J. Am. Chem. Soc.* **2012**, *134*, 11334. (d) Peryshkov, D. V.; Schrock, R. R.; Takase, M. K.; Müller, P.; Hoveyda, A. H. *J. Am. Chem. Soc.* **2011**, *133*, 20754.

[3] (a) Ibrahem, I; Yu, M.; Schrock, R. R.; Hoveyda, A. H. *J. Am. Chem. Soc.* **2009**, *131*, 3844. (b) Yu, M.; Ibrahem, I.; Hasegawa, M.; Schrock, R. R.; Hoveyda, A. H. *J. Am. Chem. Soc.* **2012**, *134*, 2788.

[4] (a) Marinescu, S. C.; Schrock, R. R.; Müller, P.; Hoveyda, A. H. *J. Am. Chem. Soc.* **2009**, *131*, 10840. (b) Marinescu, S. C.; Levine, D.; Zhao, Y.; Schrock, R. R.; Hoveyda, A. H. *J. Am. Chem. Soc.* **2011**, *133*, 11512.

[5] (a) Wang, C.; Yu, M.; Kyle, A. F.; Jacubec, P.; Dixon, D. J.; Schrock, R. R.; Hoveyda, A. H. *Chem. Eur. J.* **2013**, *19*, 2726. (b) Wang, C.; Haeffner, F.; Schrock, R. R.; Hoveyda, A. H. *Angew. Chem. Int. Ed.*, **2013**, *52*, 1939.

[6] (a) Liu, P,; Xu, X.; Dong, Xj.; Keitz, B. K.; Herbert, M. B.; Grubbs, R. H.; Houk, K. N. *J. Am. Chem. Soc.* **2012**, *134*, 1464. (b) Keitz, B. K.; Endo, K.; Patel, P. R.; Herbert, M. B.; Grubbs, R. H. *J. Am. Chem. Soc.* **2012**, *134*, 693. (c) Keitz, B. K.; Fedorov, A.; Grubbs, R. H. *J. Am. Chem. Soc.* **2012**, *134*, 2040. (d) Herbert, M. B.; Marx, V. M.; Pederson, R. L.; Grubbs, R. H. *Angew. Chem. Int.* **2013**, *125*, 310. (e) Keitz, B. K.; Endo, K.; Herbert, M. B.; Grubbs, R. H. *J. Am. Chem. Soc.* **2011**, *133*, 9686. (f) Endo, K.; Grubbs, R. H. *J. Am. Chem. Soc.* **2011**, *133*, 8525. (g) Miyazaki, H.; Herbert, M. B.; Liu, P.; Dong, X.; Xu, X.; Keitz, B. K.; Ung, T.; Mkrtumyan, G.; Houk, K. N.; Grubbs, R. H. *J. Am. Chem. Soc.* **2013**, *135*, 5848. (h) Marx, V. M.; Herbert, M. B.; Keitz, B. K.; Grubbs, R. H. *J. Am. Chem. Soc.* **2013**, *135*, 94.

[7] Gerber, L. C. H.; Schrock, R. R.; Müller, P.; Takase, M. K. *J. Am. Chem. Soc.*, **2011**, *133,* 18142.

[8] Gerber, L. C. H.; Schrock, R. R.; Müller, P. *Organometallics*, **2013**, *32*, 2373.

[9] (a) Oskam, J. H.; Schrock, R. R. *J. Am. Chem. Soc.* **1992**, *114*, 7588. (b) Oskam, J. H.; Schrock, R. R. *J. Am. Chem. Soc.* **1993**, *115*, 11831.

[10] (a) Bazan, G. C.; Khosravi, E.; Schrock, R. R.; Feast, W. J.; Gibson, V. C.; O'Regan, M. B.; Thomas, J. K.; Davis, W. M. *J. Am. Chem. Soc.* **1990**, *112*, 8378 – 8387. (b) Feast, W. J.; Gibson, V. C.; Marshall, E. L. *J. Chem. Soc., Chem. Commun.* **1992**, 1157 – 1158. (c) O'Dell, R.; McConville, D. H.; Hofmeister, G. E.; Schrock, R. R. *J. Am. Chem. Soc.* **1994**, *116*, 3414 – 3423.

[11] Schrock, R. R.; Lee, J.-K.; O'Dell, R.; Oskam, J. H. *Macromolecules,* **1995**, *28*, 5933 – 5940.

[12] Klatt, T. ROMP of Functionalized Monomers with Group 6 Imido Alkylidene Catalysts. Master's Thesis, Technischen Universität München, Munich, Germany, 2011.

[13] Serjeant, E. P.; Dempsey, B. *International Union of Pure and Applied Chemistry. Commission on Equilibrium Data. Ionisation Constants of Organic Acids in Aqueous Solution*; Oxford, New York: Pergamon Press, 1979.

[14] Duchateau, R.; Cremer, U.; Harmsen, R. J.; Mohamud, S. I.; Abbenhuis, H. C. L.; van Santen, R. A.; Meetsma, A.; Thiele, S. K.-H.; van Tol, M. F. J.; Kranenburg, M. *Organometallics*, **1999**, *18*, 5447.

[15] Saltiel, J.; Wang, S.; Watkins, L. P.; Ko, D.-H. *J. Phys. Chem. A* **2000**, *104* 11443.

[16] Jeong, H.; Kozera, D. J.; Schrock, R. R.; Smith, S. J.; Zhang, J.; Ren, N.; Hillmyer, M. A. *Organometallics*, Accepted.

[17] Schrock, R. R.; Jiang, A. J.; Marinescu, S. C.; Simpson, J. H.; Müller, P. *Organometallics* **2010**, 29, 5241.

[18] (a) La, D. S.; Sattely, E. S.; Ford, J. G.; Schrock, R. R.; Hoveyda, A. H. *J. Am. Chem. Soc.* **2001**, 123 7767. (b) Pilyugina, T. S.; Schrock, R. R.; Müller, P; Hoveyda, A. H. *Organometallics* **2007**, 26, 831.

[19] (a) Hartung, J.; Grubbs, R. H. *J. Am. Chem. Soc.* **2013**, 135, 10183. (b) Wakamatsu, H.; Blechert, S. *Angew. Chem., Int. Ed.*, **2002**, *41*, 2403. (c) Kannenberg, A.; Rost, D.; Eibauer, S.; Tiede, S.; Blechert, S. *Angew. Chem., Int. Ed.*, **2011**, *50*, 3299. (d) Tiede, S.; Schlesiger, D.; Rost, D.; Lühl, A.; Blechert, S. *Angew. Chem., Int. Ed.* **2010**, 49, 3972. (e) Liu, Z.; Rainier, J. D. *Org. Lett.* **2005**, 7, 131. (f) Krause, J. O.; Nuyken, O.; Wurst, K.; Buchmeiser, M. R. *Chem. Eur. J.* **2004**, 10, 777. (g) Katayama, H.; Nagao, M.; Ozawa, F. *Organometallics* **2003**, 22, 586. (h) Mayo, P.; Tam. W. *Tetrahedron* **2002**, 58, 9513. (i) Katayama, H.; Urushima, H.; Nishioka, T.; Wada, C.; Nagao, M.; Ozawa, F. *Angew Chem., Int. Ed.* ***2000***, 39, 4513.

[20] (a) Nuyken, O.; Müller, B. *Des. Monomers Polym.* **2004**, 7, 215. (b) Eyrisch, K. K.; Müller, B. K. M.; Herzig, C.; Nuyken, O. *Des. Monomers Polym.* **2004**, 7, 661.

[21] Tabor, D. C.; White, F. H.; Collier, L. W.; Evans, S. A. *J. Org. Chem.* **1983**, 48, 1638.

[22] Koch, H. *Monatsh. Chem.* **1962**, 93, 1343.

[23] Höfler, T.; Grießer, T.; Gstrein, X.; Trimmel, G.; Jakopic, G.; Kern, W. *Polymer* **2007**, *48*, 1930.

[24] Ryu, D. H.; Zhou, G.; Corey, E. J. *Org. Lett.* **2005**, *7*, 1633.

Laura C. H. Gerber

Massachusetts Institute of Technology
Department of Chemistry
77 Massachusetts Avenue
Cambridge, MA 02139

EDUCATION

Massachusetts Institute of Technology, Cambridge, MA 2013
Ph. D. Candidate in Inorganic Chemistry
Relevant Coursework: Principles of Inorganic Chemistry II & III, Organometallic Chemistry, Organometallic Catalysis, Physical Inorganic Chemistry

Brandeis University, Waltham, MA 2007
B.A./M.S. in Chemistry and Minor in Environmental Studies

EXPERIENCE

Massachusetts Institute of Technology, Graduate Research 2008 - Present
Advisor: Prof. Richard R. Schrock

- Designed olefin metathesis catalysts for selective reactions, especially ring opening metathesis polymerization
- Developed novel synthetic routes for olefin metathesis catalysts allowing new ligands to be incorporated, analyzed compounds using x-ray crystallography, and NMR, IR, and UV-Visible spectroscopy, several projects in the group now utilize the findings
- Studied reaction mechanism to understand catalyst selectivity for polymerization by variable temperature NMR spectroscopy
- Trained and mentored an undergraduate student in organometallic synthesis

Fulbright Fellowship, University of Bergen, Norway 2007 – 2008
Advisor: Prof. Reiner Anwander

- Studied reactivity of trimethyl and heterobimetallic rare earth metal complexes
- Presented research at a department seminar and for Fulbright Fellows in all fields

Brandeis University, Undergraduate Research 2005 - 2007
Advisor: Prof. Oleg V. Ozerov

- Synthesized transition metal complexes containing rare bonding modes including the first bis(methylidene) complex
- Presented findings at anAmerican Chemical Society meeting and at an undergraduate research symposium

University of Notre Dame, Environmental Molecular Science Institute 2005
Undergraduate Research
Advisor: Prof. Patricia Maurice

- Studied the sorption and dissolution mechanisms of siderophores with montmorillonite using a variety of techniques including UV-visible spectroscopy and powder x-ray diffractometry

LEADERSHIP

Chemistry Student Seminar, MIT 2011 - Present
Organizer of a weekly student run seminar series. Recruited speakers, obtained funding, and organized logistics.

Teaching Assistant, General and Inorganic Chemistry Laboratory Courses, MIT 2008 - 2009
Prepared pre-lab lectures, quizzes, optimized experiments, and assisted students (15 students for inorganic lab and 60 for general chemistry lab) during lab hours.

Undergraduate Departmental Representative, Brandeis Univ. Chemistry Dept. 2005 - 2007
Planned informational and community events. Served as a liaison between the students and department

HONORS AND AWARDS

Fulbright Fellowship 2007 - 2008
Awarded by the U.S. Department of State

Melvin E. Snider Prize in Chemistry 2007
Awarded by the Brandeis University Dept. of Chemistry

Presidential Scholarship 2003 - 2007
Awarded by Brandeis University

COMMUNITY ACTIVITIES

Chemistry Outreach Program, MIT 2009 - Present
Volunteer to visit high school science classes to demonstrate science concepts

Cambridge Symphony Orchestra, Cambridge, MA 2011 - Present
Member of a community orchestra that performs for local events in the Boston area

SKILLS

Manipulation of air-sensitive compounds by drybox and Schlenk technique; 1D, 2D, and multinuclear, and variable temperature NMR spectroscopy; x-ray crystallography; IR and UV-Visible spectroscopy.

PROFESSIONAL AFFILIATIONS

American Chemical Society, Division of Inorganic Chemistry, Northeastern Section of the American Chemical Society, MIT Women in Chemistry

PUBLICATIONS

Yuan, J.; Schrock; R. R.; Gerber, L. C. H.; Müller, P.; Smith, S. **Synthesis and ROMP Chemistry of Decafluoroterphenoxide Molybdenum Imido Alkylidene and Ethylene Complexes.** *Organometallics,* **2013**, *32*, 2983 - 2992.

Gerber, L. C. H.; Schrock, R. R.; Müller, P. **Molybdenum and Tungsten Monoalkoxide Pyrrolide (MAP) Alkylidene Complexes That Contain a 2,6-Dimesitylphenylimido Ligand.** *Organometallics,* **2013**, *32*, 2373 - 2378.

Flook, M. M.; Börner, J.; Kilyanek, S. M.; Gerber, L. C. H.; Schrock, R. R. **Five-Coordinate Rearrangements of Metallacyclobutane Intermediates during Ring-Opening Metathesis Polymerization of 2,3-Dicarboalkoxynorbornenes by Molybdenum and Tungsten Monoalkoxide Pyrrolide Initiators.** *Organometallics,* **2012**, *31*(17), 6231 - 6243.

Gerber, L. C. H.; Schrock, R. R.; Müller, P.; Takase, M. K. **Synthesis of Molybdenum Alkylidene Complexes That Contain the 2,6-Dimesitylphenylimido Ligand.** *J. Am. Chem. Soc.*, **2011**, *133* (45), 18142 - 18144.

Flook, M. M.; Gerber, L. C. H.; Debelouchina, G. T.; Schrock, R. R. **Z-Selective and Syndioselective Ring-Opening Metathesis Polymerzation (ROMP) Initiated by Monoaryloxidepyrrolide (MAP) Catalysts.** *Macromolecules,* **2010**, *43* (18), 7515 - 7522.

Takaoka, A.; Gerber, L. C. H.; Peters, J. C. **Access to Well-Defined Ruthenium(I) and Osmium(I) Metalloradicals.** *Angewandte Chemie, International Edition,* **2010**, *49* (24), 4088.

Gerber, L. C. H.; Le Roux, E.; Törnroos, K. W.; Anwander, R. **Elusive Trimethyllanthanum: Snapshots of Extensive Methyl Group Degradation in La-Al Heterobimetallic Complexes.** *Chemistry: A European Journal,* **2008**, *14*, 9555 - 9564.

Gerber, L. C. H.; Watson, L. A.; Parkin, S.; Weng, W.; Foxman, B. M.; Ozerov, O. V. **A Bis(methylidene) Complex of Tantalum Supported by a PNP Ligand.** *Organometallics,* **2007**, *26* (20), 4866 - 4868.

PRESENTATIONS

Gerber, L. C. H. **Exploration of Steric Bulk in Molybdenum and Tungsten Olefin Metathesis Catalysts.** Inorganic Seminar Series, Massachusetts Institute of Technology Department of Chemistry, December 19, 2012.

Gerber, L. C. H.; Schrock, R. R. **Molybdenum and tungsten olefin metathesis catalysts containing a 2,6-dimesitylphenylimido ligand.** 244th ACS National Meeting & Exposition, Philadelphia, PA, United States, August 19-23, 2012.

Gerber, L. C. H.; Schrock, R. R. **Molybdenum olefin metathesis catalysts containing a 2,6-dimesitylphenylimido ligand.** 242nd ACS National Meeting & Exposition, Denver, CO, United States, August 28-September 1, 2011.

Gerber, L. C. H.; Schrock, R. R. **Mechanistic studies of ring-opening metathesis polymerization with molybdenum monoaryloxide monopyrrolide catalysts.** 240th ACS National Meeting, Boston, MA, United States, August 22-26, 2010.

Litlabø, R., Gerber, L. C. H., Anwander, R. **Reactivity of Homoleptic Lanthanide(III) Tetraalkylaluminate Complexes.** Seminar in Inorganic and Nanochemistry. University of Bergen. May 15, 2008.

Gerber, L. C. H. **Lanthanide Chemistry.** Presentation at Meeting for U.S. Fulbright Fellows in Norway, February 14, 2008.

Gerber, L. C. H.; Ozerov, O. V.; Weng, W.; Foxman, B. M. **Synthetic approaches to pincer complexes with tantalum-carbon multiple bonds.** 232nd ACS National Meeting, San Francisco, CA, United States, Sept. 10-14, 2006.

Laura C. H. Gerber, Oleg V. Ozerov, Wei Weng, Bruce M. Foxman. **New Tantalum Pincer Compounds: En route to Group 5 Alkylidynes.** Research Experience for Undergraduates Symposium. Brandeis University. August 10, 2006.

Laura C. H. Gerber, Elizabeth Haack, Patricia Maurice. **The Sorption of Acetohydroxamic Acid by Montmorillonite.** Research Experience for Undergraduates Symposium. Environmental Molecular Science Institute, University of Notre Dame. August 5, 2005.

Acknowledgements

There are many people who I would like to thank for their encouragement and support along this path. First, I would like to thank my advisor Richard Schrock. I am grateful for the opportunity to work in his research group, despite my late start. I have enjoyed my time in the group and I have learned so much from Dick. He has always been available to discuss my latest results and provide insight when I ran into roadblocks in my research. I admire his enthusiasm and creativity for solving chemical problems, qualities I hope to embody throughout my career as a chemist. I would like to thank my thesis committee chair, Christopher Cummins. Our discussions have always been extremely productive and his perspective has been invaluable. I greatly appreciate Yogesh Surendranath joining my thesis committee on short notice. Thanks are also due to the other Inorganic faculty. I have learned a lot from each of them throughout my years at MIT.

Much gratitude goes to those who have fostered my inclination towards chemistry. My high school chemistry teacher, Keith Zeise, made chemistry intuitive and kept class interesting with his creative analogies. I appreciate the encouragement and patience from my undergraduate advisors, Oleg Ozerov and Bruce Foxman. Professor Foxman provided my first introduction to inorganic chemistry. His dedication to teaching and his encouragement to explore inorganic chemistry further through research started me on my path to becoming a chemist. Oleg Ozerov was a superb research advisor. I was thrilled to be working on my own independent project from the start, and Oleg seemed to always know the right balance between providing guidance and allowing me to work independently. I appreciate his patience and how his door was always open when I wanted to discuss research.

My colleagues at MIT have been one of the greatest assets of working here. Daily discussions with my labmates and friends have helped me evolve into the chemist I am today. Their insight has shaped my research and their support has helped me through many frustrations. I would like to thank Ayumi Takaoka, Nate Szymczak, and Neal Mankad for helping me get started in lab during my first year of grad school. I am so grateful to Annie King and Maggie Flook who helped me get started in the Schrock Group. They helped make the transition easy. I would especially like to thank Maggie Flook who I shared a glove box and office with for over two years. She was easy to work with and always willing to discuss results and help me interpret my spectra. I have learned so much from all the past and present members of the Schrock Group and I am grateful to have worked with such a friendly and talented group of people. Special thanks go to Smaranda Marinescu, Keith Wampler, Erik Townsend, Jon Axtell, Hyangsoo Jeong, Alex Lichtscheidl, Dima Peryshkov, Stephan Kilyanek, and Graham Dobereiner for helpful discussions. My lab and officemates in 6-421 have made the day-to-day work enjoyable. I appreciated the opportunity to work with undergraduate Betsy Flowers. Her enthusiasm for chemistry was contagious. All current group members have proofread portions of this thesis. Thank you Will Forrest, Hyangsoo Jeong, Matt Cain, Jon Axtell, Graham Dobereiner, and especially Erik Townsend.

I need to thank my friends and family for their support and understanding, especially my parents Ann Heidkamp and Jim Gerber, my brother Alan Gerber, my grandmother Jane Gerber, and my cousin Eleanor Heidkamp-Young. Most of all, I would like to thank my husband Mark Zegarelli. His support and encouragement have been endless, and I appreciate it more than I can express.